Springer-Verlag Berlin Heidelberg GmbH

Ashraf M. T. Elewa
(Editor)

Morphometrics

Applications in Biology and Paleontology

With 104 Figures and 35 Tables

Springer

EDITOR:
Dr. Ashraf M. T. Elewa
Associate Professor
Minia University
Faculty of Science
Geology Department
Egypt
E-mail: *aelewa@link.net*

ISBN 978-3-642-05980-3 ISBN 978-3-662-08865-4 (eBook)
DOI 10.1007/978-3-662-08865-4

Library of Congress Control Number: 2004103476

A catalog record for this book is available from the Library of Congress.
Bibliographic information published by Die Deutsche Bibliothek
Die Deutsche Bibliothek lists this publication in die Deutsche Nationalbibliographie; detailed bibliographic data is available in the Internet at <http://dnb.ddb.de>.

Originally published by Springer-Verlag Berlin Heidelberg New York in 2004
Softcover reprint of the hardcover 1st edition 2004

Cover Design: Erich Kirchner, Heidelberg
Typesetting: Camera-ready by the editor

Printed on acid free paper 30/3141/LT – 5 4 3 2 1 0

Dedication

This book is dedicated to

Almighty Allah asking him for forgiveness

My parents, my wife, my son and daughter

My brother and sister

My learners

Preface

F. James Rohlf

Department of Ecology and Evolution, State University of New York at Stony Brook, USA, rohlf@life.bio.sunysb.edu

This new edited volume is a welcome addition to the literature of geometric morphometrics. It differs from previous collections of papers in that it does not represent an outcome of one of the many morphometric workshops but is an independent collection of papers concerned with real applications of geometric morphometric methods to problems in systematics. Thus, the papers are expected to be more in depth than many of the exemplary expositions found in earlier edited volumes. This should make it especially useful to many potential users of geometric morphometric methods.

This publication is a timely development for the field as it is now in a period of transition from its early years, where it was considered a promising but rather complicated approach, to the present where for many types of applications it can be applied routinely (with suitable care, of course). Methods for data consisting of coordinates of landmarks in two dimensions are especially well developed. There are now standard protocols and several choices of software that can be used both for the computations and for visualizations. The extensions to semilandmark points along curves in two dimensions (both complete outlines as well as partial) are also readily available. The main challenges for a practical application are, as they should be, decision about what structures to study, how to capture the relevant shape variation through carefully chosen suites of landmark and/or semilandmark points, and how to interpret the results.

The mathematical and statistical properties of the methods are also quite well understood for 2-dimensional data for the usual case in which one can assume that variation in shape is relatively small. There are, however, still some important technical problems to be solved. An important one of interest to many workers is that of how to make statements about the relative amounts of variability at different landmarks. This is not as straightforward a problem as one might think because the results depend on how the configurations of landmarks are superimposed prior to the analysis. The generalized Procrustes superimposition can induce different amounts and patterns of variation at different landmarks. These need to be distinguished from differences due to biological reasons.

While studies using coordinates of 3-dimensional points are becoming standard in some fields, such as physical anthropology, they present more technical challenges. A distinct advantage of the use of 3-dimensional coordinates is that the definitions of landmark points are often much less arbitrary in three dimensions than they are in 2-dimensional projections. Some landmarks in 2-dimensional views do not actually exist as points on the object itself. Another problem is that the actual digitization of the coordinates requires more sophisticated (and hence expensive) instrumentation. That is one of the reasons that only a few studies in this volume are concerned with the analysis of 3-dimensional data. In addition to devices that record 3-dimensional coordinates, laser surface scanners, micro CT scanners, and MRI scanners make it possible to capture surfaces and volumes in three dimensions. Such data are likely to be much more informative that of configurations of points. Unfortunately, statistical methods for dealing with such additional data are still in their infancy. There are also great challenges in the development of methods for the effective visualization of shape variation for 3-dimensional data whether for points or more complicated data structures. The next few years we are likely to see very exciting new developments that should add even more power to morphometric studies in systematics.

The present volume represents an important step towards the goal. The editor, Ashraf Elewa, is to be commended for his efforts in producing this volume - I am looking forward to reading the papers.

Table of Contents

1 Introduction

Ashraf M. T. Elewa

Geology Department, Faculty of Science, Minia University, Egypt,
aelewa@link.net; aelewa@m-link.net

Since 1917, when Sir D'Arcy Wentworth Thompson published his celebrated book on growth and form, broader developments of morphometrics, theory and practice, have been brought into play.

As biologists and paleontologists are usually interested in the processes regulating shape over ontogeny and/or phylogeny, therefore, they need the different methods of morphometrics as tools for coherent quantitative reports that do not waste data.

The concept of "Multivariate Morphometrics" was introduced by Blackith and Reyment (1971), in which the authors made routine applications of standard methods of multivariate data analysis (canonical variate analysis, principal component analysis, and related methods) to standard measures on organisms – lengths, heights, breadths – in short, the usual distances measured between diagnostic features. The same general scope was maintained in the second edition (Reyment et al. 1984) in which the analysis of variation in shape as a distinct topic was awarded greater importance than in the first edition.

The principal component method, adapted for analyzing size and shape, that was originally proposed by Teissier in 1938, and its subsequent development in the hands of numerous workers, has been used now for more than 30 years; it has been accepted by statisticians and it is to be found in most texts on applied multivariate analysis as an established method, however, for the present purposes, it is usually not as informative as it could be because, in some cases, it is unsuitable for a reasonable quantification of change in shape.

In a very interesting review of the use of morphometrics in the field of phylogeny, Jensen (2003) noted that there has been resistance to the use of continuous characters in phylogenetic studies whether they are obtained from traditional or from geometric morphometric analyses. One reason is the arbitrariness of methods to reduce continuous characters to discrete states so they can be used in cladistic software. In addition, there are still many researchers using morphometric methods who have not yet made the step to the more powerful modern morphometric methods. Zelditch et al. (2000), Swiderski et al. (2002), and Bookstein (2002) have proposed methods to generate characters that can be used in cladistic studies. Some others used morphometrics for finding new, and sharpening the definition of old, character states (e.g. MacLeod 2002a, 2002b) and by the use of previously established phylogenies to aid in the interpretation of morphometric data (e.g. MacLeod 2001a; Rohlf 2002). However, Adams and

Rosenberg (1998) and Rohlf (1998) raise concerns about the former approaches. Bookstein (1994) notes some theoretical problems concerning the use of morphometric variables for such studies. It is worth noting that Jensen in his review has discussed the use of principal component analysis (PCA) for isolating size and shape as separate components. Based on the idea of isolating size and shape, Garcia-Rodriguez et al. (this volume) gave a good example for using sheared principal component analysis (SPCA) to differentiate between two populations of the blue spiny lobster *Panulirus inflatus* Street from NW Mexico.

Using multivariate data analysis techniques to analyze morphological data is not new, however, morphometrics received a considerable improvement in the 1990's as a result of the rapid development of freely distributed software supporting the quick and easy analysis of morphometric data (e.g., the SUNY Morphometrics Site: http://life.bio.sunysb.edu/morph/, the PaleoNet Pages FTP Site: http://www.nhm.ac.uk/hosted_sites/paleonet/ftp/ftp.html) as well as the increase of published articles on the subject (Bookstein 1986, 1991, 2002; Kendall 1986; Mardia and Dryden 1989; Goodall 1991; Rohlf 1993; MacLeod 1999).

Consequently, two edited volumes of papers on morphometrics have appeared in the last decade: Marcus et al. (1993) and Marcus et al. (1996). Both of these volumes were the results of international workshops basically devoted to teach systematists in the new, more geometric approach to morphometrics and edify them how to use available software packages. In fact, these two volumes were very successful. Both were split between review articles, articles introducing new methods, and applications articles. Actually, they drew their authorship from the rolls of the workshop participants and instructors. Certainly, I have a different type of collection in mind.

One problem with the two previous Marcus et al. compilations has to do with their focus. In both cases the main point of the volumes was to discuss and demonstrate some of the newer 'geometric' methods of morphometric data analysis that were the subjects of the courses. Traditional approaches to the analysis of such data (e.g. discriminant function analysis and Fourier analysis) were, for the most part, left out of these volumes. Even more importantly (1) the relations between the older and newer approaches to morphometric data analysis went largely unexplored (2) many of the applications contributions to these volumes run toward the 'me too' style of exposition and fail to come to grips with any meaningful or generalized research questions (other than that the techniques of geometric morphometrics can be applied to organism *x*). At this point in time in the field's development, a more up-to-date and careful treatment of the use of morphometric procedures in a wide variety of contexts is needed; one that provides answers to real-world questions for real-world systematists. MacLeod (2001b) represents the sort of comparative approach I feel would be useful in to both practitioners and theorists alike. Moreover, it is my belief that some of the newer methods of automated object recognition have the potential to cause yet another methodological revolution in this field. Preliminary descriptions and evaluations of exciting new developments in this area are included, notably in chapters contributed by Polly and Head, and by O. Hammer.

I deem I am so lucky to have, in this book, such group of contributors representing long-established workers as well as talented newcomers (e.g. N. MacLeod, P. D. Polly, I. Pavlinov, O. Hammer, H. D. Sheets, J. Kaandorp, M. Cavalcanti), and individuals with excellent national standing who have yet to come to the attention of international audiences. The chapters covered by these authors also show a convincing diversity ranging from micro-organisms to mammals and including such ever-popular subjects as trilobites, dinosaurs, birds, and human evolution.

According to Bookstein (1991), the way to learn morphometrics is to think closely and skeptically through dozens of applications, as varied as one can find. This is what I aimed at when I decided to edit this book. Subsequently, I focused my effort on collecting a quantity of papers that could show readers how to apply morphometrics to a wide range of living and fossil groups including vertebrates and invertebrates (both macro- and micro-organisms), using most of the known common morphometrics techniques from multivariate morphometrics (based on distance-measure) through relative warps and thin plate spline analyses to outline analysis of shape and others.

Following this advice, I arranged the book to look like an evolutionary story starting with invertebrates, micro-organisms, then, macro-organisms including trilobites. Followed by vertebrates including sharks, dinosaurs, birds, and guppies and ending with human evolution.

In general, three main goals were kept in mind during the preparation of this book:

1. To present new methods in the field of morphometrics that are relevant to the great revolution in this field. definitely, chapters (5, 6, 7, 14) written by Hammer, Sheets et al., Kaandorp and Garcia Leiva, and Polly and Head, respectively.
2. To attract a large audience by applications made to a very wide variety of organisms (invertebrates, both micro- and macro-organisms, and vertebrates).
3. The assembly of works of both biologists and paleontologists in the same book. This first step may encourage the specialists in these two sciences to start solving their taxonomic problems in a compatible manner, without contradictions in results between these two teams (a serious problem in taxonomy and systematics).

I hope that the book could be of great interest to both students and researchers, and would be very valuable to have something that presented the various aspects of the tools and their applications.

Finally, I would like to express my deep gratitude to all people who played an important role for the completion of this book. I, specifically, acknowledge, Prof. Norman MacLeod of the Department of Paleontology, the Natural History Museum Cromwell Road, London, UK and Prof. Richard Reyment of the Stockholm Natural History Museum, Sweden, for their unstinting help, valuable comments, and encouragement throughout the course of the editing process. I am deeply indebted to Prof. F. James Rohlf of the State University of New York, USA, for writing the preface as well as reviewing this introduction and two chapters for this book. Actually, without his help, guidance and advice this work could not be completed in this suitable form.

Of course, we cannot pay no heed to the reviewers of the chapters who are representing a famous group of experts in the field of morphometry: F. James Rohlf, R. Reyment, N. MacLeod, D. Polly, M. Corti, H. D. Sheets, R. Strauss, J. Kaandorp, O. Hammer, M. Cavalcanti, I. Pavlinov, E. Brouwers, J. Lynch, M. Plant, J. Stone, A. Russel, K. Schaefer, G. Cuenca, F. Korner-Nievergelt. All of them are deeply acknowledged for their efforts in reviewing the chapters of the book.

Thanks to all contributors for devoting their time in preparing their chapters for this book. Really, they did a very great work and without their contributions this project could not be completed.

A special word of thanks is due to the publishers of Springer-Verlag for their continuous help they offered during the several steps of editing this book. I also appreciate the great help of all members of the Minia University of Egypt.

References

Adams, DC, Rosenberg, MC, (1998) Partial warps, ontogeny and phylogeny: a comment on Zelditch and Fink (1995). Syst Biol. 47: 168-173

Blackith RE, Reyment RA (1971) Multivariate morphometrics. Academic Press, London, 412 pp

Bookstein FL (1986) Size and shape spaces for landmark data in two dimensions. Statistical Science 1: 181–242

Bookstein FL (1991) Morphometric tools for landmark data: geometry and biology. Cambridge University Press, Cambridge

Bookstein FL (1994) Can biometrical shape be a homologous character?. In: Hall B (ed) Homology: the hierarchical basis of comparative biology. Academic Press, San Diego, pp 197-227

Bookstein, F.L. (2002) Creases as morphometric characters. In: MacLeod N, Forey PL (eds) Morphology, shape and phylogeny. Taylor & Francis, London, pp 139–174

Goodall CR (1991) Procrustes methods in the statistical analysis of shape. Journal of the Royal Statistical Society, Series B 53: 285–339

Jensen RJ (2003) The conundrum of morphometrics. Taxon, pp 663-671

Kendall DG (1984) Shape manifolds, procrustean metrics and complex projective spaces. Bulletin of the London Mathematical Society 16: 81–121

MacLeod N (1999) Generalizing and extending the eigenshape method of shape visualization and analysis. Paleobiology 25 (1): 107–138

MacLeod N (2001a) The role of phylogeny in quantitative paleobiological analysis. Paleobiology 27: 226–241

MacLeod N (2001b) Landmarks, localization, and the use of morphometrics in phylogenetic analysis. In: Edgecombe G, Adrain J, Lieberman B (eds) Fossils, phylogeny, and form: an analytical approach. Kluwer Academic/Plenum, New York, pp 197–233

MacLeod N (2002a) Phylogenetic signals in morphometric data. In: MacLeod, Forey PL (eds) Morphology, shape and phylogeny. Taylor & Francis, London N, pp 100–138

MacLeod N (2002b) Geometric morphometrics and geological form-classification systems. Earth-Science Reviews 59 (2002): 27–47

Marcus L F, Bello E, García-Valdecasas A (1993) Contributions to morphometrics. Museo Nacional de Ciencias Naturales 8, Madrid

Marcus L F, Corti M, Loy A, Naylor GJP, Slice DE (1996) Advances in morphometrics. NATO ASI Series. Plenum Press, New York

Mardia KV, Dryden I (1989) The statistical analysis of shape data. Biometrika 76: 271–282

Reyment, RA, Blackith, RE, Campbell, NA (1984) Multivariate morphometrics. Second edition, Academic Press, London, 233 pp

Rohlf FJ (1993) Relative warp analysis and an example of its application to mosquito wings. In: Marcus LF, Bello E, García-Valdecasas A (eds) Contributions to Morphometrics. Museo Nacional de Ciencias Naturales 8, Madrid, pp 131–160

Rohlf FJ (1998) On applications of geometric morphometrics to studies of ontogeny and phylogeny. Syst Biol. 47: 147-158

Rohlf FJ (2002) Geometric morphometrics and phylogeny. In: MacLeod N, Forey PL (eds) Morphology, shape and phylogeny. Taylor & Francis, London, pp 175–193

Swiderski, DL, Zelditch, MI, Fink, WL (2002) Comparability, morphometrics and phylogenetic systematics. In: MacLeod, N, Forey PL (eds) Morphology, shape and phylogeny. Taylor & Francis, London, pp 67–99

Teissier G (1938) Un essai d'analyse factorielle. Les variants sexuels de *Maia squinada*. Biotypologie 7: 73-96

Zelditch, MI, Swiderski, DL, Fink, WL (2000) Discovery of phylogenetic characters in morphometric data. In: Wiens, J (ed) Phylogenetic analysis of morphometric data. Smithonian Institution Press, Washington, pp 37-83

2 Application of geometric morphometrics to the study of shape polymorphism in Eocene ostracodes from Egypt and Spain

Ashraf M. T. Elewa

Geology Department, Faculty of Science, Minia University, Egypt,
aelewa@link.net; aelewa@m-link.net

2.1 Abstract

Methods of geometric morphometrics applied to Eocene ostracodes from Wadi El Rayan, Eastern Desert, Egypt, and Aragon region, Spain, enable ostracode workers to define the size and shape variation in these ostracodes in the following manner. *Loxoconcha vetustopunctatella* Bassiouni, Boukhary, Shamah and Blondeau displays different shape parameters. The relative warps and thin-plate spline analyses led to recognizing five morphs (morph 1 to morph 5) within this ostracode species. The defined morphs could be arranged according to their degree of similarity to morph 1 (the typical morph), where morph 4 is the closest form to morph 1, followed by morph 5, morph 2 and morph 3, respectively. On the other hand, the analysis of three species of *Echinocythereis* (*E. isabenana* Oertli, *E. aragonensis* Oertli, *E. posterior* Oertli), using relative warps and thin-plate spline analyses, arrived at the same conclusions of Reyment (1985, 1988) in showing that the speciation events were accompanied by significant change in shape. However, the geometric morphometrics have the advantage over the techniques used by Reyment (1985, 1988) in identifying shape-patterns. Current results indicate that benefits can be expected to accrue from geometric morphometrics applied, as superior to any other relevant technique, to solve problems arising from polymorphism in not only ostracodes but also other crustaceans.

Keywords: Geometric morphometrics, shape polymorphism, Ostracoda, Eocene, Egypt, Spain.

2.2 Introduction

Morphometric methods are widely used in the fields of biology and paleontology due to their ability to describe the morphological variability exhibited by organisms. Fortunately, frequently updated computer programs for doing calculations of

morphometrics are available free of charge. Consequently, the account of classical and geometric morphometry in ostracodology has increased in the last decade.

The genus *Loxoconcha* Sars 1866 (type species: *Cythere rhomboidea* Fischer 1855) has a medium to large carapace with rhomboidal or ovate carapace that exhibits a compressed postero-ventral margin. Bassiouni et al. (1984) described their new species *Loxoconcha vetustopunctatella* as having a sub-quadrate carapace with straight dorsal margin, strongly convex ventral margin, rounded anterior margin and a caudal process at the posterior end. The carapace is ornamented by coarse central reticulation which gradually decreases in size towards the periphery. Scanning all the available specimens of *Loxoconcha vetustopunctatella* Bassiouni, Boukhary, Shamah and Blondeau of middle Eocene age, as well as the work of Reyment and Elewa (2002) suggested the strong possibility of this species being polymorphic with respect to shape.

Bassiouni et al. (1984), stated that they recognized specimens exhibiting transitional forms between *L. pseudopunctatella* and *L. vetustopunctatella*. Reyment and Elewa (2002) reported that *L.* vetustopunctatella shows tripartite subdivision of the shapes and interpreted this pattern phenomenon to be an example of polymorphism.

On the other hand, three species of the genus *Echinocythereis* Puri, 1954 (type species: *Cythereis garretti* Howe and McGuirt 1935) (*E. isabenana* Oertli, *E. aragonensis* Oertli, *E. posterior* Oertli) were subjected to geometric morphometrics analyses to assure the results of Reyment (1985, 1988), that were reported using traditional morphometrics before geometric morphometrics had been born, from one side, and to identify the shape variations in the *E. isabenana-E. aragonensis-E. posterior* lineage, from the other side. The *E. isabenana* has a relatively large carapace that, having a rounded tubercle ornamentation pattern, is the ancestor of the two other species. The *E. aragonensis* has a relatively small carapace with small lateral papillae, partly in contact, some of which are united by filaments. This species was originally erected at the subspecific level. The third species, *E. posterior*, has a relatively small carapace with a surface ornamented by pustules superimposed on a network of riblets forming a reticular pattern; this species was originally erected as a chronological subspecies. In summary, the difference between these three species is principally in size of carapace and ornamentation. The question arises, are there any shape variations within each of these three species? if yes, then a polymorphic phenomenon should exist. Reyment (1988) concluded that this phenomenon might be occurring within these species, using eigenshape analysis technique; however, he did not define the types of shape polymorphism of these species in his 1985 paper.

The idea that polymorphism in ostracodes can be described usefully through geometric morphometric analysis originated with Reyment (1993, 1995b) and Reyment and Elewa (2002). The aim of the present study is to analyze the available specimens of the considered species to document any shape-based relationships in the studied Egyptian *Loxoconcha* species, and within and/or between the studied Spanish *Echinocythereis* species.

2.3 Brief notes on morphometrics

The Hungarian artist Albrecht Dürer was the first, in the 16th century, who used a geometric technique. D'Arcy Wentworth Thompson followed the Dürer technique to devise a quasi-geometric device to express form changes as deformations. He called his diagrams Cartesian coordinate transformations, but nowhere in his original work of 1917, nor in the many subsequent reprints and revisions did he say how he had obtained them. Bookstein took up the subject and came to the same inescapable conclusion of Huxley (1932) that Thompson had merely produced his celebrated transformations by freehand and actually geometrically inaccurate (for more information on the subject see Reyment 1998).

Teissier (1938) introduced a more accessible approach which used the algebraic mode of analysis by principal components. Teissier's approach was inarguably more successful than Thompson's approach in that it was taken up by and used to analyze real biological data decades before anyone figured out how to use the deformation-grid approach in anything resembling a genuine mathematical analysis.

This idea was seized by Jolicoeur and Mosimann (1960) and became very popular in taxonomic studies. Later in 1963, Jolicoeur improved the principal components method by relating it to the allometric model. Hopkins (1966) then improved Jolicoeur's (1963) method of assessing multivariate allometry by means of a factor-analytical model for a reduced rank covariance matrix (see Reyment and Elewa 2002).

In 1971, Blackith and Reyment introduced the term multivariate morphometrics for the application of multivariate statistical analysis to the study of variation in the morphological characteristics of animals and plants. The emergence of a new era of multivariate morphometry, namely, geometric morphometry, was introduced by Bookstein (1989, 1991) with competing procedures (Reyment 1995).

Bookstein (1989, 1991, 1995) has developed a powerful geometric technique, which he terms the morphometric synthesis, for the analysis of within-population and between-population shape change, based on reference points (= landmarks). There are three types of landmarks that Bookstein recognized in 1991 and the concept has undergone substantial change since then (e.g., through the recent addition of the concept of semi-landmarks). Also, the concept of the landmark bears a subtle and interesting relation to the concept of homology. For more information about landmarks and morphometrics in general (see MacLeod 1999, 2001, 2002a, 2002b).

Landmarks contain essential information on size, shape, scaling and orientation. As a consequence, it is quite possible to restore aspects of the appearance of the measured object (the ostracode carapace herein) with respect to the points selected for study by plotting the coordinate pairs on graph paper, as it is figured hereafter (for more information see Reyment 1997).

Two main methods are common in the field of geometric morphometrics (Rohlf 1996). The first is named the superimposition method and is based on the least square method. It is most efficient if overall similarity depends on few landmarks. The second is the thin-plate spline method which works best when the similarity

depends on many landmarks, and therefore, just weekly localizable. This second method consists of fitting a thin-plate spline, an interpolating function, to the x and y coordinates of the landmarks located on each of N specimens in a sample. The variation among the specimens is described in terms of variance in the parameters of the fitted functions. This requires a reference configuration. The computations of the warps depend on this reference which is often the mean configuration of landmarks after some suitable alignment of specimens. The relative warps are the principal component vectors, they depict the main features of variation in shape among specimens as deformations (i.e. warps). In conclusion, the relative warp is only a pattern of proportionality among directed landmark displacements (see Reyment 1995).

2.4 Polymorphism in ostracodes

Ostracodes, like any other crustaceans, show evidence of polymorphism in their life-cycles. Generally, two kinds of ornamental variations are shown by ostracodes: ecophenotypic variation and genotypic variation. The first kind is often continuous and is under the control of various environmental factors such as temperature, depth, salinity and others (e.g. Reyment 1985, 1988). The second kind is discontinuous and involves co-occuring morphs without the presence of intermediate forms. However, this kind of polymorphism can be confounded by the superposition of ecophenotypic reactions (e.g. Reyment 1963, 1966).

The studied *Loxoconcha* and *Echinocythereis* species display a richness of polymorphism in both ornamental and shape characters. The ornamental and shape variations in *Loxoconcha* species are mainly: the type of reticulation, the shape of the carapace, the straight versus convex dorsal margin, and the straight versus convex postero-dorsal margin. The variations in *Echinocythereis* species belong to two main categories (shape and ornamental variations). The shape variations include: asymmetric as opposed to symmetric rounded anterior margin; concave versus straight or slightly convex postero-dorsal margin; underslung venter and concave dorsal margin; and a presumed polymorphism in the length of the posterior process. The ornamental variations include: the development of smooth lateral fields; the presence or absence of posterior spinosities (usually one central spine); the development of two to three rows of tubercles on the anterior zone; papillae are united to a greater or lesser extent by fine filaments; coalesced papillae; the development of sub-reticular ornament; the incomplete development of the anterior reticulations; and reticulate lateral ornament. There is a distinct possibility that environmental factors control the development of ornament of the studied lineage of *Echinocythereis* carapace in part. There seems to be a rather obvious relationship between the oscillatory regressive phase of the late Lutetian and the speciation event, on one hand, and the shift from papillation to reticulation, on the other. (see Reyment 1985 for more details).

As the analyses of the studied ostracode species are based on geometric morphometrics of landmarks, only the shape polymorphism will be considered throughout the course of the present study.

2.5 Materials and methods

The studied material is represented by seventeen specimens of the Egyptian *Loxoconcha* species, all of them identified as females, and thirteen Spanish *Echinocythereis* species (4 specimens of *E. isabenana*; 7 specimens of *E. aragonensis*; 2 specimens of *E. posterior*). The analysis was made on their left views of carapaces. With respect to occurrence, specimens of the Egyptian *Loxoconcha* species were collected by the author from the Midawara Formation (sandy marl to sandy shale facies) of Wadi El Rayan at the south of Fayoum area in the Western Desert of Egypt (Fig. 1; Table 1), for more information about the lithology of these sediments, see Elewa (1999). The material of the Spanish *Echinocythereis* species were provided to the author from Richard A. Reyment of the Museum of Natural Sciences of Sweden. This material was collected by geologists of the ELF Petroleum Company from the Rio Isabena section, Aragon, Spain, with a control sequence from the Rio Campo, some 60 km distant. The Rio Isabena section lies some 140 km northeast of Zaragoza (Fig. 2); the sequence begins near the Ypresian-Lutetian boundary (Eocene) and continues to late in the Lutetian, encompasses more than 1000 m of marine sediments, mainly marls, with occasional intercalations of sandstone (Table 1). For more information about the lithology and description of the three species, see Oertli (1960) and Reyment (1985, 1988).

Bassiouni et al. (1994) placed *Loxoconcha vetustopunctatella* as one of three typical species of the open platform environment, which Wilson (1975) described as a shallow water environment embracing open lagoons and bays behind the outer platform edge, where water circulation is moderate and salinity varies from normal marine to hypersaline. On the other hand, it is necessary to be aware of the possibility that quite marked differences in ornamental patterns can be caused by a deficiency or a surplus of calcium ions during molting and secreting a new shell (McKenzie and Peypouquet 1984).

Six landmarks, considered to be diagnostic, were selected on each carapace for analysis of *Loxoconcha vetustopunctatella* (Fig. 3); these are located at four points on the circumference of the left shell (nos. 1, 4, 5, 6), as well as one at the eye-tubercle (no. 2) and one at the adductorial site (no. 3). The last two are first-order landmarks, being located at fix-points on the shell. The other four are located at

Table 1. Biostratigraphical data for the occurrence of the studied species from Egypt and Spain

Country	Egypt	Spain
Age	Middle Eocene (Lutetian)	Middle Eocene (Lutetian)
Species	*Loxoconcha vetustopunctatella* Bassiouni et al.	*Echinocythereis posterior* Oertli (younger); *Echinocythereis aragonensis* Oertli; *Echinocythereis isabenana* Oertli (older)
Sections and lithology	Wadi El Rayan (Fayoum area, Western Desert); sandy marl to sandy shale facies	The Rio Isabena and Rio Campo sections, Aragon region, northern Spain; marl with occasional intercalations of sandstone facies

points of inflexion as follows: one at the mid-point of the anterior margin (no. 1), one at the contact between the dorsal and posterior margins (no. 4), one at the maximum end of the posterior margin (no. 5) and one at the mid-point of the ventral margin (no. 6). For the *Echinocythereis* species, seven landmarks are considered to be diagnostic as follows (Fig. 4). One at the mid-point of the anterior margin (no. 1), one at the eye-tubercle (no. 2), one at the contact between the dorsal and posterior margins (no. 3), one at the maximum end of the posterior margin (no. 4), one at the contact between the ventral and posterior margins (no. 5), one at the contact of the anterior zone with the ventral margin (no. 6) and one at the adductorial site (no. 7). Landmarks 2, 7 are first-order landmarks, while the others located at points of inflexion. In the original sense of the term "landmarks", were supposed to be located at homologous sites on the organism, however, it has been found useful to expand this concept so as to encompass "pseudolandmarks" which are located at mid-points of rounding of the outline of the organism.

All of these landmarks were digitized on the basis of SEM photographs and sketches of outlines using a computer program made by F. J. Rohlf (1998a), and then, subjected to relative warps and thin-plate spline analyses. The Egyptian and Spanish materials are treated separately from each other.

The programs used for the thin-plate spline and relative warps analyses were written by F. J. Rohlf (1997, 1998b), versions 1.15 and 1.20, respectively.

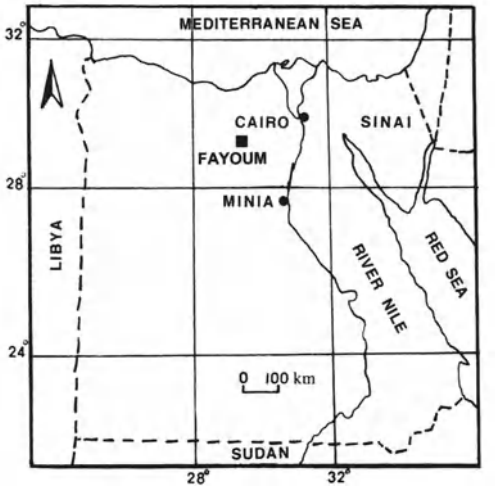

Fig. 1. Location map of Egypt. Black square represents location of the area from which specimens of the studied species were collected

Fig. 2. Location map of Spain. Black square represents location of the area from which specimens of the studied species were collected

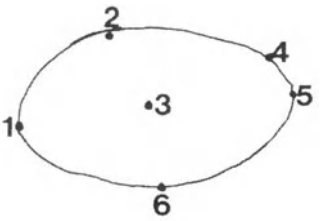

Fig. 3. Sketch showing the locations of the six landmarks (after Reyment and Elewa 2002) on the carapace of *Loxoconcha vetustopunctatella* Bassiouni et al. Figure based on morph 3

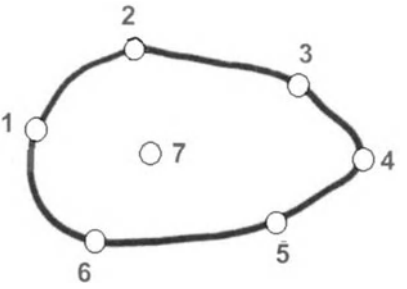

Fig. 4. Sketch showing the locations of the seven landmarks on the carapace of *Echinocythereis* species. Figure based on *E. isabenana*

2.6 Results

2.6.1 The Egyptian material

First, to examine the normal distribution within the selected specimens for this study, the Q-Q probability plot for the distance from landmarks is given (Fig. 5). This figure indicates that the selected specimens show no important outliers, and thus, are of normal distribution.

Non-affine shape differentiation in the studied species

The ordination for the 1st and 2nd warps (Fig. 6) is the representation of the non-affine (= non uniform) shape variation. The first singular value for these data constitutes more than 33% of the variance, the second one comprises more than 27% of the variance, therefore, more than 61% of the variance is included within the first two relative warps (Table 2). This is sufficient for interpreting the major as-

pects of shape variation within the studied material. Figure 6 shows a plot of the 1st vs. 2nd relative warp scores and indicates that the 1st and 2nd relative warps have a tendency to separate the studied specimens into five groups. Group 1 with sub-quadrate, pointed posterior shape (no. 1 in the graph), this form represents the typical shape of the studied species with short caudal process at the posterior end. Group 2 with sub-rectangular, rounded posterior shape (nos. 7, 8). Group 3 with

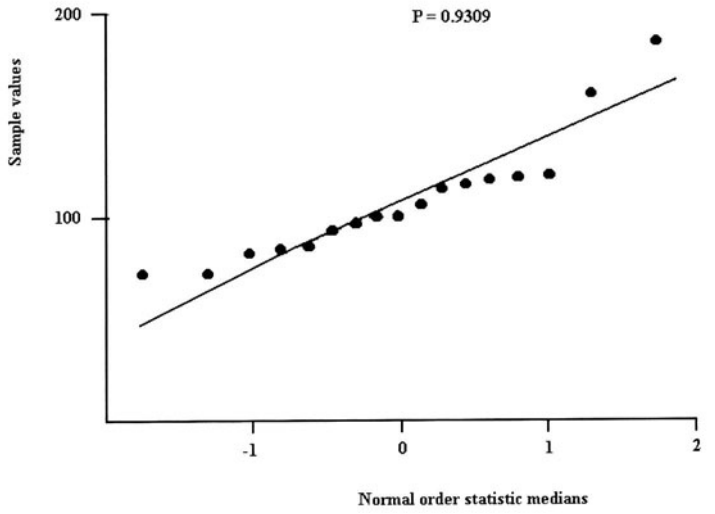

Fig. 5. Q-Q probability plot for the distance from all landmarks of the studied *Loxoconcha* specimens

sub-rectangular, pointed posterior shape (nos. 2, 3, 4, 5, 6, 9, 10, 11, 12, 14). Group 4 with sub-ovoid, pointed posterior shape (no. 13). Group 5 with sub-ovoid, rounded posterior shape (nos. 15, 16). The ordination yielded by this analysis produces a certain degree of morphological variation which suggests polymorphism to be present, however, more available specimens is insistent to hold these results to the species as a whole.

Table 2. Summary of relative warps analysis for *Loxoconcha vetustopunctatella*

Components	Eigenvalues	% variance
1	0.134	33.74
2	0.121	27.44

Affine (= uniform) shape differentiation in the studied species

The representation of the 1st vs. 2nd uniform axes is given in Figure 7. This figure indicates that the 1st relative warp has a tendency to separate specimens with straight postero-dorsal margin (right; like nos. 3, 10, 13, 16) from those with convex postero-dorsal margin (left; like nos. 1, 2, 4, 15), while the 2nd relative warp separates specimens with convex dorsal margin (the upper section of the graph; like nos. 2, 3, 4, 16) from those with straight dorsal margin (the lower section; like

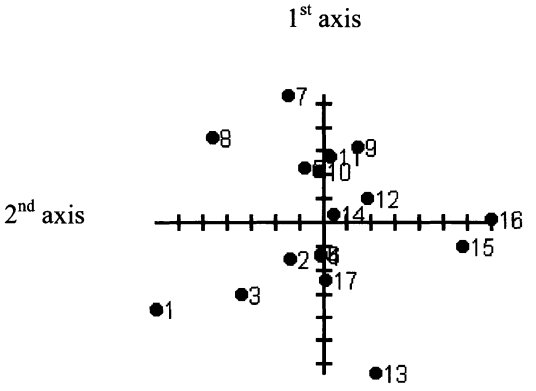

Fig. 6. Ordination by the non-affine shape components for the studied species

nos. 6, 7, 16). It can be concluded that the uniform projection provides additional information about the shape of the studied specimens, specifically the dorsal margin, but could not discriminate between the groups obtained by the non-uniform ordination.

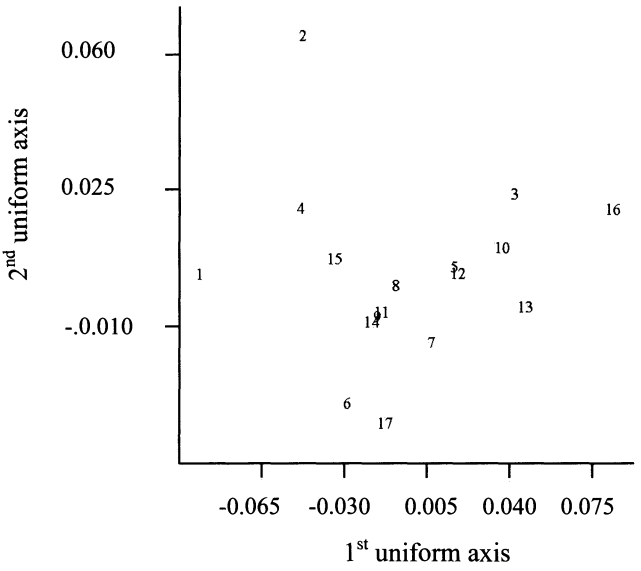

Fig. 7. Ordination by the affine (uniform) shape components for the studied species

Thin-plate spline comparisons for typical specimens of the recognized morphs

The thin-plate spline is a tool for doing the comparison of two average shapes proceeds by the fit of one image to the other with the landmarks forming the points that must correspond. It provides the mathematical approach for doing the fit but without any intrinsic biological significance, however, it does permit a realistic partitioning of shape variation into categories of specific biological interest on an increasingly more local level, a case similar to using the scanning electron microscope for increasing the magnification of an organism. At the lowest magnification the whole shell is visible, with higher magnification, more local features appear.

The graphical representations of mapping from one shape to another are given in the next step to find out the relationships between the recognized morphs. Left view of five females of the five recognized morphs (one specimen for each) were considered as typical (reference) specimens for the thin-plate spline analysis. Figure 8 portrays the mapping of the non-affine case of morph 1 into morph 2. The deformation is strong and the bending energy (an expression borrowed from the mechanics of thin metal plates; it is the energy required to bend the metal plate, therefore, the landmarks change their position appropriately) is 0.07012. The postero-dorsal zone (the caudal process area) is more affected than any other side. Weak dilatation towards the posterior margin and strong dorsal and ventral

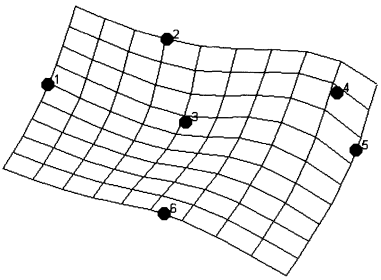

Fig. 8. The non-affine deformation for the comparison between typical specimens of morph 1 and morph 2

compressions are detected. Figure 9 displays the warp of morph 1 into morph 3. The bending energy is 0.07973 and the effect is greater than the previous case. The figure shows that the postero-dorsal margin is more affected than other sides. There are also strong dorsal and ventral compressions. From Figure 10, showing the warp of morph 1 into morph 4, it is clear that the deformation is relatively weak with bending energy equal 0.05824. The ventral zone is more affected than other sides. Figure 11 shows the warp of morph 1 into morph 5. It is obvious that the deformation is greater than the previous case with bending energy equal 0.06570.

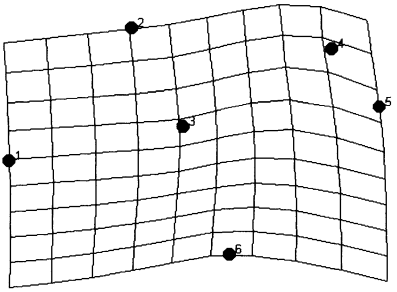

Fig. 9. The non-affine deformation for the comparison between typical specimens of morph 1 and morph 3

The deformation is strong at the ventral margin. In conclusion, morph 4 is the closest form to morph 1, followed by morph 5, morph 2 and morph 3, respectively. Photomicrographs of some representatives of the studied forms are shown in Fig. 12.

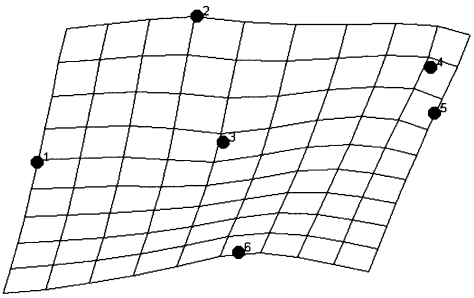

Fig. 10. The non-affine deformation for the comparison between typical specimens of morph 1 and morph 4

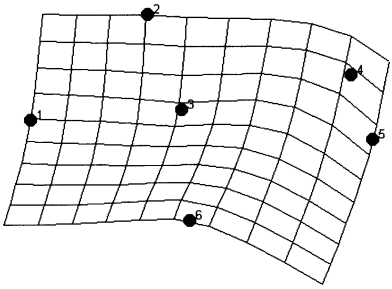

Fig. 11. The non-affine deformation for the comparison between typical specimens of morph 1 and morph 5

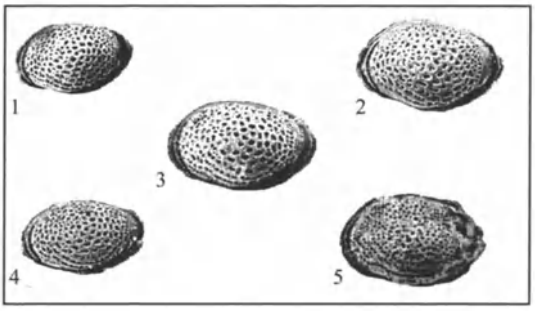

Fig. 12. Figures of some representatives of the studied forms of *Loxoconcha vetustopunctatella* Bassiouni et al. (x 200). 1, 3, 4 (morph 3); 5 (morph 5)

2.6.2 The Spanish material

The Q-Q probability plot for the distance from all landmarks (Fig. 13). shows no distinct outliers which indicate a normal distribution of the selected specimens.

Non-affine shape differentiation in the studied species

The scores for the non-affine projection show that the 1st warp score constitutes about 51% of the variance, the second one comprises more than 21% of the variance, thus, more than 72% of the variance is included within the first two relative warps (Table 3). These are suitable for interpreting the shape variation within the studied *Echinocythereis* species. From Figure 14, showing the plot of 1st and 2nd non-affine warp scores, the 1st relative warp axis seems to separate between the forms having a concave postero-dorsal margin (left; nos. 1, 2, 3, 4, 5, 6, 9), from the specimens having straight to slightly convex postero-dorsal margin (right; nos. 7, 8, 10, 11, 12, 13). The concave postero-dorsal margin as opposed to a straight, or slightly convex, margin is an example of shape polymorphism (type 2) that was introduced by Reyment (1985) for the genus *Echinocythereis*. He mentioned that this variation is found throughout the entire sequence at about the same frequency

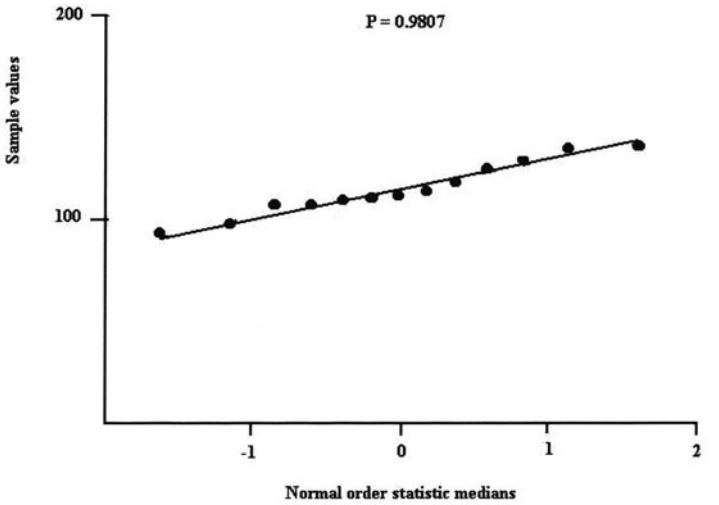

Fig. 13. Q-Q probability plot for the distance from all landmarks of the studied *Echinocythereis* specimens

Table 3. Summary of relative warps analysis for the studied *Echinocythereis* species

Components	Eigenvalues	% variance
1	0.146	50.93
2	0.095	21.64

and is, consequently, not of particular evolutionary significance. The same figure indicates that the 2nd relative warp axis have a tendency to separate the specimens with regularly rounded anterior margin (lower section; nos. 4, 6, 7, 8, 12, 13) from those with asymmetrically rounded anterior (upper section; nos. 1, 2, 3, 5, 9, 10, 11).The swung rounded anterior as opposed to a regularly rounded anterior margin is another example of shape polymorphism (type 1) of Reyment (1985). This type of polymorphism occurs throughout the entire observed sequence and is, therefore, not involved in the evolutionary changes. It is clear that the two types of polymorphism that was observed using the non-affine projection have no evolutionary significance, and thus, are not involved in speciation events.

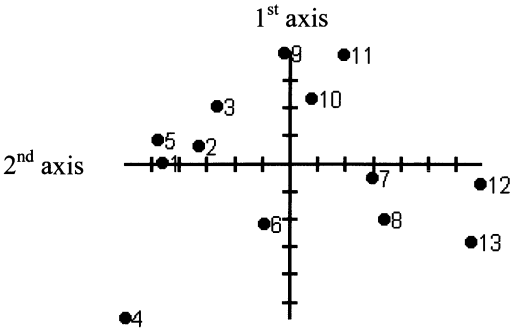

Fig. 14. Ordination by the non-affine shape components for the studied species

Affine (= uniform) shape differentiation in the studied species

In the next step, the uniform relative warps analysis was applied to the same data and the representation of the 1st vs. 2nd uniform axes is given (Fig. 15). Figure 15 indicates that the 1st relative warp axis shows the polymodality in the length of the posterior process with increased values at the right section of the graph (nos. 1, 2, 5, 10) and decreased at the left (nos. 3, 4, 7, 13). The genetic background of this polymorphism is not clear (type 5 of Reyment 1985). The 2nd relative warp axis separates the specimens with concave dorsal margin (the upper section of the graph; nos. 6, 10, 11, 13) from those with straight to convex dorsal margin (in the lower section; nos. 2, 3, 4, 9) (type 4 of Reyment 1985).

Reyment (1985) stated that this variant appears about halfway throughout the range of *E. aragonensis*, but does not become relatively common until the range of *E. posterior*, this seems to be an evolutionary conditioned feature. However, specimen no. 13, in Figure 15, is identified as *E. posterior* and exhibits a concave dorsal margin (see Fig. 20). It can be concluded that the uniform projection provides additional information about the shape of morphs within the studied material.

Thin-plate spline comparisons for selected specimens from the three species

The left view of five specimens of the *Echinocythereis* species (one specimen for *E. isabenana*; tow specimens from the earliest and late *E. aragonensis*; and two specimens of *E. posterior*) were considered as typical (reference) specimens for the thin-plate spline analysis. Figure 16 portrays the mapping of the non-affine case of *E. isabenana* (no. 1; Fig. 20) into *E. aragonensis* (no. 8; Fig. 20). The bending energy is 0.03012 and the anterior margin is more effected than any other side. This could be the shape polymorphism (type 1) of Reyment (1985).

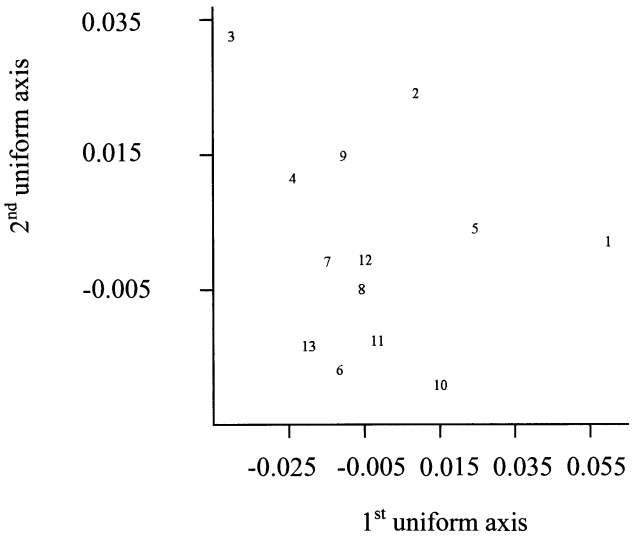

Fig. 15. Ordination by the affine (uniform) shape components for the studied *Echinocythereis* species

Figure 17, showing the warp of *E. isabenana* (no. 1; Fig. 20) into the early *E. posterior* (no. 13; Fig. 20), clarifies that the deformation is relatively strong with bending energy equal 0.04202. The anterior and posterior zones are more affected than other sides (types 1, 2 of Reyment 1985).

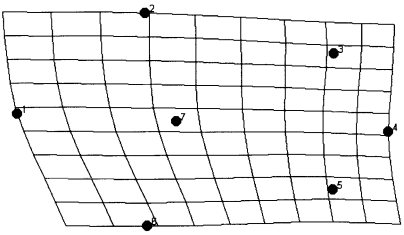

Fig. 16. The non-affine deformation for the comparison between typical specimens of *Echinocythereis isabenana* (no. 1 in Fig. 20) and the late *E. aragonensis* (no. 8 in Fig. 20)

In order to decide whether the polymorphism (type 3) is not common at the higher levels above the *E. aragonensis*, and consequently, is significant for speciation, according to Reyment (1985), the mapping of the earliest *E. aragonensis* (no. 7; Fig. 20) into the early *E. posterior* (no. 12; Fig. 20) is shown (Fig. 18). It is obvious that the deformation has a bending energy equal to 0.02200, and is greater at the dorsal margin than other sides (type 4). Figure 19 shows the mapping of the late *E. aragonensis* (no. 8; Fig. 20) into the early *E. posterior* (no. 12; Fig. 20), and indicates a weak deformation with bending energy equal 0.01507. The deformation is relatively greater at the ventral margin (type 3). The last figure suggests that the ventral margin is relatively affected (underslung venter), therefore, the type 3 of Reyment could be common in the transition from *E. aragonensis* into *E.*

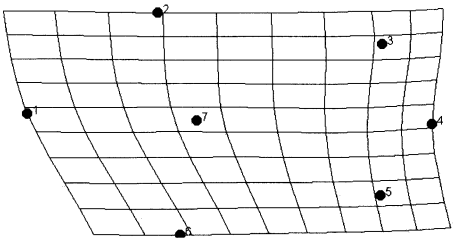

Fig. 17. The non-affine deformation for the comparison between typical specimens of *Echinocythereis isabenana* (no. 1 in Fig. 20) and the early *E. posterior* (no. 13 in Fig. 20)

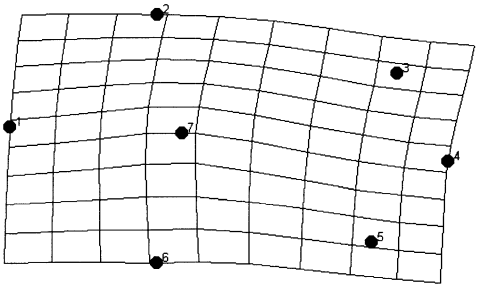

Fig. 18. The non-affine deformation for the comparison between typical specimens of the late *Echinocythereis aragonensis* (no. 7 in Fig. 20) and the early *E. posterior* (no. 12 in Fig. 20)

posterior, and has no evolutionary significance. Outlines of the thirteen *Echinocythereis* specimens are shown in Figure 20 with their stratigraphical levels.

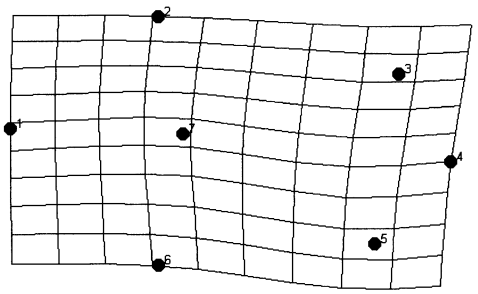

Fig. 19. The non-affine deformation for the comparison between typical specimens of the late *Echinocythereis aragonensis* (no. 8 in Fig. 20) and the early *E. posterior* (no. 12 in Fig. 20)

2.7 Conclusions

It is possible to tie together the various lines of argument used in interpreting the results from the geometric morphometric analysis of shape variation within the forms of *Loxoconcha vetustopunctatella*, and the shape variation within and between the studied transition of *E. isabenana-E. aragonensis-E. posterior.*

Loxoconcha vetustopunctatella seems to be an endemic Egyptian species and has been shown to encompass a range of morphometrical variability. My study of this species did not focus on the ornamental variability, which was discussed in detail by Bassiouni et al. (1984). However, geometric morphometrics did provide good results with respect to shape variability.

The analysis of this Egyptian species revealed the distinction of morphs to be existing within the studied specimens, with different shape characteristics. This type of shape variation belongs to the environmentally cued polymorphism that results under the control of environmental factors. It seems that the occurring polymorphism within this species could be related to deficiency or a superfluity of calcium ions during molting and secreting a new shell as a result of changes in degrees of water salinity in the study area.

On the other hand, the three Spanish species of the genus *Echinocythereis* could clarify the advantage of using geometric morphometrics on ostracode carapaces for solving problems arising from the variability in shape resulting from polymorphism which is a common phenomenon in ostracodes as well as other crustaceans.

The results support the idea of Reyment (1985) attributing the evolution in the *Echinocythereis* lineage to two different mechanisms. The transition of *E. isabenana- E. aragonensis* was rapid, with many disjunct features, as it is clear from the thin-plate spline projections (Figs. 16-21). The second transition (*E. aragonensis-E. posterior*) was slow and the variations are more of degree than of kind.

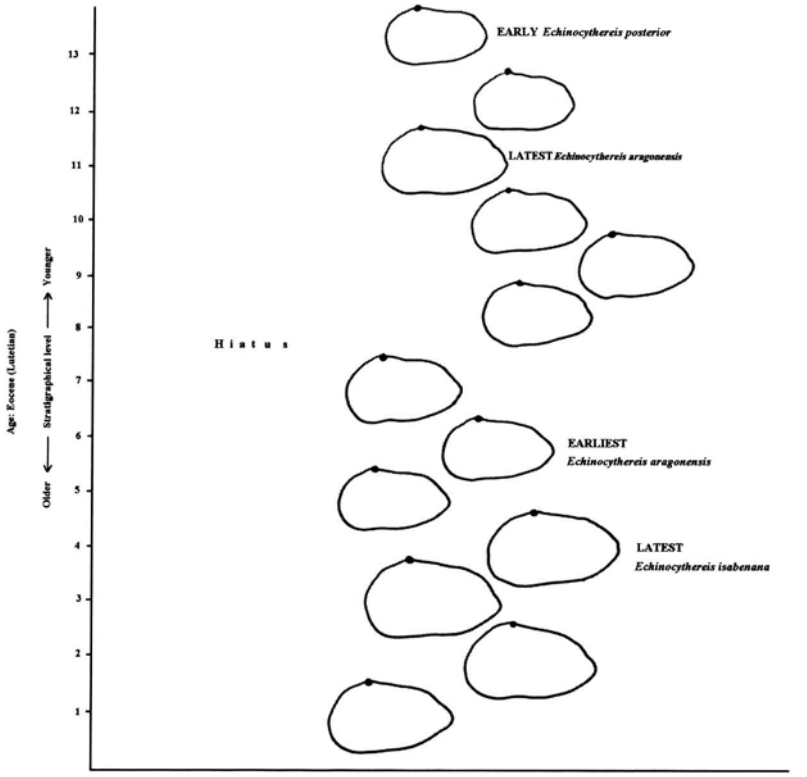

Fig. 20. Figures of the outlines of the studied *Echinocythereis* species with their stratigraphical levels (after Reyment 1988)

The advantage of using geometric morphometrics in this example is that the types of shape polymorphism that were previously recognized under the microscope are discriminated and, more important, the relationship between these shape variations are established. In contrast, the traditional morphometrics could only give a general conclusion stating that the speciation events were accompanied by a reduction in size and significant shifts in shape. However, these techniques provided me with a preliminary strategy when I started working on this material.

It is worth mentioning that the two examples studied could successfully achieve the usefulness of geometric morphometrics in discriminating shape variation (shape polymorphism) in a manner that is superior to any other techniques. The idea is not to speak about population (this needs more sample size) but the efficiency of the modern approach (geometric morphometrics) in a better way than classical techniques (traditional morphometrics) do.

2.8 Acknowledgements

I would like to express my deep gratitude to Prof. R. A. Reyment of the Swedish Natural History Museum, for his kind help throughout the course of the present study, critical reading of the manuscript as well as providing me with the Spanish material. I am much indebted to Prof. N. MacLeod of the Department of Paleontology, the Natural History Museum Cromwell Road, London, UK, and Prof. E. Brouwers of the US Geological Survey, USA, for their kind help, valuable comments, as well as critical reviewing of the manuscript.

References

Bassiouni MA, Boukhary MA, Shamah K, Blondeau A (1984) Middle Eocene ostracodes from Fayoum, Egypt. Geologie Méditerranéenne 11(2): 181-192

Bassiouni MA, Hamza FH, Morsi AM (1994) Ostracode and microfacies study of the Eocene sequence in the northwestern part of the Eastern Desert, Egypt. Revue de Paléobiologie 13(1): 259-280

Blackith RE, Reyment RA (1971) Multivariate morphometrics. Academic Press, London, 412 pp

Bookstein FL (1989) Principal warps: thin-plate spline and the decomposition of deformations. I.E.E.E. Transactions on Pattern Analysis and Machine Intelligence 11: 567-585

Bookstein FL (1991) Morphometric tools for landmark data: geometry and biology. Cambridge University Press, New York, 435 pp

Bookstein FL (1995) The morphometric synthesis for landmarks and edge-elements in images. Terra Nova 7: 393-407

Elewa AMT (1999) The use of allochthonus microfossils in determining paleoenvironments: A case study using Middle Eocene ostracodes from Wadi El Rayan, Fayoum, Egypt. Bulletin of Faculty of Science, Assiut University, 28 (2): 33-52.

Hopkins JW (1966) Some considerations in multivariate morphometry. Biometrics 22: 747-760

Huxely J (1932) Problems of relative growth. London: Methuen (2.1, 2.3, 3.2, 7.4.2).

Jolicoeur, P (1963) The multivariate generalization of the allometry equation. Biometrics 19: 497-499

Jolicoeur P, Mosimann JE (1960) Size and shape variation in the Painted Turtle, a principal component analysis. Growth 24: 339-354

MacLeod N (1999) Generalizing and extending the eigenshape method of shape visualization and analysis. Paleobiology 25(1): 107–138

MacLeod N (2001) Landmarks, localizability, and the use of morphometrics in phylogenetic analysis. In: Edgecombe G, Adrain J, Lieberman B (eds) Fossils, phylogeny, and form, an analytical approach. Kluwer Academic/Plenum, New York, 197–233

MacLeod N (2002a) Morphometrics. In: Pagel MD (ed) Encyclopedia of Evolution, Academic Press, London, 768–771

MacLeod N (2002b) Phylogenetic signals in morphometric data. In: MacLeod N, Forey PL (eds) Morphology, shape and phylogeny. Taylor and Francis, London, 100–138

Mckenzie KG, Peypouquet JP (1984) Oceanic paleoenvironment of the Miocene Fyansford Formation from Fossil Beach near Mornington, Victoria, interpreted on the basis of Ostracoda, Alcheringa 8: 291-303

Oertli H (1960) Evolution d'une espèce d'*Echinocythereis* dans le Lutètien du Rio Isabena (Prov. Huesca, Espagne). Rev Micropaléont 3: 157-166

Reyment RA (1963) Studies in Nigerian Upper Cretaceous and Lower Tertiary Ostracoda. Part 2: Danian, Paleocene and Eocene Ostracoda. Stockh Contr Geol 10: 1-286

Reyment R. A. (1966) Studies in Nigerian Upper Cretaceous and Lower Tertiary Ostracoda. Part 3: Stratigraphical, paleoecological and biometrical conclusions. Ibid 14: 1-151

Reyment RA (1985) Phenotypic evolution in a lineage of the Eocene ostracod *Echinocythereis*. Paleobiology 11(2): 174-194

Reyment RA (1988) Evolutionary significant polymorphism in marine ostracods. In: Hanai T, Ikeya N, Ishizaki K (eds) Evolutionary biology of Ostracoda (its fundamentals and applications). Proc 9th Internat Sympos Ostracoda: 987-1001, Shizuoka

Reyment RA (1993) Ornamental and shape variation in *Hemicytherura fulva* McKenzie, Reyment, Reyment (Ostracoda; Eocene, Australia). Revista Española de Paleontologia 8(2): 125-131

Reyment RA (1995a) On multivariate morphometrics applied to Ostracoda. In: Ostracoda and Biostratigraphy, Proc. 12th Intnl. Symp. on Ostracoda, Prague (1994), 203-213. Balkema, Rotterdam

Reyment RA (1995b) Analysis of geographic shape-variation in *Vargula hilgendorfii* (Ostracoda, Crustacea). Revista Española de Paleontologia. Homenaje al Dr. Guillermo Colom: 26-30

Reyment RA (1997) Evolution of shape in Oligocene and Miocene *Notocarinovalva* (Ostracoda, Crustacea): A multivariate statistical study. Bulletin of Mathematical Biology 59(1): 63-87

Reyment, RA (1998) Book review: Morphometric tools for landmark data (geometry and biology) by FL Bookstein. Palaeogeogr Palaeoclimat Palaeoecol 141 (1998): 171-173

Reyment RA, Elewa AMT (2002) Size and shape variation in Egyptian Eocene *Loxoconcha* (Ostracoda) studied by morphometric methods. In: Thiergärtner H (ed) Mathematical methods and data bank application in paleontology, Mathematische Geologie 6: 3-14, CPress Verlag, Germany

Rohlf FJ (1996) Morphometric spaces, shape components and the effect of linear transformations. In: Marcus L., Corti M., Loy A., Slice D. (eds) Advances in morphometrics. N.Y.; L.: Plenum Press, 131-152

Rohlf FJ (1997) TPSsplin: thin-plate spline, version 1.15. New York, State Univ. at Stony Brook. (program)

Rohlf FJ (1998a) TPSdig, version 1.20. New York, State Univ. at Stony Brook. (program)

Rohlf FJ (1998b) TPSrelw: relative warps, version 1.20. New York: State Univ. at Stony Brook. (program)

Teissier G (1938) Un essai d'analyse factorielle. Les variants sexuels de *Maia squinada*. Biotypologie 7: 73-96

Thompson DW (1942) On Growth and Form. Second edition of 1917 publication, Cambridge University Press, Cambridge, 1116 pp

Wilson JJ (1975) Carbonate facies in geologic history. Springer, Berlin, 471 pp

3 Morphometric analysis of population differentiation and sexual dimorphism in the blue spiny lobster *Panulirus inflatus* (Bouvier 1895) from NW Mexico

Francisco Javier García-Rodríguez[1], José de la Cruz Agüero[2], Ricardo Pérez-Enriquez[1] and Norman MacLeod[3]

[1]Centro de Investigaciones Biológicas del Noroeste. Mar Bermejo No. 195, Col. Playa Palo de Santa Rita, La Paz, B.C.S. 23090, México, fjgrodri04@cibnor.mx;
[2]Centro Interdisciplinario de Ciencias Marinas-IPN, La Paz, 23090, México;
[3]Natural History Museum, London, Cromwell Road, London, SW7 5BD, UK.

3.1 Abstract

Population differences based on a morphometric analysis were studied in blue spiny lobster *Panulirus inflatus* (Bouvier 1895) from the Pacific coast of Mexico. Seventeen morphometric distances defined by eight landmarks were recorded for 129 specimens and Sheared PCA (SPCA) and Burnaby size-adjusted principal component analysis were performed. Sexual dimorphism was detected in each locality by analysis of covariance (ANCOVA), so comparison between localities were separately performed by sex. Males and females showed some geographic differences, however, the results indicate a low differentiation level. Morphometric differences between populations can be due to plasticity in response to local environmental conditions, but further analysis should to considered to a better understanding of stock structure of blue spiny lobster.

Keywords: *Panulirus*, lobster, Mexican Pacific, morphometric analysis, sheared principal components analysis, truss, distance measures, sexual dimorphism.

3.2 Introduction

The spiny lobster's fishery is a important economic activity in the northwest coast of Mexico. Lobster commercial exploitation has been known since the end of the 19th Century, however management regulations by Mexican government did not begin until 1930. The actual annual catch in the Mexican Pacific coast is approxi-

mately 1,800 tons (Vega-Velázquez et al. 1996; Perez-González et al. 2002) and it is composed of three species: the red spiny lobster *Panulirus interruptus* Randall 1840; the blue spiny lobster *P. inflatus* (Bouvier 1895), and the green spiny lobster *P. gracilis* Streets 1871. *Panulirus interruptus* is the most temperate species, with a distributional range from California, USA, to Baja California Sur (BCS), Mexico, including some areas in Gulf of California (Hendrickx 1995). *Panulirus inflatus and P. gracilis* inhabit subtropical and tropical waters, from Bahía Magdalena, (BCS), to Oaxaca, Mexico, throughout the Gulf of California. Annual landings for these species in Mexico are estimated to be around 500-650 tons (Perez-González et al. 2002).

Several studies have been conducted on *Panulirus* spp. in the NW Mexico, mainly focused on optimization of the regulatory mechanisms of their fisheries, better understand environmental influences on the catches, document larval recruitment (Phillips and Booth 1994), or further develop fishery biology data (Ayala 1983; Briones and Lozano 1992; Pérez-Gonzalez et al. 1992, Pérez-González y Ortega Salas 1992). However, the relationships between disjunct populations along the Mexican coast have been scarcely studied (*e.g.* Perez-Enriquez et al. 2001).

The main purpose of this study was to compare morphologically the carapace of *P. inflatus* sampled from separate locations of NW Mexico. Morphometric differences within related populations could be linked to local adaptation to habitat conditions due to a high degree of phenotypic plasticity (Doadrio et al. 2002), or may indicate the presence of genetic stock structuring due to well-differentiated phenotypes that have been isolated long enough to warrant a taxonomic reappraisal.

Biological identification at any taxonomic category or fishery stock level ("individuals within a population with a spatial and temporal integrity to consider them as self-perpetuating units", *sensu* Pawson 1995) is the first step in determining the status of the resources and for developing a rational fishery management (Skillman 1989). There are several examples showing that, when the stock composition and boundaries are unclear, effective management of fisheries resources has been hampered (see: Austin et al. 1998). Actually, the main regulations in the lobster fishery along the Mexican coast include a closed season, a minimum legal size, prohibition of catching egg-bearing females, and controlling the fishing effort. However, the tropical lobster fisheries in Mexico show considerable annual and decadal scale variations in landings (Pérez-González et al. 2002).

In this study we used multivariate morphometry based on distance data, which has been shown previously to be an informative tool to assess distinctness between closely related taxa (Corti et al. 1981; Creech 1992; Elliot et al. 1995; Eisenhour et al. 1997; Lourie et al. 1998). Morphometric methodology permits quantification of differences of variations in size and body shape among organisms based on corresponding anatomical features. Also, distance-based methods permit the partitioning of allometric from non-allometric variation, in terms of Huxley's log-linear model of allometry. Particularly, multivariate morphometrics has been applied to study the intra-population variations in several lobster species (Harding et al. 1993; Cadrin 1995; Castro et al. 1998; Debuse et al 2001) and in general in fishery

researches (Krause et al. 1994; Tzeng et al. 2001). On the other hand, landmark-based geometric morphometric methods (procrustes analysis and warp analyses; e.g. Bookstein 1991) that emphasize the analysis of geometry of morphological structures could be applied, to an appropiate lobster's data set, to generate a graphical representation of the shape. This will be our intend in the future research.

3.3 Material and methods

The lobsters used in this study were caught from localities in NW Mexico, between September 2002 and January 2003 (Fig. 1). Specimens from the Pacific coast of the Baja California Peninsula (BCP) were obtained from commercial fishery landings using conventional lobster traps from Bahia Magdalena. Specimens from mainland's coast of the Gulf of California (MGC) were fished using tangle nets and skin diving and hooking, as usually captured by fishermen in that area, at Mazatlan.

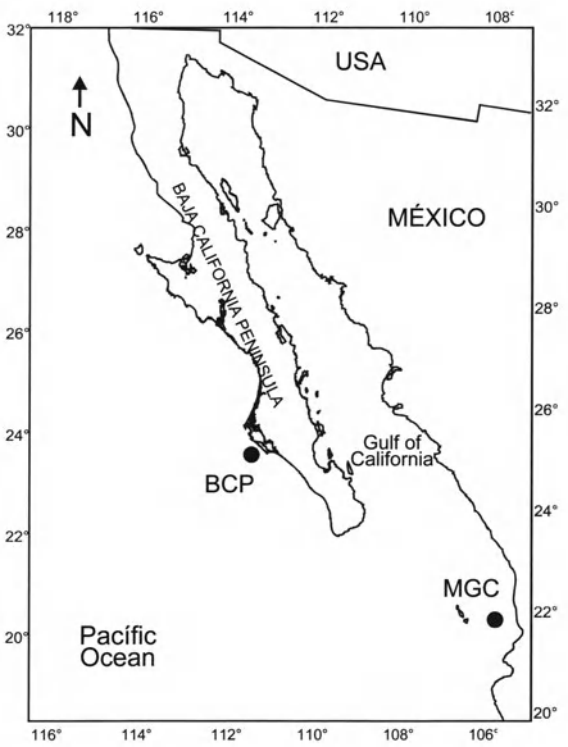

Fig. 1. Map of northwest Mexico. Lobster collection sites are represented by black circles

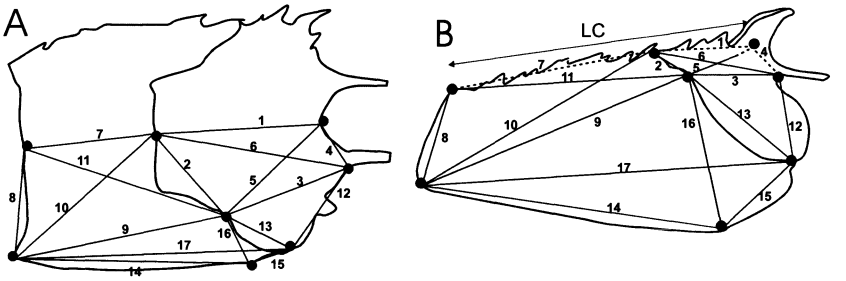

Fig. 2. Dorsal (A) and lateral (B) view of carapace of *Panulirus inflatus* and landmarks taken. Dots and asscociated number indicate the landmarks used and morphometric distances produced, respectively

Seventeen morphometric distances from a modified truss protocol (Strauss and Bookstein 1982) derived from eight carapace landmarks (Fig. 2), were measured on 129 male and female lobsters (BCP, n=75; MGC, n=54) using an electronic vernier caliper (to an accuracy of 0.01 mm). These landmarks were chosen because they represent unambiguous points in the morphology of specimens and a good representation of carapace shape. To minimize bias in the measuring procedure, all measurements were done by the same person (FJGR). The order in which the males and females were measured was random and all morphometric distances were recorded on the same side (right side) of each specimen. Carapace length (CL) was considered as an estimate of the body size and it was measured from anterior to posterior margin, on the median dorsal line. These data were divided into two subsets for males and females at each region (BCPm and BCPf – MGCm and MGCf) to test the effects of gender and size.

Analysis of covariance (ANCOVA) was used to summarize sexual dimorphism and population variation at each region, regressing each of the morphometric variables against CL. Because CL was not significantly different between sex in specimens from BCP, we also compared males and females in that site performing a multivariate analysis of variance (MANOVA) using log-transformed data. Sexual dimorphism for each region was also explored by multivariate allometry using principal component analysis (PCA). Data matrix was standardized previous to the PCA. Our results represent only the statistical sample and not the two statistical populations in the studied two regions.

Differences in body shape between populations were analyzed performing two sheared principal component analysis (SPCA); one to compare males and the other to compare females. SPCA method (Bookstein et al. 1985) allows an overall comparison of body shape among similar species or morphs because it restricts the variation due to size to the first component so that subsequent components are strictly shape related (Humphries et al. 1981). In consequence, differences between populations were illustrated by plotting the second or third SPCA. To test the significance of differences we compared SPCA scores using univariate ANOVA. Similar steps were performed using Burnaby size-adjusted principal component analysis (Rohlf and Bookstein 1987). SPCA and Burnaby methods

were performed using SHEAR-PCA and BURNABY routines, a computer procedures written by Norman MacLeod (available at http: // life.bio.sunysb.edu/morph/). All other computations were performed using Statistica 5.5 (Statsoft, Inc.).

3.4 Results

Lobster sizes (CL) ranged between 55.7 mm and 108.8 mm. Specimens from BCP were significantly larger (F=166.19, P<0.05) than MGC, with a mean CL of 88.7 mm and 71.9 mm, respectively (Table 1, Fig. 3). While MGCm were larger than MGCf (F=7.755, P=0.0075), the difference in BCP was not significant between sexes (F=0.47, P=0.41968). ANCOVA demonstrate significant differences in some variables, indicating different growth pattern between males and females. In other variables, homogeneity of regression was not found; thus, although an ANCOVA could not be performed because equality of slopes is an assumption required for the test of intercepts (Tabachnick and Fidell 1989), it was concluded that the rate of change in each variable with the generalized size variable (CL) differed across the dataset; Table 2; Fig 4).

Table 1. Mean and Standard Deviation values (mm ± SD) from lobster size (CL: carapace length) and 17 morphometric distances (variables), produced by 8 landmarks, in two populations of blue spiny lobsters from NW México

Character	MGC		BCP	
	FEMALES MGCf (n=31)	MALES MGCm (n=23)	FEMALES BCPf (n=27)	MALES BCPm (n=48)
CL	69.1 ±6.96	75.6 ±10.25	88.1 ±5.92	89.0 ±5.74
1	32.8 ±3.76	35.5 ±5.34	42.0 ±3.40	42.6 ±3.05
2	20.2 ±2.14	21.5 ±2.84	25.4 ±1.87	25.1 ±1.57
3	23.5 ±2.96	26.1 ±3.86	30.1 ±2.60	30.3 ±2.17
4	14.3 ±1.29	15.0 ±1.96	17.9 ±1.48	17.9 ±1.11
5	28.7 ±3.33	30.9 ±4.86	37.1 ±3.90	36.7 ±2.54
6	36.7 ±3.82	39.9 ±5.77	46.7 ±3.47	47.2 ±3.12
7	35.2 ±3.31	39.0 ±5.06	45.0 ±2.81	45.6 ±2.92
8	34.6 ±3.34	35.4 ±3 88	43.7 ±3.07	41.5 ±2.48
9	55.4 ±5.28	60.6 ±8.04	70.0 ±4.39	70.7 ±4.56
10	52.9 ±5.19	56.8 ±7.19	66.8 ±3.86	66.5 ±3.76
11	49.2 ±4.72	54.0 ±7.22	62.3 ±4.13	63.0 ±4.01
12	22.2 ±2.24	24.0 ±2.88	28.0 ±2.12	27.9 ±1.80
13	33.3 ±3.25	35.5 ±5.09	41.8 ±3.09	41.8 ±2.81
14	59.9 ±5.67	65.5 ±9.60	75.9 ±5.61	77.0 ±5.09
15	18.0 ±2.14	20.0 ±3.24	23.0 ±1.81	23.0 ±1.87
16	35.6 ±3.58	38.1 ±5.54	45.4 ±3.58	44.9 ±2.95
17	72.6 ±7.22	79.9 ±11.43	91.9 ±6.33	93.4 ±6.04

MGC mainland's Gulf of California; *BCP* Baja California peninsula, *f* Females, *m* Males

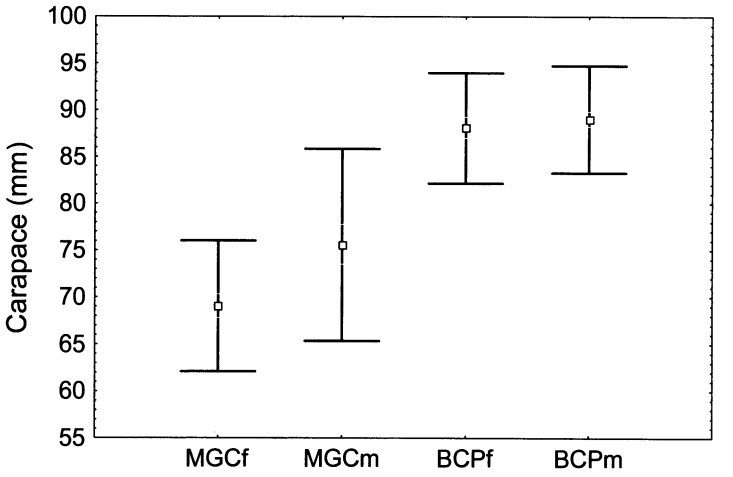

Fig. 3. Means of carapace length of each sample (see text for explanation on abbreviations)

Table 2. ANCOVA results showing significantly different morphometric characters between males and females

Character	MGC		BCP	
	ANCOVA	TP	ANCOVA	TP
1	0.0003*	0.4815	0.5765	0.2951
2	0.0627	0.5827	0.0160*	0.1892
3	0.5802	0.2205	0.5794	0.1316
4	0.0344*	0.4390	0.5491	0.3917
5	0.0004*	0.9426	-	< 0.0001*
6	0.1546	0.3872	0.8585	0.4816
7	0.0038*	0.2614	0.5481	0.4011
8	-	0.0270*	< 0.0001*	0.2269
9	0.5930	0.3499	0.9516	0.2318
10	0.0225*	0.2673	0.0003*	0.8710
11	0.2562	0.2342	0.6847	0.8466
12	0.7223	0.1995	0.0592	0.5180
13	0.0007*	0.2278	0.0555	0.6521
14	-	0.0019*	0.5160	0.3098
15	0.7255	0.8591	0.1893	0.7922
16	0.0428*	0.1996	0.0002*	0.0582
17	-	0.0383*	0.1331	0.8630

* Significant differences (P< 0.05) between males an females, *TP* Test of parallelism

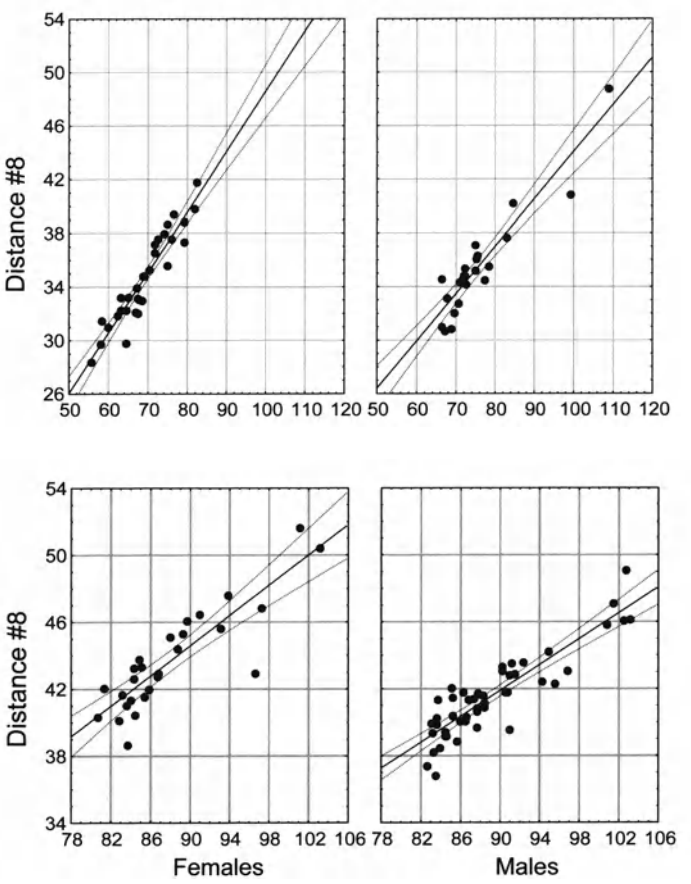

Fig. 4. ANCOVA of distance # 8. Data from MGC (above) and BCP (under)

MANOVA results among BCP's specimens for the seventeen morphometric variables (log-transformed), revealed significant differences (Wilk's Lambda = 0.2971; F = 7.9321, P< 0.0001). In BCP's data set the ANCOVA test also indicated significant differences in some variables (Table 2).

Raw PCA detected sexual dimorphism in each locality. The first principal component accounted for 94.7% of the recorded variation in MGC and 87.2% in BCP. These components were interpreted as representing overall carapace size (as one would expect, all PC1 loadings were positives and scores PC1 were significantly correlated with CL; r= 0.98, P<0.05, for BCP, and r= 0.99, P<0.05, for MGC). In both geographical areas (mainly in BCP) PC2 scores were more overlapped when the PC1 score values were lower (Fig. 5). This means, that the differences between males and females become more evident in larger-sized individuals, as in BCP compared to MGC. Because of this sexual dimorphism and size

affect on the morphometric measurements of lobster's carapace, a separate analysis of males and females, and the subsequent correction for size, is needed for comparison between regions.

Prior to shearing and Burnaby methods, PC1 accounted for 95.63%, PC2 for 1.0% and PC3 for 0.78% of the total variation in males (n=71). In females (n= 58), PC1 accounted for 0.97%, PC2 for 0.60% and PC3 for 0.46% (Table 3). The higher variance accounted by PC1 was consequence of the wide range of size and the intraspecific nature in our samples. This behavior (a high reflected variance in PC1) is commonly found when the specimens analyzed are different in size (Stauffer 1991). Differences in size result commonly from environmental effects (e.g. food level) whereas differences in shape are produced by underlying genetic variation, perhaps reflecting localized adaptations and/or the formation of subspecies across geographic ranges. Therefore we think that little variations, expected in putative individuals of a same species, are important at that level.

For both sexes, the highest SPCA loadings in SPC2 and SPC3 were associated to variables 3, 4, and 15 (Table 4). In BCPm and MGCm samples, ordination of individual component scores revealed overlap between localities on the sheared SPC2 (83.0% overlap) and SPC3 (total overlap) axes (Fig. 6). An ANOVA of SPC2 scores revealed significant differences between males (F=33.55, P<0.05), irrespective of the high overlap in scores indicating similar shape or subtle differ-

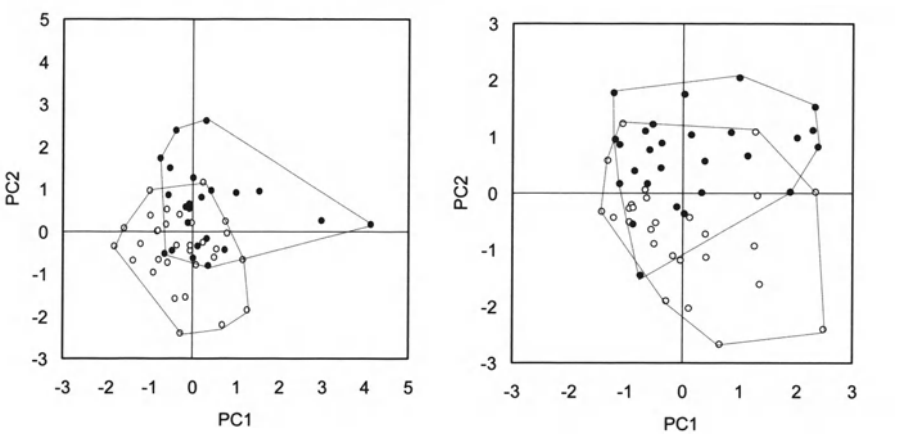

Fig. 5. Principal component analysis in MGC (left) and BCP (right). Black dots= males, white dots=females

ences. In BCPf and MGCf samples, the SPC2 scores showed a total overlap between localities and the SPC3 axes a 58.6% non-overlap (Fig. 6). Significant differences were found by an ANOVA test only for SPC3 (F=42.80, P<0.05). Similar results were found applying Burnaby's method. In BCPm and MGCm samples, individual component scores on the PC3 were totally overlapped while the PC2 scores shown significant differences (F=33.28, P<0.05). In females sam-

ples (BCPf and MGCf), the PC2 sores were overlapping but the PC3 scores revealed significant differences (F=42.61, P<0.05).

Table 3. Eigenvalues of three principal components prior to shearing as males and females

Principal components	Males		Females	
	% variance	Accumulated variance	% variance	Accumulated Variance
1	95.64	95.64	97.03	97.03
2	1.02	96.66	0.60	97.62
3	0.77	97.43	0.46	98.09
Remaining PCs	2.57	100	1.91	100

Table 4. Sheared principal component scores for 17 carapace morphometric distances, derived fron 8 landmarks, for males and females specimens of blue spiny lobster (*Panulirus inflatus*) from NW Mexico

	Males			Females		
	PC1	Sheared PC2	Sheared PC3	PC1	Sheared PC2	Sheared PC3
1	0.270	0.060	-0.312	0.257	0.019	0.350
2	0.231	0.089	-0.510	0.237	-0.298	0.059
3	0.243	-0.281	-0.257	0.264	0.000	0.533
4	0.240	0.526	0.406	0.220	-0.792	-0.268
5	0.264	-0.005	-0.154	0.274	-0.040	0.247
6	0.253	-0.005	-0.204	0.245	-0.026	0.189
7	0.233	0.129	0.366	0.237	0.281	-0.376
8	0.215	0.330	-0.020	0.231	-0.007	-0.257
9	0.237	-0.027	0.096	0.233	0.136	-0.154
10	0.229	0.037	0.150	0.234	0.150	-0.207
11	0.237	0.086	0.090	0.235	0.148	-0.241
12	0.223	0.076	0.028	0.236	-0.089	-0.205
13	0.250	0.046	-0.035	0.233	-0.041	0.148
14	0.251	0.005	0.056	0.238	0.034	0.012
15	0.246	-0.690	0.391	0.258	0.353	-0.007
16	0.252	-0.022	-0.098	0.246	0.025	-0.167
17	0.244	-0.107	0.072	0.238	0.058	-0.004

3.5 Discussion

Size and shape are obvious biological properties of organisms arising from their genetic basis and its interaction with the environment. Therefore, conspicuous dif-

ferences among related organisms are often those in the size and shape. Shape and size often vary together, but shapes can be described in a size-free manner.

In lobster, the size has tried to be removed by examining larvae or restricting the size range (Harding et al. 1993). However, the analysis on larvae does not guarantee a shape size-free analysis, because it has been found that larvae size from several sites may differ as consequence of temperature and feeding condition (Deevey 1960). Additionally, selecting individual of a certain size range restricts the shape comparison within this range, reducing the covariance and limiting a description of significant differences among groups (Bookstein et al. 1985; Cadrin 1995). Instead, adult morphometry can be useful because sexual dimorphism can

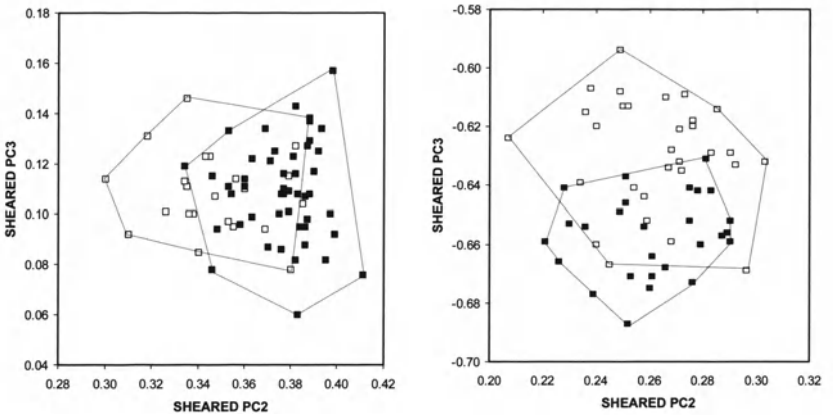

Fig. 6. Sheared Principal components 2 and 3 in males (left) and in females (right), *BCP* black square, *MGC* white square

be used to find differences among populations (Cadrin 1995).

In the present study, lobsters collected in BCP were larger than those collected in MGC. These differences could be a consequence of the different methods in the capture of specimens. However, in BCP, where traps are used and the capture is composed only of legal-sized individuals, lobster were bigger. Conversely, in MGC, where lobsters were captured using less selective methods (e.g., tangle net or diving and hooking with a J-shaped metal hook; Pérez-González et al. 2002) smaller specimens were recorded. Thus, the catch in MGC probably provides an unbiased estimate of smallest size (Pérez-González et al. 2002). Alternatively, these size differences could have a biological origin. Previous studies on BCP (Vega-Velázquez 1996) and MGC (Pérez-González 1986) found similar results. Whether the size differences are result of the influence of the environment and the fishery or have a genetic basis (BCP and MGC are different populations) remains to be explained.

Pérez-González (2002) suggests that the mean size of lobsters from the fishery at MGC has decreased significantly during the last three decades, as a result of the lack of compliance of fishermen to fishery regulations. Alternatively, differences

in lobster size can be enhanced by environmental factors, such as temperature and food availability. These two variables have been noticed to have the higher effect on the size of planktonic crustaceans (Deveey 1960). For instance, warmer waters, as in MGC, induce the presence of smaller sexually mature lobsters (Harding et al. 1992). In contrast, a greater food availability in adults provides a better nutritional state of the individuals, resulting in an increase in size. The high productivity Southern of BCP, mainly in Bahia Magdalena (Lluch-Belda2000), has an important role. In fact, this is a very important fishery zone of many other resources as the Red Spiny Lobster (Vega-Velázquez et al. 1996) and Pacific sardine, *Sardinops sagax* (Rodríguez-Sánchez et al. 1996). Thus, it is perhaps not surprising that *P. inflatus* populations living in this area reach larger sizes.

Based on our data, sexual differences were noted in each zone. There are many factors that could, in principle, be responsible for the patterns we document, including polymorphism. However we are reporting the results about a valid test of a null hypothesis.

Comparisons of sexual dimorphism in other crustaceans have been based on notoriously different body structures (*e.g.* abdomen and chelae) between females and males (Cadrín 1995; Debuse et al. 2001). However, because sexual differences in the carapace of *P. inflatus* are not so evident, an analysis to compare males with females was necessary. Our results suggest differences between males and females in carapace morphomtery do exist. Females showed a higher Variable/CL relation or higher slopes than males (Fig. 4) indicating them to have bigger dimensions for the same size. At both regions (mainly BCP) PC1 scores were highly correlated with size. These differences between males and females were clearer at higher PC1 values (higher size) suggesting a progressive allometric differentiation. Allometry differences between males and females have been shown for many crustacean species (Hartnoll 1982).

Change in the growth rate in lobsters generally appears with sexual maturity due to different biological, ecological, and behavioural requirements after the juvenile stage (Diaz et al. 2001). Since only mature specimens (above 47 mm; Pérez-González 1992), were analyzed in this study, we assumed that growth rate for each variable in each data set was constant at a different size. Ecological and behaviour studies will be necessary to complement our analysis and resolve the issue.

Morphometric differences were found between regions both in males and females. Using secondary sexual characters (characteristics of the chela and abdomen), Cadrin (1995) clearly discriminat inshore and offshore populations of the American lobster (*Homarus americanus*) from Southern New England. Harding et al. (1993) also showed clear differences among American lobster populations from Canada, analyzing the morphometry of lobster larvae. In contrast, Debuse et al. (2001) found only slight morphological differences among populations of European lobster (*Homarus gammarus)* females in nine UK locations According to our data, a geographic differentiation between regions does exist in NW Mexico. While this differentiation was more evident in females, these results suggest a low differentiation level.

Lobster discrimination in NW Mexico may be consequence of adaptive responses to local differences in environmental factors. The possibility of reproductive isolation is purely speculative at this point. Isolation can be diminished by the long periods of larval stage of lobster (6 to 11 months, Pérez-Gonzáles 1992) promoting a higher dispersal and consequent gene flow. For fishery management purposes, present results suggest that estimation of population parameters should be made in each region independently.

The Blue Spiny Lobster exhibits morphometric differences apparently as a consequence of different environmental conditions at each region. Based on our results, studies with more sensitive morphometric techniques such as landmark-based analysis of geometric morphometrics (e.g. Hood 2000; MacLeod 2002; Rosenberg 2002) combined with analysis using molecular nuclear or mitochondrial DNA markers (e.g. Sarver et al. 1990; Ovenden et al. 1994; Silberman et al. 1994; Harding et al. 1997), should be considered to define more clearly stock structures of lobsters and to develop a better understanding of the ecological and biological aspects of this fishery resource, and help for a better management strategies.

3.6 Acknowledgements

We would like to thank Raul González from the Facultad de Ciencias del Mar, Universidad Autónoma de Sinaloa, México, and his students for their help during the sampling at MGC. The authors are also grateful to "Marsen" fish market, located in La Paz, B.C.S., Mexico to allow the measurements of BCP samples. FJGR is a CONACYT fellow. RPE received funds from project RP13 of CIBNOR. JDA thanks the grants by SNI, COFAA-IPN and EDI-IPN.

References

Austin HM, Scoles D, Abell AJ (1998) Morphometric separation of annual cohorts within mid-Atlantic bluefish, *Pomatomus saltatrix*, using discriminant function analysis. Fish Bull 97:411-420

Ayala MY (1983) Madurez sexual y asepctos reproductivos de la langosta roja *Panulirus interruptus* (Randall 1840) en la costa oeste central de la Peninsula de Baja California, México. Ciencia Pesq 4:33-48

Bookstein, FL (1991) Morphometrical tools for landmark data: geometric and biology. Cambridge University Press, Cambridge

Bookstein FL, Chernoff B, Elder RL, Humphries JM, Smith GR, Strauss R (1985) Morphometrics in evolutionary biology. Special Publication No. 15. The Academy of Natural Sciences of Philadelphia

Briones-Fourzán P, Lozano-Alvarez E (1992) Aspects of the reproduction of *Panulirus inlfatus* (Bouvier) and *P gracilis* Strets (Decapoda: Palinuridae) from the Pacific coast of Mexico. J Crust Biol 12:41-50

Cadrin S (1995) Discrimination of American lobster (*Homarus americanus*) stocks off southern New England on the basis of secondary sex character allometry. Can J Fish Aquat Sci 52:2712-2723

Castro M, Gancho P, Henriques P (1997) Comparison of several population of Norway lobster, *Nephrops norvegicus* (Linneo 1758), from the Mediterranean and adjacent Atlantic: a biometrics study. Sci Mar 62:71-79

Corti M, Thorpe R, Sola S, Sbordoni L, Cataudella V (1981) Multivariate morphometrics in aquaculture: a case study of six stocks of the common carp (*Cyprinus carpio*) from Italy. Can J Fish Aquat Sci 45:1548-1554

Creech S (1992) A multivariate morphometric investigation of *Atherina boyeri* Risso, 1810 and *A. presbyter* Cuvier, 1829 (Teleostei: Atherinidae): morphometric evidence in support of the two species. J Fish Biol 41: 341-353

Lluch-Belda D (2000) Centros de actividad biológica en la costa occidental de Baja California. In: Llich-Belda D, Elorduy-Garay J, Lluch-Cota SE, Ponce-Diaz G (eds) BAC Centros de Actividad Biológica del Pacífico mexicana. Centro Investigaciones Biológicas del Noroeste, SC, Centro Interdisciplinario de Ciencias Marinas, Consejo de Ciencia y Tecnología, México, pp 49-64

Debuse VJ, Addison JT, Reynodls JD (2001) Morphometric variability in UK population of the European lobster. J Mar Biol Ass U K 81: 369-479

Deevey GB (1960) Relative effects of temperature and food on seasonal variations in length of marine copepods in some American and western European water. Bull Bingh Ocean Col Pap 17:55-86

Diaz GA, Smith SG, Serafy JE, Ault JA (2001) Allometry of the growth of pink shrimp *Farfantepenaeus duorarum* in a subtropical bay. Trans Amer Fish Soc 130:328-325

Doadrio I, Carmona J, Fernández-Delgado C (2002) Morphometric study of the Iberian *Aphanis* (Actinopterygii, Cyprinodontiformes), with description of a new species. Folia Zool, 51(1): 67-79

Elliot NG, Haskard K, Koslow JA (1995) Morphometrics analysis of orange roughly (*Hoplostethus_atlanticus*) off continental slope of southern Australia. J Fish Biol 46: 202-220

Eisenhour D (1997) Distribution and systematics of *Notropis wickliffi* (Cypriniformes: Cyprinidae) in Illinois. Transactions of the Illinois State Academy of Science 90 (1 and 2): 65-78

Harding G, Kenchington E, Zheng Z (1993) Morphometrics of American lobster (*Homarus americanus*) larvae in relation to stock determinations in the Maritimes, Canada. Can J Fish Aquat Sci 50:43-52

Harding G, Kenechington E, Bird CJ, Pezzack DS, Landry DC (1997) Genetic relationships among subpopulations of the American lobster (*Homarus americanus*) as revealed by random amplified polymorphic DNA. Can J Fish Aquat Sci 54:1762-1771

Harnoll RG (1982) Growth. *In* Abele LB (ed) The biology of Crustacea. Embriology, Morphology, and genetics, Vol 2, Academic Pres, New York, pp 111-197

Humphries JM, Bookstein FL, Chernoff B, Smith GR, Elder RL, Poss G (1981) Multivariate discrimination by shape in relation to size. Syst Zool 30:291-308

Krause MK, Arnold WS, Ambrose Jr WG (1994) Morphological and genetic variation among three population of calico scallops, *Argopecten gibbus*. Journal of Shellfish Research 13 (2): 529-537

Lourie SA, Pritchard JC, Casey SP, Truong SK, Hall HJ, Vincent ACJ (1996) The taxonomy of Vietnam's exploited seahorses (family Syngnathidae). Biological Journal of the Linnean Society 66: 231-256

MacLeod N (2002) Phylogenetic signals in morphometric data. In: MacLeod N, Forey PL (ed) Morphology, shape and phylogeny. Systematics Association Special Volume Series 64. Taylor and Francis, London, pp 110-138

Ovenden JR, Drasher DJ (1994) Stock identify of the red (*Jasus edwardsii*) and green (*J. verreauxi*) rock lobster inferred from michondrial DNA analysis. In: Philllips BF, Cobb JS, Kittaka J (eds) Spiny Lobster management. Fishing News Books, Cambridge, pp 230-249

Pawson MG (1995) Biogeographical identification of English Channel fish and shellfish stocks. Fish Res Tech Rep MAFF 99: 1-72

Pérez-Enríquez R, Vega VA, Avila S, Sandoval JL (2001) Population genetics of red spiny lobster (*Panulirus interruptus*) along the Baja California Peninsula, Mexico. Mar Fresh Res 52: 1541-1549

Pérez-Gonzáles R (1986) Aspectos generales de la biología y la pesquería de las *langostas Panulirus inflatus* y *P.gracilis* en la bahía de Mazatlán, Sinaloa, México. Bcs. Thesis, ENEP-Eztacala (UNAM)

Pérez-González R, Flores-Campaña LM, Núñez-Pasten A (1992) Análisis de la distribución de tallas, captura y esfuerzo en la pesquería de las langostas *Panulirus inflatus* (Bouvier, 1985) y *P. gracilis* Streets, 1871 (Decapoda: Palinuridae) en las costas de Sinaloa , México. Proc San Diego Soc Natural Hist 15:1-5

Péres-González R, Ortega Salas AA (1992) Algunos aspectos de la reproducción en *Panulirus inflatus* (Bouvier) y *P gracilis* Stretts (Decapoda: Palinuridae) en el sureste del Golfo California, México. Inv Mar CICIMAR 7: 25-33

Pérez-Gonzalez R, Munõz I, Valadez LM, Borrego ML (2002) The current status of the fishery for spiny lobsters *Panulirus inflatus* and *P. gracilis* (Decapoda: Palinuridae) along the Mexican Pacific coast. In: Hendrickx ME (ed) Contributions to the Study of East Pacific Crustaceans [Contribuciones al estudio de los crustáceos del Pacífico Este Instituto de Ciencias del Mar y Limnología, UNAM. 250 pp

Phillips BF, Booth JD (1994) Design, use, and effectiveness of collectors for catching the puerulus stage of spiny lobster. Rev Fish Sci 2:255-289

Rodríguez-Sánchez R, Hernández-Vázques S, Lluch-Velda D, Félix-Uraga R, Ortega-García S, Villa-Arce J, Ponce-Diaz G, Lluch-Cota D (1996) Pesquerías de pelágicos menores (sardinas y anchovetas) In: Casas-Valdez M, Ponce-Diaz G (eds) Estudio del Potencial Pesquero y Acuícola de Baja California Sur. CICIMAR, La Paz, BCS, Mexico, pp 317-350

Rolfh FJ, Bookstein FL (1987). A comment on shearing as a method fro "size correction". Syst Zool 36 (4): 356-367

Rosenberg M (2002) Fiddler crab claw shape variation: a geometric morphometric analysisi across the genus *Uca* (Crustacea: Brachyura: Ocypodidae) Biol JLinn Soc 75:147-162

Sarver SK, Silberman JD, Walsh PJ (1998) Mitochondrial DNA sequence evidence supporting the recognition of two subspecies or species of the Florida spiny lobster *Panulirus argus*. J Crust Biol 18: 177-186

Satuffer Jr JR (1991) description of a facultative cleanerfish (Teleosti: Cichlidae) from lake Malawy, Africa. Coppeia 1991: 141-147

Silberman JD, Shane SK, Walsh PJ (1994) Mitochondrial DNA variation in seasonal cohorts of spiny lobster (*Panulirus argus*) postlarvae. Mol Mar Biol Biotech 3:165-170

Skillman RA (1989) Status of Pacific Billfish stock. In: Troud RH (ed) Planning the future of billfishes: Research and management in the 90's and beyond. Fishery and stock synopses, data needs and management (Part 1). Marine Recreation Fisheries Series 13, Kailua-Kona, Hawaii, pp 175-195

Strauss RE, Bookstein FL (1982) The truss: body form reconstruction in morphometrics. Syst Zool 31: 113-135

Tabachnick BG, Fidel LS (2001) Using multivariate statistics. Allyn & Bacon, Needhamm Heights MA

Tzeng TD, Chiu CS, Yeh SY (2001) Morphometric variation in red-spot prawn (*Metapenaeopsis barbata*) in different geographic water off Taiwan. Fisheries Research 53: 211-217

Vega VA, Espinoza-Castro G, Gómez-Rojo C (1996) Pesquería de la langosta *Panulirus* spp In: Casas-Valdez M, Ponce-Diaz G (eds) Estudio del Potencial Pesquero y Acuícola de Baja California Sur. CICIMAR, La Paz, BCS, Mexico, pp 227-262

Hood C (2000) geometric morphometric approaches to the study of sexual size dimorphism in mammals. Hystrix 11(1): 77-90

4 The effect of alcohol and freezing preservation on carapace size and shape in *Liocarcinus depurator* (Crustacea, Brachyura)

Marta Rufino[1], Pere Abelló[1] and Andrew B. Yule[2]

[1]Institut de Ciències del Mar - CMIMA (CSIC), Pg. Maritim de la Barceloneta, 37-49, 08003 Barcelona, Spain, mrufino@icm.csic.es; [2]University of Wales-Bangor, School of Ocean Sciences. Menai Bridge, Anglesey, Gwynedd Wales, UK

4.1 Abstract

Morphometric and shape analysis are usually performed on preserved specimens. The current paper examines the effect of two common preservation methods, freezing and alcohol, on the shape and magnitude of crab's carapace. The carapace widths and images of the carapace of two batches of the swimming crab, *Liocarcinus depurator* were taken before and after preservation. The carapace width was measured by two operatives and discrepancy between the two was analysed. The carapace images were analysed using geometric morphometric analysis. The carapace widths decreased significantly, though minimally, after preservation. Geometric morphometric indicated significant differences after preservation in the uniform shape components only indicating global differences rather than localised differentials.

Keywords: *Liocarcinus depurator*, alcohol, freezing, preservation, shape differences, geometric morphometry, crab.

4.2 Introduction

Since crustaceans have hard exoskeletons and potentially numerous "landmarks" they should constitute an ideal group for the application of geometric morphometric methods. Few such studies on Crustacea can, however, be found. Cadrin (1995) applied box-truss methods to discriminate between sexes and potential fishery stocks of the American lobster, *Homarus americanus* (Milne Edwards). Rosenberg's (1997) work on the shape difference between major and minor chelipeds of the fiddler crab *Uca pugnax*, (Smith) probably pioneered the use of land-

mark-based morphometric analysis in extant crustaceans (see Reyment for works on fossil Crustacea). The differences observed suggested that the major claw could produce more crushing power, and that selection for "fight effectiveness" may have played an important role in the evolution of the cheliped shape. Rufino et al. (2004) used geometrical morphometric techniques to elucidate subtle differences in the carapace shape of male and female *Liocarcinus depurator*.
Recently, reviews of the techniques applied to crustaceans can be found in, Rosenberg (2002, claw shape variation across the genus *Uca*), Cadrin and Friedland (1999, lobster stock identification) and Cadrin (2000, fisheries stock identification).

In many field studies, individuals are not measured immediately after capture, but are preserved for later measurement. The effect of the preservation on the size of the individuals is often ignored, however significant. The ultimate effect of preservation distortion may largely depend on the degree of accuracy needed for each specific study. The effect is often quite variable, for example, many fish species, both adults and larvae, either shrink or enlarge after preservation with alcohol, formaldehyde or freezing (e.g. *Sprattus sprattus*, *Encheylopus cimbrius* and *Pomatoschistus minutus* (Fey 1999); *Clupea harengus* and *Osmerus eperlanus* (Fey 2002); *Mullus barbatus* and *M. surmuletus* (Al-Hassan et al. 2000)). The few studies carried out on crustaceans include that of Melville-Smith (2003) who showed that the carapace of the rock lobster (*Panulirus cygnus*) shrank significantly after cooking and freezing, although the shrinkage was minimal. No study has been conducted on the effect of preservation procedure on the over-all shape of the individuals and whether preservation acts in a differential manner on different parts of the body.

Clearly, the interpretation of significant differences in morphometry between species is difficult if the preservation method causes a differential effect between species. Such differential effects of preservatives on different parts of an organism will cause differences in shape, which will be more readily appreciated with geometric morphometry than with any other technique.

The present study examines the effect of different preservation methods on size and shape in the portunid crab *Liocarcinus depurator* (Linnaeus). It is the dominant brachyuran by-catch (untargeted species) in Mediterranean demersal fisheries and shows a wide bathymetric range throughout the continental shelf and upper slope (Abelló et al. 1988; Abelló et al. 2002; Rufino et al. submitted). *L. depurator* inhabits several types of substrata, although it is most commonly found on mud (Minervini et al. 1982; Rufino et al. submitted). A wide-ranging species, *L. depurator* has been reported from Mauritania and the Canary Islands to Norway in the eastern North Atlantic and throughout the Mediterranean Sea (d'Udekem d'Acoz 1999).

4.3 Materials and methods

Individuals of *Liocarcinus depurator* were collected by trawling off Barcelona (western Mediterranean). The carapace widths (CW) of 120 fresh individuals (60 males and 60 females) were measured by two operatives using the same digital calipers with a resolution of 0.01 mm. The upper view of the carapace was also scanned into a digital image using a calibrated HP Precisionscan 3.1. Thirty male and 30 female crabs, randomly-selected, were frozen (~ –20°C) and the remaining 30 males and females were stored in 70% ethanol. Three weeks later, the frozen crabs were defrosted and the measurements repeated on both groups of crabs.

Landmarks (see Fig. 1) were used to quantify carapace shape and "Centroid" magnitude (defined as the squared root of the summed, squared distance of all landmarks in relation to the geometric centroid [calculated using tpsRel (Rohlf 2003b)]) was used as a measure of crab size in addition to CW.

Figure 1 shows the locations of the 15 landmarks identified for the geometrical morphometric analysis. The first landmark was located centrally on the posterior margin of the carapace. The second landmark was the point of maximum curvature of the posterior carapace margin. Landmarks 3 to 11 represent the tips of and anterior notch formed by the four anterolateral teeth. Landmarks 12 to 14 represent the tips of and the notch between the two anterior teeth. Landmark 15 along with landmark 3 delineated the maximum carapace width. Coordinates of the landmarks were digitised using tpsDig (Rohlf 2003a).

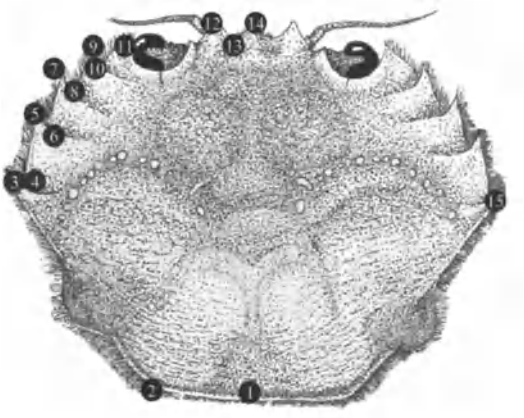

Fig. 1. Landmarks selected on the *Liocarcinus depurator* carapace

Details on the procedures for geometrical morphometric analysis can be found in Adams et al. (2003), nevertheless only a brief description is given here. After digitising, landmark maps were rotated, scaled (to unit centroid size) and translated through a Generalised Least squares Superimposition (GLS) procedure (generalised procrustes) to eliminate scale and orientation distorsions ('*tpsRel*' (Rohlf 2003b)). A thin-splate spline procedure was used to fit an interpolated function to an average map (consensus configuration) of the carapace shape and

derive the uniform and non-uniform (partial warps) components of shape variation. The two uniform components describe differences that affect all parts of the carapace equally (global differences). The magnitude of the first of these indicates the degree of stretching along the x-axis relative to the average carapace map. Whereas the magnitude of the second indicates compressions or dilatations along the y-axis (Cavalcanti et al. 1999). The non-uniform shape components (partial warps) describe localised departures from the average carapace map.
The approach followed in the data treatment was to calculate the difference between the operative's measurements and between before/after conservation, in order to obtain independent samples. A two-sample Wilcoxon test was used to test differences between genders and the non-parametric one-sample Wilcoxon test corrected for tied observations (exactRankTests package in R-project (Ihaka and Gentleman 1996)) was used to test if the CW change due to the conservation or different author measurements, was significantly different from zero (which would correspond to absence of a significant change). Ninety-five percent confidence intervals were estimated using one-sample Wilcoxon test corrected for tied observations (exactRankTests package in R-project (Ihaka and Gentleman 1996)).

4.4 Results

Carapace width (CW) measurements were not normally distributed and the variances between treatments were not approximately equal. Therefore, differences between operators' measurements and before and after preservation were analysed separately.

Within the size ranges measured, no significant difference ($p>0.05$) between measurements on males or on females was found (Wilcoxon test corrected for tied observations: $W = 7622$, p-value = 0.4332) so, in the remaining analyses, both sexes were pooled.

There were no significant differences between median operator differences across the groups of male and female crabs before or after preservation (Mood's median Test Chisquared = 9.54, $df = 7$, $p = 0.216$). Fig 2 shows boxplots of the difference data for each group showing how one or two outliers are evident but that the bulk of the differences were very small. There are no discernible patterns between genders or preservation methods nor between before and after preservation. The median differences between the measurements made by the two operators was 0.01mm and proved highly significant (Wilcoxon 1-sample test $W=7484.5$, $p<0.001$, $N=238$).

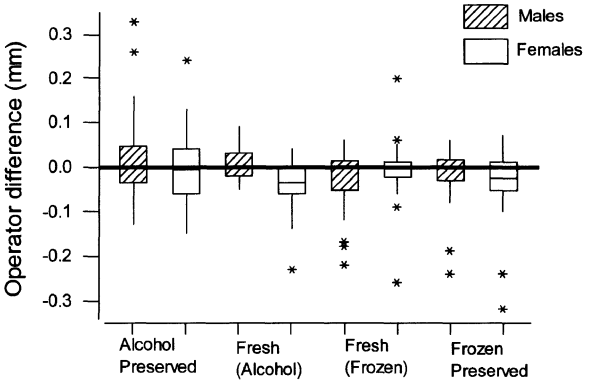

Fig. 2. Box plots of the differences in measurements on individual *L.depurator* carried out by two different operators

Since the average carapace width being measured was 39.4 mm to find a systematic error of 0.025% between operatives is remarkably good, despite the "significance". With such large numbers of observations even tiny and essentially trivial differences tend to become "statistically significant". There was no significant correlation ($r = -0.074$, $df = 236$, $p = 0.256$) between operatives' and the size of the crabs, confirming a standard systematic error between operatives which did not vary with crab dimension or applied treatment.

From the geometric morphometry, Centroid size was significantly correlated with CW ($r = 0.992$, $df = 118$, $p < 0.001$ see Fig.3).

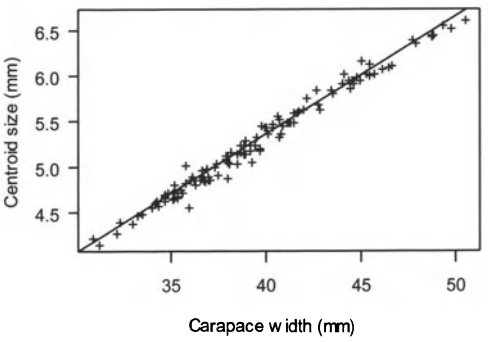

Fig. 3. Relationship between carapace width (measured with a digital caliper) and the centroid size (based on 15 landmarks on the crab's carapace) of 120 *Liocarcinus depurator* (60 males and 60 females). centroid = 0.183 + 0.129*CW

Carapace width and centroid magnitude, showed different results in relation to the effect of preservation technique. Carapace width decreased (median difference = 0.08 mm) after the animals were preserved in alcohol (Table 1), while the centroid magnitude only decreased by 0.01mm (median difference not significant, Table 1). The effect of freezing was smaller. Centroid magnitude actually increased (median difference = -0.01, but not significantly, Table 1). Carapace width, on the other hand decreased significantly (median difference = 0.07-0.05 mm, Table 1) after freezing. However, the variability associated with centroid magnitude differences after freezing was far greater than any other treatment

For both the difference in carapace width and in centroid magnitude, with preservation technique there was no significant correlation with the carapace width (i.e. size of the individual), showing no differential effect of preservation technique with crab size.

Table 1. Median difference of the carapace width (mm) and centroid size of *Liocarcinus depurator*, between before and after preservation (alcohol or frozen), and respective results of the one-sample Wilcoxon test (V: statistic and p: pvalue)

					Wilcox	
Cons	Measure	Author	Estimated median.	Median	V	p-value
Alc	Centroid		0.02	0.01	990	0.065
	CW	A	0.09	0.08	1441	0.000
		B	0.1	0.08	1709	0.000
Fro	Centroid		-0.01	-0.02	806	0.701
	CW	A	0.07	0.06	1423	0.000
		B	0.05	0.04	1619	0.000

Cons.:conservation; Alc:Alcohol; Fro: Frozen

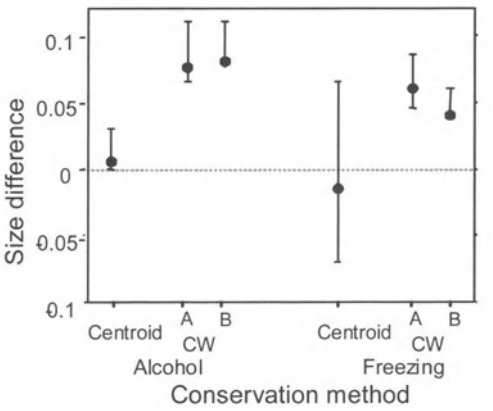

Fig. 4. Median and 95% CI (Wilcoxon), of the difference between conservation methods, on the centroid magnitude and on carapace width of *Liocarcinus depurator* for the two operatives measurements (A and B)

Analysis of the uniform components for crabs preserved in alcohol (Repeated measures MANOVA) indicated a significant effect of the preservation on the shape (Wilks = 0.743, F = 10.016, p <0.001). The resultant discriminant function was not particularly powerful (63% success for pre-preservation crabs and 65% success for post-preservation crabs). Freezing also showed a significant multivariate effect (Wilks = 0.792, F = 7.627, p = 0.001), providing an even less powerful discriminant (58% success for pre-preservation crabs and 60% for post-preservation specimens). Despite determining significant effects of preservation on the global shape parameters, the multivariate analysis could not discriminate well between preserved and fresh crabs simply on the basis of their shape.

The non-uniform shape components exhibited no significant effects of preservation for both alcohol (Manova:- Wilks = 0.177; F = 1.415; p = 0.244) and freezing (Manova:- Wilks = 0.128; F = 2.082; p = 0.068). Thus, although an over all shrinkage (global change) was evident in the preserved carapaces such was not reflected in local effects at particular landmark locations.

4.5 Discussion

Differences in carapace width measurements taken by the two operatives were always smaller than the differences measured between preserved and fresh specimens. The effect of operative was shown to be truly systematic and did not vary with treatment or crab size. The precision of each operative was very similar, again emphasising the systematic nature of the difference.

Both alcohol and freezing preservation methods caused significant shrinking of *L. depurator*'s carapace. Shrinking by alcohol preservation was slightly greater than that caused by freezing. 70% ethanol is well known for removing water from immersed specimens and presumably does so quicker than exposure to -20°C which can also create dehydration but usually only under a vacuum.

The individuals of *Liocarcinus depurator* studied ranged from 30.69 mm to 50.53 mm CW. A maximal shrinkage of a maximum of 100μm, represents a mere 0.33 to 0.20% decrease, which in practice is relatively trivial. Melville-Smith (2003) also found shrinkage of the carapace after freezing in the rock lobster *Panulirus cygnus*. Remarkably, given the severity of the treatment, Ibbot (2001) found no effect of boiling and subsequent freezing on the carapace length of the southern rock lobster (*Jasus edwardsii*).

Centroid magnitude showed no significant differences due to the different preservation methods, and seemed the most variable of the two measures, particularly for crabs that had been frozen. The inability of centroid magnitude to reflect the obvious differences in CW measured indicates its limitations as a general indicator of 'size'. It must ultimately be more variable than a single easily identifiable measure since it is composed of many, often imprecisely located, measures. In the present instance, the variability associated with centroid magnitude hid the significance of the obvious shrinkage and even resulted in the opposite effect being identified (although not significant).

Geometrical morphometric analysis indicated that the effect of preservation on crab shape was significant only in the uniform shape component. All differences in shape were global. Despite the significance, the discriminating power of the derived function was low. The potential for the technique to address tiny differences like those inflicted on the crab carapace by preservation appears limited at present. The errors in digitising, establishing landmark locations and then interpolating the shape functions are clearly greater than the difference revealed by precise measurements of a single, but easily identifiable dimension. Increasing the precision of the geometrical morphometric techniques to rival simple measures of 'size' in discriminating power must be an urgent aim. The power to analyse shape as an overall phenomenon with the precision of simple measurements will make geometric morphometry extremely valuable.

4.6 Acknowledgements

The authors would like to acknowledge Andrea Cardini, James Rohlf and Miriam Zelditch for their suggestions. This work was inserted on MMR PhD program and it was financed by Fundação para a Ciência e a Tecnologia ref. PRAXIS XXI BD /21569 / 99.

References

Abelló P, Valladares FJ, Castellón A (1988) Analysis of the structure of decapod crustacean assemblages off the Catalan coast (North-West Mediterranean). Mar Biol 98: 39-49

Abelló P, Carbonell A, Torres P (2002) Biogeography of epibenthic crustaceans on the shelf slope of the Iberian Peninsula Mediterranean coasts: implications for the establishment of natural management areas. Sci Mar 66 (Suppl.2): 183-198

Adams DC, Rohlf FJ, Slice D (in press) Geometric Morphometrics: Ten Years of Progress Following the 'Revolution'. Ital J Zool. Proceedings of the Rome Geometric Morphometrics Workshop

Al-Hassan LAJ, Bujawari JA, El-Silini OA (2000) The effect of some preservatives and freezing on certain body dimensions of two species of the family Mullidae collected from Benghazi waters, Libya. Acta Ichthyol Piscatoria 30: 127-136

Cadrin SX (1995) Discrimination of the American lobster (*Homarus americanus*) stocks off southern New England on the basis of secondary sexual character allometry. Can J Fish Aquat Sci 52: 2712-2723

Cadrin SX (2000) Advances in morphometric identification of fishery stocks. Rev Fish Biol Fish 10: 91-112

Cadrin SX, Friedland KD (1999) The utility of image processing techniques for morphometric analysis and stock identification. Fish Res

Cavalcanti MJ, Monteiro LR, Lopes PRD (1999) Landmark based morphometric analysis in selected species of serranid fishes (Perciformes: Teleostei). Zool Stud 38: 287-294

d'Udekem d'Acoz C (1999) Inventaire et distribution des crustacés décapodes de l'Atlantique nort-oriental, de la Méditerranée et des eaux continentales adjacentes au nord de 25°N. Patrimoines Naturels (M.N.H.N./S.P.N.) 40: 1-383

Fey DP (1999) Effects of preservation technique on the length of larval fish: Methods of correcting estimates and their implication for studying growth rates. Arch Fish Mar Res/Arch Fisch Meeresforsch 47: 17-29

Fey DP (2002) Length correction of larval and early-juvenile herring (*Clupea harengus* L.) and smelt (*Osmerus eperlanus* L.) after preservation in formalin and alcohol. Bull Sea Fish Inst Gdynia 155: 47-51

Ibbot S, Gardner C, Frusher S (2001) The effect of cooking on carapace length of southern rock losbter, *Jasus edwardsii* (Hutton 1875) (Decapoda, Palinuridae). Crustaceana 74: 221-224

Melville-Smith R, Thomson AW (2003) The effect of cooking and freezing on the carapace measurements of western rock lobster, *Panulirus cygnus* George 1962. Crustaceana 76: 605-609

Minervini R, Giannotta M, Falciai L (1982) A preliminary report on the decapod crustaceans in the estuarine area of the Tiber. Quad Lab Tecnol Pesca 3: 305-318

Rohlf FJ (2003a) TpsDig, version 1.39, Department of Ecology and Evolution, State University of New York at Stony Brook, Stony Brook

Rohlf FJ (2003b) TpsRel, version 1.29, Department of Ecology and Evolution, State University of New York at Stony Brook, Stony Brook

Rosenberg MS (1997) Evolution of shape differences between the major and minor chelipeds of *Uca pugnax* (Decapoda: Ocypodidae). J Crustacean Biol 17: 52-59

Rosenberg MS (2002) Fiddler crab claw shape variation: a geometric morphometric analysis across the genus *Uca* (Crustacea : Brachyura : Ocypodidae). Biol J Linn Soc 75: 147-162

Rufino MM, Abelló P, Jones DA (in press) An application of geometric morphometrics to crustaceans: male and female carapace shape differences in *Liocarcinus depurator* (Decapoda: Brachyura). Ital J Zool. Proceedings of the Rome Geometric Morphometrics Workshop

Rufino MM, Abelló P, Maynou F (in press) *Liocarcinus depurator*: Review of current knowledge on life history and fishery data. In: Tully O (ed) The assessment and management of European crustacean fisheries: EDFAM Concerted Action

5 Allometric field decomposition – an attempt at morphogenetic morphometrics

Øyvind Hammer

Physics of Geological Processes (PGP), University of Oslo, Pb. 1048 Blindern, Norway, and Geological Museum, University of Oslo, ohammer@nhm.uio.no

5.1 Abstract

In cases of large deformations caused by allometric growth and with allometric coefficients varying in space, the concepts of partial and relative warps do not have a direct interpretation in terms of morphogenetic mechanisms. This is illustrated both with a synthetic example and with an example of apertural allometry in ammonites. Allometric field decomposition will be used as an example of an alternative, morphogenetically oriented approach, at this stage tentative and partly impractical. The method is based on a growth gradient model with parameters that are fitted by repeated growth simulation and comparison with an observed ontogenetic or heterochronic sequence.

Keywords: Geometric morphometrics, morphogenesis, growth gradients, allometry, ammonites.

5.2 Introduction

The mainstream of modern geometric morphometrics involves the concepts of thin-plate splines, partial and relative warps (Bookstein 1991, Dryden and Mardia 1998). A common procedure consists in removing translation, rotation and size from a sample of landmark configurations by Procrustes fitting. The variation in shape within the sample is studied by interpolating the displacements at the landmarks using thin-plate splines (TPS), and then decomposing the TPS into partial and/or relative warps. The landmark configurations can be ordinated (projected into a low-dimensional space) by their partial or relative warp scores for visualisation purposes. Several samples can be compared using methods from multivariate statistics, and the deformations can be regressed onto size to study allometric effects. For lack of a better term, I will refer to this general approach (with all kinds of variants and extensions) as the geometric warp method.

The geometric warp method has proved to be a highly successful and powerful tool for the study of biological shape variation. It has a firm mathematical basis, a simple geometric interpretation and is easy to apply, and is likely to remain one of

the best morphometric approaches available in the foreseeable future. The geometric warp method is a purely geometric approach, and as such it is entirely theory-free when it comes to biological mechanisms. This can obviously be an advantage from the viewpoint of the philosophy of science, but for some applications it may not fully capture the patterns of interest. Most importantly, biologists are becoming more and more interested in morphogenesis and growth processes. To an evolutionary developmental biologist, the phenetic manifestation of shape is only of secondary interest - only a product (but also part) of a morphogenetic system that includes the genome. Phylogeny is thus evolution not primarily of the phenotype (the "standard" view), nor primarily of the genotype (the "selfish gene" concept), but of what could be termed the "auxotype": the growth type.

From this perspective, we would like to position organisms and organs in a morphogenetic/developmental/constructional parameter space rather than in a classical morphospace (McGhee 1999; Eble 1999). To solve this "inverse problem" we need two things, both of them usually somewhat impractical to obtain. First, we need a morphogenetic model: a theory for the processes that produce the shape. Secondly, given the model and an observed ontogenetic sequence, we need a way of estimating the parameters of the model. If we could do these things, we would have a protocol for morphogenetic morphometrics.

These ideas are far from new, and are well known to morphometricians. Moreover, the creators of modern geometric morphometrics are not claiming that their methods should be interpreted directly in terms of developmental mechanisms, except in some cases where they have developed special analytical techniques for this purpose. In other words, the aim of this paper is not to criticise the geometric warp method, but to illustrate its purely geometric nature and to loosely outline a possible alternative that can be applied in special cases.

It is also important to stress the distinction between partial warps as *shape descriptors* and their use to characterize *growth trajectories*. Four degrees of freedom are lost in the landmark data because of the removal of position, rotation and size in landmark registration. By transforming to partial warp scores (including the affine component scores) the dimensionality is reduced by four, partly solving this problem of closure (Dryden and Mardia 1998). This makes partial warps highly useful as pure shape descriptors for statistical analysis. However, special care must be taken when partial and relative warps are used to study growth trajectories, for example by regression onto size. These trajectories may or may not be linear, and must be analyzed with special methods. Considerable insight may be achieved by such careful study of growth trajectories based on partial warps (e.g. Zelditch et al. 2003).

5.3 Allometric fields

The allometric power law of Huxley (1932) must be the simplest and most well known morphogenetic model available. In its basic form, this model concerns

growth along two axes, call them x and y. Assuming a constant ratio a between their relative growth rates, we have

$$(dy/dt)/y = a(dx/dt)/x, \tag{5.1}$$

which by elimination of dt and consecutive integration yields the familiar allometric law:

$$y = kx^a \tag{5.2}$$

for an arbitrary integration constant k. In order to linearise this relationship, it has been common practice in traditional morphometrics to log-transform all linear measurements:

$$\log y = a \log x + \log k. \tag{5.3}$$

The geometric warp method does not inherently address this issue, which has caused some feeling of unease. On the other hand, log-transformation can easily be integrated into distance-based approaches such as EDMA.

The allometric power law was originally devised to explain the relationship between two linear distance variates. Later, it has been (controversially) extended to the multivariate case (Jolicoeur 1963). However, when considering growth in a continuous domain, the study of individual distances between a finite number of landmarks will not always give the whole picture. This brings us into the concept of allometric fields and corresponding analytical methods.

We may define an allometric field as follows, echoing Huxley's (1932) idea of a growth gradient:

Under the paradigm of allometric power laws, an allometric field is a continuous distribution of allometric coefficients a(x) *over an anatomical region with well-defined boundaries.*

In two- and three-dimensional domains, the position x will be a vector, and the value of a for a given x may vary with direction to allow for anisotropic growth. In the simplest anisotropic model, which will probably be adequate for most cases, a will have two (or three) orthogonal components.

A simple artificial example will illustrate the idea. Consider a square region with parametric axes u and v, varying from 0 to 1. The anisotropic allometric coefficient has two orthogonal components. For growth in the u direction:

$$a_u(u,v) = 1 \qquad \text{(isometric growth)} \tag{5.4}$$

In the v direction, we have

$$a_v(u,v) = 1+u, \tag{5.5}$$

defining an allometric gradient where cell division rates in the v direction are increasing in the u direction. The existence of morphogenetic gradients is well established within developmental biology, following the work of Wolpert (1969), and that morphogens can control cell division rates either directly or through other

growth factors is also obvious (e.g. Burke and Basler 1996). However, we do not need to assume any particular genetic mechanism, as we are only proposing a spatial variation in cell proliferation rates that must obviously be present for a shape change to take place. More complicated fields such as compartmentalized regions of constant growth rates can easily be used if necessary, but the principle of parsimony suggests the use of the simplest model.

Consider now an infinitesimally small, square (in parametric *uv*-coordinates) element *dudv*. According to the allometric power law, we will have the following relation between the lengths (*dx*, *dy*) of the sides of the corresponding rectangle in geometric *xy*-space:

$$dy = kdx^{l+u} \tag{5.6}$$

We set k=1 for convenience. Now approximating the continuous allometric field with a set of finite elements $\Delta x_i \Delta y_i$ of fixed number, we can choose a given Δx, constant over space (because of isometry in our example case), controlling overall size, and calculate the Δy using the allometric power law above. The corresponding geometric configuration is approximated by the aid of a spring model, relaxing to minimal energy (Rolland-Lagan et al. 2003). In this simple case we could probably also have calculated the shape analytically. Increasing Δx from 1 to 4.5, we produce the simulated ontogenetic sequence shown in Figure 1. Five landmarks are also indicated.

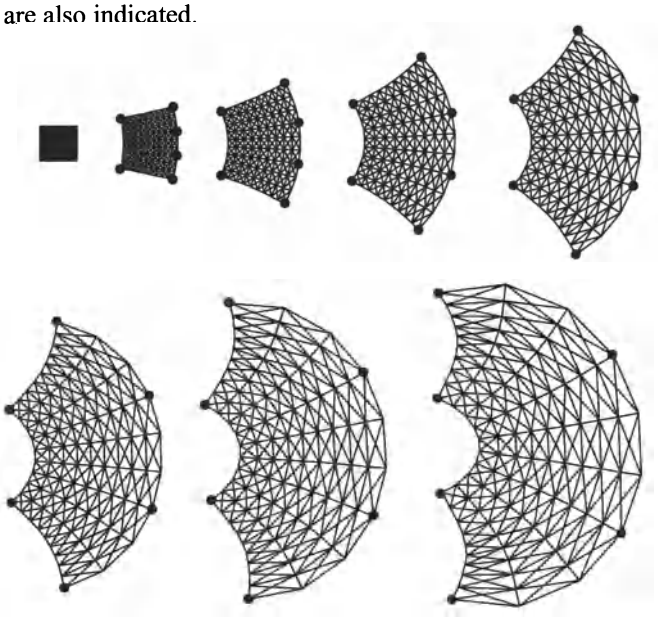

Fig. 1. Synthetic example of growth controlled by an allometric field (see text for details)

In this case the energy vanishes to zero, because a configuration exists where all grid nodes have their prescribed distances. We might say that the prescribed

strains are *internally consistent*. It is easy to construct a situation where this is not the case, for example by having a small region of fast growth constrained by a slow-growing area on all sides. Such an allometric field would not be able to control shape freely, implying an inconsistent and unsatisfactory model.

Traditional landmark-based multivariate morphometrics does not represent this simple, continuous deformation in a simple way, or at least not in a way that is easy to interpret from a morphogenetic standpoint. Consider, for example, the decomposition of deformation by the use of relative warps. We leave aside for now the difficulty of statistical treatment of large deformations due to the violation of the assumption of a flat tangent shape space (e.g. Dryden and Mardia 1998). Although the first relative warp captures important aspects of the deformation, it is not a sufficient description (Fig. 2). The second relative warp, involving a local stretching, compensates for errors in the first relative warp (Fig. 3). It is common in morphometrics to plot specimens in a relative warp space, projecting the high-dimensional shape representations down to two or three dimensions in a way that maximizes variance (e.g. Dryden and Mardia 1998). However, plotting of the first two relative warp scores for the synthetic example produces an arch, where the second warp score first decreases and then increases again through ontogeny (Fig. 4). Similar arches result from other methods of ordination, such as Principal Components Analysis of all log-transformed inter-landmark distances (Fig. 5). Although these representations can of course be subjected to non-linear regression to provide a consistent ontogenetic trend (Zelditch et al. 2003), they are not useful in revealing, let alone quantifying, the underlying morphogenetic mechanism. Figures 2-6 were produced using the software package PAST (Hammer and Harper 2001).

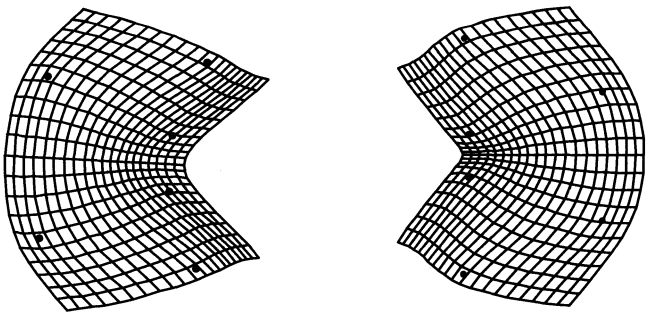

Fig. 2. Relative warps for the synthetic example. Grid deformations corresponding to Warp 1 with amplitudes +2 (left) and -2 (right). Note the incomplete, or at least unclear representation of the full deformation of Figure 1

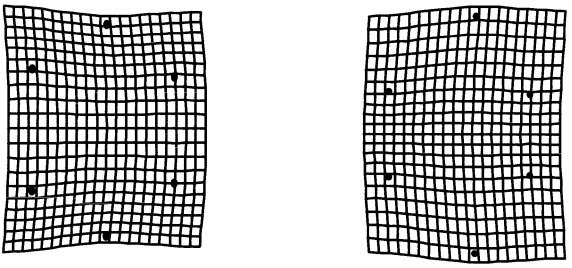

Fig. 3. Relative warps for the synthetic example. Grid deformations corresponding to Warp 2 with amplitudes +2 (left) and +- (right)

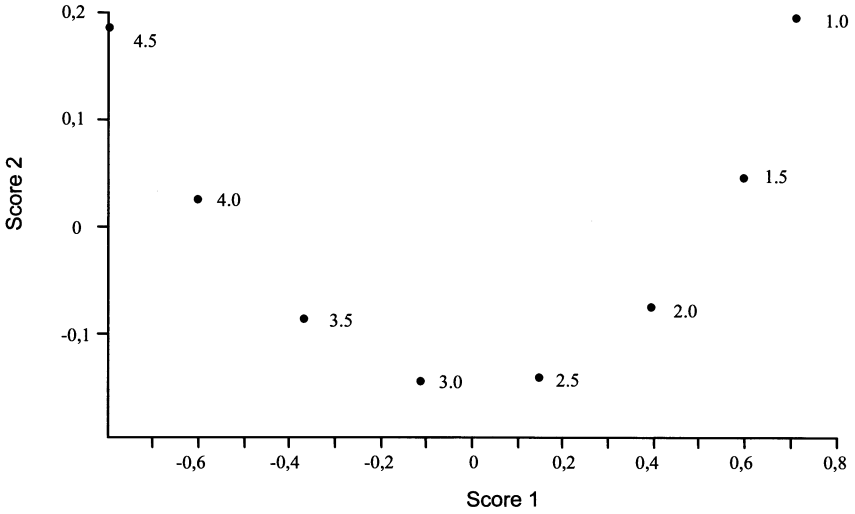

Fig. 4. First and second relative warp scores for the synthetic example. Numbers indicate growth step.

The concept of an allometric field may be compared with the vector field of Magwene (2001). Both these ideas involve a continuous growth field, but with the major difference that the allometric field describes the distribution of local growth rates under a growth model, while the vector field of Magwene (2001) describes the geometric displacement of points within the field.

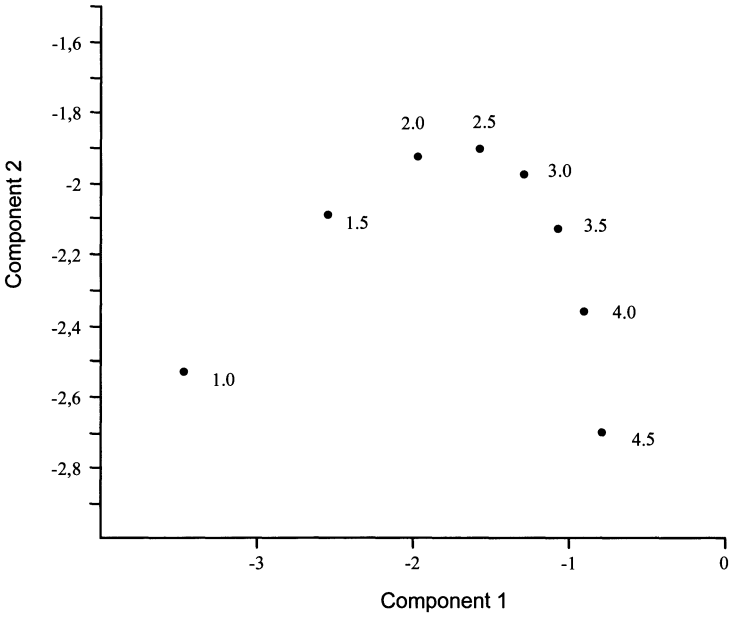

Fig. 5. PCA of all log-transformed inter-landmark distances in the synthetic example

5.4 Allometric field decomposition

Ideally, we would like to automatically and analytically deduce a representation of the allometric field from the landmark displacements through ontogeny. This inverse problem is however a rather complicated one, and must probably be attacked differently in different cases. A conceptually straightforward method is simply to simulate growth using different allometric fields, and optimize with respect to the fit to the observed landmark positions. The resulting, optimal allometric field should be represented in terms of a set of linearly independent basis functions, allowing a decomposition of the field and thereby a parameterization of developmental morphospace. The procedure might then go as follows:

1. Decide on an algebraic form for the allometric field, such as a linear combination of basis functions. For a bilaterally symmetric shape with the axis of symmetry in the v direction, such a form could be

$$(a_u, a_v)=(c_1|u|+c_2v+c_3, d_1|u|+d_2v+d_3) \qquad (5.7)$$

2. Define an (u,v) grid covering the landmark configuration of the first observed ontogenetic stage.

3. Using the allometric field for a chosen initial set of parameters, run the growth simulation up to the size of the second observed ontogenetic stage. Calculate the displaced landmark positions by interpolation in the deformed grid, and

measure the fit to the shape of the second observed ontogenetic stage using the Procrustes distance. If more than two ontogenetic stages have been observed, continue to deform the grid as in step 3, taking note of the fit to each successive stage.

4. Optimise the parameters of the allometric field by repeating the procedure in step 3 for different parameter values until a best fit to all observed ontogenetic stages is achieved. The optimisation can be automated using e.g. a steepest gradient search.

The allometric field parameters can then be subjected to any multivariate analysis method such as MANOVA, PCA, multivariate regression etc.

The use of a discrete, deforming grid may be reminiscent of the finite element method for shape change analysis (e.g. Cheverud and Richtsmeier 1986). The main differences are that the allometric field decomposition method is based on a growth model, and that the method aims to extract a small number of model parameters for further analysis. The grid can be made arbitrarily fine, and thereby approach continuity.

5.5 Case study: Ammonite allometry

The procedure will be illustrated with a limited data set of little inherent interest, but its very simplicity will hopefully convey the idea clearly. A single sub-mature specimen of the ammonite *Liparoceras* from the Lower Jurassic of Gloucestershire, England was measured using a FARO coordinate measuring machine at the University of Zürich. Four three-dimensional landmarks were defined: Venter, ventral tubercle, umbilical tubercle and umbilical seam (all on one side of the shell only). The tubercle landmarks were taken within the two rows of tubercles, but between two consecutive tubercles to avoid errors due to the breakage of tubercle tips. These landmarks were taken in a near-plane cross section of the shell tube, and projected into 2D using PCA (the third principal component being negligible). Three such landmark configurations were measured, with a spacing of a quarter of a whorl. Over the distance of these measurements, the shell tube diameter roughly doubles. The Procrustes-fitted landmark configurations and the landmark displacements corresponding to the first principal component are shown in Figure 6.

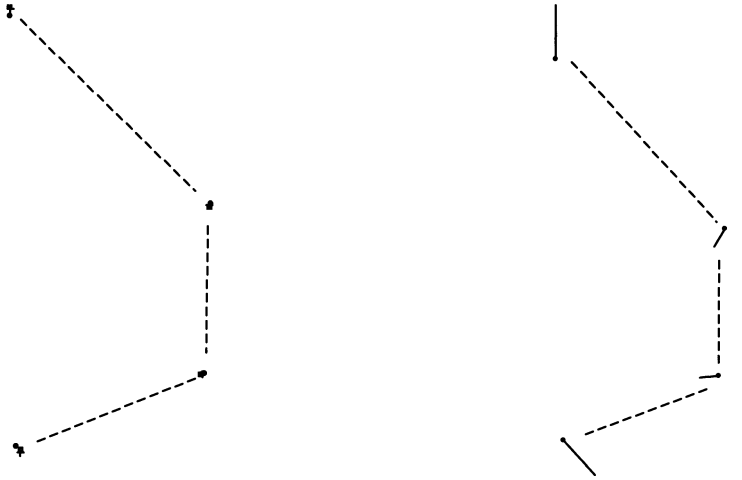

Fig. 6. Left: Procrustes fitted landmark configurations from three ontogenetic stages of a specimen of the ammonite *Liparoceras* (only one side of the shell). The apertural outline is indicated with dashed lines. Dots are stage 1, crosses stage 2, squares stage 3. Right: Landmark displacement vectors corresponding to the first principal component, drawn as lines away from the mean configuration

The landmark displacements are small, but indicate increased apertural height/width ratio and an outward displacement of the umbilical seam, reflecting a well-known ontogenetic trend for this genus.

Consideration of these displacements, and of the local thin-plate spline expansion factors and principal strain directions, suggest a model using isometric growth in the dorsoventral direction, while lateral growth is controlled by an allometric gradient increasing from umbilical seam to venter. Using the form suggested in point 1 above, we have $(a_u, a_v)=(c_2v+c_3, 1)$, giving a two-dimensional parameter space.

A square (u,v) grid of size 5 by 11 elements was defined, covering the initial landmark configuration. Running the growth simulation, the landmarks were allowed to move with the deforming grid using bilinear interpolation. The parameters c_2 and c_3 were optimized manually through a number of runs. Figure 7 shows a resulting growth simulation using the spring model. This specimen can now be placed as a point in a two-dimensional parameter space (or developmental morphospace) spanned by c_2 and c_3. Analysis of further specimens would allow operations such as ordination and hypothesis testing.

It is possible that a similar landmark displacement could have been reached using another allometric field. In other words, the inversion may not be unique (Magwene 2001). In such situations we are forced to choose among several competing models, all explaining the observed data reasonably well. Several methods have been developed for such model choice (Burnham and Anderson 1998; Zelditch et al. 2003).

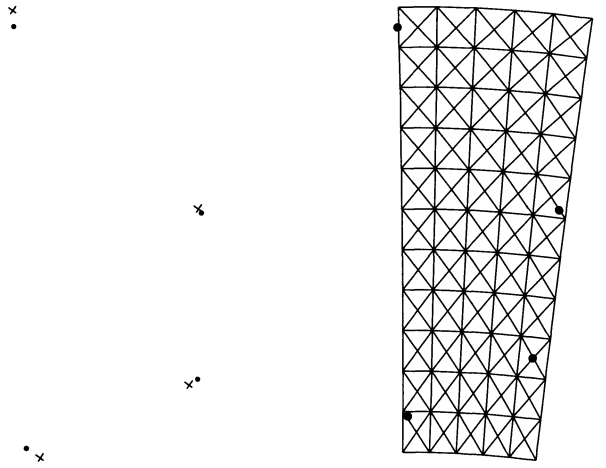

Fig. 7. Left: Landmark displacements observed in a growth model simulation of the *Liparoceras* aperture, with c_2=0.3, c_3=0.7 (see text). Procrustes fitted configurations from original (dots) to displaced (crosses) landmarks. Right: Spring model resulting from simulation beyond the observed ontogenetic stages (extrapolation), showing the relative lateral compression in the umbilical region. Rectangles were originally square

5.6 Conclusion

The point of this exercise was not to present allometric field decomposition as a new, useful method, as it is not a practical research tool at this stage. Rather, the hope was that the description of a developmentally oriented method for shape analysis, albeit almost hypothetical, would, as a contrast, highlight the purely geometric nature of the geometric warp method. A partial or relative warp score does not in itself have any direct biological interpretation in developmental terms. This takes nothing away from the usefulness of the geometric warp method for many scientific applications, which has by now been proven, but the scope of the method should be kept in mind. The extracted parameters of an allometric field decomposition will represent a *growth trajectory* and not a single shape. This illustrates the difference in aims between the two approaches.

A second goal of this paper was to inspire development of more practical methods for morphogenetic morphometrics (this may not be a good term, as the focus is not the measurement of shape, but of growth – I doubt, however, if *auxometrics* will catch on). Perhaps the fitting of model parameters by simulation as suggested here is the way forward, or perhaps a more direct, analytical approach can be found.

References

Bookstein FL (1991) Morphometric tools for landmark data: geometry and biology. Cambridge University Press, New York

Burke R, Basler K (1996) Dpp receptors are autonomously required for cell proliferation in the entire developing *Drosophila* wing. Development 122:2261-2269

Burnham KP, Anderson DR (1998) Model Selection and Inference: A practical information-theoretic approach. Springer, New York

Cheverud JM, Richtsmeier JT (1986) Finite element scaling applied to sexual dimorphism in rhesus macaque (*Macaca mulatta*) facial growth. Systematic Zoology 35:381-399

Dryden IL, Mardia.KV (1998) Statistical shape analysis. Wiley

Eble GJ (1999) Developmental and non-developmental morphospaces in evolutionary biology. In: Chapman RE, Rasskin-Gutman D, Wills M (eds) Morphospace Concepts and Applications

Hammer Ø, Harper DAT, Ryan PD (2001) PAST: Paleontological Statistics Software Package for Education and Data Analysis. Palaeontologia Electronica 4(1): 9 pp http://palaeo-electronica.org/2001_1/past/issue1_01.htm

Huxley JS (1932) Problems of relative growth. Mac Veagh, London

Jolicoeur P (1963) The multivariate generalization of the allometry equation. Biometrics 19:497-499

Magwene P (2001) Comparing ontogenetic trajectories using growth process data. Systematic Biology 50:640-656

McGhee GR Jr (1999) Theoretical morphology. Columbia University Press, New York

Rolland-Lagan A-G, Bangham JA, Coen E (2003) Growth dynamics underlying petal shape and asymmetry. Nature 422:161-163

Wolpert L (1969) Positional information and the spatial pattern of cellular differentiation. Journal of Theoretical Biology 25:1-47

Zelditch ML, Sheets HD, Lundrigan BL, Gardner T (2003) Do precocial mammals develop at a faster rate? A comparison of rates of skull development in *Sigmodon fulviventer* and *Mus musculus domesticus*. Journal of Evolutionary Biology 16:708-720

6 A combined landmark and outline-based approach to ontogenetic shape change in the Ordovician trilobite *Triarthrus becki*

H. David Sheets[1], Keonho Kim[2] and Charles E. Mitchell[2]

[1]Dept. of Physics Canisius College, 2001 Main St. Buffalo, NY 14208, USA, sheets@canisius.edu; [2]Dept. of Geology, SUNY at Buffalo, Buffalo, NY 14260, USA

6.1 Abstract

Landmark based geometric morphometrics has developed as a powerful set of statistical and visual tools for the study of the covariance patterns of organismal shape change with a range of variables or factors. The approach is limited in the kinds of shape information accessible to it, however, by the need to employ discrete landmarks as the basis for comparison. In particular, curves and complex outlines are difficult to address using strictly landmark-based methods. Information about curves may be incorporated into the study of shape by the use of semi-landmark methods, which allow information about curved surfaces to be incorporated into the framework of landmark-based geometric morphometrics. We present a discussion of several software and statistical approaches needed to carry out combined landmark and semi-landmark analysis. In particular, we demonstrate several approaches to semi-landmark alignment (including the "edgewarp" method) and compare these to standard landmark based methods utilizing a regression analysis of the Ordovician trilobite *Triarthrus becki*. Abundant landmarks on the cranidium of *T. becki* allow landmark methods to represent the shape of that structure effectively, making it a good test case for combined landmark and semi-landmark methods. We verify that patterns of ontogenetic change implied by regression models using varying combinations of landmark and semi-landmark information are consistent with one another. Thus, semi-landmark methods and standard landmark based geometric morphometric methods yield commensurate information about this ontogenetic shape transformation. These results suggests that semi-landmark methods show substantial promise for rigorously testing hypotheses that involve the comparison of shapes when an adequate set of landmarks is not available.

Keywords: ontogenetics, geometric morphometrics, trilobite, semi-landmarks, outlines.

6.2 Introduction

Landmark based geometric morphometrics has proven to be a powerful and robust tool for the study of changes in organismal shape relative to a range of effects, factors and causes (Bookstein 1991; Rohlf and Marcus 1993; Dryden and Mardia 1998). Use of landmark based methods does require the use of discrete landmark locations on organisms. Aspects of shape such as curved margins or contours on surfaces are not readily accessible to landmark based analyses. Methods for studying outlines have been developed (Lohmann 1983; Lohman and Schweitzer 1990; Rohlf 1986, 1990, 1996; MacLeod 1999), including several approaches which incorporate landmarks along curves. Outline-based methods have been criticized as not having the same emphasis on biological homology as the landmark-based method (Bookstein 1991; Zelditch et al. 1995), however, MacLeod (1999) has argued that the two methods do not have fundamentally different properties. The approaches presented by Sampson et al. (1996), Bookstein (1996a, 1997), Bookstein et al. (2002) and Green (1996) allow analysis of outlines using software and techniques developed for landmark-based analysis, by incorporating points along outlines called *semi-landmarks*. The goal of this approach is to incorporate information about landmarks and outlines into a framework for analysis based on landmark methods of representing information about shape as opposed to adding information about landmarks into outline-based methods as presented by MacLeod (1999). Incorporating information about outlines into the same form or representation as purely landmark data allows the use of many of the same software tools as landmark-based methods and allows inclusion of landmarks not lying along outlines. Despite the differences in approach, the overall goals of these landmark-based methods, and the possible concerns related to homology, are shared with the outline based methods as discussed by MacLeod (1999).

Semi-landmark methods place a series of points called semi-landmarks along curves or contours (Green 1996). The curves or contours should be homologous structures, just as the landmarks employed are homologous points on the organisms (see Bookstein 1991). The shape of the organism is represented by a set of landmark and semi-landmark points. All specimens then need to be superimposed on a reference form, which is usually an estimate of the mean form or shape of all specimens in a study. The locations of the semi-landmarks of each specimen are then allowed to "slide" along the curve defined by the set of measured semi-landmark locations on the specimen, to produce a set of semi-landmarks along the curve that represent the smoothest possible mathematical deformation of the curve on the reference form to the corresponding curve on a particular specimen (Bookstein 1996a, 1997; Green 1996), or to minimize the distance between the curve on the reference form and each individual in the sample (Sampson et al. 1996). This procedure of finding the mean form and then sliding semi-landmarks in each specimen is iterated, until a stable reference shape is obtained, that is, until successive semi-landmark alignments no longer alter the reference form, to some specified level of precision.

Typically the reference form used in land-mark based methods is the GLS Procrustes mean form of all specimens in the study (see Gower 1975, Rohlf and Slice 1990; Rohlf 1998). This choice minimizes the errors associated with approximating the curved shape space with a linear tangent space. It is possible to carry out semi-landmark alignments on a reference form other than a GLS mean specimen, should this be necessary for a given study. The extent of departure of a given data set from the linear tangent space approximation may be estimated using the program TPSSmall (Rohlf 1998a). It is particularly important to perform this test when using a reference other than the GLS Procrustes mean to ensure the linear tangent space is still a valid approximation to the curved shape space (Rohlf 1998; Slice 2001).

We present a small study of ontogenetic changes in the Middle Ordovician trilobite *Triarthrus becki* using a variety of landmark and semi-landmark configurations, and describe the use of the freely available software tools and techniques (Rohlf 2002; Sheets 2002) used to carry out this study. The specimens used here were taken from the data set used in a larger, landmark-based study of ontogenetic shape change (Kim et al. 2002). By comparing the analysis of allometric shape change using semi-landmarks to the analysis based purely on landmarks, it is possible to assess the effectiveness of semi-landmark methods for the study of shape.

Although there are a number of issues related to the use of semi-landmark based methods that merit further investigation, these initial results show that the differing combinations of landmarks and semi-landmarks utilized herein produce consistent graphical and statistical representations of the patterns of shape change in *T. becki,* indicating that the use of semi-landmarks has not distorted or obscured the information about ontogenetic shape change present in the landmark data. The inclusion of semi-landmarks in the study has also revealed information about

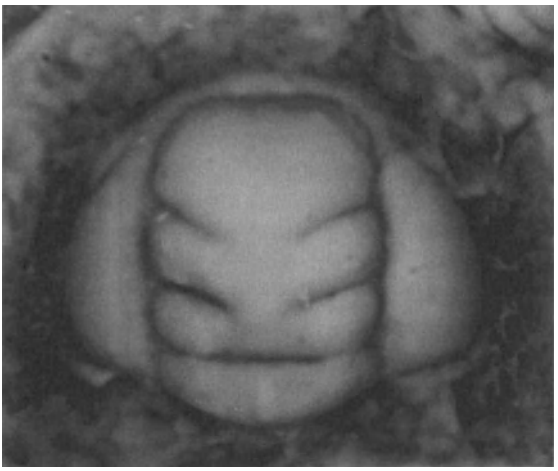

Fig. 1. A meraspid specimen of *Triarthrus becki* (NYSM 17058)

ontogenetic changes in *T. becki* that are less obvious in the landmark-only study.

These results suggest that semi-landmarks offer substantial promise for cases where discrete landmarks are not present over the entire form of interest. As we discuss below, however, there are also reasons to approach the application of semi-landmark methods with some caution.

6.3 Materials

Over 700 specimens of *Triarthrus becki*, a Middle Ordovician trilobite, were collected by Kim (Kim et al. 2002) from a single bed of the lower Dolgeville Formation in the Mohawk River Valley, New York State. Further details on the specimens and geological setting may be found in Kim et al. (2002). For this initial, limited methodological study only 13 well preserved meraspid specimens (Fig. 1) were used.

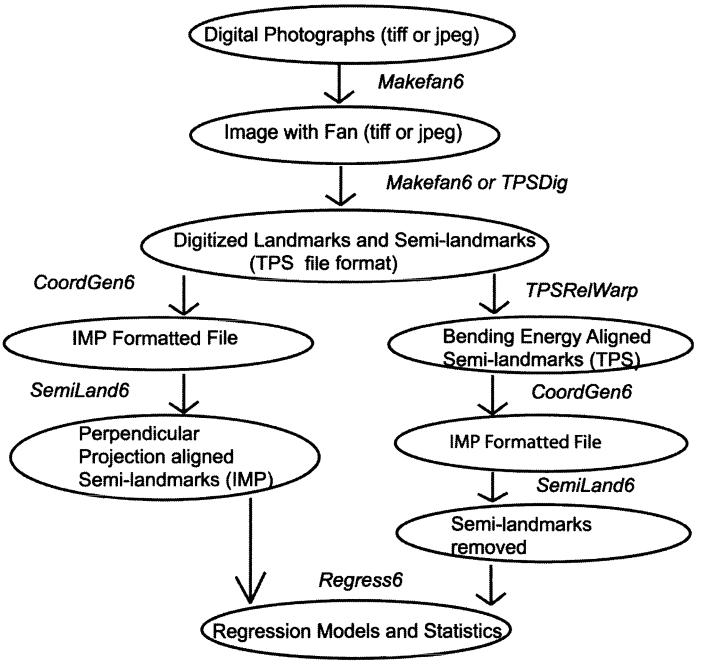

Fig. 2. A block diagram showing how data (within ellipses) is processed by software (italics) in a landmark plus semi-landmark regression analysis of shape, using either the perpendicular projection method (left) or bending energy method (right). TPS programs are by Rohlf (1998a, 2002) all other software by Sheets (2002)

6.4 Methods

The processing of the data was carried out using a series of software tools written by Rohlf (1998a, 2002) and Sheets (2002). A flow diagram of the data processing and analysis procedure and details of the software used is shown in Fig. 2.

All specimens were digitized by a single researcher (KH Kim) and images were captured using BioScan Optimas software. To digitize points evenly along contours of the specimens, guidelines with equal angular spacing were placed on the images of the specimens using MakeFan6 (Figs. 3,4). Other approaches to the spacing of landmarks along a curve are possible, an equal linear spacing would also be an obvious alternative, and additional software tools will be needed to support such approaches using landmark based data. Eleven landmarks were digitized on each specimen, 16 semi-landmarks were placed along the front edge of the cranidium and 40 semi-landmarks were digitized around the perimeter of the glabella. The number of semi-landmarks used was arbitrarily chosen in a way that visually yielded a reasonable approximation of the curves. MacLeod (1999) presents an algorithmic approach to determining the number of points necessary to represent a curve to a given level of accuracy that offers an improvement on the approach used here. As we describe below, the results of our analyses are not highly dependent on the number of semi-landmarks used, but this choice does affect the relative contribution of the outlines and discrete landmarks to measures of difference in shape between specimens.

The landmark configuration used for the analysis using only landmarks with no semi-landmarks present was taken from Kim et al. (2002), which used only the landmarks on the left-hand side of the cranidium. To form a symmetric data set for use in the current study, the left-hand side landmarks were mathematically reflected over the axis of symmetry to form a symmetric representation of the cranidium. This produced a 20 landmark configuration as shown in Figs. 3 and 7.

All landmark and semi-landmark coordinates were then used to compute an initial mean shape or reference form for all of the specimens using a GLS Procrustes procedure (Gower 1975; Rohlf and Slice 1990). All specimens were placed in a Partial Procrustes Superimposition (Dryden and Mardia 1998; Rohlf 1999) on the reference form, by minimizing the Procrustes distance (the square root of the summed squared distances between landmarks of the specimen and reference form) between them, under translation and rotation of the specimens, using a fixed centroid size (Bookstein 1991).

Two different approaches were then used to align the semi-landmarks along the curves, a *bending energy* criterion (the "edgewarp" method, see Bookstein 1996a; Green 1996) or a *perpendicular projection* criteria (similar to that used by Sampson et al. 1996).

To carry out semi-landmark alignment using the bending energy criterion, the positions of the semi-landmarks (along contours) of each specimen were allowed to slide along the direction parallel to the contours to minimize the bending energy necessary to produce the change in the contour relative to the reference form, following the semi-landmark approach developed by Bookstein (1996a, 1997),

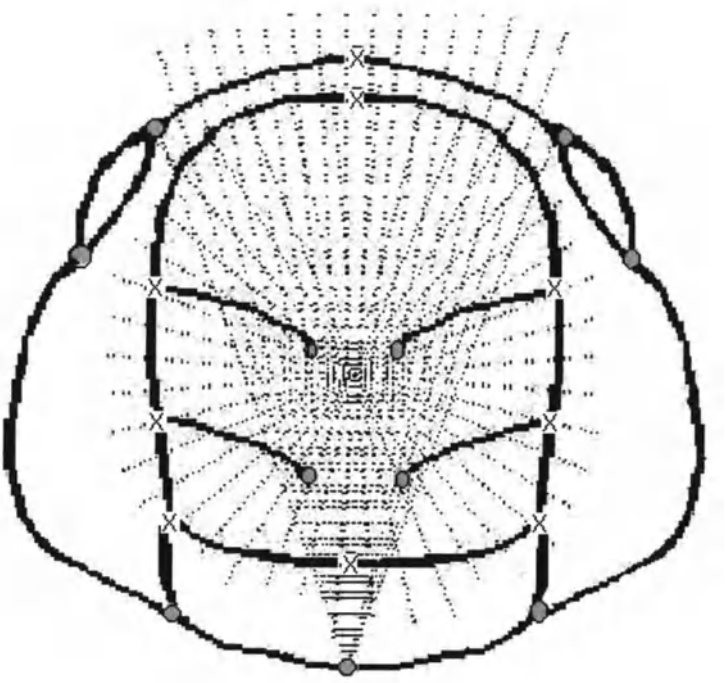

Fig. 3. The landmarks and semi-landmarks used in the study. The fans (dotted lines) shown are used to space semi-landmarks along the anterior margin of the cranidium and the perimeter of the glabella. The 11 landmarks used in conjunction with the semi-landmarks are shown as grey dots. Nine additional landmarks (each marked with an x) were used in the landmark-only portion of the study

Bookstein et al. (2002) and Green (1996). Smooth curves have low bending energy, while sharp curves have high bending energy. The requirement that semi-landmarks of the mean shape deform smoothly to the shape of a particular specimen in a manner that minimizes bending energy is equivalent to the conservative assumption that the contour on a particular specimen is the result of the smoothest possible deformation of the corresponding contour on the reference form(Bookstein 1996a). The mean shape of all specimens was then recomputed after sliding the semi-landmarks of each specimen along the respective contours, and the procedure iterated until a consistent mean form was determined, using a procedure similar to that used to producing a GLS Procrustes reference form, the only additional step being the addition of the semi-landmark processing. MacLeod (personal communication, 2003) noted that this may result in a geometric construction (the GLS reference form) having substantial influence on the analysis. One could obtain a rough estimate of the extent of this effect by using one or more biological specimens as the reference forms, rather than utilizing an iterated GLS Procrustes mean. Researchers using reference forms other than a GLS Procrustes

mean need to be aware of the issues related to the validity of the linear approximation to the curved shape space as discussed by Rohlf (1998b).

In the perpendicular projection approach used here, the portion of the difference in semi-landmark positions between the reference form and the target form that lies along the curve on the target form is mathematically removed by estimating the tangent direction to the curve at a point (using a third order polynomial fitted to the point and the two adjacent points along the curve to either side of a given point to estimate the tangent to the curve at that point) and removing the component of the difference that lies along the tangent to the curve. This results in an alignment of the semi-landmarks along the curve such that the semi-landmarks on the target form lie along the lines perpendicular to the curve that passes through the corresponding semi-landmarks on the reference form (see Sampson et al. 1996). If the curves do not have abrupt curvature changes, this criterion tends to minimize the distance between the semi-landmarks on the target and the reference.

Regression analysis of the aligned meraspid specimens was carried out, using a

Fig. 4. The landmark, semi-landmark and helper point data set for the meraspid specimens, shown after semi-landmark processing using the perpendicular projection criteria. The landmarks are open circles, semi-landmarks are solid diamonds and helper points are plus-signs (+)

variety of different protocols to specify which landmarks and semi-landmarks were to be used in the regression analysis. In some protocols, some of the points

along the contours were designated as "helper" points, and were used only to align the semi-landmarks along the contours. Helper points were then discarded prior to regression analysis. This reduces the number of semi-landmarks relative to the number of landmarks used in the study.

Since semi-landmarks contribute to the Procrustes distance (see Dryden and Mardia 1998; Rohlf 1999) in the same manner as landmarks do, a large number of semi-landmarks along a single curve will contribute more to the Procrustes distance than a single landmark representing a point on the organism does, despite the fact that the contour and the structure represented by the landmark are both homologous features. The use of helper points in conjunction with semi-landmarks may reduce this effect, while maintaining coverage of the contour during the sliding of semi-landmarks along the contour. We used two arbitrarily chosen configurations of semi-landmarks and helpers that yielded reasonable visual representations of the curves. There have been algorithm approaches to determining the number of points needed to represent a curve (MacLeod 1999), which would yield less arbitrary results. Future semi-landmark software should include this or similar approaches. Figs. 3 and 4 shows the different configurations used in the study. Note that each configuration was aligned using both the bending energy (denoted BE) and the perpendicular projection criteria (denoted as D for 'distance'), except for the landmark only configuration (in which no semi-landmarks need be aligned).

The regression analysis of shape on log centroid size was carried out using the two semi-landmark criteria (BE and D) with each of three protocols for handling reference points: 1) all landmarks and semi-landmarks (LM+SLM), 2) the landmarks only (LM), and 3) landmarks, semi-landmarks and helpers (LM+SLM+HLP). Rather than work with the landmark coordinates themselves, it is common in landmark based geometric morphometrics to use a thin-plate spline decomposition method to produce a basis set of scores along the eigenvectors of the bending energy matrix (see Bookstein 1991; Dryden and Mardia 1998). The thin-plate spline decomposition expresses the deformation of each specimen relative to the reference form as components (the Partial Warp plus Uniform Component Scores) along the eigenvectors of the bending energy matrix (the Principal Warp axes), and the patterns of deformation induced by affine deformations of the reference form (the Uniform Components, Bookstein, 1996b).

In addition to allowing for the production of the evocative deformation grid patterns that illustrate changes in shape (as seen in Figs. 5-7), the use of the thin-plate spline decomposition yields a set of variables for use in statistical analyses that have the same number of variables as degrees of freedom in the data. It is important to note that this use of the thin plate spline is not a method of data analysis or reduction that is comparable to a Relative Warp analysis (PCA based on Partial Warp scores). The Partial Warp scores are not being used to uncover "factors" influencing shape covariation or to deduce patterns of variation, but merely as a convenient set of replacement variables with which to carry out computations. The deformation diagrams, or "grid diagrams" ala D'Arcy Thompson, produced by the thin plate spline are dependent on the use of the thin-plate spline as an interpolation method for estimating deformation at points between landmarks, rather than

as a decomposition method. In fact, the thin-plate spline may be used purely as a drawing or rendering tool: any given set of predicted or measured deformation values at landmark locations may be depicted as a deformation grid by using the thin-plate spline purely as an interpolation function, without the necessity of using the partial warp scores as variables in the analysis.

In our analysis, we constructed regression models to depict the shape change that occurs during growth, as a function of change in relative (or proportionate) size. To form such a regression model, we carried out a multivariate regression of all of the Partial Warp plus Uniform Component scores on the log of the centroid size (Bookstein 1991) of the specimens. The regression model determines the portion of the variation in the shape "explained" by the covariation of shape with the relative size measure used (log centroid size). Note that this differs from a factor analysis or Principal Components Analysis approach in that we hypothesize initially that relative size is a factor influencing shape change and then determine the extent and nature of the shape change attributable to changes in relative size, rather than exploring the covariance structure within the data to determine the presence of one or more factors influencing shape change. Statistical tests are applied to the regression model to determine if the hypothesis that there is a significant correlation of shape with relative size is supported by a given data set or not.

For each protocol (LM, LM+SLM, LM+SLM+HLP) and alignment procedure (BE, D), the Partial Warp plus Uniform Component scores produced by a thin-plate spline decomposition (Bookstein, 1991) were computed using a GLS Procrustes reference form for each group, and then the multivariate regression model was computed based on this thin-plate spline decomposition. When working with semi-landmarks, the sliding of the semi-landmarks along the contour removes one degree of freedom from each semi-landmark. In addition four degrees of freedom are lost in the Procrustes superimposition process. Consequently, when the deformation is expressed as Partial Warp plus Uniform Component scores, there are still more variables than degrees of freedom in the Partial Warp plus Uniform Component scores when semi-landmarks are used in a study. Although the use of the thin-plate spline is no longer helpful statistically under these conditions, it is still of use graphically. The patterns of ontogenetic shape change in the meraspid specimens predicted by the regression model for each protocol are shown in Figs. 5 to 7. Similar results were obtained for a set of holaspid specimens not shown here.

The significance of the regression was tested using the Generalized Goodall's *F*-test (Rohlf 1998a), which computes an *F*-score from the ratio of the summed squared Procrustes distances of the shapes predicted by the regression model from the mean shape, to the summed squared Procrustes distances from the actual shapes of the specimens to the shapes predicted by the regression model. This is similar to the ratio of variance explained by the regression model to the unexplained variance. Rather than rely on an analytic model of the distribution of the Generalized Goodall's *F*-test, we employed a bootstrap procedure to determine the range of *F* scores produced under a null hypothesis of no relation between shape and log of centroid size. The percentage of bootstrap sets whose *F*-score exceeded the observed *F*-score provides an estimate of the significance of the regression

model. This resampling based test avoids the difficulties associated with the reduction in degrees of freedom in the data, and with the limited sample size relative to the number of variables used.

To form a univariate test of the significance of the regression model, we calculated the Procrustes distance of each specimen from the mean of the three smallest specimens in the group. These Procrustes distances were then regressed on log centroid size. We tested the significance of this regression model using the correlation coefficient r, and the test statistic 1/2log[(1+r)/(1-r)] (Freund and Walpole 1980), which is normally distributed with a variance of N-3, where N is the number of specimens.

6.5 Results

The meraspid specimens of *T. becki* showed statistically significant patterns of allometric shape change with log centroid size, for all configurations and alignment procedures (Table 1). Kim et al. (2002) found significant allometric changes in meraspid stage based on landmark data only with a much larger (72 specimen) data set, so the results shown here are consistent with the earlier work, despite the reduction in sample size.

The perpendicular projection method (Fig. 5 upper) yields depictions of the pattern of change that are very similar to those produced under the bending energy method (Fig. 5 lower). The patterns produced by the bending energy method are noticeably smoother than those produced by the perpendicular projection approach. Note the more abrupt changes in the grid curvature evident at the posterior lateral margins of the cranidium. This difference is a direct result of the fact in that the bending energy alignment method is based on the assumption that changes in the contours occurred in the smoothest possible manner, i.e., that this method seeks to disperse shape change over as broad a region as possible.

The landmark only configuration (Fig. 7) yields a similar pattern of overall ontogenetic shape change that is consistent with that produced by the landmark plus semi-landmark configurations (Figs. 5, 6). The landmark plus semi-landmark configurations, however, do pick up several features of ontogenetic change not visible in the diagram produced by the landmark only data. First, semi-landmark data permit resolution of ontogenetic shape change with considerably more detail. The landmark only analysis suggests a generalized widening that increases mildly to the posterior of the cranidium. In contrast, the landmark plus semi-landmark analysis reveals more localized changes in cranidium shape. Secondly, this greater definition of the shape change shows that the central part of the cranidium (the glabella) widens rather strongly relative to the surrounding regions (the "fixed cheeks"), which become dramatically

Table 1. Tests of the dependence of shape on log centroid size. For the multivariate data, the fraction of bootstraps sets that exceeded the observed *F*-value are shown along with the corresponding *p*-value

Configuration	Multivariate (Generalized Goodall's *F*)	Univariate (Correlation Coefficient *r*)
LM+SLM, D	0/100 $p<0.01$	0.9324 $p=5.71\times10^{-8}$
LM+SLM+HLP,D	0/100 $p<0.01$	0.9106 $p=.45\times10^{-7}$
LM+SLM, BE	0/100 $p<0.01$	0.9028 $p=1.28\times10^{-6}$
LM+SLM+HLP,BE	1/100 $p<0.01$	0.8663 $p=1.54\times10^{-5}$
LM Only	0/100 $p<0.01$	0.9669 $p=5.30\times10^{-11}$

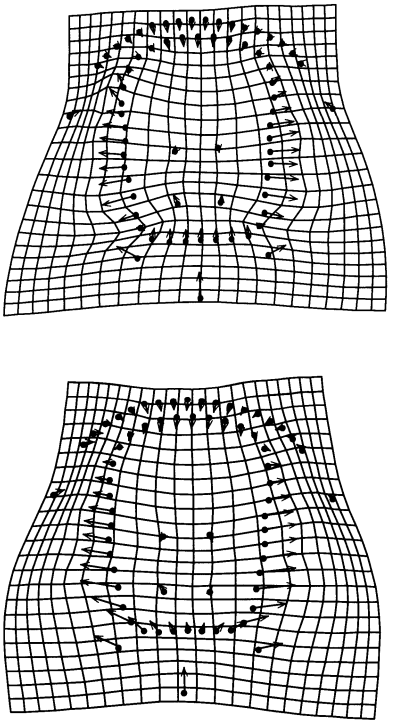

Fig. 5. A comparison of the regression models constructed from landmark plus semi-landmark data, the upper plot is the results obtained using the perpendicular projection method (D), the results based on bending energy method (BE) are shown in the lower plot

narrower. The greater definition of shape change also suggests a more pronounced anterior migration of the posterior tip of the palpebral lobe with a concomitant relative decrease in palpebral lobe length.

Thus the added detail and greater coverage of the cranidium afforded by the inclusion of semi-landmarks, not surprisingly, produces a much more nuanced description of the shape change that accompanied growth in *T. becki* meraspis. That this is a product of coverage rather than an effect peculiar to the semi- landmark technique is suggested by the intermediate degree of subtlety exhibited in the shape change description produced by the process when some of the semi- landmark points are treated as helper points (i.e., semi-landmark included in the process of aligning curves, but not in the spline decomposition of shape changes; Fig. 6).

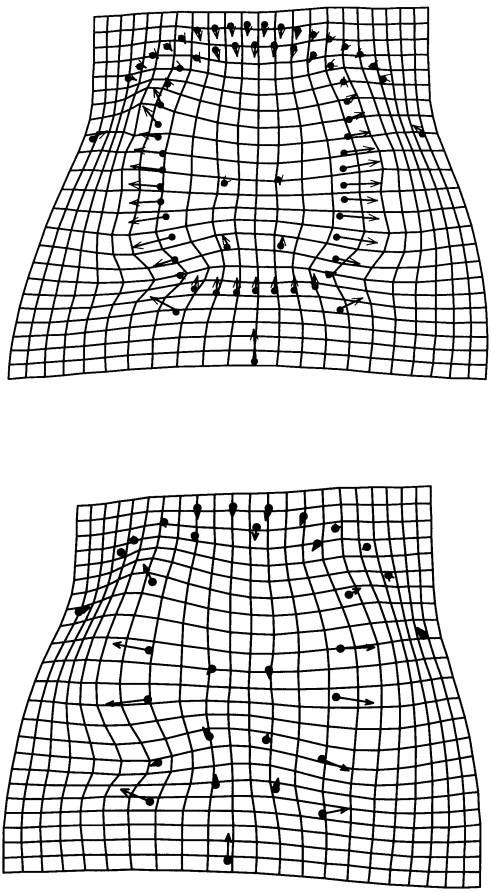

Fig. 6. A comparison of the regression models of meraspid growth based on all landmarks and semilandmarks (LM+SLM, upper plot) and on a protocol where the number of semi-landmarks was reduced by use of helper points (LM+SLM+HLP, lower plot). Perpendicular projection alignment of semi-landmarks was used in both cases

In this study, we have found that the incorporation of semi-landmark data yields results consistent with those based purely on landmark data, and may reveal features of shape change not evident in purely landmark based studies. These results are not strongly dependent on the choice of alignment procedure (perpendicular projection or bending energy) nor are they substantially altered by the choice to use helper points. This is an initial indication of the promise of semi-landmark methods for the study of shape, particularly for the inclusion of information about curved features of organisms that present few standard landmarks.

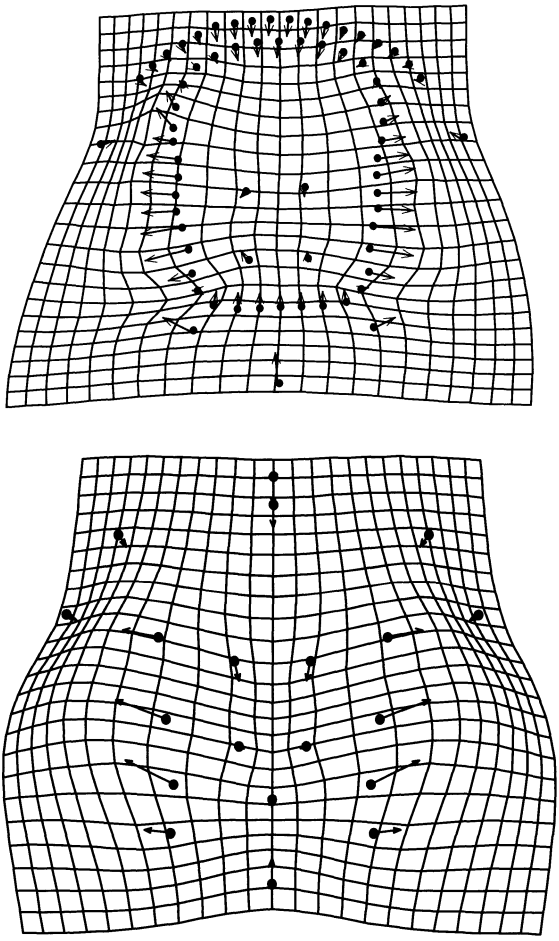

Fig. 7. A comparison of the regression models of meraspid growth based on all landmarks and semi-landmarks (LM+SLM, upper plot) and on landmarks only (LM, lower plot). Perpendicular projection alignment of semi-landmarks was used in the upper plot

6.6 Concerns about the Use of Semi-landmarks

Despite the agreement of landmark and semi-landmark based analyses seen here, and the promising features of the approach, there are some substantial concerns about the method.

1) Landmarks on two-dimensional surfaces have 2 degrees of freedom each, while semi-landmarks submitted to the semi-landmark alignment procedure have only one. All software that computes degrees of freedom based on the number of coordinates in an input file will have incorrect calculations of the degrees of freedom present when evaluating the results of statistical tests. This difficulty may be avoided by using only bootstrap or permutation based tests.

2) The number of semi-landmarks along a curve (either 16 or 40 in the two curves shown in the examples above) is much larger than the number of landmarks typically used in a study (11 in this case). This means that the semi-landmarks along a single curve may a "dominate" an analysis. One approach is to use "helper points", which are points arrayed between semi-landmarks along the curve and used to align the semi-landmarks (within Semiland6), but thereafter discarded prior to the calculations of statistics during the analysis. In his work on eigenshape methods, MacLeod (1999) has developed an algorithmic approach to determining the number of points necessary to represent a curve to a given level of accuracy, which would provide an objective criterion for the number of semi-landmarks and the number of helper points to use in a given study. Other approaches to the relative weighting of semi-landmarks and landmarks might also be possible. Additional work on software tools appears necessary.

3) The biological homology of the points along the curve has been debated (see discussions in Zelditch et al. 1995, MacLeod 1999, 2002a, 2002b). MacLeod (1999) presents a case that outline methods are not fundamentally different from landmark methods in the way they handle biological homology. While there may be debate about purely landmark methods as opposed to outline based methods, it seems clear that analyses utilizing semi-landmarks are not fundamentally different in their treatment of biological homology from outline-based methods. One must be careful to represent biologically homologous curves when setting up the study. It is the responsibility of the researcher to compare homologous features. While the thin-plate spline is a robust and reliable method for multivariate statistical analysis in many applications, it must be noted that its properties in positioning semi-landmarks along a curve have not been thoroughly explored. This issue warrants further investigation.

6.7 Acknowledgements

We thank Ashraf Elewa for the opportunity to contribute to this volume and Norman MacLeod, Mark Webster, and Jaap Kaandorp for their insightful reviews.

References

Bookstein FL (1991) Morphometric tools for landmark data:Geometry and Biology. Cambridge University Press, New York

Bookstein FL (1996a) Applying landmark methods to Biological Outline Data. In: Mardia KV, Gill CA, Dryden IL (eds) Image Fusion and Shape Variability, pages 79-87. University of Leeds Press, Leeds

Bookstein FL (1996b) Standard formula for the uniform shape component in landmark data. In: Marcus LF, Corti M., Loy A., Naylor GJP, Slice DE (eds) Advances in Morphometrics. Plenum, New York

Bookstein FL (1997) Landmark methods for forms without landmarks: Localizing group differences in outline shape. Medical Image Understanding 66:97-118

Bookstein FL, Streissguth AP, Sampson PD, Connor PD, Barr HM (2002) Corpus Callosum Shape and Neuropsychological Deficits in Adult Males with Heavy Fetal Alcohol Exposure. NeuroImage 15:233-251

Dryden IL, Mardia KV (1998) Statistical Shape Analysis. Wiley, Chicester

Freund JE, Walpole RE (1980) Mathematical Statistics. Prentice Hall, New Jersey

Green WDK (1996) The thin-plate spline and images with curving features. In: Mardia KV, Gill CA, Dryden IL (eds) Image Fusion and Shape Variability, pages 79-87. University of Leeds Press, Leeds

Gower JC (1975) Generalized Procrustes analysis. Psychometrika. 40:33-51

Kim K, Sheets HD, Haney RA, Mitchell CE (2002) Morphometric analysis of ontogeny and allometry of the Middle Ordovician trilobite *Triarthrus becki*. Paleobiology 28:364-377

Lohmann GP (1983) Eigenshape analysis of microfossils: A general morphometric procedure for describing changes in shape. Mathematical Geology 15:659-672

Lohmann GP, Schweitzer PN (1990) On Eigenshape Analysis. In: Rohlf FJ, Bookstein FL (eds) Proceedings of the Michigan Morphometrics Workshop. University of Michigan Museums, Ann Arbor

MacLeod N (1999) Generalizing and extending the eigenshape method of shape space visualization and analysis. Paleobiology 25:107-138

MacLeod N (2002a) Morphometrics. In: Pagel MD (ed) Encyclopedia of Evolution. Academic Press, London

MacLeod N (2002b) Phylogenetic signals in morphometric data.In MacLeod N, Forey PL (eds). Morphology, shape and phylogeny. Taylor and Francis, London

Rohlf FJ (1986) Relationships among eigenshape analysis, Fourier analysis and analysis of coordinates. Mathematical Geology 18:845-854

Rohlf FJ (1990) Fitting curves to outlines. In: Rohlf FJ, Bookstein FL (eds) Proceedings of the Michigan Morphometrics Workshop. University of Michigan Museums, Ann Arbor

Rohlf FJ (1996) Introduction to outlines. In: Marcus LF, Corti M, Loy A, Naylor GJP, Slice DE (eds) Advances in Morphometrics. Plenum, New York

Rohlf FJ (1998a) TPSRegress, version 1.18, TPSSmall, version 1.17. Available at http://life.bio.sunysb.edu/morph/

Rohlf FJ (1998b) On applications of geometric morphometrics to studies of ontogeny and phylogeny. Systematic Biology 47:147-158

Rohlf FJ (1999) Shape statistics: Procrustes superimpositions and tangent spaces. Journal of Classification 16:197-223

Rohlf FJ (2002) TPS software series, available at http://life.bio.sunysb.edu/morph/.

Rohlf FJ, Marcus LF (1993) A revolution in morphometrics. Trends in Ecology and Evolution 8(4):129-132

Rohlf FJ, Slice DE (1990) Extensions of the Procrustes method for the optimal superimposition of landmarks. Systematic Zoology 39:40-59

Sampson PD, Bookstein FL, Sheehan FH, Bolson EL (1996) Eigenshape analysis of left ventricular function from contrast ventriculograms. In: Marcus LF, Corti M, Loy A, Naylor GJP, Slice DE (eds) Advances in Morphometrics. Plenum, New York

Sheets HD (2002) IMP software series, available at http://www.canisius.edu/~sheets/morphsoft.html/

Slice DE (2001) Landmark coordinates aligned by Procrustes Analysis do not lie in Kendall's shape space. Systematic Biology 50(1) 141-149

Zelditch ML, Fink WL, Swiderski DL (1995) Morphometrics, homology and phylogenetics: quantified characters as synapomorphies. Systematic Biology 54:179-189

Zelditch ML, Sheets HD, Fink WL (2000) Spatiotemporal reorganization of growth rates in the evolution of ontogeny. Evolution 54:1363-1371

7 Morphological analysis of two- and three-dimensional images of branching sponges and corals

Jaap A. Kaandorp and Rafael A. Garcia Leiva

Section Computational Science, Faculty of Science, University of Amsterdam, Kruislaan 403, 1098 SJ Amsterdam, The Netherlands, jaapk@science.uva.nl

7.1 Abstract

Morphological analysis of the growth forms of corals (and other marine sessile organisms) is an important prerequisite for research on these organisms. A quantitative morphological analysis is required in studies on the morphological plasticity in marine sessile organisms. To verify simulation models of growth and form of branching sponges and corals, a morphological comparison between actual and simulated forms is essential. We will discuss a number of methods suitable for the quantitative morphological comparison of branching forms. Methods will be discussed for computing measurements based on medial axes (the morphological skeleton) in two- and three-dimensional images of branching structures.

Keywords: Scleractinian corals, sponges, morphological skeletons, morphological analysis of indeterminate growth forms.

7.2 Introduction

Many marine sessile organisms, as for example coralline algae, sponges, hydrocorals, stony corals and bryozoans, exhibit considerable morphological plasticity; in many cases this is related to the impact of the physical environment. Examples of studies in which morphological plasticity and the relation to the physical environment have been investigated are: local light intensities and growth forms of the stony corals *Montastrea annularis* (Barnes 1973; Graus and Macintyre 1982) and *Porites sillimaniani* (Muko et al. 2000); variations in morphology due to differences in exposure to water in coralline algae (Bosence 1976), the sponge *Haliclona oculata* (Kaandorp and de Kluijver 1992), the hydrocoral *Millepora* spp. (Stearn and Riding 1973; de Weerdt 1981), the scleractinian corals *Pocillopora damicornis* (Lesser et al. 1994), *Madracis mirabilis* (Sebens et al. 1997, Kaandorp

et al. 2003) and *Agaricia agaricites* (Helmuth and Sebens 1993), and the bryozoan *Electra pilosa* (Okamura and Partridge 1999).

An important complication in the morphological analysis of growth forms of scleractinian corals and many other marine sessile organisms, is that the growth forms are usually indeterminate and complex. Most methods for the analysis of growth and form use landmark-based geometric morphometrics (Bookstein 1991; Chaplain et al. 1999). These methods are more suitable for unitary organisms and less applicable for the analysis of indeterminate growth forms of modular organisms (Harper et al. 1986). In a number of cases the organism is built from well-defined modules (for example the corallites in scleractinian corals or zooids in bryozoans), in other cases the module itself has no well-defined shape but an irregular and indeterminate form (for example an osculum and its corresponding aquiferous system in sponges). For organisms with well-defined modules it is possible to apply landmark-based methods for the morphometrics of individual modules. For example, Budd et al 1994 and Budd and Guzman 1994 used landmark-based methods to measure the corallites in a scleractinian coral.

The development of methods for quantifying the morphology of indeterminate growth forms of marine sessile organisms is an important prerequisite for further research on these organisms in a number of areas. A potential application area for morphological analysis of growth forms is in studies where the growth form is used to assess the state of the physical environment. In bio-monitoring studies on current environmental conditions or studies on the paleo-environment, it might be possible to detect environmental changes based on growth forms by applying a morphological analysis, possibly aided by information obtained from simulation models. These organisms represent very suitable subjects for developing simulation models of morphogenesis, as several important simplifications concerning their growth process can be made. In many cases the growth process can be described as accretive, where layers of new material are deposited on top of the preceding growth stages, which remain unchanged. Furthermore the influence of the physical environment can be reduced to a few dominant parameters, among the most important of these the amount of water movement and local light intensities. In a number of studies (Kaandorp and Sloot 2001; Kaandorp and Kübler 2001; Merks et al. 2003) simulation models of the morphogenesis of organisms with radiate accretive growth have been developed. To verify these simulation models, a morphological comparison between actual and simulated forms is essential. One of our ultimate aims is to study the growth and form of these organisms through a combination of simulation models and morphological analysis. The idea is that by analysing growth forms from a certain marine sessile organism and morphological simulation models, it might be possible to identify some generic effects of the impact of physical environment on the overall growth form of organisms with accretive growth, and to distinguish these from species-specific morphological features, which are presumably controlled by genetic regulation.

In previous studies (Kaandorp 1999; Kaandorp and Kübler 2001; Abraham 2001) methods have been developed for the morphological analysis of two-dimensional images of branching marine sessile organisms. In these studies the analysis is based on the construction of a two-dimensional morphological skeleton

within the image of the branching object by applying a thinning algorithm (for an overview of these algorithms see Jonker and Vossepoel 1995). The morphological skeleton, or medial axis, of the branching object can be used to measure various biologically relevant parameters as for example the diameter of the branches, branching rate, branching angles and branch spacing. In for example studies on particle capture in the branching stony coral *Madracis mirabilis* (see Fig. 1) and the influence of hydrodynamics (Sebens et al. 1997), it was demonstrated that branch diameters and branch spacing are crucial morphological properties. The diameter of the branches and spacing between branches is variable and may be controlled by a combination of hydrodynamics and genetics. Sebens et al. (1997) argue that through modifications of its branch structure and branch spacing, *Madracis mirabilis* can function efficiently as a passive suspension feeder over a wide range of exposure to water movement. An important limitation in the two-dimensional studies is that this method only works well for growth forms which tend to form a branching pattern in one plane, for example the sponge *Raspailia inaequalis* analysed by Abraham (2001). For many stony corals, where usually three-dimensional branching structures are formed with branches in all directions, as for example in *Madracis mirabilis*, this method does not provide optimal results. By occlusion effects branches of the growth form overlap other branches and it is not possible to distinguish the complete branching structure on the two-dimensional image.

In a preliminary study (Kaandorp and Kübler 2001) we have have tried to solve this problem of occluding branches in complex-shaped scleractinian corals, by analysing three-dimensional images obtained with Computed Tomography scanning techniques. The three-dimensional morphological skeleton of these images was constructed by applying the thinning algorithm described by Tsao and Fu (1981). This skeleton can be used to measure several morphological properties, such as the thickness of branches and the determination of branching points, branching angles, branch spacing etc. A major problem with the thinning algorithm described by Tsao and Fu (1981) was that it gives reasonable results only for relatively simple branching objects. One of the major pitfalls in many of the three-dimensional thinning techniques is the generation of new branches due to small perturbations at the surface of the object. This phenomenon is demonstrated in Fig. 2. In Fig. 2A the morphological skeleton consists of one medial axis, and in Fig. 2B the addition of a small perturbation results in the formation of a new side branch. Especially for large complex-shaped three-dimensional objects, such as those shown in Fig. 1, the result is a highly complex ("bushy") skeleton. For practical measurements this complicated structure is virtually useless.

Recently we solved this problem of the formation of "bushy" skeletons by analyzing the images with a 3D thinning algorithm developed by Ma and Sonka (1996). This algorithm has been specifically designed to extract the skeleton of images of pulmonary airway trees. The first part of the paper will briefly introduce the thinning procedure and the extraction of medial axes (the morphological skeleton) in relatively simple 2D images of the sponge *Haliclona oculata* and discuss how various measurements can be defined, using the morphological skeleton. Measurements on 2D images of a sponge (*Haliclona oculata*), a hydro-coral (*Mil-*

(*Millepora alcicornis*) and a scleractinian coral (*Pocillopora damicornis*) can be found elsewhere (Kaandorp 1999). In the second section of the paper we will briefly describe the acquisition of the three-dimensional images of the scleractinian coral *Madracis mirabilis*, which we have used as a case-study. Finally we will briefly describe the application of the three-dimensional thinning procedure of Ma and Sonka (1996), and show measurements obtained with this method. The application will be demonstrated using a simple three-dimensional image of a simulated branching object. Preliminary results using the actual data sets depicted in Fig. 1 will be shown. Mathematical details regarding the 3D thinning algorithms are beyond the scope of this paper and can be found elsewhere (Jonker and Vossepoel 1995; Ma and Sonka 1996).

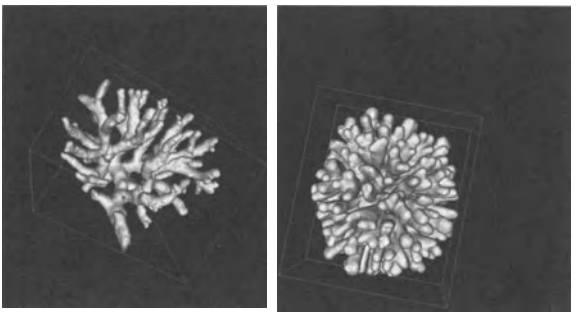

Fig. 1. Surface renderings of CT-scans of the coral *Madracis mirabilis*} (A) thin-branching low-flow morphology (B) compact high-flow morphology. Both morphs are visualized on the same scale. The dimensions of the actual objects shown in (A) and (B) are respectively 13 cm × 8 cm × 11 cm and 11 cm × 10 cm × 6 cm

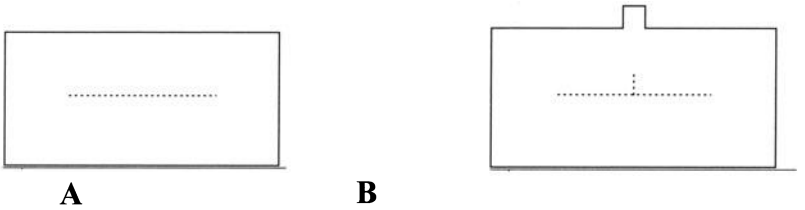

Fig. 2. A. Construction of a morphological skeleton in a cylindrical object. B. Formation of a new side branch due to a small perturbation on the surface of the object

7.3 Methods

7.3.1 Measurements in two-dimensional images

The morphological skeleton in a two-dimensional image was obtained by applying the two-dimensional thinning algorithm developed by Zhang and Suen (1984). The skeleton is defined by connecting the center points of the maximal discs which fit exactly within the contour (Rosenfeld and Kak 1982). As an example, Fig. 3A shows the morphological skeleton constructed within the contour of the sponge *Haliclona oculata* (Kaandorp 1999) in Fig. 3B. In the construction of the morphological skeleton several artefacts may be generated. By occlusion effects some branches of the growth form may overlap other branches and produce junctions that are not actually present; furthermore, contamination and damage at the object (for example at the holdfast of the organism) may produce "false" junctions. In many marine sessile organisms (for example in many sponges) real junctions are also present; these are formed by fusion of branches (anastomosis). In the morphological measurements, both "false" junctions and junctions formed by anastomosis have to be detected by comparing the images to the actual objects and are not used in the measurements.

A B

Fig. 3. A. Morphological skeleton constructed within the contour shown in B. In B the contour picture is shown of the sponge *Haliclona oculata* (Kaandorp 1999)

The diameter was measured for two types of maximal discs: the diameter *da* of the disc *a* with a center point at a junction of the morphological skeleton, and the

diameter *db* of the disc adjacent to disc *a*. Disc *b* was measured in an area of the contour which represents a younger part of the organism compared with the area where disc *a* was located. Both types of discs are shown in Fig. 4. The diameter *da* represents an estimation of the maximal thickness of a branch, while *db* is an estimation of the minimal thickness. The measurement *rb* is the branching rate, and is defined by the length of an edge connecting the centers of two successive *a* discs. A low value of *rb* indicates a high branching rate, while high values indicate relatively slow formation of branches during the growth process. Two types of angles were measured using the skeleton: *b_angle* is the branching angle, and is defined by the intersection points of the skeleton and the outer circle of disc *a*; *g_angle* is the geotropy angle, and is defined by the angle between the vector connecting two successive *a* discs and the positive *y*-axis. The *y*-axis in the construction of *g_angle* corresponds to the original growth position, and is directed away from the substrate. The angle *g_angle* expresses the degree in which the organism tends to grow away from substrate.

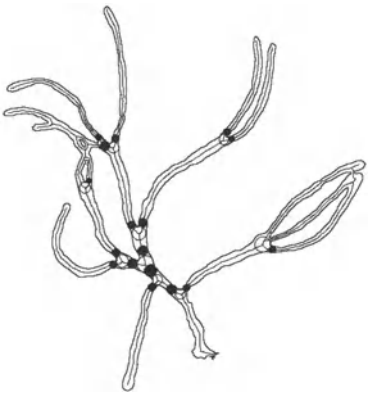

Fig 4. Construction of the maximum discs *a* (open discs) and *b* (solid discs) within the contour of the sponge *Haliclona oculata* shown in Fig. 3B

In Fig. 5 the measurements of the diameter *br_spacing* are depicted in a contour of the sponge *Haliclona oculata*. The diameter *br_spacing* is defined as the radius of a maximum disc which can be constructed using the tip of the skeleton, located at the tip of a branch, and construction stops when the outer circle of the disc intersects with a part of the skeleton which is not directly connected to a part of the skeleton situated within the maximum disc. The standard deviation of *br_spacing* expresses the degree to which branches tend to fuse; a relatively low value indicates that there is a low degree of self-intersection between branches, while a high value shows that there is no mechanism present preventing self-

intersection, and anastomosis of branches may occur. In a number of cases the value of *br_spacing* is undefined, for example when the tip of the root of the object shown in Fig. 5 is used as the center of construction. In morphological measurements these non-valid centers were not used and have to be removed in a step which involves visual inspection of the data.

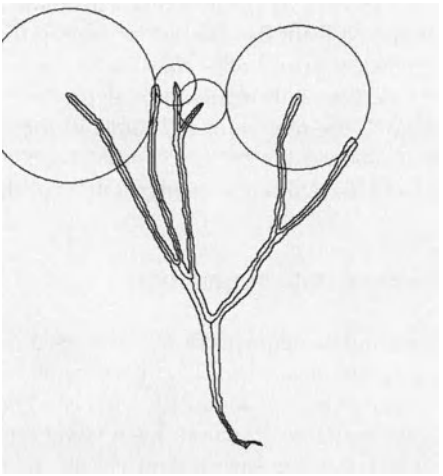

Fig 5. Construction of four *br_spacing* maximum discs using the tips of the skeleton situated in the branches of a contour of the sponge *Haliclona oculata* as centers of construction

The algorithm with which *da, d, b_angle, g_angle, rb,* and *br_spacing* were measured can be subdivided into five stages:

1. Determination of the morphological skeleton.
2. Determination of the junctions in the skeleton.
3. Determination of the *a* discs at the junctions of the morphological skeleton, where "false" junctions and junctions formed by anastomosis are detected by visual inspection of the data set and are eliminated.
4. Measurement of *b* discs, *rb* lengths, and the angles *b_angle* and *g_angle* in successive order by retracing the morphological skeleton. The endpoints of the skeleton, located within the tips of the branches, are determined. Non-valid endpoints are detected by visual inspection of the data set and are eliminated. Retracing starts at the root of the skeleton, which is close to the holdfast of the object.
5. Construction of the *br_spacing* discs, using the endpoints of the skeleton as centers of construction.

After this procedure an ordering of the *a* discs is possible. Since the skeleton is retraced starting near the holdfast, arrangement of the *a* discs in the order of emergence during the growth process can be ensured; i.e. an *a* disc which is directly connected via the skeleton to a previous *a* disc will be younger than its predecessor. Furthermore this procedure ensures that the *b* disc is positioned within the

contour (immediately after an *a* disc) representing a part of the organism which was added to the organism after the formation of the part in which the previous disc *a* is located. The branching angle, *b_angle*, is measured in branches formed after the part represented by disc *a*, while in the measurement of the geotropy angle, *g_angle*, the direction of the vector connecting two successive *a* discs can be unambiguously determined and corresponds to the growth direction. A complication in the algorithm is the occurrence of loops (in Fig. 4 several loops can be observed). The loops were caused by occlusion and fusion of branches. Before stage 4, loops have to be removed from the data set by cutting the morphological skeleton at points where branches fuse. Loops may cause the *a* discs to be arranged in reverse order to their emergence during the growth process.
Before stage 5, in stage 4, the non-valid endpoints of the morphological skeleton have to be removed. In Stage 5 the *br_spacing* discs are constructed at valid tips of the skeleton, which are located in the youngest parts of the growth form.

7.3.2 Three-dimensional data acquisition

For the three-dimensional data acquisition we have used X-ray Computed Tomography (CT) scanning techniques. The CT scan data consists of $512 \times 512 \times z$ ($20 \leq z \leq 50$) three-dimensional pixels, so-called "voxels". The slice thickness of the CT scan data is 2.5 mm in the *xy* direction. Each voxel represents a density value between 0 and 2^{12}, where 0 is the lowest density (the air around the coral skeleton), while high values indicate the calcium carbonate of the coral skeleton. In Fig 1 the CT scans of *Madracis mirabilis* are visualized with a surface rendering technique. The surface was constructed with the marching cube technique discussed in Lorensen and Cline (1987). The surface is constructed approximately at the boundary between air and the calcium carbonate skeleton of the coral. With this technique, using the original data set of $512 \times 512 \times z$ voxels, an image is reconstructed with an equal resolution in *x, y*, and *z* directions (see for details Schroeder et al. 1997). On the voxels representing the surface of the corals a triangulated mesh was constructed using this surface rendering technique. This triangulated surface representation can be used to map the form onto a lattice of 512^3 voxels, with an equal resolution in the *x, y,* and *z* directions. This lattice representation can be used as the input data set for a three-dimensional thinning algorithm.

7.3.3 Three-dimensional measurements based on the morphological skeleton

For the thinning of the three-dimensional images we have applied the algorithm from Ma and Sonka (1996). For obtaining medial axes and medial surfaces in three-dimensional images a large number of algorithms are described (an overview is given by Jonker and Vossepoel (1995). In Fig. 6 the 3D thinning algorithm was applied in a simple branching three-dimensional data set. The branching object in Fig 6 was generated with a simulation model (for details regarding the

simulation model, see Kaandorp and Kübler 2001). In Fig 6 the branching object is visualized as a transparant object, within the object the medial axis is shown as a solid line. In Fig 6 the same measurements as discussed in the section above are constructed in three dimensions. In Fig. 6A the *a*-spheres are constructed at the junctions of the morphological skeleton. In Fig 6B the *b* spheres are positioned within the surface of the branching object immediately after an *a*-sphere. The branching angle, *b_angle* (Fig 6C), is measured in branches formed after the part represented by the *a*-sphere, while in the measurement of the geotropy angle, *g_angle* (Fig. 6D), the angle between the vector connecting two successive *a*-spheres and the positive *y*-axis was computed. The branching rate *rb* (Fig. 6E) is the length of an edge connecting the centers of two successive *a*-spheres. The branch spacing *br_spacing* is the radius of a maximum sphere, the centre of the sphere is located at the tip of a branch, and the extension of the sphere stops when a part of the skeleton is reached, which is not connected to a part of the skeleton situated within the *br_spacing* sphere (Fig 6F).

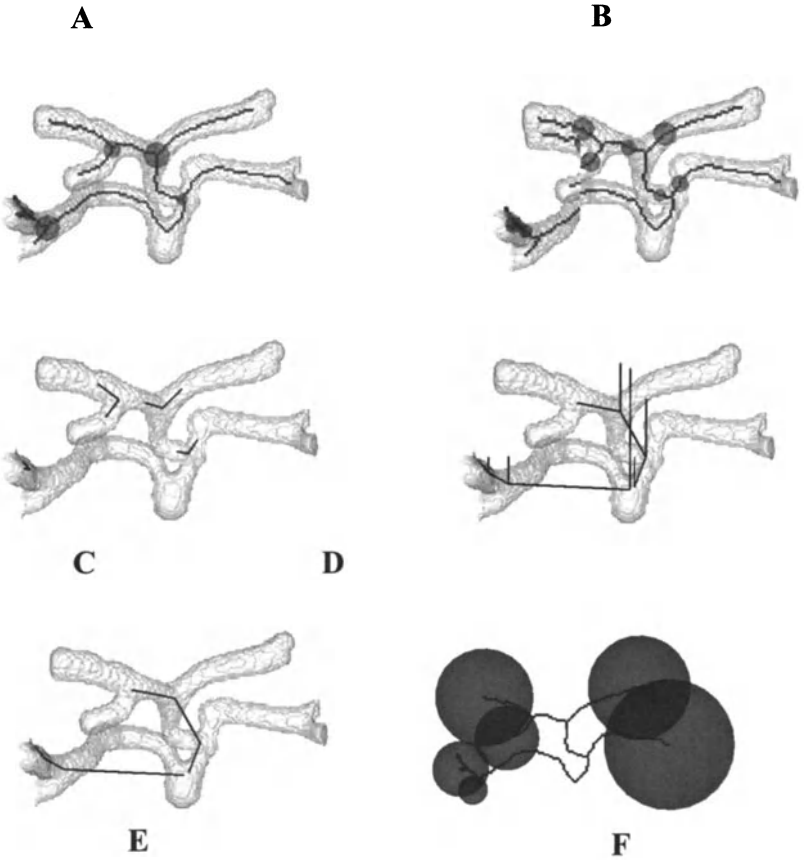

Fig 6. Construction of the *a*-spheres (A), *b*-spheres (B), branching angle *b_angle* (C), geotropy angle *g_angle* (D), branching rate *rb* (E) and branch spacing *br_spacing* (F) in a simulated object

7.4 Results

The three-dimensional thinning algorithm of Ma and Sonka (1996) was used to measure diameters of the *a*-spheres and *b*-spheres, branching angle *b_angle*, geotropy angle *g_angle*, branching rate *rb* and branch spacing *br_spacing* in the three-dimensional image of *Madracis mirabilis* shown in Fig 1. Fig. 7 shows the morphological skeleton constructed with the three-dimensional image of Fig. 1A. The measurements, based on this skeleton, are summarized in Table 1.

Table 1. Measurements of the *a*-spheres, *b*-spheres, branching angle *b_angle*, geotropy angle *g_angle*, branching rate *rb* and branch spacing *br_spacing* in the three-dimensional image of *Madracis mirabilis* shown in Fig. 1A

measurement	Number of elements	Mean value
a-sphere	234	0.32±0.08 cm
b-sphere	98	0.29±0.08 cm
b_angle	211	1.65±0.54
g_angle	101	1.37±0.63
rb	90	0.80±0.51 cm
br_spacing	228	0.31±0.50 cm

Fig. 7. Construction of the morphological skeleton within the three-dimensional image of *Madracis mirablis* colony shown in Fig. 1A

7.5 Discussion

In Fig. 7 it is demonstrated that it is possible to construct a morphological skeleton within a three-dimensional image of *Madracis mirabilis* and to use this skeleton

for measuring diameters and angles (see Table 1). Although the three-dimensional image in Fig. 1A is relatively simple, without any obvious anastomosis of branches, several loops formed in the measurement procedure. For ensuring the correctness of the measurement procedure these loops have to eliminated from the data set in a visual inspection step (stage 3 in the algorithm described above). Loops in the morphological skeleton can be formed by various causes:

1. Artificial fusion of branches due to a low resolution of the CT scan images, where branches seem to anastomose and the separation between the branches cannot be detected.
2. Real anastomosis of branches. Careful inspection of the 3D image of *Madracis mirabilis* in Fig 1B shows that especially at the base, near the holdfast of the colony, fusion of branches frequently occurs.
3. Loop formation through ``contamination'' of the data set. For example by the presence of boring and encrusting organisms, branches seem to fuse in the three-dimensional image.
4. Artificial fusion of branches due to self-occlusion in two-dimensional images.

The loop formation is still a problematic issue in the two-dimensional analysis of more complex branching structures (compared to the relatively simple images of *Haliclona oculata* shown in Fig. 3) and in the analysis of more complex three-dimensional branching structures as shown in Fig. 1B. In both cases this problem can be prohibitive in the morphological analysis. In Fig 1A it is still possible to remove the fusions manually. In Fig 1B, the thinning process results in a highly complex three-dimensional branching structure, which makes manual removal of loops virtually impossible. The loops in Fig. 1B are caused by a combination of the first three points mentioned above, which makes a useful morphological analysis of object Fig. 1B currently impossible. Furthermore it should be noted that for the determination of the branch spacing *br_spacing*, another visual inspection step in stage 4 of the algorithm is needed. Invalid construction points may lead to a very large *br_spacing* values while small perturbation at the surface may lead to the formation of very small branches, leading to a very small values of *br_spacing*. This explains the awkward values for the *br_spacing* in Table 1. For this reason, the *br_spacing* in Table 1 are not reliable.

Currrently we are working on solutions of the problems mentioned above. Here we are using the following approaches:

1. The resolution of the three-dimensional images can be improved by increasing the resolution of the CT scans.
2. Detection of real fusions and artificial anastomosis due to contaminations is still a problematic issue. It is difficult (and may be even impossible) to represent a fusion of branches in a useful mathematical form, which can be used in an algorithm.
3. Improvement of the interactive visual inspection step, required in stages 3 and 4 of the algorithm. Currently we are working on three-dimensional visualisation environments in which these data sets can be processed and loops and invalid construction points can be removed interactively. Alternatively it is possible to isolate branches from the three-dimensional image, shown in

Fig. 1B, and to simplify the loop formation problem and to do a series of measurements on separated branches.

The measuring method, based on morphological skeletons, can be used to determine morphological invariants (diameters of branches, angles etc.) in indeterminate growth forms of branching organisms, which cannot be easily morphologically characterized by landmark-based methods. In this paper we focused on six types of measurements. The branching structure can also be used in a Horton-Strahler analysis (see Kaandorp and Kübler 2001) of the ordering of branches, and analysis of various types of fractal dimensions (Kaandorp and Kübler 2001), provided that the resolution of the images is sufficient to do measurements on a range of scales. The measuring method works well in two-dimensional images of branching organisms, with a relatively simple branching pattern (for example the sponge *Haliclona oculata* shown in Fig 3). For measurements in more complex objects only a three-dimensional version of the method will provide useful results. In a three-dimensional branching structure, without too many fusions, the method (with the exception of the *br_spacing* measurements) gives reasonable results. For the analysis of more complex morphologies, as shown in Fig 1B, the development of a three-dimensional interactive visualization environment is needed, in combination with high resolution images.

7.6. Acknowledgements

The CT-scans were made within a collaborative project with R.P.M. Bak (Netherlands Institute for Sea Research), M.J.A. Vermeij (Cooperative Institute for Marine and Atmospheric Studies, Miami, USA) and L.E.H. Lampmann (St. Elisabeth Hospital Tiburg, The Netherlands) on modelling and analysis of growth and form of *Madracis* species. We would like to thank Øyvind Hammer of the Physics of Geological Processes (PGP) and the Geological Museum, University of Oslo, Norway, for going so carefully to our text.

References

Abraham ER (2001) The fractal branching of an arborescent sponge. Mar Biol 138:503-510

Barnes DJ (1973) Growth in colonial scleractinians. Bull Mar Sci 23:280-298

Bookstein FL (1991) Morphometric tools for landmark data: geometry and biology. Cambridge University Press, New York

Bosence DWJ (1976) Ecological studies on two unattached coralline algae from western Ireland. Palaeontology 19:365-395

Budd AF, Johnson KG, Potts DC (1994) Recognizing morphospecies in colonial reef corals: I. Landmark-based methods, Paleobiology 20: 484-505

Budd AF, Guzman HM (1994) *Siderastrea glynni*, a new species of scleractinian coral (cnidaria:anthozoa) from the eastern pacific. Proc Biol Soc Wash 107: 591-599

Chaplain MAJ, Singh, McLachlan JC (1999) On growth and form, spatio-temporal pattern formation in biology. Wiley, New York

de Weerdt WH (1981) Transplantation experiments with Caribbean *Millepora.* Bijdr Dierk 51:1-19

Graus RR, Macintyre IG (1982) Variation in growth forms of the reef coral *Montastrea annularis* (Ellis and Solander): a quantitative evaluation of growth response to light distribution using computer simulation, Smithson. Contr Mar Sci 12: 441-464

Harper JL, Rosen BR, White J (1986) The growth and form of modular organisms. The Royal Society London, London

Helmuth B, Sebens K (1993) The influence of colony morphology and orientation to flow on particle capture by the scleractinian coral *Agaricia agaricites* (Linnaeus). J. Exp. Mar Biol Ecol 165:251-278

Jonker PP, Vossepoel AM (1995) Mathematical morphology in 3D images: comparing 2D & 3D skeletonization algorithms. In: Wojciechowski (ed.) BENEFIT Summer School on Morphological Image and Signal Processing, Zakopane, Silesian Technical University, ACECS, Gliwice, Poland

Kaandorp JA, de Kluijver MJ (1992) Verification of fractal growth models of the sponge *Haliclona oculata* (Porifera; class Demospongiae) with transplantation experiments. Mar Biol 113:133-143

Kaandorp JA (1999) Morphological analysis of growth forms of branching marine sessile organisms along environmental gradients Mar Biol, 134:295-306

Kaandorp JA, Kübler JE (2001) The algorithmic beauty of seaweeds, sponges and corals, Springer-Verlag, Heidelberg, New York

Kaandorp JA, Sloot PMA (2001) Morphological models of radiate accretive growth and the influence of hydrodynamics, J Theor Biol 209:257-274

Kaandorp JA, Koopman EA, Sloot PMA, Bak RPM, Vermeij MJA, Lampmann LEH (2003) Simulation and analysis of flow patterns around the scleractinian coral *Madracis mirabilis* (Duchassaing and Michelotti). Phil Trans R Soc Lond B 358:1551 - 1557

Lesser MP, Weis VM, Patterson MR, Jokiel PL (1994) Effects of morphology and water motion on carbon delivery and productivity in the reef coral, *Pocillopora damicornis* (Linnaeus): diffusion barriers, inorganic carbon limitation, and biochemical plasticity. J Exp Mar Biol Ecol 178:153-179

Lorensen WE, Cline HE (1987) Marching cubes: a high resolution 3D surface construction algorithm. ACM Computer Graphics 21:163-169

Ma CM, Sonka M (1996) A fully parallel 3D thinning algorithm and its applications.Computer Vision and Image Understanding 64: 420-433

Merks RMH, Hoekstra AG, Kaandorp JA, Sloot PMA (2003) Models of coral growth: Spontaneous branching, compactification and the Laplacian growth assumption, J Theor Biol 224: 153-166

Muko S, Kawasaki K, Sakai K, Takasu F, Shigesada N (2000) Morphological plasticity in the coral *Porites sillimaniani* and its adaptive significance. Bull Mar Sci 66:225-239

Okamura B, Partridge JC (1999) Suspension feeding adaptations to extreme flow environments in a marine bryozoan. Biol Bull 196:205-215

Rosenfeld A, Kak AC (1982) Digital Picture Processing, Academic Press, New York

Schroeder W, Martin K, Lorensen B (1997) The Visualization Toolkit: An Object-Oriented Approach To 3D Graphics, 2nd edition. Prentice Hall, New Jersey

Sebens KP, Witting J, Helmuth B (1997) Effects of water flow and branch spacing on particle capture by the reef coral *Madracis mirabilis* (Duchassaing and Michelotti). J Exp Mar Biol Ecol 211:1-28

Stearn CW, Riding R (1973) Forms of the hydrozoan *Millepora* on a recent coral reef. Lethaia 6: 187-200

Tsao YF, Fu KS (1981) A parallel thinning algorithm for 3-D pictures. Computer Graphics and Image Processing 17: 315-331

Zhang TY, Suen CY (1984) A fast parallel algorithm for thinning digital patterns. Communications of the ACM 27:236-239

8 Geometric morphometric analysis of head shape variation in four species of hammerhead sharks (Carcharhiniformes: Sphyrnidae)

Mauro J. Cavalcanti

Departamento de Vertebrados, Museu Nacional/Universidade Federal do Rio de Janeiro, Quinta da Boa Vista, São Cristóvão, Rio de Janeiro, RJ, CEP 20940-040, Brazil, maurobio@acd.ufrj.br

8.1 Abstract

Patterns of head shape variation in four species of hammerhead sharks of the genus *Sphyrna* (*S. lewini*, *S. tiburo*, *S. tudes*, and *S. zygaena*) were analyzed using geometric morphometrics methods. The analysis was performed on the coordinates of 8 anatomical landmarks defined on the basis of external morphology and homologous among the species, reconstructed from distance measurements among the landmarks, using a truss scheme and a modified multidimensional scaling algorithm. The landmark coordinates for each specimen were aligned by generalized Procrustes analysis and entered into a thin-plate splines relative warp analysis. Shape differences among the species were investigated using both the uniform and non-uniform shape components. Canonical variates analysis of the partial warp scores were used to compare patterns of interspecific variation and multiple regression analysis of the shape components on centroid size was used to examine for intraspecific variation.

The uniform components accounted for most of the statistically significant shape differences among the species. There were also differences among species with respect to the non-uniform shape components. The first relative warp depicted a lateral expansion and an anterior compression of the head, whereas the second relative warp displayed a lateral compression and posterior expansion of it. *Sphyrna. tiburo* and *S. tudes* were separated from *S. lewini* and *S. zygaena* along the first relative warp. The major non-affine shape differences (local deformations) were associated to a relatively larger snout and smaller head in *S. tiburo* and *S. tudes*. Significant intraspecific shape changes with increasing size were found for two species, *S. lewini* and *S. zygaena*. The largest variation observed with size increase was associated to the uniform compression of the head on its anteroposterior axis and a localized lateral compression of the snout.

No clear evolutionary trend could be unequivocally depicted by the interspecific shape differences, though the results of the geometric morphometric analysis may support the existence of multiple head designs in hammerhead sharks.

Keywords: Hammerhead sharks, geometric morphometrics, partial-warps, thin-plate spline, relative warp scores, truss, ontogeny, phylogeny.

8.2 Introduction

The hammerhead sharks (family Sphyrnidae) are uniquely distinguished from other sharks of the order Carcharhiniformes by a lateral expansion of the head, known as the cephalofoil (Gilbert 1967; Compagno 1988). The internal structure of the cephalofoil consists of cartilaginous plates that act as support for the entire head. This internal structure in turn leads to the relative rigidity of the cephalofoil (Nakaya 1995; Lima et al. 1997).

Several hypotheses have been presented to explain the function of this lateral expansion of the head in the Sphyrnidae, such as providing lift during swimming (Thomson and Simanek 1977; Compagno 1988), improving sensory functions (Compagno 1988; Nakaya 1995), and handling prey (Chapman and Gruber 2002; Strong et al. 1990), but a clear consensus has not yet been achieved. In recent years, experimental studies have demonstrated that the cephalofoil may indeed serve as an efficient lift generating structure, or hydrofoil (Nakaya 1995; Driver 1998), at least in the larger species.

The shape of the cephalofoil varies significantly during ontogeny in hammerhead sharks, with the cephalofoils of the juveniles in larger species tending to resemble those of the adults in smaller species. The ontogenetic shape changes that occur in the head of sphyrnids seems to have no parallel in other carcharhinid sharks (Gilbert 1967), but are poorly known and so far only qualitative descriptions in single species have been done (Castro 1989).

The evolution of the cephalofoil also remains unexplained. Despite their close relationships to the carcharhinid sharks (Compagno 1988; Naylor 1992), the cephalofoil represents an autapomorphy which warrants the recognition of the hammerhead sharks as a separate family (Compagno 1988; Lima et al. 1997). There are currently two conflicting phylogenetic hypotheses of relationships within the Sphyrnidae. A phylogeny based on morphological characters (Compagno 1988) suggests that the cephalofoil evolved in the smaller species but only realized its hydrodynamic function in medium to large, more derived species; therefore, the cephalofoil as a hydrofoil could be viewed as an exaptation (*sensu* Gould and Vrba 1982). On the other hand, a phylogeny based on mtDNA sequences (Martin 1993) suggests that the larger species are less derived and that there has been a trend towards size decrease during the diversification of the sphyrnid clade; according to this view, it would not be possible to consider the hydrofoil properties of the cephalofoil as an adaptation.

Though the shape of the cephalofoil varies significantly among the hammerhead sharks, a rigorous quantification of these shape differences is required before their functional role and evolutionary patterns can be properly assessed. However, there have been very few morphometric studies of the sphyrnids and these have focused almost exclusively on the analysis of hydrodynamic properties of the cephalofoil in selected species, using measurements of surface areas, angles of attack and aspect ratios (Thomson and Simanek 1977; Nakaya 1995; Driver 1997). Only Driver (1997) did an attempt to compare shape variation in the cephalofoils of seven species of hammerhead sharks using shape coordinates and thin-plates splines analysis.

In the present study, the intra- and interespecific changes in shape of the cephalofoil in four selected species of *Sphyrna* are examined with the new techniques of geometric morphometrics, that allow the precise and detailed analysis of shape change and shape variation in organisms on the basis of positions of homologous anatomical landmarks or shapes of outlines (Rohlf and Marcus 1993). Geometric morphometric methods also allow for the graphic presentation of results for visual display and comparison of shape changes among the forms of interest. These methods represent an interesting alternative to traditional morphometrics, based on measured distances, angles, and ratios, and have demonstrated to be particularly useful to studies involving the comparison of form in fishes (Caldecutt and Adams 1998; Carpenter 1996; Cavalcanti et al. 1999; Loy et al. 1996, 1998; Reig et al. 1998; Rüber and Adams 2001; Walker 1993, 1996, 1997; Walker and Bell 2000).

8.3 Materials and methods

8.3.1 Samples

Specimens were obtained from the ichthyological collections of Museu de Zoologia, Universidade de São Paulo (MZUSP), Museu Nacional, Universidade Federal do Rio de Janeiro (MN/UFRJ), Fundação Universidade do Rio Grande (FURG), Departamento de Biologia Animal e Vegetal, Universidade do Estado do Rio de Janeiro (DBAV/UERJ), and Laboratório de Ictiologia, Departamento de Ciências Biológicas, Universidade Estadual de Feira de Santana (LIUEFS). A total of 83 specimens belonging to the four species of *Sphyrna* that are among the most common along the Brazilian coast (Figueiredo 1977) were analyzed. Choice of species for inclusion in this study was determined by the availability of an adequate size range and number of specimens. Sample sizes and body size range for each species are as follows: *S. tiburo* (Linnaeus, 1758): n = 22, 75-938 mm in total length (TL); *S. tudes* (Valenciennes, 1822): n = 18, 156-440 mm TL; *S. lewini* (Griffith & Smith, 1834): n = 30, 155-770 mm TL; and *S. zygaena* (Linnaeus, 1758): n = 13, 121-1507 mm TL.

8.3.2 Data acquisition

The analysis was performed on the Cartesian coordinates of eight two-dimensional landmarks defined on the basis of external morphology (Fig. 1). Landmarks refer to: (1) left lateral indentation; (2) right lateral indentation; (3) upper margin of the right eye; (4) distal end of the cephalofoil posterior right margin; (5) proximal end of the cephalofoil posterior right margin; (6) proximal end of the cephalofoil posterior left margin; (7) distal end of the cephalofoil posterior left margin; (8) upper margin of the left eye. After the classification of Bookstein (1991), landmarks 1, 2, 3 and 8 can be classified as Type I and landmarks 4 to 7 as Type II. Distance measurements based on a box-truss scheme (Strauss and Bookstein 1982) were taken among the landmarks with electronic calipers to the nearest 0.05 mm. The landmark coordinates for each specimen were reconstructed from these measurements by a simplified metric multidimensional scaling algorithm (Carpenter et al. 1996), using the UNFOLD program written by H.J.S. Sommer.

8.3.3 Data analysis

The geometric size of each specimen was estimated by the centroid size, defined as the square root of the sum of squared distances from all landmarks to the centroid of the configuration (Bookstein 1991). The landmark coordinates for each specimen were aligned and superimposed by the Procrustes generalized orthogonal least-squares method (Rohlf 1990; Rohlf and Slice 1990). In this procedure, the configurations were scaled to unit centroid size and then centered and rotated, in order to minimize the sum of squared distances between the landmark of each individual configuration to the corresponding landmarks of a reference or "consensus" configuration, computed as the mean landmark configuration of all specimens. This reference configuration was used to estimate the uniform components and partial warps (non-uniform components of shape). This step is required to define an adequate metric for the subsequent computation of the thin-plate splines interpolation function. The reference configuration defines the point of tangency between the non-Euclidian shape space and the approximating linear tangent space, where all statistical analyses based on the General Linear Model are done (Rohlf 1995, 1996, 1999).

Patterns of shape change were analyzed by the thin-plate splines technique (Bookstein 1989, 1991). This method models shape changes as deformations, by fitting an interpolation function to the aligned landmark coordinates of each specimen against the reference configuration, so that all homologous landmarks coincide. Differences in shape among the specimens and the reference configuration, fitted by the thin-plate spline function, are expressed as a bending energy matrix. The eigenvectors of the bending energy matrix are known as principal warps, and are relative only to the reference configuration. The eigenvalues associated to each principal warp are inversely related to the spatial scale of shape change, so that large eigenvalues correspond to eigenvectors (principal warps) de-

scribing small-scale deformations, whereas small eigenvalues correspond to eigenvectors that describe large-scale deformations. The projection of the aligned specimens onto the principal warps yield the matrix of partial-warp scores (the "weight matrix", W), that describe their deviations from the reference configuration and can be used as a set of shape variables in subsequent multivariate statistical analyses (Rohlf 1995, 1996).

The shape changes modelled by the thin-plate splines technique can be further decomposed into two parts, the uniform and non-uniform components. The uniform components (u1 and u2) express global (affine) variation in shape, whereas the non-uniform components describe local (non-affine, non-uniform) shape changes at different geometric scales, and correspond to the partial warps as described above. The first uniform component (u1) corresponds to the stretching of a landmark configuration along the x-axis, whereas the second uniform component (u2) indicates a shearing along the y-axis. In this study, the x-axis corresponds to the width of the cephalofoil, and the y-axis corresponds to its length. The uniform components were estimated by the complement method of Rohlf, Bookstein (2003). The uniform components were tested for significant differences among species by multivariate analysis of variance (MANOVA: Neff and Marcus 1980).

A relative warps analysis was performed to assess localized shape changes among the species. The relative warps are the principal components of the partial-warp scores matrix (Bookstein 1991; Rohlf 1993). The average configuration of landmarks was used as the reference configuration in the relative warp analysis, and the reference was aligned to its principal axes. The relative warps were computed with the scaling option $\alpha = 0$, that weights all landmarks equally and is more appropriate for systematic studies (Loy et al. 1993; Rohlf 1993; Rohlf et al. 1996). The relative warps were computed in the full shape space (i.e. including both the uniform and the non-uniform components). Deformation grids using thin-plate splines were used to graphically portray the patterns of shape variation among the landmarks.

Centroid size was tested for differences among species by single classification analysis of variance (ANOVA: Sokal and Rohlf 1995). The major axis of variation in partial warp space (first relative warp) was regressed on centroid size for the assessment of ontogenetic localized shape variation within each species. The uniform components were also regressed on centroid size for the assessment of ontogenetic uniform shape variation. Ontogenetic trajectories on size and shape were analyzed with a single classification analysis of covariance (ANCOVA: Sokal and Rohlf 1995), treating species as a fixed effect and centroid size as the covariate. Probabilities for homogeneity of slopes among the size and shape ontogenetic trajectories were computed by a generalization of Tukey's HSD test for unequal samples sizes (Spjotvoll, Stoline 1973). The relative contribution of uniform components to ontogenetic shape changes was estimated by a multivariate regression of shape components on centroid size. It was calculated as the difference in percentage of variance unexplained by models with and without the uniform components (Loy et al. 1998; Monteiro 1999).

Significance of cephalofoil shape differences was assessed by a canonical variates analysis (CVA: Neff and Marcus 1980) of the partial-warp and uniform components. The results were visualized directly on cephalofoil shape by regressing the partial warps and uniform components onto each canonical axis (Rohlf et al. 1996). The regression also allowed the estimation of the relative contribution of uniform components (complete integration of shape change) to among-species differences. This is given by the difference between unexplained variances after the partial warp scores matrices with and without uniform components appended were regressed onto canonical scores.

The relative warps analysis and computation of centroid size and partial-warp scores were done using the TPSRelw program, version 1.35 (Rohlf 2003). Regressions between the partial warps, centroid size and canonical variates were computed with the TPSRegrw program, version 1.26 (Rohlf 2000). All statistical analyses were performed with the STATISTICA package, version 5.5 (StatSoft 1999).

8.4 Results

There was no correlation between the x and y uniform components, but these components showed a highly significant difference among species by single classification MANOVA (Wilks $\Lambda = 0.03467$, $p << 0.0001$). The uniform compo nents do not depict large differences from the reference configuration (Fig. 2) and

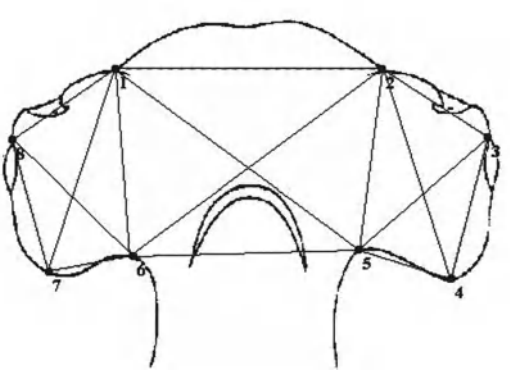

Fig. 1. Outline drawing of *Sphyrna lewini*, showing the locations of the eight anatomical landmarks (numbered points) and morphometric distance measures recorded on each individual

clearly separate the species with wide and narrow (*S. zygaena* and *S. lewini*) from the species with evenly rounded (*S. tudes* and *S. tiburo*) cephalofoils.

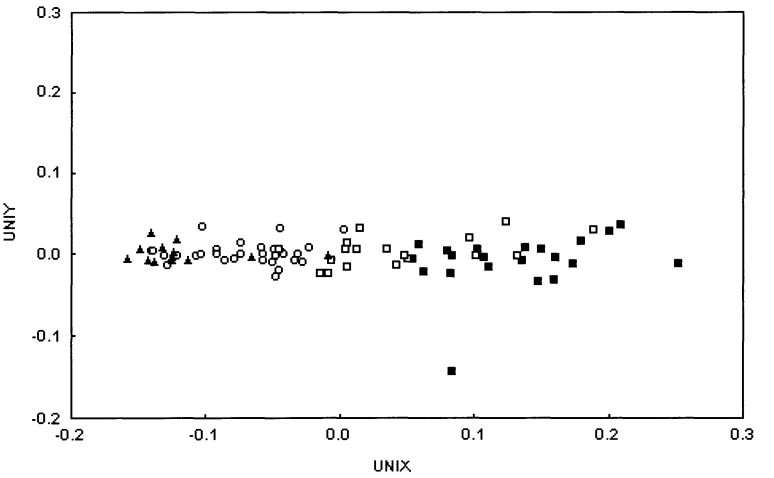

Fig. 2. Scatterplot for individual scores of all specimens of *Sphyrna* on the x and y uniform components (U1 and U2). ▲: *S. zygaena*, ○: *S. lewini*, △: *S. tudes*, ■: *S. Tiburo*

Single classification ANOVA showed a highly significant difference in centroid size ($F_{[3, 791]} = 20.48746$, $p << 0.0001$) among species.

Centroid size was significantly correlated with the uniform shape components ($R^2 = 0.4719$, $p << 0.0001$). The partial regression coefficient for the x uniform component ($r = -0.6860$, $p << 0.0001$) was much larger than that for the y uniform component ($r = 0.0656$, $p = 0.5581$).

A significant multiple correlation was also found between centroid size and the non-uniform components ($R^2 = 0.3458$, $p < 0.001$). The largest correlation was with the 3x partial warp (the projection of the x-coordinates on the third principal warp). The multiple correlation increased when both the uniform shape and non-uniform components were regressed on centroid size ($R^2 = 0.6034$, $p << 0.0001$), with the largest correlation being with the x uniform component.

The first two relative warps accounted for 78.47% of total non-uniform shape variation in the sample. Two groups are formed on the ordination of relative warps (Fig. 3), one including *S. lewini* and *S. zygaena* and the other including *S. tudes* and *S. tiburo*. Main localized shape differences between these groups are due to a relatively larger snout and smaller cephalofoil in *S. tudes* and *S. tiburo* (Fig. 4). *Sphyrna tudes* displays a broader range of non-uniform shape variation than the other three species.

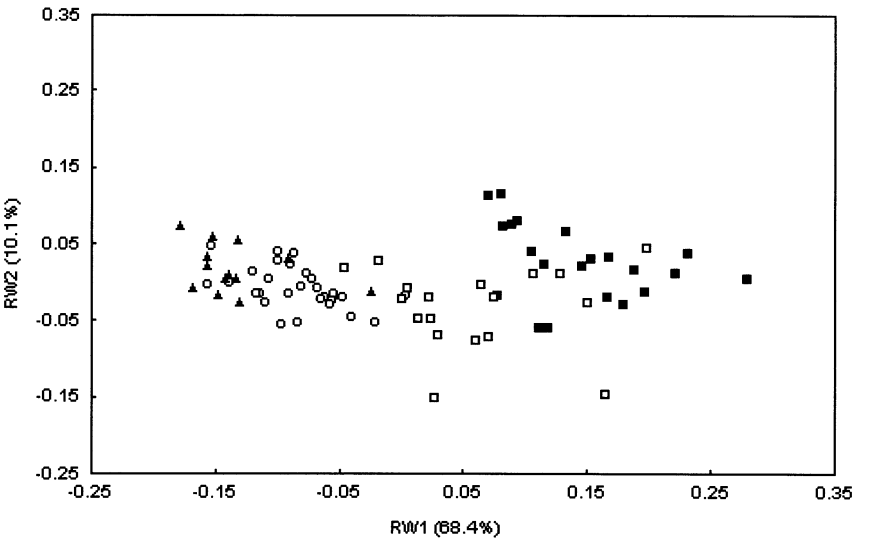

Fig. 3. Scatterplot of individual scores from the relative warps analysis of all specimens of *Sphyrna*, with the uniform component excluded ($\alpha = 0$). ▲: *S. zygaena*, ○: *S. lewini*, △: *S. tudes*, ■: *S. Tiburo*

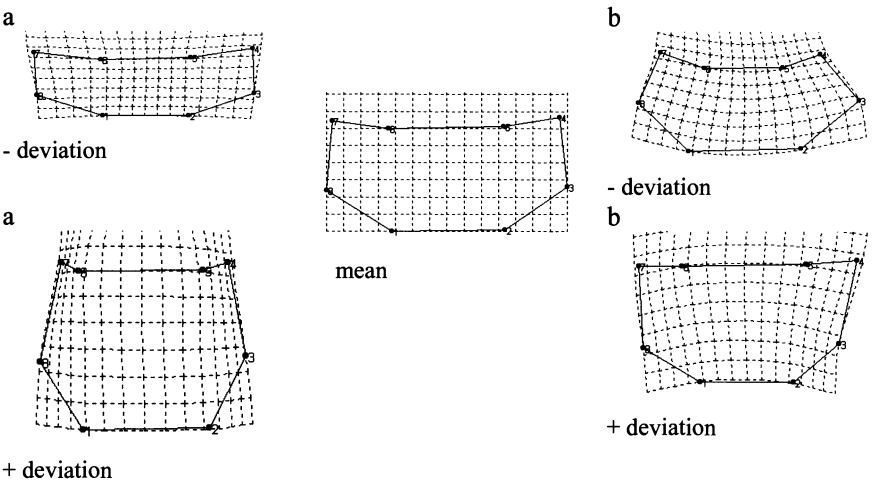

Fig. 4. Non-affine shape changes, expressed as deformations using thin-plate splines, along relative warps 1 (a) and 2 (b)

The three vectors extracted from the sample by the canonical variates analysis of partial warps and uniform components were highly significant ($\chi^2 = 248.78$, $p << 0.0001$) and contributed to shape differentiation among species (Table 1).

Shape variance due to among species differences expressed by these three vectors taken together amount to 98.7% of total variation. Decomposing the among species variation into localized and uniform components of variance showed that the partial warps (localized shape differences) were responsible for 23.34% and the uniform components for 50.38% of the total variation.

Table 1. Mahalanobis distances between species (above diagonal) and probabilities (below diagonal) for the null hypothesis of no difference between species centroids

	S. lewini	*S. tiburo*	*S. tudes*	*S. zygaena*
S. lewini	-	58.54727	23.70216	2.95959
S. tiburo	0.000000	-	16.08228	70.59877
S. tudes	0.000000	0.000000	-	35.59177
S. zygaena	0.065190	0.000000	0.000000	-

The first canonical variate (Fig. 5) separates all species but *S. zygaena* and *S. lewini*. *Sphyrna tudes* appears as an intermediate group and *S. tiburo* is very different from all other three.

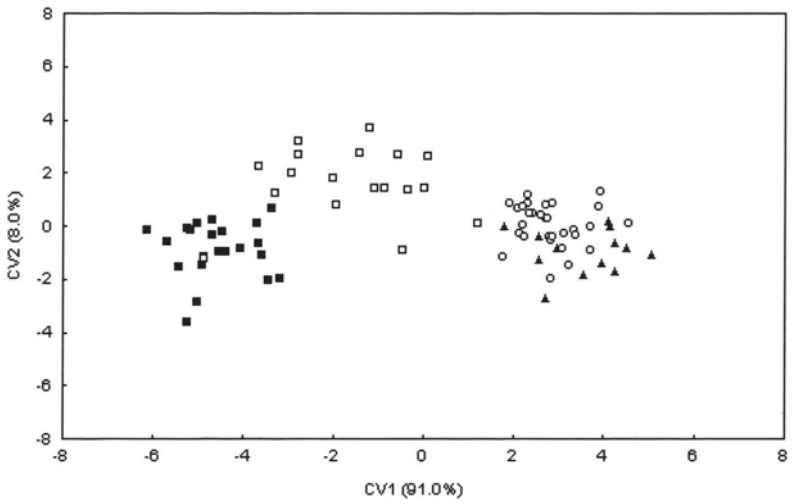

Fig. 5. Scatterplot of individual scores from the canonical variates analysis of all specimens of *Sphyrna*, with the uniform component included. ▲: *S. zygaena*, ○: *S. lewini*, △: *S. tudes*, ■: *S. tiburo*

The shape difference that separates the species is in large part due to a uniform compression on the anteroposterior axis of the cephalofoil (Fig. 6a). On one ex-

treme (*S. tiburo*) the cephalofoil is large in length but not in width. On the other extreme (*S. lewini*) it is large in width but not in length. *Sphyrna tudes* is separated from the other three species along the second canonical variate. The shape difference on this axis is mostly due to a localized enlargement on the snout of *S. tudes* (Fig. 6b).

Significant ontogenetic variation in cephalofoil shape was present in *S. lewini* (Table 2) for both the uniform and non-uniform shape components, and in *S. zygaena* for the uniform component only. *Sphyrna tiburo* and *S. tudes* showed no variation in shape with centroid size for either component (Figs. 7 and 8), but this result may only represent a lack of size variation in the specimens examined and is inconclusive with regard to patterns of ontogenetic variation within these species. The variation observed with size increase is both a uniform compression of the cephalofoil on its anteroposterior axis and a localized lateral compression of the snout. The cephalofoil is also expanded laterally during size increase (Fig. 9).

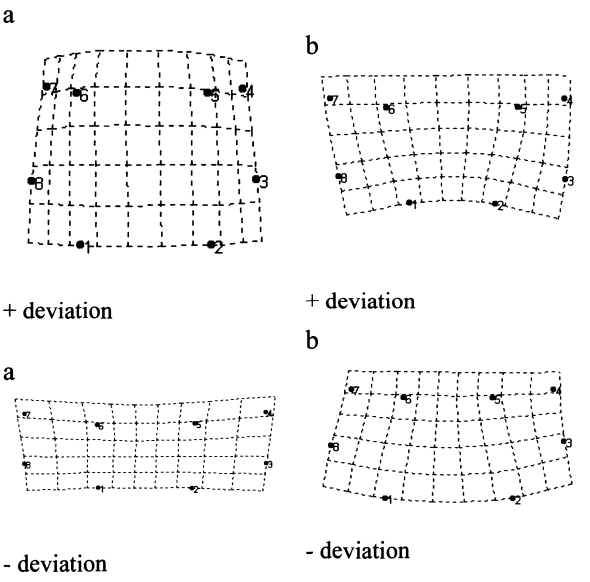

Fig. 6. Shape changes, expressed as deformation grids using thin-plate splines, as a function of size in *Sphyrna*, estimated by a multivariate regression of all shape variables (uniform components+partial warps) on canonical vectors 1 (a) and 2 (b)

Table 2. Within-group correlations with centroid size for the first relative warp and the first uniform component (ns = not significant)

	RW1		U1	
Species	r	p	r	p
S. lewini	-0.60916	< 0.002	-0.73216	< 0.0001
S. tiburo	-0.37312	ns	-0.39305	ns
S. tudes	-0.46213	ns	-0.28701	ns
S. zygaena	-0.44784	ns	-0.58945	< 0.05

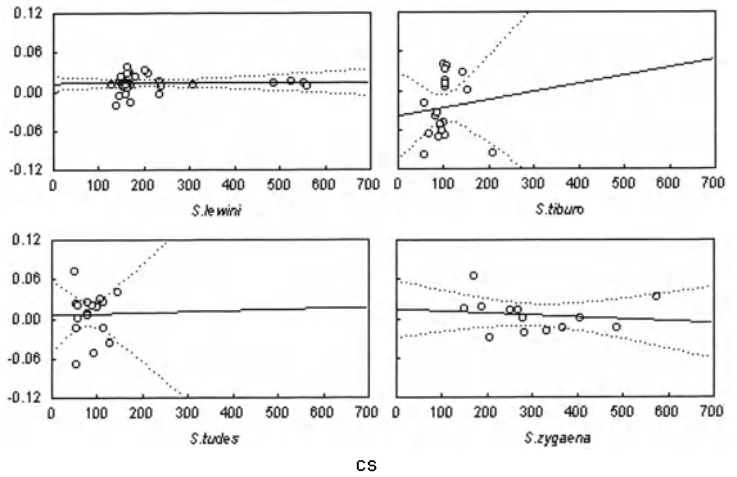

Fig. 7. Categorized plot of within-group regression of the first relative warp on centroid size, depicting the ontogenetic trajectories for each of *Sphyrna*

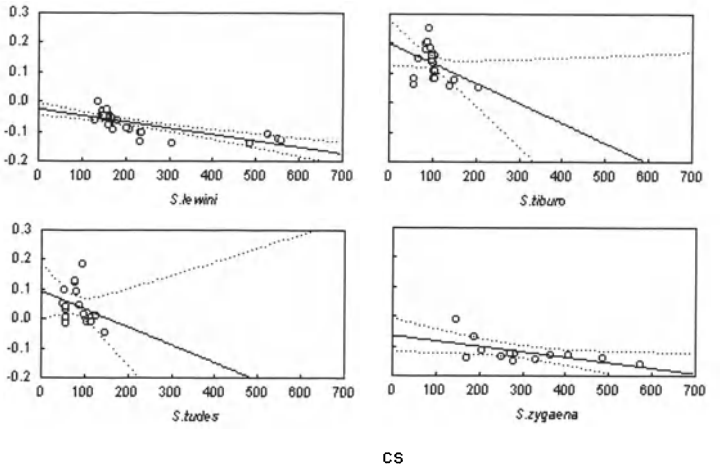

Fig. 8. Categorized plot of within-group regression of the second uniform component on centroid size, depicting the ontogenetic trajectories for each of *Sphyrna*

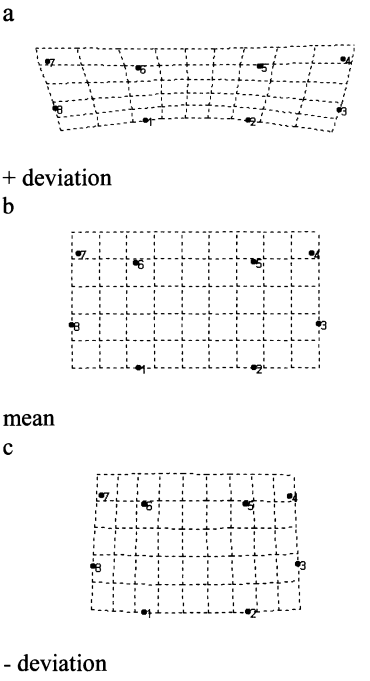

Fig. 9. Shape changes, expressed as deformation grids using thin-plate splines, as a function of size in *Sphyrna*, estimated by a multivariate regression of all shape variables (uniform components+partial warps) on centroid size. a) estimated shape for a very large specimen; b) mean configuration; c) estimated shape for a very small specimen

Size and localized shape ontogenetic trajectories have significantly similar slopes in *S. lewini* and *S. zygaena*, and the trajectories for both species differ in slope from *S. tiburo* and *S. tudes* (Table 3). The latter species has a slightly steeper ontogenetic trajectory. The trajectories on uniform shape differences also differ among species, except between *S. lewini* and *S. zygaena*. The fact that *S. tudes* shows a steeper slope in the localized shape ontogenetic trajectory might be due to the fact that more different ontogenetic phases were sampled for that species alone.

Table 3. Probabilities for homogeneity of slope in size and shape ontogenetic trajectories on the first relative warp (above diagonal) and the first uniform component (below diagonal). Significant values ($p < 0.05$) are marked with an asterisk

	S. lewini	*S. tiburo*	*S. tudes*	*S. zygaena*
S. lewini	-	0.000148*	0.000148*	0.032199
S. tiburo	0.000148*	-	0.000150*	0.000148*
S. tudes	0.000148*	0.000148*	-	
S. zygaena	0.034264	0.000148*	0.000148*	-

Size variation causes 31.52% of total shape variation in the samples. Of this percentage of variation, 5.36% are due to partial warp variation and 26.15% are due to uniform components variation.

8.5 Discussion

The geometric morphometric analysis of shape variation in the cephalofoil of these four species of *Sphyrna* indicates that the evolutionary and ontogenetic lateral expansion of the head does not occur only by a simple expansion of the blades but by a modification of the entire head structure.

The uniform components contribute to a larger part of the interspecific shape differences than the partial warps, suggesting that the cephalofoil is a highly integrated and constrained structure in the evolutionary sense. The large contribution of the uniform components to intraspecific shape changes also point to a high level of integration during ontogeny in these species.

Because evolutionary shape changes are mostly due to uniform components, the localized shape changes do not contribute to the widening of the cephalofoil. Instead, they are responsible for specific differences that separate each species from the other. This might be interpreted as supporting the suggestion of Martin (1993) with respect to the existence of multiple cephalofoil designs in hammerhead sharks, as a result of selection forces acting at different times along the evolution of this group.

However, the results of the present study do not allow to unequivocally interpret the trajectory of cephalofoil evolution in the sphyrnids. The morphometric pattern of cephalofoil shape variation places *S. zygaena*, *S. lewini* and *S. tiburo* as extremes of shape variation and *S. tudes* as an intermediate group (that also differs

from the other species by more subtle shape differences as reflected by the localized shape components), yet offer no clear indications of the evolutionary direction of shape change in the cephalofoil of these species.

Additional phylogenetic information is required to test the alternative hypotheses of cephalofoil evolution in the sphyrnids. An interesting perspective for future work is the possibility of assembling the available sphyrnid phylogenies into a more comprehensive phylogenetic "supertree" (Sanderson et al 1998) that combines all or most of the information from the source trees, and onto which shape data could be fitted by a procedure of the type suggested by Rohlf (2002). The effect of the phylogeny on shape variables could then be studied by the method of independent contrasts (Felsenstein 1985; Harvey and Pagel 1991) or other phylogenetic comparative methods. Westneat (1995) has applied this approach quite successfully in his study of functional morphology in labrid fishes.

Nonetheless, it can be anticipated that as the investigation of intra- and interespecific morphometric variation in the sphyrnids continues, with the inclusion of more species in further studies, there will be some resolution of the evolutionary histories of these organisms. The precise spatial view of shape changes only made possible by the powerful analytical tools of geometric morphometrics can make a significant contribution toward this goal.

8.6 Acknowledgements

This paper is dedicated to the memory of Leslie F. Marcus, for his great contribution to morphometrics and evolutionary biology. I thank José Lima de Figueiredo (Museu de Zoologia, Universidade de São Paulo), Gustavo Wilson Nunan (Museu Nacional, Universidade Federal do Rio de Janeiro), Carolus Maria Vooren (Fundação Universidade do Rio Grande), and Ulisses Leite Gomes (Departamento de Biologia Animal e Vegetal, Universidade do Estado do Rio de Janeiro) for permission to examine specimens under their care. I also thank H.J.S. Sommer III (Department of Mechanical Engineering, Pennsylvania State University) for the software to reconstruct landmark coordinates from truss distance data and advice. I am also grateful to Maisa da Cruz Lima, Ulisses Leite Gomes and Paulo Roberto Duarte Lopes for their invaluable help in collecting the data for this study. I especially thank Kim Honey Driver for many helpful discussions and encouragement over the years, and Richard Strauss for providing constructive criticisms and valuable suggestions that contributed to the improvement of an earlier version of the manuscript. Leandro Rabello Monteiro participated in valuable discussions on geometric morphometric methods. The kind support of the editor, Prof. Ashraf M.T. Elewa, is much appreciated. The author has been continuously supported by grants of the Brazilian Coordenação para Aperfeiçoamento de Pessoal do Ensino Superior (CAPES).

References

Bookstein FL (1989) Principal warps: thin-plate splines and the decomposition of deformations. IEEE Trans Pattern Anal Mach Intell 11: 567-585

Bookstein FL (1991) Morphometric tools for landmark data: Geometry and biology, Cambridge University Press, Cambridge

Caldecutt WJ, Adams DC (1998) Morphometrics of trophic osteology in the threespine stickleback, *Gasterosteus aculeatus*. Copeia 1998: 827-838

Carpenter KE (1996) Morphometric pattern and feeding mode in emperor fishes (Lethrinidae, Perciformes). In: Marcus LF, Corti M, Loy A, Naylor G, Slice DE (eds) Advances in Morphometrics. Plenum Publishing, New York, p. 479-487

Carpenter KE, Sommer HJ, Marcus LF (1996). Converting truss interlandmark distances to Cartesian coordinates. In: Marcus LF, Corti M, Loy A, Naylor G, Slice DE (eds) Advances in Morphometrics. Plenum Publishing, New York, 103-111

Castro JI (1989) The biology of the golden hammerhead, *Sphyrna tudes*, off Trinidad. Environ Biol Fish 24: 3-11

Cavalcanti MJ, Monteiro LR, Lopes PRD (1999) Landmark-based morphometric analysis in selected species of serranid fishes (Perciformes: Teleostei). Zool Stud 38: 287-294

Chapman DD, Gruber SH (2002) A further observation of the prey-handling behavior of the great hammerhead shark, *Sphyrna mokarran*: predation upon the spotted eagle ray, *Aetobatus narinari*. Bull Mar Sci 70: 947-952

Compagno LJV (1988) Sharks of the Order Carcharhiniformes. Princeton University Press, Princeton, New Jersey

Driver KH (1997) Hydrodynamic Properties and Ecomorphology of the Hammerhead Shark (Family Sphyrnidae) cephalofoil, Ph D thesis, University of California, Davis

Felsenstein J (1985) Phylogenies and the comparative method. Am Nat 125: 1-15

Figueiredo JL (1977) Manual de Peixes Marinhos do Sudeste do Brasil. I. Introdução. Cações, Raias e Quimeras. Museu de Zoologia da Universidade de São Paulo, São Paulo, Brasil

Gilbert CR (1967) A revision of the hammerhead sharks (family Sphyrnidae). Proc US Natl Mus 119: 1-88

Gould SJ, Vrba ES (1982) Exaptation – a missing term in the science of form. Paleobiology 8: 4-15

Harvey PH, Pagel MD (1991) The Comparative Method in Evolutionary Biology. Oxford University Press, New York

Lima MC, Gomes UL, Souza-Lima W, Paragó C (1997) Estudo anatômico comparativo da região cefálica pré-branquial de *Sphyrna lewini* (Griffith & Smith) e *Rhizoprionodon lalandii* (Valenciennes) (Elasmobranchii, Carcharhiniformes) relacionados com a presença do cefalofólio em *Sphyrna* Rafinesque. Revta Bras Zool 14: 347-370

Loy A, Corti M, Marcus LF (1993) Landmark data: size and shape analysis in systematics. A case study on Old World Talpidae (Mammalia, Insectivora). In Marcus LF, Bello E, García-Valdecasas A (eds) Contributions to Morphometrics. Museo Nacional de Ciencias Naturales, Madrid, p 213-240

Loy A, Cataudella S, Corti M (1996) Shape changes during the growth of the sea bass, *Dicentrarchus labrax* (Teleostea: Perciformes), in relation to different rearing conditions. An application of thin-plate spline regression analysis. In: Marcus LF, Corti M,

Loy A, Naylor G, Slice DE (eds) Advances in Morphometrics. Plenum Publishing, New York, p 399-405

Loy A, Mariani L, Bertelletti M, Tunesi L (1998) Visualizing allometry: geometric morphometrics in the study of shape changes in the early stages of the two-banded sea bream, *Diplodus vulgaris* (Perciformes, Sparidae). J Morph 237: 137-146

Martin A (1993) Hammerhead shark origins. Nature 364: 494

Monteiro LR (1999) Multivariate regression models and geometric morphometrics: the search for causal factors in the analysis of shape. Syst Biol 48: 192-199

Morrison DF (1990) Multivariate Statistical Methods. McGraw-Hill, New York

Nakaya K (1995) Hydrodynamic function of the head in the hammerhead sharks (Elasmobranchii: Sphyrnidae). Copeia 1995: 330-336

Neff NA, Marcus, LF (1980) A Survey of Multivariate Methods for Systematics. Privately published, New York

Reig S, Doadrio I, Mironovsky AN (1998) Geometric analysis of size and shape variation in barbel from Lake Tana (Ethiopia). Folia Zoologica 47: 35-51

Rohlf FJ (1990) Rotational fit (Procrustes) methods. In: Rohlf FJ, Bookstein FL (eds) Proceedings of the Michigan Morphometrics Workshop. The University of Michigan Museum of Zoology, Ann Arbor, p 227-236

Rohlf FJ (1993) Relative warp analysis and an example of its application to mosquito wings. In: Marcus LF, Bello E, García-Valdecasas A (eds) Contributions to Morphometrics. Museo Nacional de Ciencias Naturales, Madrid, p 131-159

Rohlf FJ (1995) Multivariate analysis of shape using partial-warp scores. In Mardia, KV Gill, CA (eds) Proceedings in Current Issues in Statistical Shape Analysis. Leeds University Press, Leeds, p 154-158

Rohlf FJ (1996) Morphometric spaces, shape components, and the effects of linear transformations. In: Marcus LF, Corti M, Loy A, Naylor G, Slice DE (eds) Advances in Morphometrics. Plenum Publishing, New York, p 117-129

Rohlf FJ (1999) Shape statistics: Procrustes superimposition and tangent spaces. J Class 16: 197-223

Rohlf FJ (2000) tpsRegr: Shape regression. Department of Ecology and Evolution, State University of New York, Stony Brook

Rohlf FJ (2002) Geometric morphometrics and phylogeny. In: MacLeod N, Forey PL (eds) Morphology, Shape and Phylogeny. Taylor and Francis, London, p. 175-193

Rohlf FJ (2003) tpsRelw: Analysis of relative warps. Department of Ecology and Evolution, State University of New York, Stony Brook

Rohlf FJ, Bookstein FL (2003) Computing the uniform component of shape variation. Syst Biol 52: 66-69

Rohlf FJ, Loy A, Corti M (1996) Morphometric analysis of Old World Talpidae (Mammalia, Insectivora) using partial-warp scores. Syst Biol 45: 344-362

Rohlf FJ, Marcus LF (1993) A revolution in morphometrics. Trends Ecol Evol 8: 129-132

Rohlf FJ, Slice DE (1990) Extensions of the Procrustes method for the optimal superimposition of landmarks. Syst Zool 39: 40-59

Rüber L, Adams DC (2001) Evolutionary convergence of body shape and trophic morphology in cichlids from Lake Tanganyika. J Evol Biol 14: 325-332.

Sanderson MJ, Purvis A, Henze C (1998) Phylogenetic supertrees: assembling the trees of life. Trends Ecol Evol 13: 105-109

Sokal RR, Rohlf FJ (1995) Biometry: the principles and practice of statistics in biological research. Freeman, San Francisco

Spjotvoll E, Stoline MR (1973) An extension of the T-method of multiple comparison to include the cases with unequal sample sizes. J Amer Stat Assoc 68: 976-978

StatSoft (1999) STATISTICA for Windows. StatSoft Inc, Tulsa

Strauss RE, Bookstein FL (1982) The truss: body form reconstruction in morphometrics. Syst Zool 31: 113-135

Strong WR, Snelson FF, Gruber SH (1990) Hammerhead shark predation on stingrays: an observation of prey handling by *Sphyrna mokarran*. Copeia 1990: 836-840

Thomson KS, Simanek, DE (1977) Body form and locomotion in sharks. Amer Zool 17: 343-354

Walker JA (1993) Ontogenetic allometry of three-spine stickleback body form using landmark-based morphometrics. In: Marcus LF, Bello E, García-Valdecasas A (eds) Contributions to Morphometrics. Museo Nacional de Ciencias Naturales, Madrid, p 193-214

Walker JA (1996) Principal components of body shape variation within an endemic radiation of threespine stickleback. In: Marcus LF, Corti M, Loy A, Naylor G, Slice DE (eds) Advances in Morphometrics. Plenum Publishing, New York, p 321-334

Walker JA (1997) Ecological morphology of lacustrine threespine stickleback *Gasterosteus aculeatus* L. (Gasterosteidae) body shape. Biol J Linn Soc 61: 3-50

Walker JA, Bell MA (2000) Net evolutionary trajectories of body shape evolution within a microgeographic radiation of threespine sticklebacks (*Gasterosteus aculeatus*). J Zool 252: 293-302

Westneat MW (1995) Feeding, function, and phylogeny: analysis of historical biomechanics in labrid fishes using comparative methods. Syst Biol 44: 361-383

9 Morphometric stock structure of the Pacific sardine *Sardinops sagax* (Jenyns, 1842) off Baja California, Mexico

José De La Cruz Agüero[1] and Francisco Javier García Rodríguez[2]

[1]Centro Interdisciplinario de Ciencias Marinas (CICIMAR-IPN), Coleccion Ictiológica Apartado Postal 592, La Paz, Baja California Sur, Mexico 23000, jcruz@ipn.mx; [2]Centro de Investigaciones Biológicas del Noroeste (CIBNOR). Mar Bermejo No. 195, Col. Playa Palo de Santa Rita, La Paz, B.C.S. 23090, México

9.1 Abstract

The existence of a stock structure in the Pacific sardine (*Sardinops sagax*) along its geographic range, has been discussed at length by fishery biologists in the last sixty years. Samples of the Pacific sardine collected in the west coast of Baja California, Mexico, the southern limit of its distribution, were compared by canonical variate analyses (CVA) to test for the presence of stock structuring. The raw data of morphological characters were depured and adjusted to obtain size-free CVs of body shape measurements, excluding outliers, testing properties and transforming variables. Because sexual dimorphism was detected in morphometric characters, females and males were analyzed separately. According objectives, an overall portrayal of the morphometric structure of *S. sagax* was needed; therefore an additional CVA was made using all data disregarding gender or locality. Significant differences in shape variables were found between groups analyzed, however the environmental properties of the spawning and development areas in Baja California, migratory behavior, and genetic data available indicate that present morphological differences found may reflect environmentally induced morphotypes, and therefore will not be reliable indicators of stock identity.

Keywords: *Sardinops sagax,* Pacific sardine, stocks, morphometrics, Baja California.

9.2 Introduction

The clupeoid fishes, sardines, anchovies, and herrings, are of great importance in the world's fisheries, representing about one-third of the total world fish catch (Blaxter and Hunter 1982). For most of recent years, either *Sardinops* or *Engraulis* has supported the world's largest fisheries and the former has been the largest single component of the world's harvest of fish (Parrish et al. 1989). Consequently, the Pacific sardine *Sardinops sagax* (Jenyns 1842) has been the most important species for fisheries in northwest Mexico in recent decades (Cisneros et al. 1995), making an important contribution to protein resources and the economy of the country.

The taxonomy of the Pacific sardine, as many other clupeoid fishes, has been controversial. In spite of several studies and revisions of the group (e.g. Regan 1916; Thompson 1926; Hubbs 1929; see also a thorough discussion in Parrish et al. 1989), the use of different binomen for the Pacific sardine continues (e.g. *Sardinops sagax, Sardinops caeruleus, Sardinops sagax sagax, Sardinops sagax caeruleus, Sardinops sagax caerulea*).

Moreover, the question of the stock composition of the Pacific sardine along the eastern Pacific coast also has been discussed at length. Existence, quantity, and geographical ranges of stocks of *Sardinops* in the California current system has been of considerable interest to fishery biologists in the last sixty years (e.g. Janssen 1938; Clark and Janssen 1945; Clark 1947, Vrooman 1964; Mais 1972; Hedgecock et al. 1989; Radovich 1995).

Biological identification of individuals, at the genus, species or fishery stock rank, is an important step far beyond the scope of taxonomy, and is mainly used for determining the status of the resources and developing a rational strategy for conserving them via fishery management (Skillman 1989). Overexploitation of stocks may result in a loss of genetic diversity and may reduce the resilience of the species as a whole, because it is unlikely the exploitation rate on individual biological stocks can be optimized when fish are being harvested from a mixture of such stocks (Pawson 1995). Also, exist examples when, because the stock composition and boundaries are unclear, the effective management of fish resources has been difficult (e.g. Austin et al. 1998).

The Pacific sardine inhabits coastal waters from the British Columbia, Canada, southward to Baja California, Mexico, including the Gulf of California. Several approaches to stock or subpopulation identifications have been investigated along its distribution range based on tagging and marking (Clark and Janssen 1945), meristic variables (Clark 1947), egg and larval surveys (Ahlstrom 1954), blood types (Vrooman 1964), growth parameters (Wolf and Daugherty 1964), morphometry and genetics (Hedgecock et al. 1989), and cohort analysis (Félix et al. 1996). However, for the southern part of the geographical distribution of *S. sagax* (Pacific coast of Baja California) most of the studies have been on reproduction, size-length relationships, and analysis of catch data (*e.g.* Torres-Villegas et al. 1985; Félix et al. 1996).

Detection of morphological differences within fish populations in its geographical range may indicate the presence of stock structuring. Therefore, the main purpose of this study was to make a morphological comparison among two populations of the Pacific sardine exploited along the west coast of Baja California, Mexico, to determine if constitute morphometrically differentiated stocks.

For the purpose of the present study, we use the term *stock* as groups of individuals within a species population that have sufficient spatial and temporal integrity to warrant consideration as self-perpetuating units (Pawson 1995). Multivariate morphometry has been chosen because it represents an appropriate tool to assess distinctness between closely related taxa as in the study of geographic variation and racial affinities (e.g. Corti et *a*l. 1988; Creech 1992; Elliot et al. 1995).

9.3 Materials and methods

9.3.1 Sample collection and treatment of data

All fish used in this study were obtained from the commercial fishery at Isla de Cedros, Baja California and Bahia Magdalena, Baja California Sur, Mexico, (Fig. 1) between February and June 1994.

Sampling gear was that of existing sardine fisheries of the zone, mainly purse seines. Specimens collected were preserved immediately after catch with 10% Formalin and carefully dissected for gonad examination.

For each specimen, nine landmarks were established and allowed 19 distance measurements (*truss elements*) to be defined, which were made to the nearest ± 0.01 mm using an electronic calliper. The morphometric characters are segments of box truss protocol (Strauss and Bookstein 1982) defined by landmarks that describe body shape of each fish. These landmarks are true and unambiguous points from specimen to specimen (e.g. points of insertion of fin rays and anatomical features of the head), which allow one to compare and detect variation of linear di-

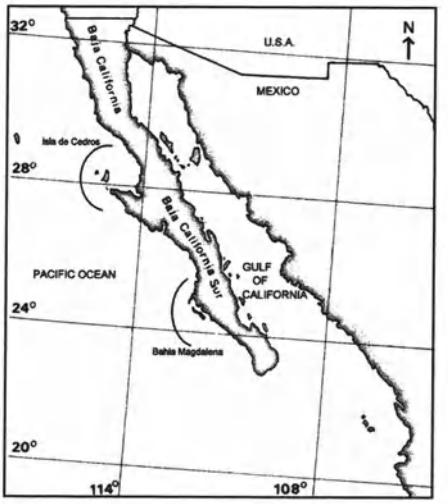

Fig. 1. Map of northwest Mexico indicating sampling locations for Pacific sardine, *Sardinops sagax*

mensions in horizontal, vertical, and oblique directions throughout the entire body (Creech 1992; Elliot et al. 1995). All distances were taken on the left side of the fish. In Figure 2 are listed the code and definitions of landmarks and truss elements used. To minimize bias in the measuring procedure, all measurements were made by the same person (FJGR) using the same digital caliper over a period of two months, and alternating individual specimens from each area.

In the present work, the outline perimeter (*Pe*) was used as a standard estimator of overall size, and was calculated as the summation of the contiguous distances of the landmarks (excepting landmark 8, the pectoral fin origin). The sex of each fish was determined before the morphometric characters were measured; therefore the data were divided into two subsets for each locality to test the effect of gender and size on body measurements. The raw data of fish measured was analyzed for outliers. Analyses were restricted to adult specimens between 300 and 400 mm of *Pe* because availability range size in fish factories and to minimize bias related to growth allometry (Table 1).

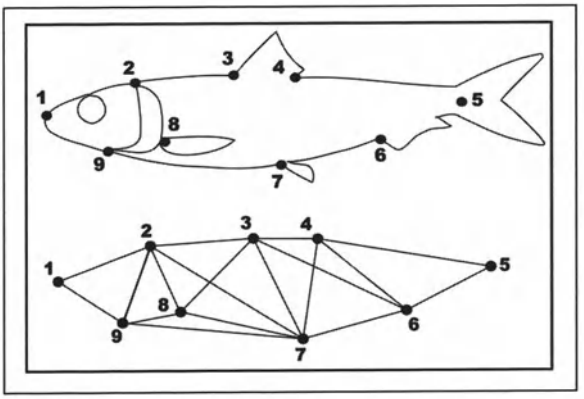

Fig. 2. Description of the truss elements resulting from 9 external landmarks (points) used in the canonical variate analysis (19 interpoint distances or measurements): 1-2 = Dorsal head length (tip of snout to occiput); 1-8 = Distance of snout to pectoral fin origin; 1-9 = Maxilla length; 2-3 = Predorsal length (occiput to dorsal-fin origin); 2-7 = Distance of occiput to pelvic fin origin; 2-8 = Distance of occiput to pectoral fin origin; 2-9 = Distance of occiput to maxilla rear margins; 3-4 = Dorsal-fin base; 3-6 = Distance of dorsal fin origin to anal fin origin; 3-7 = Distance of dorsal fin origin to pelvic fin origin; 3-8 = Distance of dorsal fin origin to pectoral fin origin; 4-5 = Distance of dorsal fin insertion to base of the middle caudal rays; 4-6 = Distance of dorsal fin insertion to anal fin origin; 4-7 = Distance of dorsal fin insertion to pelvic fin origin; 5-6 = Distance of the base of the middle caudal rays to anal fin origin; 6-7 = Distance of the anal fin origin to pelvic fin origin; 7-8 = Distance of pelvic fin origin to pectoral fin origin; 7-9 = Distance of pelvic fin origin to maxilla rear margins; 8-9 = Distance of pectoral fin origin to maxilla rear margins

Table 1. Number of specimens of Pacific sardines *(Sardinops sagax)* sampled and analyzed by sex and location along the west coast of Baja California, Mexico (February - June 1994)

Location	Sex	Specimen Measured	Ouliers	Specimens Out/range *	Specimens Analyzed
I de C	M	55	1	14	40
I de C	F	59	3	15	41
Subtotal		114	4	29	81
B. M.	M	65	3	11	51
B. M.	F	35	1	3	31
Subtotal		100	4	14	82
Totals		214	8	43	163

I de C Isla de Cedros, B. M. Bahía Magdalena, M male, F female, *Pe* perimeter of the box truss (estimator of total length), * < 300 mm > 400 mm of *Pe*.

9.3.2 Data analysis

The influence of the gender on morphometric traits was examined within-group (each location) by a bivariate analysis of covariance (ANCOVA) by the regression of each morphometric character against *Pe*. A significant interaction term between the regressor and character indicates heterogeneity of regression, suggesting differences between males and females and precluding direct group comparison (Tabachnick and Fidell 1989). In each case, tests of homogeneity of characters regression slopes were made. The differences of morphometric traits between-group (by gender; male-to-male, female-to-female) were explored by an ANCOVA, by a univariate analysis of variance (ANOVA) and a canonical variate analysis (CVA). Previously to ANOVA and CVA, *Pe* was compared to detect differences in size among specimens selected. From the results of the latter test on *Pe*, all morphometric measurements were standardized to minimize the variation resulting from allometric growth and to remove the influence of size in shape measures. Standardization was made using the formula:

$$Mt = Mo\ (Pe_{ov} / Po)^{b} \qquad (18.1)$$

where Mt = standardized measurement, Mo = observed character length, Pe_{ov} = the overall mean perimeter for all fish in all groups, Po = the perimeter of a specimen, and b = slope of the regression of log Mo to log Po for each subset (Karakousis et al. 1991; Reist 1985). Parameter b was estimated according Elliot et al. (1995) to reduce the effects of *Pe* on group differences in the standardized data.

Standardized measurements were transformed to natural logarithms to reduce the magnitude of the variances between groups and to obtain a better approximation to multivariate normality (Schaefer 1989; Mayden et al. 1991). Additionally, tests of normality were made on standardized measurements and those characters that not present normality and homoscedasticity were excluded. Then, an ANOVA

using measurements logarithmically transformed was made between-group (e.g. locations).

Canonical variate analysis (CVA) was used to determine linear combinations of variables (canonical variates) with maximum separation among specimens of different gender or from different geographical locations. CVA has been used in numerous works where the objective was the identification of different populations using morphometric characters (e.g. Castro et al. 1998). The CVA orders groups along axes of maximum variation in such a way as to maximize among-group variances relative to within-group variances (Corti et al. 1988). Moreover, the coefficients of the canonical variate may be used to determine the discriminatory value of each original variable, and allow the calculation of the likelihood of misclassification of specimens into another group analyzed (Humphries 1993). A scatter diagram based on the main canonical variates gives a visual portrayal of the relative similarity of the groups.

The CVA was made on the basis of gender, considering the results of variable checking for different criteria of inclusion (e.g. standardized sizes and morphometric characters with normality and homoscedasticity). We computed Mahalanobis distances (e.g. Klecka 1980: 55) to examine differences between sexes and location-group centroid. Because an overall portrayal of the morphometric structure of *S. sagax* was needed, a third CVA was made using all data disregarding gender or location (four groups) but considering the same variable checking criteria described above. Mahalanobis squared distances and their approximation to the F statistic was used to quantify the multivariate differences between the populations centroid (Manly, 1991). Univariate and multivariate analysis was done using *Statistica for Windows*, Version 5.0

9.4 Results

9.4.1 Data improvement

Before statistical analysis, eight fish were eliminated because their measurement of *Pe* was greater than three standard deviations from the mean and therefore were outliers (four for each location). From the rest, 43 specimens were discarded because of the variation in size ranges of the samples, restricting analyses to 163 fish with values of *Pe* in the predefined range (300 - 400 mm of *Pe*; see Table 1).

9.4.2 Univariate analysis

Univariate analysis of covariance (ANCOVA) within-group indicated that at least for one character the slopes of the log-log regressions of morphometric traits against *Pe* were significant. For Isla de Cedros, the truss elements 1-2, 1-8, 2-8, 2-

9, 3-4, 3-7, and 4-7 (Fig. 2) differ significantly between sexes ($P < 0.05$), whereas for Bahia Magdalena the differences between males and females were more subtle and only one measurement, 1-9, was significant ($P < 0.05$). These results therefore preclude a direct analysis to show sexual dimorphism in the morphometric measurements used.

ANCOVA between-groups indicated differences for males in the truss measurement: 1-2, 1-8, 1-9, 2-3, 2-7, 3-6, 3-7, 3-8, 4-6, 4-7, and 8-9 ($P < 0.05$). In the other three (5-6, 7-8, and 7-9), homogeneity tests were not made because of heterogeneity of slopes. For females, truss elements: 1-8, 2-7, 2-8, 2-9, 3-6, 3-7, 3-8, 4-6, 4-7, 5-6, 6-7, and 7-8 differ significantly ($P < 0.05$). Three others, 1-2, 3-4, and 4-5, show interactions with *Pe* and therefore homogeneity tests were not done.

ANOVA of the outline perimeter (*Pe*) indicated significant differences between males and females of Bahia Magdalena ($F_{(1, 80)} = 16.20$, $P < 0.000$) but not within males and females of Isla de Cedros ($F_{(1, 79)} = 0.136$, $P = 0.713$). Because of the results of later tests, the morphometric measurements were standardized. After size adjustment, no transformed measurement showed significant correlation with *Pe* (ANOVA, $P > 0.05$). Normality in six of nineteen standardized measurements: 2-3, 4-6, and 4-7 in females from Bahia Magdalena, 2-9 and 3-8 for females from Isla de Cedros, and 7-8 for males of Bahia Magdalena, was rejected ($P < 0.05$).

ANOVA between-groups of resulting measurements, logarithmically transformed, indicated differences for males in the truss elements: 1-2, 1-8, 1-9, 2-3, 2-7, 3-8, 4-5, 7-9, and 8-9 ($P < 0.05$). For females, measurements: 1-8, 2-7, 2-8, 3-6, 5-6, 6-7, and 7-8 differ significantly ($P < 0.05$). For males in three measurements the homoscedasticity was not proven: 2-9, 3-7, and 4-7 ($P < 0.05$), and in two for females: 1-9 and 3-7 ($P < 0.05$).

9.4.3 Multivariate analysis

For males the CVA was run using fifteen measurements, because of their normality and homoscedasticity: 1-2,1-8, 1-9, 2-3, 2-7, 2-8, 3-4, 3-6, 3-8, 4-5, 4-6, 5-6, 6-7, 7-9, and 8-9. For females, twelve truss measurements were use for CVA, 1-2, 1-8, 2-7, 2-8, 3-4, 3-6, 4-5, 5-6, 6-7, 7-8, 7-9, and 8-9. For the CVA including overall data, but using the same variable checking criteria, ten truss elements were selected, 1-2, 1-8, 2-7, 2-8, 3-4, 4-5, 5-6, 6-7, 7-9, and 8-9.

The canonical variate analysis for females yielded a significant difference between the populations of Isla de Cedros and Bahia Magdalena (Wilks' Lambda = .4717; $P < 0.000$). Females of the Pacific sardine are clearly separated into two distinct groups whose centroid distance was significant (Mahalanobis distance = 4.567; $F_{(12, 59)} = 5.499$; $P < 0.000$). Three specimens for Isla de Cedros and six for Bahia Magdalena were misclassified by the CVA, but the accuracy of the classification was high for both groups for an overall 88% (93% for females of Isla de Cedros and 81% for Bahia Magdalena).

In the CVA for males, the canonical correlation for the CV obtained was significant (Wilks' Lambda = .6422; $P < 0.001$). As females, the males were separated in two groups along the canonical variate. The centroid distance between

groups was significant (Mahalanobis distance = 2.261; $F_{(15, 75)} = 2.783$; $P< 0.001$). Specimens from Bahia Magdalena showed the greatest degree of correct classification, 82%, whereas about 78% of male fish from Isla de Cedros were classified correctly. Nine fish per location were misclassified.

The CVA using the four groups (each sex and location) produced three canonical variates, the first two significant and accounting for 91% of the variation (first 61%, second 30%). This CVA produced three variates with a Wilks' Lambda ($F_{(30, 440)} = 3.822$; $P < 0.000$), that reveals significant differences between the group centroids. Females from Bahia Magdalena exhibit the greatest Mahalanobis distances compared to the other groups, all significant at $P < 0.05$. However, the classification accuracy was low. On average, 54% of fish were correctly classified: 41% for males from Bahia Magdalena (30 misclassified) 54% in Cedros' females (19 misclassified); 58% for Bahia Magdalena's females (13 misclassified); and 68 for Isla de Cedros' males (13 misclassified) (Fig 3).

Examination of the scatter-plot of the first canonical variates shows the CVI separated Magdalena's females from all other groups, whereas the CVII discriminated between males and females from Isla de Cedros. Male fish from Bahia Magdalena showed a high overlap in both canonical variates with the rest of specimens.

9.5 Discussion

In multivariate statistics, it is desirable to have sample sizes several times larger than the number of variables to avoid overfitting (Tabachnick and Fidell 1989; Elliot et al. 1995). Shaklee and Tamaru (1981) demonstrated the effect of sample size on the multivariate analysis, concluding that as the number of individuals in a sample decreased below 15, the separation of the species became dependent of the individuals used in the analysis. Harris (1975) has suggested that if the number of individuals minus the number of variables used is greater than 30, then the sample can be considered adequate. In the present study, that criterion gives a value of 144, assuming therefore an appropriate sample size. Discarding the measurements expressing the variation in size and sexual dimorphism produced a more objective and essentially size-free CVA.

Several authors, based on distinct criteria, had established the existence of subpopulations of *Sardinops sagax* along the eastern Pacific coast. Clark (1947), on the basis of vertebral counts found two groups, the first from British Columbia to northern Baja California and the second in the Gulf of California and southern Baja California. Felin (1954) and Radovich and Phillips (1952), found heterogeneous growth rates between distribution areas of the Pacific sardine. Mais (1972) using combined meristic and morphometric characters, found the existence of three stocks, located in California (USA), Baja California (Mexico), and the Gulf of California. Vrooman (1964), by blood studies, found three genetically distinct subpopulations: "northern", which ranges from California to northern Baja California, "southern", which ranges from southern Baja California to southern Cali-

fornia, and "gulf" which is confined to the Gulf of California. Hedgecock et al. (1985; 1989), found that the five Pacific sardine populations studied by them are virtually genetically identical at the gene loci examined. The morphometric analysis by Hedgecock et al. (1989) on the same specimens, genetically investigated, concluded that *S. sagax* shows a north to south cline in size-at-age. However, the size interval they used (145 mm to 240 mm SL), sample size of subsets analyzed, inclusion of SL in the statistical analysis, measurements along the general length axis of the fish, and the untested effect of sex and size within populations studied, can have caused bias and failure to differentiate populations morphometrically (e.g. Shaklee and Tamaru 1981; Reist 1985; Creech 1992). More recently, Félix et al. (1996) by analysis of catch data and temperatures suggests the existence of three stocks along the coast of Baja California.

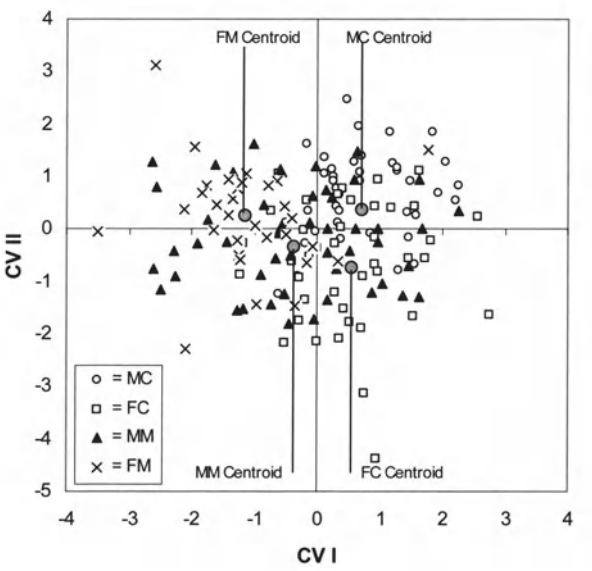

Fig. 3. Canonical variate scores for each individual of *Sardinops sagax* from the west coast of Baja California. Canonical variate axes, CVI (61% of the variance of data) and CVII (30%) produced by 163 specimens and 10 morphometric measurements. Classification accuracy, 54% in average. Significant differences between the group centroids (see text). MC and FC = males and females from Isla de Cedros, n = 40 and 41, respectively; MM and FM = males and females from Bahia Magdalena, n = 51 and 31 respectively

Although the genetic evidence argues for the absence of spatial variation in allozyme frequencies (Hedgecock et al. 1989), the present morphological analysis considering a restricted size interval, based on patterns of body shape size-free, and excluding the influence of sexual dimorphism, reveals significant differences between the two populations of the Pacific sardine exploited along the west coast of Baja California, Mexico. These morphological differences were more evident when comparing specimens separately by gender, attributing the lower percentage

of accuracy in the overall CVA (four groups) to sexual dimorphism detected in the truss measures and that specimens belong to the same species.

Differences observed between morphometrics and allozymes by Hedgecock et al. (1989), maybe linked to relatively reduced number of loci analyzed, preventing detection of differences between compared stocks. Moreover, the allozymes analysis has not detected interpopulation differences, where de DNA mitochondrial analysis has been capable to determine genetic differences among populations (Billington and Hebert 1991).

Hence, it would appear that morphometrical differences are a result of the phenotypic plasticity in *S. sagax*. Phenotypic plasticity describes a profile of potential phenotypes from a fixed genotype affected by temporal and spatial variation of the environment (Lin and Dunson 1999). This event is quite common in nature and environmental cues often result in behavior or morphological development appropriate to local conditions (Adkinson 1995).

The Pacific sardine is a multiple-batch spawner (Torres-Villegas 1997) with dispersal of the eggs and larvae along its geographic range (Ahlstrom 1954, 1959) and strong evidence of adult seasonal migration along the west coast of Baja California (Félix et al. 1996). Therefore overlapping generations reduce the potential for random genetic differentiation from genetic drift.

That is, that morphological characters can be environmentally determined, because the environment in the spawning and juvenile development areas of the Pacific sardine varies spatially and temporally (Lluch et al. 1989) and genetic homogeneity can occur despite differences in selective regimes (Lin and Dunson 1999).

Morphological differences between specimens in the present study may reflect environmentally induced morphotypes, a plausible case of uncoupling of organismal and molecular evolution, where organismal divergence is accompanied by molecular conservatism (Clayton 1981), and therefore those morphological differences will not be reliable indicators of stock identity (*sensu* Pawson 1995). Knowledge of the stock structure or identification of stocks of *Sardinops sagax* is important to the fishery management of the species. Further studies combining morphological variables, environmental factors, biological characters, and other analytical procedures used on specimens at same time, such as geometric morphometrics and biomolecular markers (related with DNA nuclear and mitochondrial) will contribute to our knowledge of the origin of individual differences.

9.6 Acknowledgements

The authors thank to Laboratorio de Morfofisiologia (CICIMAR-IPN) for providing the fish samples and L. Perezgomez for laboratory assistance. This research was supported by grants from the Consejo Nacional de Ciencia y Tecnologia (CONACYT), EDI-IPN, COFAA-IPN, and SNI to JDA. FJGR was supported by fellowships from PIFI-IPN and Programa Beca de Posgrado IPN.

References

Adkinson MD (1995) Population differentiation in the Pacific salmon: local adaptation, genetic drift or the environment?. Can J Fish Aquat Sci 52:2762-2777

Ahlstrom EH (1954) Distribution and abundance of egg and larval populations of the Pacific sardine. Fish Bull 56:83-140

Ahlstrom EH (1959) Distribution and abundance of eggs of the Pacific sardine, 1952-56. Fish Bull 60:185-213

Austin HM, Scoles D, Abell AJ (1998) Morphometric separation of annual cohorts within mid-Atlantic bluefish, *Pomatomus saltatrix*, using discriminant function analysis. Fish Bull 97:411-420

Blaxter JH, Hunter JR (1982) The biology of the clupeoid fishes. Advan Mar Biol 20: 1-223

Billington N, Hebert PDN (1991) Mitochondrial DNA diversity in fishes and its implications for introduction. Can J Fish Aquat Sci 48:80-94

Castro M, Gancho P, Henriques P (1998) Comparison of several populations of Norway lobster, *Nephrops norvegicus* (Linneus), from the Mediterranean and adjacent Atlantic: a biometric study. Sci Mar 62:71-79

Cisneros MA, Nevarez MM, Hammann GM (1995) The rinse and fall of the Pacific sardine, *Sardinops sagax caeruleus* Girard, in the Gulf of California, Mexico. CalCoFi Inv Rep 36:136-143

Clark FN, Janssen JF (1945) Movements and abundance of the sardine as measured by tag returns. Fish Bull 61:7-42

Clark FN (1947) Analysis of population of the Pacific sardine on the basis of vertebral counts. Fish Bull 65:1-26

Clayton JW (1981) The stock concept and the uncoupling of organismal and molecular evolution. Can J Fish Aquat Sci 38:1515-1522

Corti M, Thorpe RS, Sola L, Sbordoni V, Cataudella S (1988) Multivariate morphometrics in aquaculture: a case study of six stocks of the common carp (*Cyprinus carpio*) from Italy. Can J Fish Aquat Sci 45:1548-1554

Creech S (1992) A multivariate morphometric investigation of *Atherina boyeri* Risso, 1810 and *A presbyter* Cuvier, 1829 (Teleostei: Atherinidae): morphometric evidence in support of the two species. J Fish Biol 41:341-353

Elliot NG, Haskard K, Koslow JA (1995) Morphometrics analysis of orange roughly (*Hoplostethus atlanticus*) off continental slope of southern Australia. J Fish Biol 46:202-220

Felin FE (1954) Population heterogeneity in the Pacific pilchard. Fish Bull 54:201-225

Félix UR, Alvarado RM, Carmona PR (1996) The sardine fishery along the west coast of Baja California, 1981-1994. CalCoFi Inv Rep 37:188-192

Harris RJ (1975) A primer of multivariate statistics. Academic Press, New York

Hedgecock D, Hutchinson E, Nelson K, Sly F (1985) Morphological and biochemical genetic variation in the Pacific sardine *Sardinops sagax caerulea*. Memories Annual CalCoFi Conference, pp 16

Hedgecock D, Hutchinson E, Li G, Sly F, Nelson K (1989) Genetic and morphometric variation in the Pacific sardine, *Sardinops sagax caerulea*: comparison and contrasts with historical data and with variability in the northern anchovy, *Engraulis mordax*. Fish Bull 87:653-671

Hubbs CL (1929) The generic relationships and nomenclature of the California sardine. Proc Calif Acad Sci 18:261-265

Humphries PA (1993)Comparison of the mouth morphology of three co-occurring species of Atherinid. J Fish Biol 42: 85-593

Janssen JF (1938) Tag recoveries from the first thousand sardines. Calif Fish and Game 24: 69-71

Karakousis Y, Triantaphyllidis C, Economidis SP (1991) Morphological variability among seven populations of brown trout, *Salmo trutta* Linnaeus, in Greece. J Fish Biol 38:807-817

Klecka WR (1980) Discriminant Analysis. Sage Publications, Beverly Hills

Lin HC, Dunson WA (1999) Phenotypic plasticity in the growth of the self-fertilizing hermaphroditic fish *Rivulus marmoratus*. J Fish Biol 54:250-266

Lluch BD, Crawford RJM, Kawasaki T, MacCall AD, Parrish RH, Schwarloze RA, Smith PE (1989) Worldwide fluctuations of Sardine and anchovy stocks: the regime problem. S Afr J Mar Sci 8:195-205

Mais KF (1972) A subpopulation study of the Pacific sardine. Calif Fish and Game 58:296-314

Mayden LR, Rainboth JW, Buth GD (1991) Phylogenetic systematics of the cyprinid genera *Mylopharodon* and *Ptychocheilus*: comparative morphometry. Copeia 4:819-834.

Manly BF (1991) Multivariate Statistical Methods: a Primer. Chapman & Hall, London

Parrish RH, Serra R, Grant WS (1989) The monotypic sardines, *Sardina* and *Sardinops*: their taxonomy, distribution, stock structure, and zoogeography. Can J Aquat Fish Sci 46:2019-2036

Pawson MG (1995) Biogeographical identification of English Channel fish and shellfish stocks. Fish Res Tech Rep MAFF 99:1-72

Radovich JR (1995) Effects of sardine spawning stock size and environment on year class production. Calif Fish and Game 48: 23-140

Radovich JR, Phillips JB (1952) Distribution and abundance of young sardines. Fish Bull 87:1-63

Regan CT (1916) The British fishes of the subfamily Clupeinae and related species in other seas. Ann Mag Nat Hist 18: 1-19

Reist JD (1985) An empirical evaluation of several univariate methods that adjust for size variation in morphometric data. Can J Zool 63:1429-1439

Schaefer K M (1989) Morphometric analysis of yellowfin tuna *Thunnus albacares* from the eastern Pacific ocean. Inter Trop Tuna Comm Bull 19:387-427

Shaklee JB, Tamaru CS (1981) Biochemical and morphological evolution of Hawaiian bonefishes (*Albula*). Syst Zool 30:125-146

Skillman RA (1989) Status of Pacific Billfish stock. In: Troud RH (ed) Planning the future of billfishes: Research and management in the 90's and beyond. Fishery and stock synopses, data needs and management (Part 1). Marine Recreation Fisheries Series 13, Kailua-Kona, Hawaii, pp 175-195

Strauss RE, Bookstein FL (1982) The truss: body form reconstruction in morphometrics. Syst Zool 31:113-135

Tabachnick BG, Fidell L (1989) Using Multivariate Statistics. Harper & Collins Publishers, New York

Thompson WE (1926) The California sardine and the study of the available supply. Fish Bull 11:8-17

Torres-Villegas JR (1997) La reproducción de la sardina monterrey *Sardinops caerulea* (Girard, 1854) en el Noroeste de México y su relación con el ambiente. Ph D thesis, Universidad Politecnica de Cataluña

Torres-Villegas JR, Ochoa BRI, Perezgomez AL, Garcia MG (1985) Comparison of seasonal variability in the reproduction of Pacific sardine (*Sardinops sagax*) from the Baja California Sur, Mexico, in the years 1982-1992. Sci Mar 59:255-264

Vrooman AM (1964) Serologically differentiate subpopulations of the Pacific sardine, *Sardinops caerulea*. J Fish Res Board Can 21: 691-701

Wolf R, Daugherty AE (1964) Age and length composition of the sardine catch off the Pacific coast of the United States and Mexico in 1961 and 1962. Calif Fish and Game 50: 241-2

10. Sauropod Tracks – a geometric morphometric study

Luis Azevedo Rodrigues and Vanda Faria dos Santos

Museu Nacional de História Natural (MNHN), Universidade de Lisboa, Rua da Escola Politécnica, 58, P-1250-102 Lisboa, Portugal, lmrodrigues@fc.ul.pt

10.1 Abstract

Geometric morphometrics are used to characterize shape variations in different *Sauropodomorpha* ichnotaxa and unclassified ichnites. Ten landmarks were collected from each of 30 specimens. Landmark configurations were superimposed, and residuals were modeled with the thin-plate spline interpolating function (to visualize shape changes). This group of techniques allows to discriminate tendencies in shape changes (providing quantitative descriptors). The multivariate analysis of shape variables on the centroid size indicates the absence of allometry in our sample of *Sauropodomorpha* tracks.

Keywords: *Sauropoda pes* tracks, *Brontopodus*, geometric morphometrics, allometry, relative warps.

10.2 Introduction

Application of Geometric Morphometric (GM) techniques in the ichnological record haven't received much attention. Some applications have been made on dinosaur tracks particularly the *Theropoda* and *Ornithopoda* ichnological record (Rasskin 1995; Rasskin et al. 1997). This work presents the first GM study on the *Sauropodomorpha* ichnological record. Here we constrast a descriptive study based on four sauropod ichnological morphotypes with a geometric morphometric approach.

The discovery and documentation of many new sauropod tracksites in Portugal over the last ten years have yielded valuable information to better understand sauropod *manus* and *pes* prints morphologies. Nevertheless, well-preserved sauropod *manus* and *pes* prints are still rare in the general fossil record.

Until 1990 a small number of well-preserved specimens were known worldwide and few ichnogenus were considered valid scientific names. Middle Jurassic sauropod ichnites from Morocco were described as *Breviparopus taghbaloutensis* (Dutuit and Ouazzou 1980).

Brontopodus birdi was named on the basis of well-preserved sauropod trackways from Albian carbonates from Texas (Farlow et al. 1989). *Parabrontopodus mcintoshi* was proposed from narrow-gauge Upper Jurassic sauropod trackways (Lockley et al. 1994a)

The record of the ichnogenus *Brontopodus* is worldwide distributed - Portugal (Lockley et al. 1994a,b), Croatia (Mezga and Bajraktarevic 1999), Switzerland (Meyer 1993), Spain (e.g. Moratalla 1993), Poland (Gierlinski 2002), United Kingdom (Romano et al. 1999), China (Lockley et al. 2002), South Korea (e.g. Lim et al. 1994), Australia (e.g. Thulborn et al. 1994), USA (Farlow et al. 1989).

More recently, Lower Cretaceous sauropod footprints from Croatia were described and named as *Titanosaurimanus nana* (Dalla Vecchia and Tarlao 2000).

In the present study were used *Sauropodomorpha* footprints outlines from several works (Table 1).

Most of the sauropod footprints are oval- or egg-shaped without diagnostic digit impressions, due to inadequate substrate conditions, and further unfavorable conservation factors (e.g. Leonardi 1987; Lockley 1991; Gatesy et al. 1999; Garcia-Ramos et al. 2000; Nadon 2001). Nevertheless, several of these poorly preserved ichnites have received formal names despite the fact that other well-preserved specimens have not (Lockley et al. 1986).

Up to now, no Geometric Morphometric analysis of shape variation in a sample of *Dinosauria – Sauropodomorpha* footprints of the world ichnological record has been conducted and just only the preliminary results of the application of this methodological approach on 22 specimens were presented (Rodrigues and Santos 2003). The aim of this paper is to discuss the contribution of the Geometric Morphometrics analysis to improving the discrimination of *Sauropodomorpha* footprints and, possibly, to improving the characterization of ichnological shape variation.

In this paper we use GM analysis on *pes* prints attributed to *Sauropoda* and other marks attributed to *Prosauropoda* footprints in order to provide a contribution to *Sauropodomorpha* footprints discrimination. We chose a total of 30 *Sauropodomorpha pes* tracks from the world ichnological record (range of standard length 5.8–94.0 cm) (see Table 1).

10.3 Materials and methods

10.3.1 Samples

Good general preservation and presence of, at least, four digit impressions determined selection of specimens. With these selection criteria, we tried to reduce the taphonomical bias.

The descriptions of sauropod tracks were based on several features characteristics of *Sauropoda autopodia*. Concerning *pes* prints the following distinctive features were characteristic:

- subcircular/suboval/subtriangular shape of the *pes* print with asymmetrical expanded proximal portion (entaxonic);
- outward rotated;
- four or five digit impressions usually outward rotated or laterally oriented;
- strongly curved and usually triangular impressions;
- claws on digits I, II, III.

We grouped the specimens into four morphotypes, based on the ichnotaxonomy proposed by different authors in the literature. Morphotype 1 (MT1) – this morphotype gathers *Brontopodus birdi/Brontopodus* sp.; Morphotype 2 (MT2) – *Brontopodus* aff. *B. birdi* / *Brontopodus type* / *Brontopodus*; Morphotype 3 (MT3)– *Prosauropoda* ichnites (*Tetrasauropus/ Pseudotetrasauropus/ Paratetrasauropus*); Morphotype 4 (MT4) – miscellaneous and unidentified ichnites.

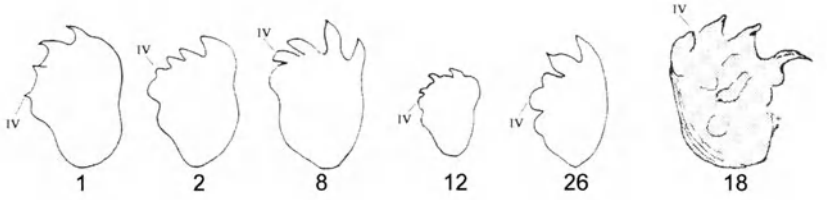

Fig. 1. Examples of specimens used in this study – Specimen 1 (Morphotype 1), Specimen 2 (Morphotype 2), Specimen 8 (Morphotype 4), Specimen 12 (Morphotype 1), Specimen 26 (Morphotype 2) and Specimen 18 (Morphotype 3). Parataxonomy and references in Table 1. IV – fourth digit. (Adapted from Lockley et al. 1994a, Santos et al. 1994, Thulborn 1990)

10.3.2 Obtaining Landmarks coordinates

Due the inherent characteristics of the materials analyzed in this study, the type of landmarks applied were Type III (Bookstein 1991).

Silhouettes and photos of *Sauropodomorha* footprints in literature were used and digitized with Hp 5470C scanner.

Images were treated digitally (digital clearness) using Paint Shop Pro 7.0 (Jasc Software 2002).

We assumed that all specimens were left *pes*. When only right *pes* existed, the specimens were reflected (mirror effect) using Paint Shop Pro 7.0 (Jasc Software 2002).

The coordinates of the specimens were determined with TpsDig 1.37 (Rohlf 2003a). Since we used figures from different literature sources, they presented different sizes. In order to correct this we used scale factor in every specimen.

Some of the specimens studied have been measured in terms of length and width, applying the measure tool on TpsDig 1.37 (Rohlf 2003a). This procedure was applied because those measurements are not mentioned in the literature.

10.3.3 Description of landmarks

1- maximum *hypex* of digit I; 2 - *hypex* between digits I and II; 3 - maximum *hypex* of digit II; 4 - *hypex* between digits II and III; 5 - maximum *hypex* of digit III; 6 - *hypex* between digits III and IV; 7 - maximum *hypex* of digit IV; 8 – intersection point between a perpendicular line (from mid point of landmark 7 and 9) and the ichnite contour; 9 – most posterior point of the print considering its axis; 10 - intersection point between a perpendicular line (from mid point of landmark 1 and 9) and the ichnite contour .
All ichnological terms and definitions follows Leonardi (1987) and Thulborn (1990). The long axis of the footprint employed in the landmarks 8, 9 and 10 follows the definition of Leonardi (1987).

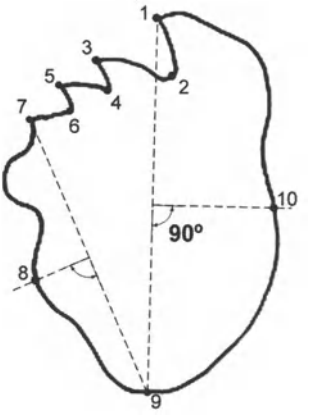

Fig. 2. Orientation terminology and position of the 10 landmarks used in this study. Landmark 1 and 9 are in the anterior and posterior region of the track, respectively; landmark 8 and 10 are in the lateral and medial region of the track, respectively

The mid points between landmarks 1 and 9 and between 7 and 9 were calculated. Marking of a perpendicular line to the referred mid points and the point of intersection of that line with the contour of the footprint. These calculations were performed with Microsoft Visio 2000 (Microsoft Corporation 2000).

A full, detailed, mathematical description of the GM methodology used in this study is outside the range of this paper. Theoretical background of these methdologies are reviewed in different literature sources (e.g. Bookstein 1989a, b, 1990, 1991, Rohlf and Marcus 1993, Marcus et al. 1996, Rohlf and Bookstein 2003).

For each specimen, centroid size and weight matrix (with both uniform components appended) were computed. The weight matrix is the matrix of the partial warp scores. Centroid size was tested for differences by single classification analysis of variance (ANOVA) (Sokal and Rohlf 1995). All specimens were scaled to unit centroid size before alignment by the method of Generalized Procrustes Analysis (GPA) superimposition.

10.4 Relative warp analysis

The coordinates of all aligned specimens were used for thin-plate splines relative warp analysis (Bookstein 1991; Rohlf 1993).

The Relative Warps (RW) analysis was performed with the scaling option $\alpha=0$ (Rohlf 1993) that weights all landmarks equally, with the uniform component included - complement method (Rohlf and Bookstein 2003).

Relative warps analysis corresponds to a Principal Components Analysis of the covariance matrix of the partial warp scores, which are different scales of a thin-plate spline transformation of landmarks. The thin-plate spline is a smooth interpolation function that computes and visualizes transformations of Cartesian Coordinates in a way similar to D'Arcy Thompson's transformation grids (Thompson 1917). A rectangular grid is projected over Procrustes aligned landmark configurations and the bending of the grid visually depicts the difference in landmark locations between two configurations

The columns of the weight matrix represent the shape variables (Partial warps), being the last two columns the uniform shape components (Unif X, shearing, and Unif Y, stretching along the major axis of the consensus configuration). The first n-2 columns characterize more localized shape components (non uniform shape components).

10.5 Multiple regression analysis

Centroid size, the square root of the sum of the squared distances between all homologous landmarks and the center of gravity of the landmarks, is commonly used as general size measure in geometric morphometrics.

To explore the existence of size allometry (i.e. shape change as a function of size), a multivariate regression of the weight matrix (with uniform components appended) onto log centroid size was performed. The log of centroid size was used as our size variable because most of shape change occurs early in ontogeny (e.g. Zeldich et al. 2000).

10.6 Software

Procrustes superimposition, weight matrix, graphical material and centroid size were performed using TPSRelw 1.35 (Rohlf 2003b); TPSRegr 1.26 (Rohlf 2003c). Statistical analysis and scatterplots – SPSS 10.0 (SPSS Inc., 2000).

10.7 Results

Centroid size was tested for differences among specimens by ANOVA ($F= 4.126$, $p< 0.05$) and was significant. The centroid size is moderately correlated with the uniform component x ($r=-0.379$, $p<0.05$) and not correlated with uniform component y.

10.7.1 Relative warps analysis

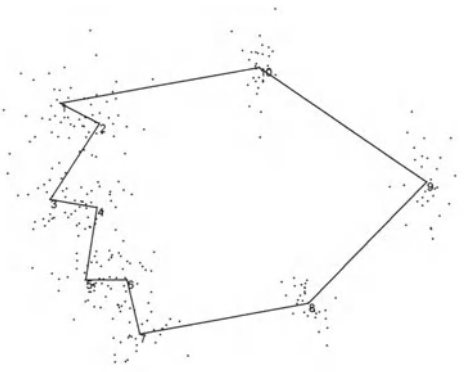

Fig. 3. Scatterplot of mean consensus configuration with individual specimens superimposed by Generalized Procrustes Analysis (GPA)

There is large variability in most of the landmarks as visualized in Fig. 3. In landmarks 8, 9 and 10 the observed variability is mostly latero-medial.

The first three relative warps account for 66.46% of the total variation of the specimens. RW1 accounts for 35.52% of total shape variability. There is a significant correlation between centroid size and the first relative warp (r=0.404, P <0.05).

RW2 accounts for 18.40% for shape variability and is not correlated with centroid size. RW3 explains 12,54% of shape variability and is not correlated with centroid size.

The distribution of the four morphotypes is presented in a scatterplot of Relative Warp 1 (RW1) and Relative Warp 2 (RW2) (Fig. 4).

Distribution of specimens presents some tendencies: specimens 16, 17 and 18 (*Prosauropoda* origin) clearly separated from other specimens; specimens 1, 2, 12, 24 and 26 are morphological related despite their different morphotype classification; Croatia specimens (27, 28, 29 and 30) are closely associated with the exception of specimen 30. This could be explained as probable misidentification of digit polarity. All other specimens present a distribution very similar with the consensus and without clear grouping.

Patterns of shape change along the two first relative warps are illustrated in Fig.5. Most of the variance from the consensus, along RW1 axis (negative to positive deviations), is due to the rotation of digits from an inward (medial) position to an outward (lateral) position. Similar tendency in relative shape change is observed in the heel region. This shape variation along this axis is also a consequence of a medial bending. In addition, we detected an antero-posterior shortening associated with digit rotation (both outward and inward). The correlation between centroid size and the first relative warp support this size shift.

RW2 differences from the consensus (negative to positive deviations) are due: 1- reduction in relative length of digits I and II; 2 – digits I, II and III becoming narrow.

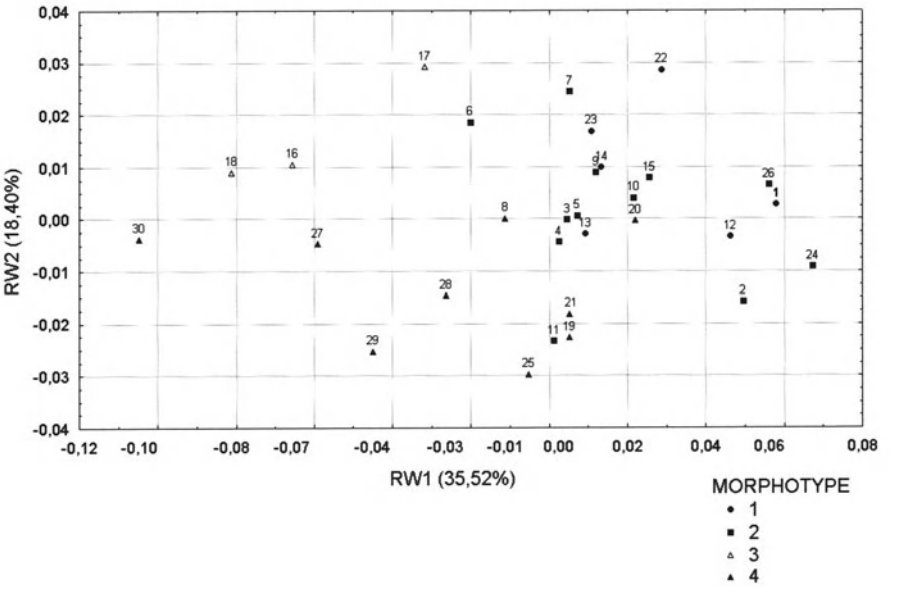

Fig. 4. Scatterplot of RW1 and RW2 of the specimens and respective Morphotypes

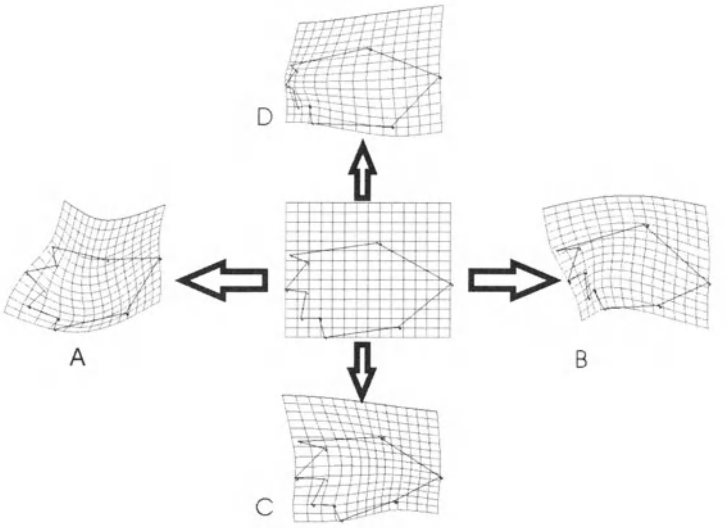

Fig. 5. Shape changes depicted by the RW1 and RW2. (A) Deformation relative to the mean shape toward the negative direction of RW1. (B) Deformation relative to the mean shape toward the positive direction of RW1. (C) Deformation relative to the mean shape toward the negative direction of RW2. (D) Deformation relative to the mean shape toward the positive direction of RW2

10.7.2 Multiple regression analysis

Regressing the full set of partial warps on log centroid size showed no significant differences (Wilks' Lambda = 0.4372, F (16, 13) = 1.046, P>0.4). Size explains only 4.91% of the shape variation in our sample. Clearly, in our sample, shape is not a function of size.

The isometric growth of appendicular skeleton in sauropods has been noted (e.g. Carpenter and McIntosh 1994). For instance, the limbs of *Camarasaurus* show evidence of isometric growth with very little indication of allometry (Wilhite 1999, 2003). Some authors also noted isometric growth in the limbs of *Apatosaurus* (Carpenter and MacIntosh 1994).

10.8 Discussion and conclusions

Ichnology can complement information from the dinosaur osteological record, for instance, by providing complementary data on *autopodia* shape and structure as well on limb posture. (Lockley and Hunt 1995; Gatesy et al. 1999; Wilson and Carrano 1999).

GM techniques were applied for the first time in the *Sauropodomorpha* ichnological record, as far as we are aware. This methodology allowed to descriminate between tendencies in shape changes in our sample as well as to confirm the absence of allometry.

The shape variation observed in our sample are caused by:

relative digit position (inward/medial to outward/lateral rotation);

medial region bending (directly associated with outward/lateral rotation of digits) and relative heel position (inward/medial to outward/lateral rotation).

We have observed and quantified that specimens attributed to prosauropods (*Tetrasauropus, Pseudotetrasauropus* and *Paratetrasauropus*) are closely related to each other in comparison to the mean shape and to specimens attributed to sauropods (i.e. there is a morphological discontinuity between the *Prosauropoda* and *Sauropoda* tracks). As a consequence of this GM analysis, we can maintain the idea of a *Prosauropoda* origin for Morphotype 3, which includes the above referred ichnogenus type *Tetrasauropus*. An opposite ichnotaxonomical proposal is the attribution of *Tetrasauropus* to the *Sauropoda* ichnological record (Lockley et al. 2001).

The general sauropod track record suggests that *pes* prints are slightly longer than wider and present a trend as an outward rotation of four or five externally rotated digit impressions (e.g. Farlow et al. 1989; Lockley 1991; Meyer et al. 1994). These features are reliable with character 64 on the sauropod phylogenetic hypothesis of Wilson and Sereno (1998) - "*Pedal unguals, orientation: aligned with (0), or deflected lateral to (1), digit axis*".

Digit rotation is the most important factor in the shape variation in our sample. Despite this, there are other factors contributing to the variability of shape observed.

This analysis allows us to suggest that *Brontopodus birdi* present more outward rotated digits than the Portuguese specimens 3, 4, 5 and 8. These specimens present a digit rotation very similar to mean shape.

Specimens from Croatia (27, 28, 29 and 30) were attributed to a *Titanosauria* origin (Dalla Vecchia and Tarlao 2000). In this analysis, they are the most extreme specimens regarding inward digit rotation, which is close associated with Morphotype 3 (*Prosauropoda* origin) and distant to Morphotypes 1 and 2 (*Sauropoda* origin). This may suggest a slightest non-*sauropoda* origin hypothesis or digit misidentification (i.e. digit I could be digit IV, inverting the digit rotation course). This methodology could permit the recognition of misidentified tracks as long as other factors could be included (e.g. stratigraphical age, wide or narrow-gauge trackway).

Morphotypes 1 and 2 are morphologically comparable, which is confirmed by its parataxonomical origin affinity. This GM study corroborates the majority of previous ichnotaxonomical classifications.

The multivariate regression analysis on the centroid size supports the lack of allometry in different taxa of *Sauropoda* limbs (Wilhite 1999, 2003; Carpenter and MacIntosh 1994). This geometric study corroborates the osteological results on absence of allometry on *Sauropoda* appendicular structures.

Other multivariate analyses are currently under study using as independent variables: velocity; wide/narrow gauge trackway; geological/stratigraphical frame; illustration authors. This latter variable study is justified by the ichnological interpretation that precedes each track illustration. It means the author of the illustration is a very important variable in geometric morphometric studies that uses track contours.

Table 1. Reference, morphotype, parataxonomy, age, literature consulted and standard dimensions of the specimens analyzed. * - measurements made by the authors; ** - measurements made by the authors on the most external contour; LT- Late Triassic; J- Jurassic MJ- Middle Jurassic UJ- Upper Jurassic; LC – Lower Cretaceous.

Reference	Morphotype	Parataxonomy	Age	Authors	Length	Width
1	1	*Brontopodus birdi*	LC	Thulborn 1990, p. 170, fig. 6.16.a	89*	65*
2	2	*Brontopodus aff. B. birdi*	UJ	Santos 2003, p. 249, fig. 6.15.9.	80	58
3	2	*Brontopodus aff. B. birdi*	UJ	Santos 2003, p. 241, fig. 6.15.5.	72*	56*
4	2	*Brontopodus aff. B. birdi*	UJ	Santos 2003, p. 241, fig. 6.15.5.	80	50
5	2	*Brontopodus aff. B. birdi*	UJ	Santos 2003, p. 186, fig. 6.7.3.	85	68
6	2	*Brontopodus aff. B. birdi*	UJ	Santos 2003, p. 186, fig. 6.7.3.	70	60
7	2	*Brontopodus aff. B. birdi*	UJ	Santos 2003, p. 188, fig. 6.7.4.	60	60
8	4	*Polyonichnus gomesi*	MJ	Santos 2003, p. 124, fig. 6.1.7.	90	60
9	2	*Brontopodus aff. B. birdi*	UJ	Lires 2000, p. 33	74*	56*
10	2	*Brontopodus aff. B. birdi*	UJ	Lires 2000, p. 34	62*	58*
11	2	*Brontopodus aff. B. birdi*	UJ	Lires 2000, pers. commun.	52	36
12	1	*Brontopodus sp.*	UJ	Lockley & Mickelson 1997, p. 136	60	46
13	1	*Brontopodus sp.*	UJ	Lockley & Mickelson 1997, p. 136	55	40
14	1	*Brontopodus sp.*	UJ	Lockley & Mickelson 1997, p. 136	55	40
15	2	*Brontopodus (?)*	LC	Thulborn 1990, p. 170, fig. 6.16.f	70	65*
16	3	*Pseudotetrasauropus*	LT	Thulborn, 1990, p. 178, fig. 6.23.b	49	39*
17	3	*Paratetrasauropus*	LT	Thulborn 1990, p. 178, fig. 6.23.e	28	22*
18	3	*Tetrasauropus*	LT	Thulborn 1990, p. 178, fig. 6.23.c	44	41*
19	4	Non-identified	J	Thulborn 1990, p. 170, fig. 6.16.e	80	51*
20	4	Non-identified	LC	Woodhams 1998, pers. commun.	58*	36*
21	4	Non-identified	LC	Woodhams 1998, pers. commun.	62*	51*
22	1	*Brontopodus birdi*	LC	Ray Stanford 2003, pers. commun.	5.8	5
23	1	*Brontopodus birdi*	LC	Ray Stanford 2003, pers. commun.	5.8	5
24	2	*Brontopodus type*	MJ	Romano et al. 1999, p. 365, fig. 3A	94	70
25	4	*Breviparopus type*	MJ	Romano et al. 1999, p. 365, fig. 3B	81	67
26	2	*Brontopodus type*	UJ	Lockley et al. 1994, p.143, fig. 6.b	83*	51*
27	4	*Titanosaurimanus nana*	LC	Dalla Vecchia & Tarlao, 2000, p. 261, fig. 29E	34.5**	32**
28	4	*Titanosaurimanus nana*	LC	Dalla Vecchia & Tarlao, 2000, p. 261, fig. 29G	33**	29**
29	4	*Titanosaurimanus nana*	LC	Dalla Vecchia & Tarlao, 2000, p. 261, fig. 29B	31**	23**
30	4	*Titanosaurimanus nana*	LC	Dalla Vecchia & Tarlao, 2000, p. 261, fig. 29F	34**	29**

10.9 Acknowledgements

The authors would like to thank: Prof. James Rohlf (Stony Brook University, USA) for all of his helpful comments and support; Dr. Ângela Delgado Buscalioni and Jesus Marugán-Lóbon (Universidad Autónoma, Madrid) for helpful comments; Jose Lires (University of Oviedo, Spain) for giving information about sauropod *pes* natural casts of Upper Jurassic of Asturias, Spain; Ray Stanford (*Mesozoic Track Project*) for the two small *Brontopodus birdi* specimens (22, 23) and all of his helpful comments; Dr. Kenneth Woodhams for the specimens 20 and 21; Sara Bárrios for assistance in data processing. A special thanks to Prof. Galopim de Carvalho (MNHN/University of Lisbon) for all of his support. The manuscript was greatly improved by the comments of two anonymous reviewers. This work was partially funded by Project Fundação para a Ciência e Tecnologia (FCT) POCTI/PAL/36550/2000 - "Dinosaur Osteological and Ichnological studies of the Mesozoic of Portugal (DINOS)".

References

Bookstein FL (1989a) Principal warps: thin-plate splines and the decomposition of deformations, IEEE trans. Pattern Analysis and Machine Intelligence 11(6): 567-585.

Bookstein FL (1989b) "Size and Shape": a comment on semantics. Systematic Zool 38: 173-180

Bookstein FL (1990) Introduction to methods for landmark data. In: Rohlf FJ, Bookstein FL (eds) Proceedings of the Michigan morphometric workshop. Univ.Michigan Mus. Zool. Spec. Publ., Ann Arbor (Michigan), 2: 215-225

Bookstein FL (1991) Morphometric Tools for Landmark Data. Geometry and Biology. Cambridge University Press, New York

Carpenter K, McIntosh JS (1994) Upper Jurassic sauropod babies from the Morrison Formation, pp. 265-278. In: Carpenter K, Hirsch KF, Horner JR (eds) Dinosaur Eggs and Babies. Cambridge University Press, New York, pp 265-278

Dalla Vecchia FM, Tarlao A (2000) New Dinosaur track sites in the Albian (Early Cretaceous) of the Istrian peninsula (Croatia) - Parte II - Paleontology. Mem Sci Geologiche 52(2): 227-292

Dutuit JM, Ouazzou A (1980) Découverte d'une piste de dinosaure sauropode sur le site d'empreintes de Demnat (Haut-Atlas Marocain). Mém Soc Géol France, NS 139: 95-102

Farlow JO, Pittman JG, Hawthorne JM (1989) Brontopodus birdi, Lower Cretaceous sauropod footprints from the U. S. Gulf coastal plain. In: Gillette DD, Lockley MG (eds) Dinosaur Tracks and Traces. Cambridge University Press, Cambridge, pp 371-394

Garcia-Ramos JC, Aramburu C, Piñuela L, Lires J (2000) La costa de los dinosaurios. Consejería de Educación y Cultura del Principado de Asturias, Oviedo

Gatesy SM, Middleton KM, Jenkins F, Shubin NH (1999) Three-dimensional preservation of foot movements in Triassic theropod dinosaurs. Nature 399:141-144

Gierlinski G (2002) Dinosaur Tracks in the Late Jurassic of Poland. Journal of Vertebrate Paleontology 22(3): 58A

JASC SOFTAWRE (2002) Inc Paint Sho Pro version 7.0. USA

Leonardi G (1987) Glossary and Manual of Tetrapod Footprint Palaeoichnology. Departmento Nacional da Produção Mineral, Brasilia

Lim SK, Lockley MG, Yang S-Y, Fleming RF, Houck KA (1994) Preliminary report on sauropod tracksites from the Cretaceous of Korea. Gaia 10: 109–117

Lires J (2000) Icnitas de dinosaurios cuadrúpedos del Jurásico de Asturias. Morfometría, morfología e interpretación. (Memoria de Investigación, Dept Geol, Universidad de Oviedo)

Lockley MG (1991) Tracking Dinosaurs: a new look at an ancient world. Cambridge University Press, Cambridge

Lockley MG, Hunt AP (1995) Dinosaur tracks and other fossil footprints of the western United States. Columbia University Press, Cambridge

Lockley MG, Mickelson D (1997) Dinosaur and pterosaur tracks in the Summerville and Bluff (Jurassic) beds of eastern Utah and northeastern Arizona. New Mexico Geological Society Guidebook, 48th Field Conf. Four Corners Region pp 133-138

Lockley MG, Farlow JO, Meyer CA (1994a) Brontopodus and Parabrontopodus ichnogen nov. and the significance of wide- and narrow-gauge sauropod trackways. Gaia 10: 135-145

Lockley MG, Meyer CA, Santos VF (1994b) Trackway evidence for a herd of juvenile sauropods from the Late Jurassic of Portugal. Gaia 10: 43-48

Lockley MG, Houck KJ, Prince NK (1986) North America's largest dinosaur trackway site: implications for Morrison paleoecology. Bull Geol Soc Am 97: 1163-1176

Lockley MG, Wright JL, Hunt AP, Lucas SG (2001) The Late Triassic sauropod track record comes into focus: old legacies and new paradigms. New Mexico Geological Society Guidebook, 52nd Field Conference, Geology Llano Estacado

Lockley MG, Wright J, White D, Matsukawa M, Jianjun L, Lu F, Hong L (2002) The first sauropod trackways from China Cretaceous Research 23: 363–381

Marcus LF, Corti M, Loy A, Naylor G, Slice DE (1996) Advances in morphometrics. Plenum, New York

Meyer CA (1993) A sauropod megatracksite from the Late Jurassic of northern Switzerland, Ichnos 2:1–10

Meyer CA, Lockley MG, Robinson JW, Santos VF (1994) A comparison of well-preserved sauropod tracks from the Late Jurassic of Portugal, and the western United States: Evidence and implications. Gaia 10: 57-64

Mezga A, Bajraktarevic Z (1999) Cenomanian dinosaur tracks on the islet of Fenoliga in southern Istria, Croatia Cretaceous Research 20: 735–746

Microsoft Corporation (2000) Microsoft Visio 2000 (2000), USA

Moratalla JJ (1993) Restos indirectos de dinosaurios del registro español: paleoicnología de la Cuenca de Cameros (Jurásico Superior-Cretácico Inferior) y paleoología del Cretácico Superior, Tesis Doctoral, Facultad de Ciencias, Univ Autónoma de Madrid 729 p (inédita)

Nadon GC (2001) The Impact of Sedimentology on Vertebrate Track Studies. In: Tanke DH, Carpenter K (ed) Mesozoic Vertebrate Life. Indiana Univ Press, Bloomington, pp. 395-407

Rasskin-Gutmann D (1995) Modelos Geométricos y Topológicos en Morfología. Exploración de los limites del morfoespacio afin. Aplicaciones en Paleobiologia. Ph D thesis, Universidade Autónoma de Madrid

Rasskin-Gutman D, Hunt G, Chapman RE, Sanz JL, Moratalla JJ (1997) The shapes of tridactyl dinosaur footprints: Procedures, problems and potentials. In: Wolberg/Stump/Rosenberg, Dinofeast International, pp 377—383

Rodrigues LA, Santos VF (2003) Quantitative description of sauropod tracks – a geometric morphometrics study. Journal of Vertebrate Paleontology 23(3):90A

Rohlf FJ (1993) Relative warp analysis and an example of its application to mosquito wings. In: Marcus LF, Bello E, Garcia-Valdecasas, A (eds) Contributions to Morphometrics. Museo Nacional de Ciencias Naturales (CSIC), Madrid, pp 131-159

Rohlf FJ (2003a) tpsDig, version 1.37. Department of Ecology and Evolution, State University of New York, Stony Brook

Rohlf FJ (2003b) tpsRelw, version 1.35. Department of Ecology and Evolution, State University of New York, Stony Brook

Rohlf FJ (2003c) tpsRegr, version 1.26. Department of Ecology and Evolution, State University of New York, Stony Brook

Rohlf FJ, Bookstein FL (2003) Computing the uniform component of shape variation. Systematic Biology 52: 66-69

Rohlf FJ, Marcus LF (1993) A revolution in morphometrics. Trends Ecology and Evolution 8:129–132

Romano M, Whyte MA, Manning PL (1999) New sauropod dinosaur prints from the Saltwick Formation (Middle Jurassic) of the Cleveland Basin, Yorkshire. Proceedings of the Yorkshire Geological Society 52: 361-369

Santos VF (2003) Pistas de dinossáurio no Jurássico-Cretácico de Portugal Considerações paleobiológicas e paleoecológicas. Ph D thesis, Universidade Autónoma de Madrid

Santos VF, Lockley MG, Meyer CA, Carvalho J, Galopim de Carvalho AM, Moratalla JJ (1994) A new sauropod tracksite from the Middle Jurassic of Portugal. GAIA 10: 5-13

Sokal RR, Rohlf FJ (1995) Biometry: the principles and practice of statistics in biological research. 3rd edition. WH Freeman and Co, New York, 887 pp

SPSS Inc. (2000) SPSS 10.0 for Windows (2000), Chicago, USA.

Thompson DW (1917) On growth and form. Cambridge University Press: London 753 pp

Thulborn RA (1990) Dinosaur Tracks. Chapman and Hall, London

Thulborn RA, Hamley T, Foulkes P (1994) Preliminary report on sauropod dinosaur tracks in the Broome sandstone (Lower Cretaceous) of Western Australia. Gaia 10: 85-96

Wilhite R (1999) Ontogenetic variation in the appendicular skeleton of the genus Camarasaurus. Master's thesis, Brigham Young University

Wilhite R (2003) Biomechanical reconstruction of the appendicular skeleton in three North American Jurassic sauropods. Ph D thesis, Louisiana State University

Wilson JA, Carrano MT (1999) Titanosaurs and the origin of 'wide-gauge' trackways: a biomechanical and systematic perspective on sauropod locomotion. Paleobiology 25: 252-267

Wilson JA, Sereno P (1998) Early evolution and higher level phylogeny of sauropod dinosaurs. Journ Vert Paleontol 18(2): 1- 68

Zelditch ML, Sheets HD, Fink WL (2000) Spatiotemporal reorganization of growth rates in the evolution of ontogeny. Evolution, 54(4): 1363-1371

11 Morphometric approach to Titanosauriformes (Sauropoda, Dinosauria) femora: Implications to the paleobiogeographic analysis

José I. Canudo and Gloria Cuenca-Bescós

Área y Museo de Paleontología. Facultad de Ciencias. Universidad de Zaragoza. 50009 Zaragoza, Spain, jicanudo@unizar.es; cuencag@unizar.es

11.1 Abstract

A morphometric approach to Titanosauriformes sauropod dinosaur femora provides an interesting tool for systematic and paleobiogeographic studies. The femur is an element of phylogenetic interest, being the proximal one third deflected medially or lateral bulge one of the autapomorphies of Titanosauriformes. Some of the selected 20 landmarks use to be reference anatomical points for the femur measurements, yet never attempting to apply for the Geometric Morphometrics. The landmarks are located at the posterior femora outline, except for the fourth trochanter that is a medial projection of this feature. The Procrustes Superimposition Analysis reveals that there are differences among some Titanosauriformes clades, for instance between the Titanosauria from Laurasia and Gondwana. This may indicate they separate at the end of the Jurassic times, when supercontinents were the Pangea, and it is unnecessary to resort to intercontinental bridges during the Upper Cretaceous to explain the existence of Titanosauria in Laurasia

Keywords: Titanosauriformes, Sauropoda, femora, biogeography, APS.

11.2 Introduction

At the end of the Jurassic the definitive rupturing of Pangea started. This formed the super-continent of Laurasia, whereas the continents of the southern hemisphere shaped Gondwana. The fragmentation between these two super-continents is more significant at the beginning of the Cretaceous with the opening of the central Atlantic and its interaction with the Tethys (Bonaparte and Kielan Jaworoska 1987; Calvo and Salgado 1996; Le Loeuff 1997; Sereno 1999).

The oceanic masses constitute a formidable barrier for terrestrial organisms. It's certain that this would have hindered the movement of terrestrial organisms be-

tween Laurasia and Gondwana during most of the Lower Cretaceous. This isolation has been the reason for the notorious divergence between the cretaceous faunas on each side of these continental masses. Some of the cretaceous taxa are considered as laurasiatic or gondwanic, according to their presence or abundance on each continental mass. The occasional presence of these taxa outside Laurasia or Gondwana respectively, has frequently been explained as the dispersion from their place of origin through terrestrial bridges (Le Loeuff and Buffetaut 1991; Forster 1999). The common taxa may be the result of faunal migrations between Laurasia and Gondwana or at least from a specific flow in both directions during the Cretaceous. However shared taxa can also be explained, in biogeographic terms, as a result of dispersion from the place of origin or by vicariance, which means the partition of an ancestral taxon and its posterior evolution separated by a geographic barrier (Foster 1999; Canudo and Salgado 2003).

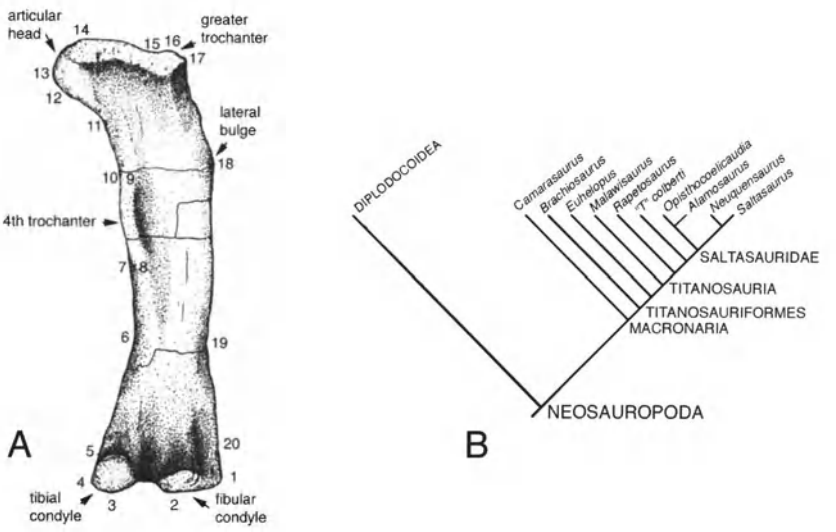

Fig. 1. A: Landmarks position (LM: 1-20) and terminology used in this paper. LM's are located on a posterior view of a right femur of *Phuwiangosaurus sirindhornae* (slightly modified from Martin et al. 1999). B: Neosauropoda Phylogeny (Wilson 2002)

Sauropoda are the terrestrial vertebrates that have reached the largest size in the Earth's history. During the last years there has been a considerable effort to understand their phylogenetic relationships and most important clades (Salgado et al. 1997; Wilson and Sereno 1998; Upchurch 1998; Wilson 2002), which has permitted the reconstruction of the phylogeny of Sauropoda. Titanosauriformes is well differentiated by unmistakable sinapomorphies. One of the femur sinapomorphies is the lateral bulge of the shaft (Salgado et al. 1997; Wilson and Sereno 1998; Wilson 2002), which means that the proximal one third is deflected medially (LM 18 in Fig. 1A).

Titanosauriformes originated during Jurassic before Pangea's fragmentation. One of the oldest taxa known is *Brachiosaurus*, which is found at the end of the

Tanzanian and USA Jurassic. Actual cladistic studies consider *Brachiosaurus* as the most basal titanosauriform (Salgado et al. 1997; Wilson 2002, Fig.1B). During the Lower Cretaceous they show an important diversification (McIntosh 1990; Hunt et al. 1994). As well as their broad distribution, as per their pangeatic origin, Titanosauriformes (specially Titanosauria) have been used to make palaeobiogeographic reconstructions mainly as proof of the existence of intercontinental bridges (Le Loeuff 1993; Casanovas-Cladellas and Santafé-Llopis 1993; Foster, 1999). Nevertheless, the presence of Titanosauriformes in the Jurassic Pangea explains its cretaceous distribution as a consequence of a vicariant evolution (Canudo and Salgado 2003).

The objective of this work is to study the variation of the shape of the Titanosauriformes femora and the use of the Geometric Morphometrics as a tool for paleobiogeographic studies.

Table 1. Sauropod femur illustration used in this study

Taxa	Figuration	E	G. S.
Aegyptosaurus baharijiensis Stromer, 1932	Stromer 1932	LC	Afr
Alamosaurus sanjuanensis Gilmore, 1922 #	Lehman Coulson 2002	LC	NA
Ampelosaurus atacis Le Loeuff, 1995	This paper	LC	Eur
Antarctosaurus wichmannianus Huene, 1927	Bonaparte 1996	LC	SA
Aragosaurus ischiaticus Sanz et al., 1987	This paper	EC	Eur
Brachiosaurus altithorax Riggs, 1901	McIntosh 1990	LJ	NA
Brachiosaurus brancai Janensch, 1914 #	Janensch 1961	LJ	Afr
Brachiosaurid	Blows 1995	EC	Eur
Chubutisaurus insignis del Corro, 1975 #	Salgado 1993	LC	SA
Euhelopus zdanskyi Wiman, 1929 #	Wiman 1929	EC	Asia
Lirainosaurus astibiae Sanz et al., 1999	Sanz et al. 1999	LC	Eur
Magyarosaurus dacus Nopcsa, 1915	McIntosh 1990	LC	Eur
Magyarosaurus dacus Nopcsa, 1915 #	Jianu Weishampel 1999	LC	Eur
Neuquensaurus australis(Lydekker, 1883)	Huene 1929	LC	SA
Neuquensaurus robustus(Huene, 1929)	Huene 1929	LC	SA
Opisthocoelicaudia skarzynskii Borsuk-Bialynicka, 1977 #	Borsuk-Bialynicka 1977	LC	Asia
Phuwiangosaurus sirindhornae Martin et al., 1994 #	Martin et al. 1999	EC	Asia
Pleurocoelus nanus Marsh, 1888 #	Glut 1997	EC	NA
Saltasaurus loricatus Bonaparte & Powell, 1980	Bonaparte Powell 1980	LC	SA
Tangvayosaurus hoffeti Allain et al., 1999 #	Allain et al. 1999	EC	Asia
Tangvayosaurus? falloti Hoffet, 1943 #	Hoffet 1943	EC	Asia
Titanosauriformes indet.	This paper	EC	Eur
"Titanosaurus" indicus *Lydekker, 1877	McIntosh 1990	LC	Asia
"Titanosaurus" indicus *Lydekker, 1877 #	Swinton 1947	LC	Asia

G.S: Geographical Situation. Afr: Africa NA: North America Eur: Europe SA: South America LJ: Late Jurassic EC: Early Cretaceous LC: Late Cretaceous E: Epoch #: Reversed *: *Titanosaurus indicus* has recently revised by Wilson and Upchurch (2003), they concluded that the genus *"Titanosaurus"* and family "Titanosauridae" may be likewise abandoned, for this reason we use inverted commas.

11.3 Materials and methods

Data has been collected from 24 figures of whole femurs of Titanosauriformes (Table 1 and Figures 2 and 3). The landmarks are situated on the posterior view of the femur perimeter except the ones showing the fourth trochanter position.

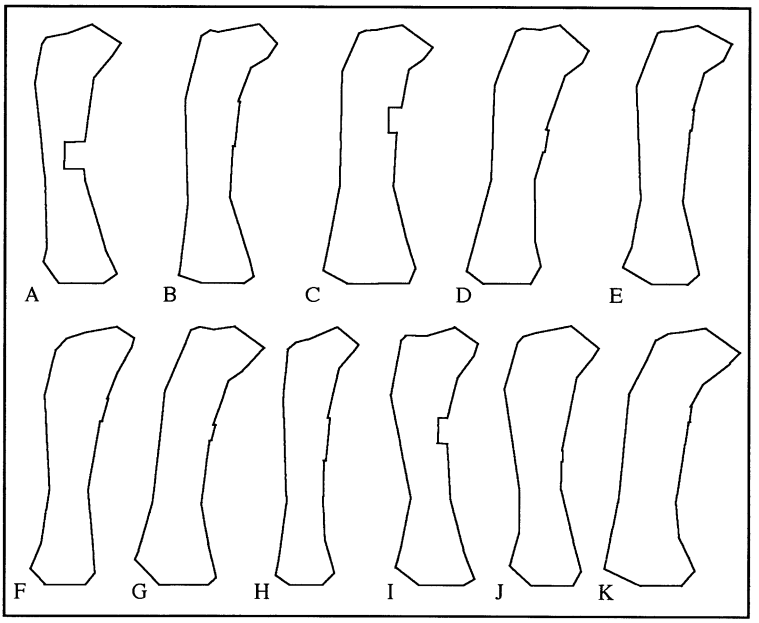

Fig. 2. Outline femora made with the landmarks junction. A: *Euhelopus zdanskyi*. B: *Phuwiangosaurus sirindhornae*. C: *Tangvayosaurus hoffeti*. D: *Brachiosaurus altithorax*. E: *Brachiosaurus brancai*. F: Brachiosaurid. G: *Aragosaurus ischiaticus*. H: Titanosauriformes indet. I: *Pleurocoelus nanus*. J: *Chubutisaurus insignis*. K: *Tangvayosaurus? falloti*. References are in table 1

The landmarks have been obtained through outlines drawn from the figures of the posterior views published by the authors and in some cases straight from our own images. The femur has been selected to do this study because it is an element of great systematic interest, furthermore one of the diagnostic characteristics of Titanosauriformes (lateral bulge) can be found on the femur (Salgado et al. 1997; Wilson 2002). Due to the relevance of this element the femur is well figured in almost every study. Moreover, the Sauropoda femur is sufficient straight to assume that the anterior and posterior outlines record the morphology of the specimens. Ideally the drawing should be collected directly from the specimen, but due to collections being all over the world it is non viable. In some cases, as in the femur outline of *"Titanosaurus" indicus* of Swinton (1947), the draft is taken at the anterior view, and as the fourth trochanter is situated medially the landmarks are similar at both views.

Previous to the digitalisation of the landmarks and to eliminate the size factor, the figures have been reduced to the same scale, using as baseline the row between LM 2 and 3. Following the perpendicular to this baseline the scale is adjusted using a vectorial, drawing programme (Free-Hand 8.0). Apart from scaling, this program has also been used to associate every femur according to a left femur in the posterior view to eliminate variables associated with asymmetry and we assume that the Sauropoda femurs are perfectly symmetrical. Due to the scarcity of material this assumption cannot be verified. The digitalisation and principal component analysis of the landmarks from each specimen studied has been done with APS (The Procrustes Superimposition Software, Penin 2003).

The landmarks or anatomic points selected represent the femur morphology of Sauropoda's posterior view. In general these points are of a mixed kind as in cases 1 and 2 of Bookstein (Rabello Monteiro and Furtado dos Reis 1999). As per the fourth trochanter case the projection of the landmarks has been used where this element is situated against the plane of the posterior view of the femur (except for *"Titanosaurus" indicus* as indicated).

The landmarks selected are those that can be identified in Fig 1. At the beginning the landmarks selected were some of the ones related to the condyles like the proximal terminals of the condyles, but in the illustrations exists a certain degree of a different interpretation of the articulated surfaces of the condyles for what degree of subjectivity that could exist, something that should be avoided. In Figures 2 and 3, the landmarks and outlines are considered in the 24 femora studied.

Some of the landmarks considered in this study are used to be the reference anatomical points for femur measurements but no attempt to apply the geometric morphometric methodology has been done. They are the following (Figs. 1-3):

1. Lateral end of the fibular condyle.
2. Distal end of the fibular condyle. This is the lateral end of the string that forms the baseline of the femur.
3. Distal end of the tibial condyle. This is the medial end of the baseline.
4. Medial end of the tibial condyle.
5. Proximal end of the tibial condyle. Generally this point is reflected on the outlines of the Sauropoda femurs as a consequence of a change from concave to convex as seen in *Opisthocoelicaudia* (Borsuk-Bialynicka 1997). Although in some sauropods the condyle, practically has not this medial spreading out which can be interpreted as the non-existence of this concavity. In this case the landmark taken is the projection of the proximal end of the tibial condyle on the outline.
6. Medial point where the diaphysis has its minimum medial lateral diameter. It coincides with the point of maximum concavity of the distal half of the femur on its medial side.
7. Medial projection on the outline of the distal end of the fourth trochanter.
8. Distal end of the fourth trochanter. In the sauropod femurs where the fourth trochanter is medial the points 7 and 8 coincide and even stick out from the outline.
9. Proximal end of the fourth trochanter.

10.Medial projection on the outline of the proximal end of the fourth trochanter. As in landmarks 7,8, LM 9 and 10 may coincide and yet LM 9 can protrude medially. In this case the 4th trochanter is seen as a convex feature in the femur profile.
11.Medial-distal end of the articular head. This point is an inflexion, which marks the limit between the epiphysis and the proximal end of the shaft.
12.Point of inflexion between the concave and convex profile of the articular head.

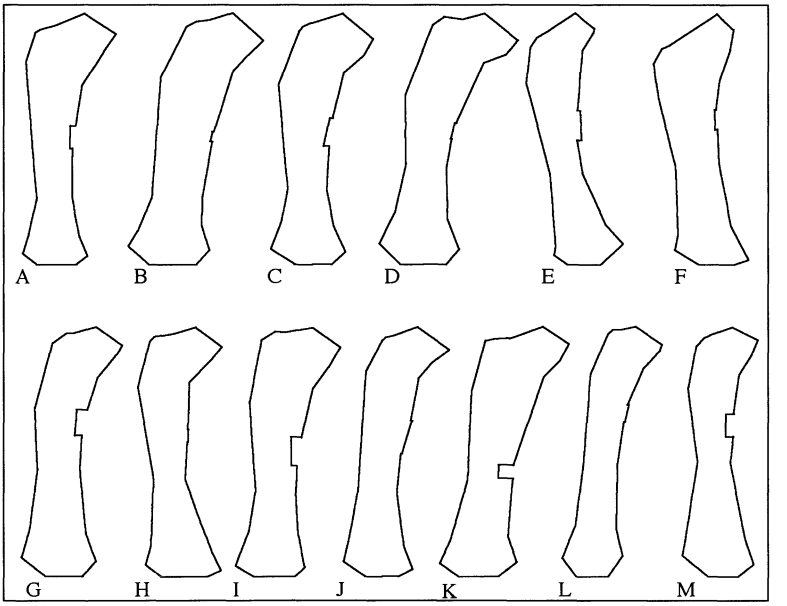

Fig. 3. Outline femora made with the landmarks junction lines. A: *Antarctosaurus wichmannianus*. B: *Saltasaurus loricatus*. C: *Neuquensaurus australis*. D: *Neuquensaurus robustus*. E: *Lirainosaurus astibiae*. F: *Ampelosaurus atacis*. G: *Magyarosaurus dacus*. H. *Magyarosaurus dacus* Jianu. I: *Alamosaurus sanjuanensis*. J: *Aegyptosaurus baharijiensis*. K: *Opisthocoelicaudia skarzynskii*. L: *"Titanosaurus" indicus*. M: *"Titanosaurus" indicus*. References are in table 1

13.Point of greatest medial distal convexity of the articulated head. In the majority of the Sauropoda, it coincides with the most medial point of the whole of the femur.
14.The most proximal point of the articular head. Generally, it corresponds to the furthest point from the distal condyles of the whole femur.
15.Most depressed point between the greater trochanter and the articular head. Coincides with the depression of the intertrochanteric fossa.
16.Greater trochanter. In some sauropods has practically disappeared, reason why in these cases has been made to coincide, this point with point 17.
17. Latero-proximal corner of the greater trochanter.

18.Greatest lateral expansion of the proximal third. This expansion is the most lateral end of the femur or "Lateral Bulge" of Salgado et al. (1997).
19.Lateral part where the diaphysis acquires its minimum diameter. Coincides in the same transversal plane as point 6, practically parallel to the distal plane where the baseline is found.
20.Lateral projection at the proximal beginning of the fibular condyle. Discussion as in LM 5.

11.4 Results and discussions

The results of the morphometric study of the sauropod femora seem to be a useful tool in biogeography as well as systematic. Our results are expressed in Figures 4 y 5. The analysis of the landmarks position variability is expressed in its principal component analysis (PCA) Figure 4 shows the analysis of all the Titanosauriformes whereas Figure 5 illustrates only the Upper Cretaceous Titanosauria. In both PCA diagrams the taxa grouping is greatly significant, temporarily as well as biogeographically. The Figure 4 allows infer three assemblages; on the one hand all the laurasiatic Titanosauriformes of the Lower Cretaceous and in the other, the two groups of the Upper Cretaceous, laurasiatic and gondwanic Titanosauria. Some taxa like *Euhelopus*, *Opisthocoelicaudia* or *Aegyptosaurus* are not part of any of these groups, which is interpreted in posterior paragraphs. A different case is both species of *Brachiosaurus*, which are situated in a non-apparent paleobiogeographic distribution, which makes sense because the separation of continents was unclear at the end of Jurassic, meaning that Gondwana and Laurasia were together and there must have been easy communication between both land-masses.

11.4.1 Titanosauriformes of the Lower Cretaceous

The fossil record of Titanosauriformes is rare at the Lower Cretaceous both in Europe and North America. Nevertheless our study of the femur reveals a close phylogenetic relation between these groups. Following the authors, during the Barremian, faunas of Titanosauriformes and possibly similar Titanosauria roamed throughout both continental masses (Tidwell and Carpenter 2002). This seems to agree with our results (Fig. 4) since the studied femurs indicate that there are Laurasiatic Titanosauriformes from Asia, Europe and North America that are grouped altogether.

As seen in Figure 4 these Titanosauriformes are found far away from the genus *Euhelopus*, which (at least in our studies) represents a morphologically distant group from the rest of the Titanosauriformes of Lower Cretaceous of Laurasia. This taxon is interpreted in a different way according to the diverse phylogenetic propositions. On the one hand it comes out of the neurosauropods clade of Fig. 1B because it is related to other Jurassic Chinese sauropods (Upchurch 1998) and on the other hand it is regarded as a representative of the Titanosauriformes clade, as

a group closely related to Titanosauria (Wilson and Sereno 1998; Wilson 2002). Our studies may indicate that in Asia there would have been two groups of well-differentiated Titanosauriformes, on one side *Euhelopus* and on the other the rest, or also the possibility that *Euhelopus* does not belong to the Titanosauriformes clade.

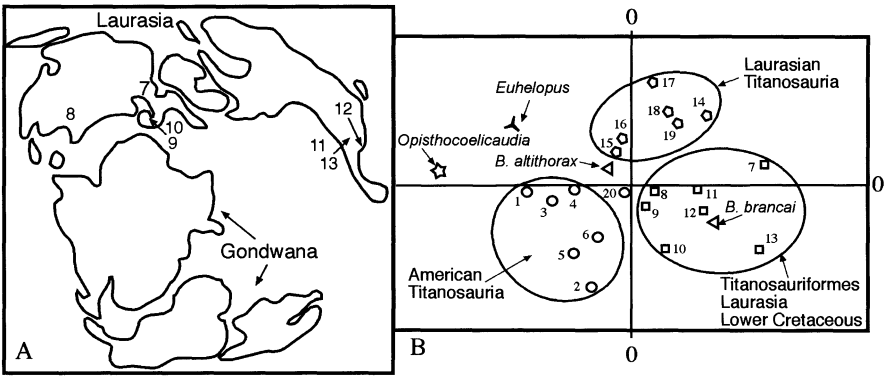

Fig. 4. A. Lower Cretaceous paleogeographic map modified from Le Loeuff (1997) The numbers are Titanosauriformes Lower Cretaceous taxa from Laurasia. B. Principal Component Analysis of the Titanosauriformes femora using the generalized Procrustes Superimposition Software (APS, Penin, 2003). 1: *Chubutisaurus insignis*. 2: *Saltasaurus loricatus*. 3: *Alamosaurus sanjuanensis*. 4: *Neuquensaurus australis*. 5: *Antarctosaurus wichmannianus*. 6: *Neuquensaurus robustus*. 7: Brachiosauridae indet. 8: *Pleurocoelus nanus*. 9: Titanosauriformes indet. 10: *Aragosaurus ischiaticus*. 11: *Tangvayosaurus hoffeti*. 12: *Phuwiangosaurus sirindhornae*. 13: *Tangvayosaurus? falloti*. 14: *"Titanosaurus" indicus* after McIntosh (1990). 15: *Lirainosaurus astibiae*. 16: *Magyarosaurus dacus* after McIntosh (1990). 17: *"Titanosaurus" indicus* after Swinton (1947). 18: *Ampelosaurus atacis*. 19: *Magyarosaurus dacus* sensu Jianu and Weishampel (1999). 20: *Aegyptosaurus baharijiensis*. References are in table 1

11.4.2 Titanosauria and Titanosauridae

The type taxon of the Titanosauridae family is *"Titanosaurus" indicus*. It was initially described on the basis of two caudal vertebras and a partial femur of the Lameta formation in India (Lydekker 1877; Wilson and Upchurch 2003). Although in the original description Lydekker (1877) doesn't give a formal diagnosis of *"Titanosaurus"* he describes the caudal vertebras as strongly procelic, which permits the differentiation with other Dinosauria genus and also permits the recognition of sauropods with similar character in different parts of the world, like in the Lower Cretaceous of England and the Upper Cretaceous of Argentina (see discussion in Salgado 2003; Wilson and Upchurch 2003). The "titanosaurids" are the group of Neosauropoda most diversified, especially for the tendency to assign to this family any of the rest of Sauropoda of the Upper Cretaceous of Gondwana (McIntosh 1990; Foster 1999). Recent phylogenetic analysis (Salgado et al. 1997;

Upchurch 1998; Wilson and Sereno 1998; Wilson 2002) clarifies the monophyly of this clade, which traditionally has been considered as Titanosauridae. Due to the fragmentary nature of the original material of *"Titanosaurus"*, several propositions have been made to consider it *nomina dubia* (Wilson and Upchurch 2003) and to substitute Titanosauridae for Saltasauridae, to establish the systematic of the traditionally considered as more derived titanosaurids, mostly from South America (Sereno 1999; Wilson 2002). The last phylogenetic propositions demonstrate that the classic titanosaurids are a diverse group, which are part of the Titanosauria clade (Fig. 1). This group would include the family Saltasauridae and the subfamilies Nemegtosaurinae, Saltasaurinae or Opisthocoelicaudinae (Wilson 2002). Our study reveals the partition into American and Laurasiatic Titanosauria by grouping these forms in two separate clades

11.4.3 Titanosauria of Laurasia

When analysing Titanosauriformes as a whole, as well as only Titanosauria (Figs. 4, 5) it can be observed that Titanosauria from Laurasia group together, including *"Titanosaurus" indicus*. This means that they represent a group broadly distributed throughout Asia and Europe well away from gondwanic taxa. It is surprising to note the association of *T. indicus* with European Titanosauria, since the most accepted proposition is that the *"Titanosaurus"* genus represents a relict of gondwanic fauna, which enters into Laurasia as a consequence of the clash between the Indian and Asian plaques during the migration of India to the north during the Maastrichtian. However our data tells a different story, which is that, the titanosaurs analyzed are more coherent like laurasiatic emigrants who colonized India after the collision. The existing argument, which considers *"Titanosaurus"* as a gondwanic emigrant, means that we should consider Titanosauria as gondwanic taxa, which is incorrect (Canudo and Salgado 2003). It also lacks the registration of previous Maastrichtian Cretaceous dinosaurs in India, which could have corroborated the gondwanic origin. In India exist a mosaic of gondwanic and laurasiatic vertebrates from which at least a third are laurasiatic (Bonaparte 1984). It doesn't seem to be problematic in this context that the femurs from the analysed *"Titanosaurus"* are not gondwanic and belong to laurasiatic Titanosauria.

The position of *Opisthocoelicaudia*, a Sauropoda from the end of the Mongolian Cretaceous, poses a different problem (Figs. 4, 5). In the original description it was classified as a Camarasauridae (Borsuk-Bialinicka 1997) and therefore was outside of Titanosauriformes clade. However, in the cladistic analysis have situated it in Titanosauria (Salgado et al. 1997; Wilson and Sereno 1997) and also have proposed the subfamily Opisthocoelicaudinae (Wilson 2002). In our Figures 4 and 5 it can be seen how its femur stays separated from laurasiatic Titanosauria as well as from gondwanic although in both cases it is closer to the gondwanic taxa. Also other authors, and referent to this Wilson (2002) considers that *Alamosaurus* and Opisthocoelicaudinae are part of the same subfamily. Therefore both taxa probably will have to be considered as a gondwanic emigrant in Laurasia. Nevertheless, as our study shows, due to the different morphology presented by

the femur it is possible that it could be a representative member of the Titanosauria family non-related to the groups considered in this study.

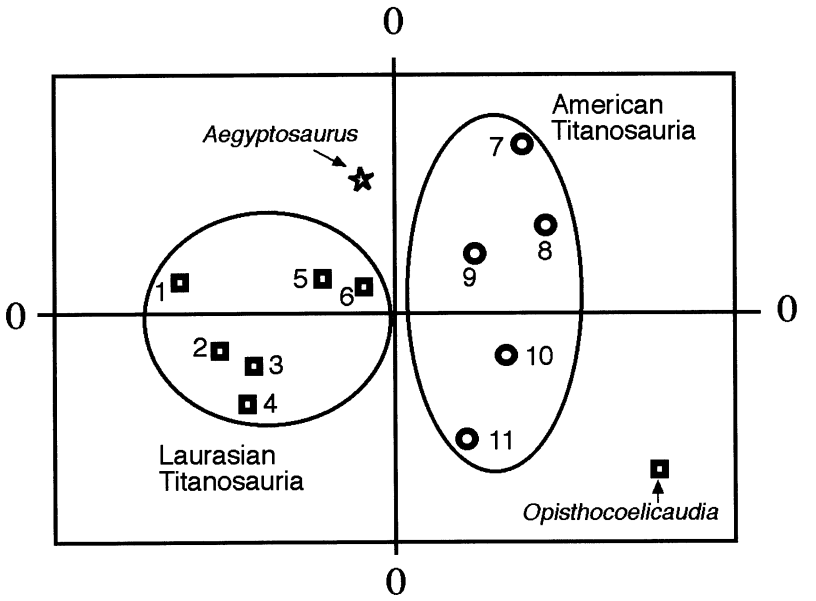

Fig. 5. Principal Component Analysis of the Titanosauria femora using the generalized Procrustes Superimposition Software (APS, Penin, 2003). 1: *"Titanosaurus" indicus* after McIntosh (1990). 2: *"Titanosaurus" indicus* after Swinton (1947). 3: *Ampelosaurus atacis*. 4: *Magyarosaurus dacus* from McIntosh (1990). 5: *Magyarosaurus dacus* from Jianu and Weishampel (1999). 6: *Lirainosaurus astibiae*. 7: *Antarctosaurus wichmannianus*. 8: *Saltasaurus loricatus*. 9: *Neuquensaurus australis*. 10: *Alamosaurus sanjuanensis*. 11: *Neuquensaurus robustus*. References are in table 1

11.4.4 Titanosauria of Gondwana of Upper Cretaceous. *Alamosaurus*, the emigrant

Traditionally the Titanosauria taxa have been considered as gondwanic faunas with their presence in the laurasiatic Upper Cretaceous (i.e. *Alamosaurus*) explained as migrations. Nevertheless the oldest rests of Titanosauria are from Laurasia, in the European Barremian (Le Loeuff 1993) as well as the North American (Britt et al. 1997). The presence of Titanosauria in Gondwana is posterior, since it was found for the first time in the Aptian of Africa and South America (Taquet 1976; Salgado 1993). These dinosaurs could have taken advantage of a connexion between Laurasia and Gondwana, and almost certainly it happens at the end of the Barremian. The faunas are the evidence (Canudo and Salgado 2003). This could be the reason why Titanosauria came from Laurasia and at the

end of the Lower Cretaceous colonised Gondwana, to diversify during the Upper Cretaceous.

Figures 4 and 5 show the results obtained from the morphometric analysis of the femurs. When we analyse Titanosauriformes as a whole or Titanosauria individually, the South American taxa are separated from the European and Indian. Even the oldest taxon, which is *Chubutisaurus insignis*, is separated. The genus *Aegyptosaurus*, the only gondwanic taxon studied from Africa is separated from South American Titanosauria, which could be expected to be closer, but also stays separated from laurasiatic taxa. Future studies may indicate the existence of a group of African Titanosauria that have a vicariant evolution in relation to the South American and laurasiatic taxa. Accordingly the best-known African Titanosauria is *Rapetosaurus krausei* from the Maastrichtian of Madagascar (Curry Rogers and Foster 2001). The last phylogenetic revision of Wilson (2002) situates it in a different clade to the South American Titanosauria, which could be an argument connected to the vicariant hypothesis.

One of the particularities of the associations of dinosaurs from the North American Upper Cretaceous is the almost Sauropoda vacuum, when in similar ages they are present in the rest of Laurasia and Gondwana. The species *Alamosaurus sanjuanenesis* is the only reported sauropod. It is found at the end of the Cretaceous of southern regions of North America (Lucas and Hunt 1989; Lehman and Coulson 2002). Different paleobiogeographic interpretations try to explain this: Lucas and Hunt (1989) consider that *Alamosaurus* is an emigrant from South America, that took advantage of an earth bridge before the Maastrichtian, and through which, in the opposite direction, also migrated hadrosaurs to South America (Bonaparte and Kielan Jaworowska 1987) Also it has been suggested that there could have been an Asiatic emigrant (Rusell 1995) which could also have been a representative of a North American group of Titanosauria, that as described previously were present during the Lower Cretaceous, although it was absent from the paleontological record for most of the Cretaceous (Britt et al. 1997; Foster 1999, Tidwell and Carpenter 2002).

Various argentinean authors (Salgado et al. 1997) proposed the morphological similitude of *Alamosaurus* and South American titanosaurids. In their cladistic study they suggest that *Alamosaurus* is related to the sudamerican taxa. Our study agree with these authors and indicates that *Alamosaurus* is integrated into the group of American Titanosauria and is well differentiated from the group of laurasiatic Titanosauria including *"Titanosaurus"*. Therefore it has been discarded that *Alamosaurus* could be an Asiatic immigrant because it is more coherent for it to have been a gondwanic immigrant from South America during the Upper Cretaceous.

11.5 Conclusions

The application of the Procrustes Superimposition Analysis of the femurs of the Titanosauriformes has revealed that this could be a strong discriminative tool ap-

plicable in paleobiogeographic studies, allowing the discrimination of systematic and geographic groups. Because of the fragmentary nature of the Cretaceous Sauropoda fossil record, our conclusions can only be accepted as hypothetical. Even though it has permitted us to confirm proposed paleobiogeographic hypothesis like the one about the gondwanic origin of *Alamosaurus* or the close relationship between laurasiatic Titanosauriformes during the Upper Cretaceous except for *Euhelopus*. But in some other cases the results have been unexpected like the clear differences found between the European and Indian Titanosauria and the South American, which appears to indicate that their separation was earlier during the Upper Jurassic when Laurasia and Gondwana where together in Pangea. The most immediate conclusion is that it is unnecessary to resort to intercontinental bridges during the Upper Cretaceous to explain the existence of Titanosauria in Laurasia.

11.6 Acknowledgements

This study is part of the VECOBA (Vertebrados Continentales del Barremiense) project, supported by the Ministerio de Ciencia y Tecnología (BTE 2001-1746), the Fundación Conjunto Paleontológico de Teruel, the Departamento de Educación y Cultura of the Aragón Government (DGA). Marta Cuenca and Danniel Metcalf helped improve the English version. Two anonymous reviewers help to improve an earlier draft of the manuscript as a result of their careful comments.

References

Allain R, Taquet P, Battail B, Dejax J, Richir Ph, Véran M, Limon-Duparcmeur F, Vacant R, Mateus O, Sayarath P, Khenthavong B, Phouyavong S (1999) Un nuouveau genre de dinosaure sauropode de la formation des Grés supérieurs (Aptien-Albien) du Laos. C R Acad Sci Paris 329: 609-616

Blows WT (1995) The Early Cretaceous brachiosaurid dinosaurs *Ornithopsis* and *Eucamerotus* from the Isle of Wight, England. Palaeontology 38: 187-197

Bonaparte JF (1984) Late Cretaceous faunal interchanges of terrestrial vertebrates between the Americas. In: Reif WE, Westphal F (eds) Third Symposium on Mesozoic Terrestrial Ecosystems, Short Papers. Attempto Verlag, Tübigen, pp.19-24

Bonaparte JF (1996) Cretaceous tetrapods of Argentina. Münchner Geowissenchaftliche Abhandlungen (A) 30: 73-130

Bonaparte J F, Kielan-Jaworowska Z (1987) Late Cretaceous dinosaur and mammal faunas of Laurasia and Gondwana. In: Currie P, Koster EH (eds) Fourth Symposium on Mesozoic Terrestial Ecosystems, Short Papers, Tyrrell Museum of Palaeontology, Drumheller, pp. 24-29

Bonaparte JF, Powell JE (1980) A continental assemblage of tetrapods from the Upper Cretaceous of Northwestern Argentina (Sauropoda-Coelurosauria-Carnosauria-Aves). Mém Soc Géol France 139: 19-28

Borsuk-Bialynicka M (1977) A new camarasaurid sauropod *Opisthocoelicaudia skarzynskii* gen. n. sp. from the Upper Cretaceous of Mongolia. Palaeontologia Polonica 37: 5-64

Britt BB, Stadtman KL, Scheetz RD, McIntosh JS (1997) Camarasaurid and Titanosaurid sauropods from the Early Cretaceous Dalton Wells Quarry (Cedar Mountain Formation) Utah. Journal of Vertebrate Paleontology 17 Supl: 34A

Calvo JO, Salgado L (1996) A land bridge connection between South America and Africa during Albian-Cenomanian times based on sauropod dinosaur evidences. XXXIX Congr Brasil de Geol 7: 392-393

Canudo JI, Salgado L (2003) Los dinosaurios del Neocomiense (Cretácico Inferior) de la Península Ibérica y Gondwana Occidental: Implicaciones biogeográficas. In: F Perez-Lorente (ed). Actas del primer congreso Internacionacional sobre Dinosaurios y otros Reptiles Mesozoicos en España, Logroño, in press

Casanovas-Cladellas LM, Santafé-Llopis, V (1993) Presencia de Titanosáuridos (Dinosauria) en el Cretácico Superior de Fontllonga (Lleida, España). Treb Mus Geol Barcelona 3: 67-80

Curry Rogers K, Forster CA (2001) The last of the dinosaur titans: a new sauropod from Madagascar. Nature 412: 530-534

Forster CA (1999) Gondwanan dinosaur evolution and biogeographic analysis. Journal of African Earth Sciences 28: 169-185

Glut D (1997) Dinosaurs-The Encyclopedia. McFarland Press, Jefferson

Hoffet JH (1943) Description de quelques ossements de Titanosauriens du Sénonien du Bas-Laos. Comptes Rendus des séances du Conseil des Recherches Scientifiques de lndochine1er Semestre: 1-8

Huene FVon (1929) Los Saurisquios y Ornitisquios del Cretaceo Argentino. Anales del Museo de La Plata 3: 1-196

Hunt AP, Lockley MG, Lucas SG, Meyer CA (1994) The Global sauropod fossil record. Gaia 10: 261-279

JanenschW (1961) Die gliedmaszen und gliedmaszengürtel der sauropoden der Tendaguru-schichten. Palaeontographica Suppl 7: 178-233

Jianu CM, Weishampel DB (1999) The smallest of the largest: a new look at possible dwarging in sauropod dinosaurs. Geologie en Mijnbouw 78: 335-343

Lehman TM Coulson AB (2002) A juvenile specimen of the sauropod dinosaur *Alamosaurus sanjuanensis* from the Upper Cretaceous of Big Bend National Park, Texas. Journal of Paleontology 76: 156-172

Le Loeuff J (1993) European titanosaurids. Revue de Paléobiologie vol spéc 7: 105-117

Le Loeuff J (1997) Biogeography. In:Currie PJ, Padian K. Encyclopedia of Dinosaurs. Academic Press, pp. 51-56

Le Loeuff J, Buffetaut E (1991) *Tarascosaurus salluvicus* nov. gen., nov. sp. dinosaure théropode du Crétacé supérieur du sud de la France. Geobios 25: 585-594

Lucas SG, Hunt AP (1989) *Alamosaurus* and the sauropod hiatus in the Cretaceous of the North American Western Interior. Geological Society of America Special Paper 238: 75-85

Lydekker R (1877) Notice of new and other Vertebrata from Indian Tertiary and Secondary rocks. Records of the Geological Survey of India 10: 30-43

Martin V, Suteethorn V, Buffetaut E (1999) Description of the type and referred material of *Phuwiangosaurus sirindhornae* Martin, Buffetaut and Suteethorn, 1994, a sauropod from the Lower Cretaceous of Thailand. Oryctos 2: 39-91

McIntosh JS (1990) Sauropoda. In: DB Weishampel, P Dodson, H Osmólska (eds) Dinosauria. University of California Press, Berkeley Los Angeles Oxford, pp. 345-390

Penin X (2003) APS Statistical Shape Analysis Freewares

Rabello Monteiro L Furtado dos Reis S (1999) Principios de Morfometría geométrica. Holos, Ribeirao Preto

Russell DA (1995) China and lost worlds of the dinosaur era. Historical Biology 10: 3-12

Salgado L (1993) Comments on *Chubutisaurus insignis* del Corro (Saurischia, Sauropoda). Ameghiniana 30: 265-270

Salgado L (2003) Should we abandon the name Titanosauridae? some comments on the taxonomy of Titanosaurian sauropods (Dinosauria). Revista Española de Paleontología 18: 15-21

Salgado L, Coria RA, Calvo JO (1997) Evolution of titanosaurid sauropods. I: Phylogenetic analysis based on the postcranial evidence. Ameghiniana 34: 3-32

Sanz JL, Powell JE, Le Loeuff J, Martínez R, Pereda-Suberbiola X. (1999) Sauropod remains from the Upper Cretaceous of Laño (Northcentral Spain). Titanosaur phylogenetic relationships. Est Mus Cienc Nat de Alava 14 Núm Espec 1: 235-255

Sereno PC (1999) A rationale for dinosaurian taxonomy. Journal of Vertebrate Paleontology 19: 788-790

Stromer E (1932) Wirbeltier-reste der Baharije-Stufe (unterstes Cenoman). 11. Sauropoda. Abh Bayer Akad Wissensch Math -naturwiss Abt 10: 1-21.

Swinton W (1947) New discoveries of *"Titanosaurus" indiens*. Ann Mag Nat His. (ser. 11) 14: 112-123

Taquet P (1976) Geologie et Paleontologie du gisement de Gadoufaoua (Aptian du Niger). Cahiers de Paleontologie, pp. 1-191

Tidwell V, Carpenter K (2002) Bridging the Atlantic: new correlations of Early Cretaceous Titanosauriformes (Sauropoda) from England and North America. Journal of Vertebrate Paleontology Supplement to number 3: 114A

Upchurch P (1998) The Phylogenetic Relationships of Sauropod Dinosaurs. Zoological Journal of the Linnean Society 124: 43-103

Wilson JA. (2002) Sauropod dinosaur phylogeny: critique and cladistic analysis. Zoological Journal of the Linnean Society 136: 215-275

Wilson JA, Sereno PC (1998) Early evolution and higher-level phylogeny of sauropod dinosaurs. Society of Vertebrate Paleontology Memoir 5: 1-68.

Wilson JA, Upchurch, P (2003) A revision of *"Titanosaurus"* Lydekker (Dinosauria - Sauropoda), the first dinosaur genus with a "Gondwanan" distribution. Journal of Systematic Palaeontology 1: 125-160

Wiman JC (1929) Die Kreide-Dinosaurier aus Shantung. Palaeontologia Sinica (Ser. C) 6: 1-67

12 Geometric morphometrics in macroevolution: morphological diversity of the skull in modern avian forms in contrast to some theropod dinosaurs

Jesús Marugán-Lobón[1] and Ángela D. Buscalioni [1, 2]

[1]Unidad de Paleontología, Departamento de Biología. Universidad Autónoma de Madrid, 28049 Cantoblanco (Madrid), Spain, jesus.marugan@uam.es; [2]Konrad Lorenz Institute for Evolution and Cognition Research, Alternberg, Austria

12.1 Abstract

Birds are the most diversified forms of modern terrestrial vertebrates. They are archosaurs, and are related to Theropoda within Dinosauria. Even though bird morphology has been a subject of interest for centuries, most studies have focused solely on discrete morphological characters, leaving a gap in the understanding of morphological organization and integration in macroevolution. We present this chapter to exemplify a quantitative exploration of the macroevolutionary trends of skull morphological diversity in theropod dinosaurs including modern birds. Using a sample with taxa representative of all of known modern avian Orders, skull disparity is described over a morphospace modeled from shape variables obtained by General Procrustes methods. High taxonomical categories imply large-scale morphological difference, thus landmarks were selected according to evolutionary homologous and developmental conservative areas. Morphological diversity of the skull relies mainly on craniofacial variation, and can be found within the first four dimension of a PCA. Modern avian forms have a strikingly localized, but not morphologically independent, variation at the rostrum. Craniofacial variation unfolds in a range of structurally straight-flexed appearance dependant on the covariation between the rostrum and braincase, structurally mediated by the antorbital cavity. Extinct theropods occupy a region within morphospace resembling an extreme straight skull. Major macroevolutionary changes are likely associated to expansion of the braincase.

Keywords: Archosauria, aves, disparity, macroevolution, morphology, morphospace, phenotypic Integration, Theropoda.

12.2 Introduction

12.2.1 Theoretical perspective

Birds and crocodiles are the living representatives of the Archosaurian lineage. Modern birds are the most diversified forms of the group, and perhaps of all extant terrestrial vertebrates (Witmer 1997). They are abundant in both populations and species (there are over 9000), they live on every continent, and occupy virtually all available ecological niches (Chaterjee 1999). This strikingly high degree of diversity is what has probably raised avian morphology to be such a well studied subject over centuries.

Studies regarding the morphology of the skull in modern birds, however, have directed more attention to the description of variability at the species and subspecies levels (Zusi 1993), concentrating on the study of discrete characters and on their functional significance, rather than on the variation of entire integrated morphological complexes. For instance, the rostrum is known to be a strikingly variable structure from which examples of adaptation can be called straightforward. It is commonly thought that its morphological characters only reflect a response to trophic demands (see e.g. Proctor and Lynch 1993; Feduccia 1999; Grant and Grant 1993). Since birds are a paradigmatic example for the analytical consideration of discrete anatomical elements, very little attention is paid to the structural properties of the whole, (e.g. the rostrum is a unit that belongs to the craniofacial system), thus leaving a gap in the understanding of architectural properties, phenotypic integration and constraints of their skull, or put another way, whether if it functions as a cohesive morphological system or not.

We must therefore propose to study skull morphology by developing approaches that help decipher the properties and organization of the whole (Dullemeijer 1972). It must be kept in mind though, that morphological organization can, and needs, to be studied at different taxonomical levels to unveil and understand the main events that occurred in its macroevolution (Raff 1996). In regard to the morphological organization of the skull in archosaurs previous studies have revealed the existence of a structural geometric configuration, which was found to be a constructional constant (Marugán-Lobón and Buscalioni 2003). When plotted over morphospace of skull proportions, real organisms only occupied 18% of the 100% that was theoretically available. This resulted from a constraining rule of morphological organization governing the three main constituent modules of the skull (rostrum, orbit and braincase), which was dictated by a negative correlation between the braincase and rostrum proportions common among all archosaurs. A numerical relationship between braincase and orbit proportions was also characteristic within the pattern. A special case within the trend were, for instance, flying forms (namely pterosaurs and birds), forms which show a more restrictive braincase/orbit ratio relationship, unbalanced towards larger orbital proportions.

In contrast to the use of proportions, however, geometric morphometrics provide a major operative advance in the field of morphometrics (Bookstein 1991; Rohlf and Marcus 1993), and is now a practice gaining worldwide application in

morphological research, as many of its mathematical properties are now better understood. In accordance to the theoretical standpoint anticipated in the paragraph above, it is important to highlight that geometric morphometrics makes it possible to analyze biological form whilst preserving its physical integrity by including information that pertains to the geometry of the whole (Richtsmeier et al. 2002), thereby upholding what was its initial operative purpose. Thus, we have chosen the use of General Procrustes methods of superimposition to obtain the variables for the construction of an empirical morphospace (McGhee 1999) to describe disparity in terms of shape variation, and to provide further interpretations about morphological covariation in terms of evolutionary processes (Debbaut and Davis 2002).

We have hereby abstracted the whole skull into a series of landmarks placed homogeneously across conservative and homologous areas of the skull of avian and theropod forms, using a sample that covers 100% of known avian Orders and 10 theropod dinosaurs, from which we aim to explore the patterns of phenotypic covariation among the structural units that construct their skull, and to track the morphological evolution of the avian skull by exploring the variation across characters and modules. Our purpose is to exemplify a preliminary approximation of how to prospect for common or different macroevolutionary trends of the structural variation between birds and theropods.

12.2.2 Morphology

Overall features that illustrate the external appearance of the skull of modern birds in contrast to other diapsids are (Fig. 1); a large braincase (because of the presence of a larger brain in relation to body weight; Jerison 1973; King and King 1979), where the large brain housed in fits so tightly that the walls within the braincase externally conforms its shape (Jerison 1973). The large orbital cavities resemble the large eyes they house (King and King 1979; Martin 1985), and finally, a rostrum strikingly variable in length and shape (Zusi 1993; Feduccia 1999). The rostrum also houses the olfactory chambers (Bang 1971), associated to the external nares, the latter also highly variable in topography and typology (see, Zusi 1993).

The skull of modern birds is also very variable in its craniofacial arrangement, which becomes conspicuous from the topographical orientation between the braincase and the rostrum. Taking, for instance, the occipitals as a reference in lateral view, the rostrum is angled in regard to the braincase within a range between 90° up to approximately 165-170°, or even higher angles (Gaup 1906; Marinelli 1928; Duijm 1951; Hofer 1952; Fig. 4). Several typologies have been proposed and named in regard to the different configurations qualitatively described, but little agreement has been reached about the nature of these arrangements and the causal factors underlying them.

The skull of modern birds is kinetic (Fisher 1955; Bock 1965; Büller 1981), being able to allow the rostrum to pivot independently from the braincase. While a kinetic skull is not uncommon in diapsids, in modern birds it has its own structural and biomechanical properties, and is variable across taxa. The spectrum of kinetic

types embraces *Prokinetic* types, for those in which the upper jaw maintains its shape as it pivots at the craniofacial hinge, and the various types of *Rhynchokinetic*, with several and different points of flexure along the rostrum.

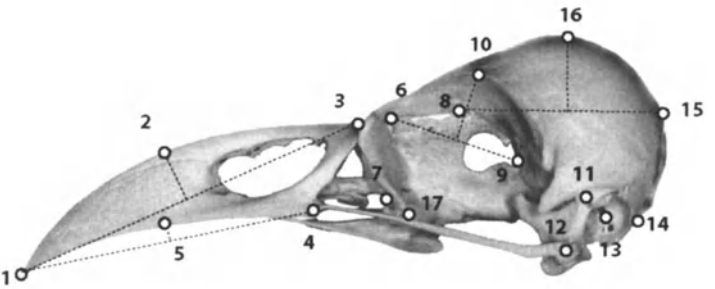

Fig. 1. Example of a modern avian skull in lateral view (*Corvus corax*, O. Passeriformes), with landmarks (descriptions on Table 1)

12.2.3 Phylogenetic context

It is broadly accepted that modern birds belong to the monophyletic group Archosauria (Reptilia: Diapsida), but within this group, they have been historically related to several different groups; basal thecondonts, crocodylomorphs, and theropod dinosaurs (the 'thecodontian', 'crocodylomorph' and 'theropod' hypotheses respectively) (Padian 2001). Ostrom (1973) provided decisive evidence that pioneered the revalidation of the latter, the theropod hypothesis, a proposal that nowadays is the most extended and accepted avian phylogenetic hypothesis.

Within the Coelurosauria, it is the consensus (Norell et al. 2001) to include birds in Maniraptora as Avialae (Gauthier 1986; Aves *sensu*, Cracraft 1986; Chiappe 1995; Padian and Chiappe 1998). While the monophyly of modern forms (Neornithes *sensu*, Chiappe 1995) remains stable, the relationships within the neornithine clades have also been highly contentious. Classic subdivisions within the clade divide Neornithines in two groups, the Paleognathae and Neognathae. Cracraft and Clarke (2001) have recently argued in favour of the monophyly of Neornithes and subgroups within.

Operatively, we will use the term "modern birds" or "birds" when referring to our extant Neornithes sample. When including other extinct dinosaurs, we will refer to 'extinct theropods', meaning Coelurosaurian theropods (e.g. *Dromaeosaurus*, *Velociraptor*, or *Oviraptorids*) and Non-Coelurosaurian theropods (e.g. basal forms as *Herrerasaurus*, or more derived and popular *Allosaurus* or *Tyrannosaurus*).

12.3 Materials and methods

The sample consists of 93 skulls from a sample of modern adult birds which comprising 100% of described Orders following Morony et al. (1975; 25 Orders). Sampling was not random, but rather, the intention was to extend the sample to include representatives from all Orders of birds. However, election of specimens was also dependant on availability and/or anatomical preservation of necessary features (e.g. good preservation of all the structures on the same specimen for landmark placement). Studied specimens are housed at the Vertebrate Collections of the Museo Nacional de Ciencias Naturales de Madrid (MNCN), the Collection of the Museum of Anatomy at the University of Valladolid (MAUV) and the Collection or Ornithology at the American Museum of Natural History (AMNH) in New York.

The skulls were all digitised in lateral view and using the same procedure to avoid parallax distortion. For this purpose, lenses were set at maximum telephoto (8x), and the digital camera was placed at varying distances to fit specimens at the same frame within the lenses; the minimum was for smaller specimens at 2.5m. A squared grid underneath each specimen's skull served to align the mid sagittal plane to a line of the grid (from the Premaxillary Symphysis as the most anterior point to the sagittal crest close to the foramen magnum at the occipital region caudally), and at that position, the skull was set completely perpendicular to the focus axis of the camera. At the same time, the camera was placed still on a tripod parallel to the ground plane. However, we have not checked for possible digitising distortions in this study, a potential source of error within analyses. Notwithstanding the possibility of error due to parallax, it should be expected that morphological differences at a high taxonomic level would still be the largest source of variation (see e.g., Duijm 1951). The small sub-sample consists of 9 extinct theropods that were digitised from either from real fossil material, casts, or literature (see Fig. 4).

We have selected a series of 17 arguably homologous landmarks delimiting the constituent units that build the skull; the rostrum, the orbital cavity and the braincase, (Fig. 1, Table 1). Landmarks have been placed within the skull according to homologous features stable at development and evolution, e.g. cranial nerves, and/or boundaries between units (rostrum, antorbital, orbit, braincase, otic and articular areas). When including dinosaurs, not all landmarks designated for modern forms could be used because of absence due to preservation (see Table 1). Landmark series were recorded with TPSdig (v. 1.34, Rohlf 2003). All anatomical descriptions follow the *Nomina Anatomica Avium* (Baumel and Witmer 1993).

Landmark superimposition was carried out using Generalised Procrustes Analysis (GPA, *a.k.a* Generalised Least Square Superimposition, GLS; Bookstein 1991). This methodology removes all information unrelated to shape minimizing the distance between landmarks by translating, rotating and scaling all forms to a consensus (the average) while preserving all shape differences among specimens (Rohlf and Slice 1990). Resistant Fit superimposition (Siegel and Benson 1982) was also used for exploratory purposes. Principal Component Analysis (PCA) has

been used on the residuals of landmarks after GPA superimposition to explore trends of morphological variation.

Centroid Size will be the geometric expression of skull size (as the squared root of the sum of the square distances between landmarks). All geometric morphometrics were performed using GRFnd (Slice 1994), the TPS series (Rohlf 2003), and Morpheus (Slice 2000). All programs a freeware and can be currently found at http://life.bio.sunysb.edu/morph/, to download and for any further information.

12.4 Results

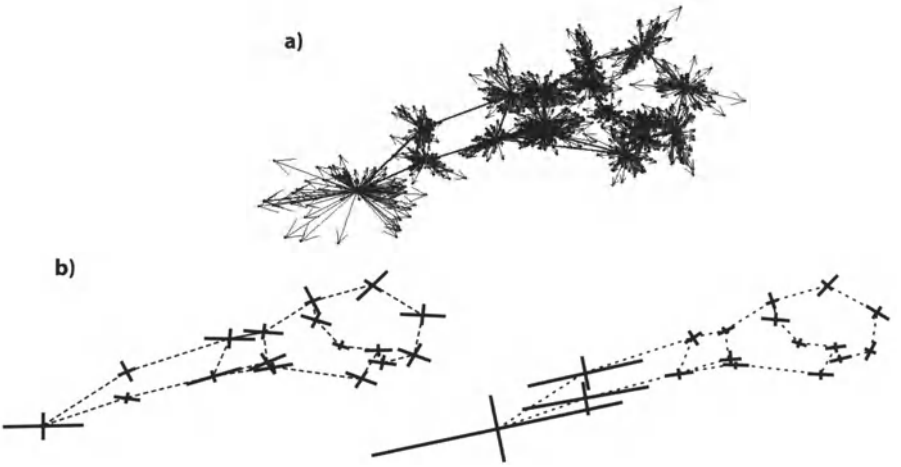

Fig. 2. a) Superimposed specimens over consensus after GPA (average configuration drawn by lines between landmarks). Scatters are not homogeneous. The tip of the rostrum seems to be the most variable region. b) Intra-landmark PCAs; (left) after GPA, (right) after Resistant Fit superimposition. Note difference in magnitude of variation around rostrum, in comparison to braincase region

When all specimens were plotted after GPA superimposition, clusters of homologous landmarks did not display the same degree of dispersion. Although all clusters were heterogeneously scattered, dispersion of landmark 1 seemed much more scattered than the remainder caudal to it (Fig. 2). To aid visualization, Figure 2 depicts intra-landmark PCAs (PTPCA command on GRFnd), variation also appears to be on landmark 1, variation associated therefore to the tip of the rostrum (premaxillary symphysis). However, more or less variation cannot be confidently described from the degree of scatter within each cluster, as it could be an effect of the superimposition technique used. Resistant Fit showed that variation was strongly localized at the anterior region of the rostrum (landmarks 1, 2 and 3), closely resembling a Pinocchio Effect (see, Bookstein 1991; Fig. 2), and thus also displaying that remainder regions of the skull (namely, the braincase) are morphologically more conservative.

Table 1. Landmarks, skull in lateral view. Asterisks (*) indicate missing landmarks in extinct dinosaurs. See also Fig. 1 to find profiled anatomical structures of the skull

Number	Anatomical description
1	Premaxillary symphysis at the tip of the rostrum
2	Perpendicular at midpoint between landmarks 1 and 3 to dorsal margin of the rostrum
3	Joint in lateral view of the nasal and lachrymal bones at craniofacial hinge
4	Path of the maxillary nerve (Maxillary Ramus of N. V) at anterior and ventral-most edge of antorbital cavity
5	Perpendicular at midpoint (between landmarks 1 and 4) for lower margin of rostrum
6*	Foramen orbitonasalis (N. I)
7*	Junction between the palatines dorsally with the interorbital septum
8*	Emergence of Nerve I (olfactory) at laterosphenoid bone
9*	Foramen Opticum (N. II)
10	Perpendicular at midpoint to upper margin of the orbit (between landmarks 8 and 10) to reach the upper margin of orbit
11	Insertion of quadrate bone to the braincase
12	Articulation of jugal bar to the quadrate
13*	Central area of the external ear (Auditory Meatus)
14	Junction of parietal and squamosal at most caudal point at the occipital crest
15	Mid-point of foramen magnum at the paraoccipital area in lateral view
16*	Perpendicular at midpoint to upper margin of cranial vault (between landmarks 19 & 16) for to display its maximum height
17*	At the ectethmoid bone (Lamina Orbitonasalis), at its ventral-most point

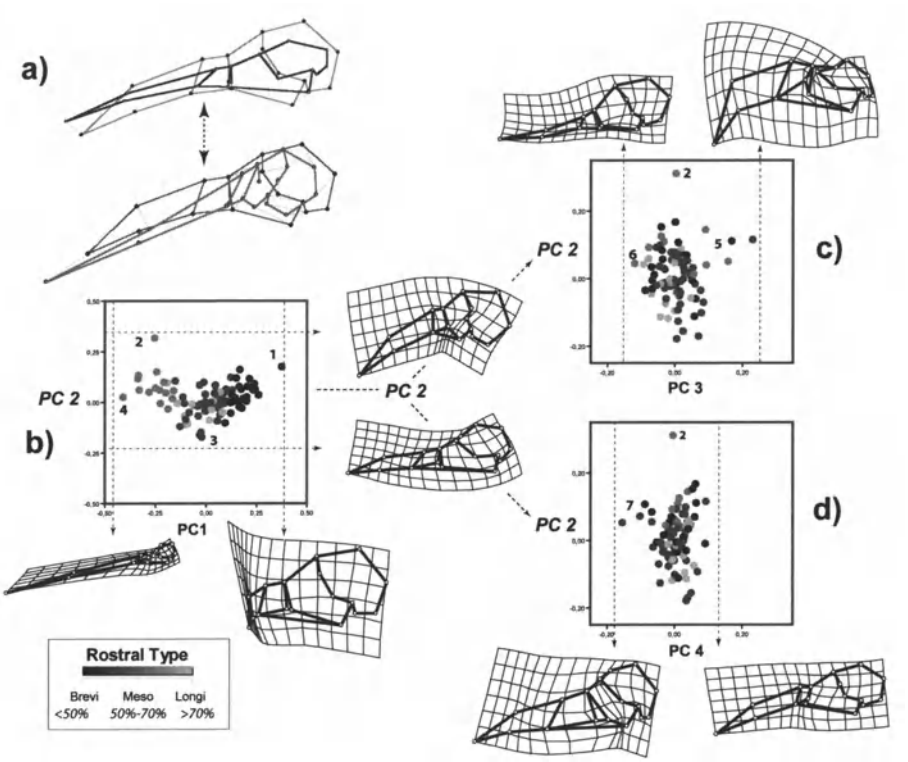

Fig. 3. a) (Above, in black) Typical straight form, *Phalacrocorax* (see text), compared to mean shape, (Below, in light gray) typical kinked form, *Scolopax*, compared to mean shape. Vectors show direction of variation in comparison to mean. b) PC1 with PC2 plot. Note distribution of rostral types along PC1, with main deformation is at anterior region of rostrum. PC2 shows deformation around the antorbital cavity c) PC2 with PC3 plot, and d) PC2 with PC4. Dashed arrows connect PC2 between all graphs, dotted arrows approximate natural morphological boundaries. (1) *Micropsitta*, (2) *Scolopax*, (3) Penguins, (4) *Pelecanus*, (5) Parrots and *Phoenicopterus*, (6) *Recurvirostra* (7) Strigiformes. Only modern birds included in this analysis

PCA on the residuals after superimposition of modern birds shows that much of the of the total variance is captured by the first four dimensions, with over 80% of variance is explained. However, there is a dominant trend, PC1, which explains 59.24% of the total variance. We considered useful to proceed describing more dimensions because all PCs, from 1 to 4, correlate with size (although at different p levels; Table 2), and PC1 scores are neither homogeneous in magnitude or in sign (not shown).

Shape variation along PC1 axis involves a very localized variation at the anterior region of the rostrum, characterized by its stretching and compression (region between landmarks 1, 2 and 4; Fig 3). Within this trend, stretching of the rostrum implies also its whole straightening, while compressing implies its downward cur-

vature. A dorso-ventral variation associates with the described trend is affecting the whole skull. When strong stretching occurs at the anterior region of the premaxilla, the spline shrinks dorso-ventrally, and the opposite occurs when the rostrum is compressed at opposite signs on the axis. Yet, it is not clear to us whether this effect can be attributed to the behavior of the spline or a real morphological episode.

The second dimension, PC2, explains a 14.10% of variance (PC1+PC2 accumulate a 73.34% of total variance). It describes an interesting trend that involves a flexion of the skull localized mainly at the antorbital region (antorbital cavity, landmarks 3, 4, 6, 7 and 17) (Fig. 3). The reduction or extension of the jugal bar covaries within this trend, in conjunction with variation at the region of the base of the brain, demarked by landmarks 8, 9. PC1 with PC2 depicts a distinctive graph over morphospace (Fig. 3), with a curved distribution within which we find four morphological extremes; *Micropsitta* (Psittaciformes) and *Pelecanus* (Pelecaniformes) for PC1, and *Scolopax* (Charadriformes) and *Penguins* (Sphenisciformes) for PC2. The former extremes differ on PC1 for their rostral proportion, and the latter, on PC2, represent extreme conditions for craniofacial flexion. *Micropsitta* and *Scolopax* are further aside from the overall sample within morphospace (Fig. 3).

PC3 explains a 7.04% of total variance (total explained variance reaches 80.37%; Fig. 3). This dimension corresponds to a trend of more homogeneous variation across landmarks within the skull than the former PC1 and PC2 dimensions. Deformation is at the rostrum, with a dorso-ventral compression of the rostrum morphologically covarying with its bending or straightening at its mid portion. The antorbital cavity also varies accordingly, although expanding or contracting. There is also a conspicuous deformation located at the orbital region, here implying that the base of the brain (e. g. landmark 8) appears to be "invading" the orbital cavity. On the score values opposite in sign within PC3, there is not such invasion, but rather, the brain remains behind the eye.

Within the graph between PC2 and PC3 (Fig. 3), *Phoenicopterus* (Phoenicopteriformes), two parrots (Psittaciformes) and *Rhyticeros* (Coraciiformes) are outliers from the main distribution from their values on PC3, and *Recurvirostra* (Charadriformes) is an extreme (not and outlier) in opposite location. *Scolopax* remains an outlier because of its extreme values for PC2.

PC4 (3.72% of explained variance; total explained variance 84.09%) describes variation at the antorbital cavity (its shrinkage or overall expansion), accompanied morphologically by variation at the jugal region and by invasion of the ectethmoid region within an area located beneath the orbit (landmarks 7 and 17). Outliers for the scatter between PC2 and PC4 are merely Strigiformes (i.e. Owls; Fig. 3).

PCA including extinct theropods embraces a first dimension explaining a 51.84% of total variation, and a second, PC2, explaining a 24.19% of the variation (76.03% of total variance). We restrain description of variation to the first two dimensions because the impossibility to place landmarks across morphologically relevant regions, such as the orbit and the antorbital fenestra (Fig. 4), to prevent conclusions biased by the lack of morphological information. PC1 remains associated to the same morphological variation as when only modern forms were ana-

lyzed (see paragraphs above). PC2 regards variation across all landmarks, and is more conspicuous at the braincase, although it also affects the rostrum, and implies a craniofacial structural bending.

Table 2. Correlations of PCs to Centroid Size are tested for the avian sample to explore association of size to shape variation. Matrix of correlation coefficients (*r*); (**) p<0.01; (*) p<0.05

		PC1	PC2	PC3	PC4	Cent. Size
PC1	r	1.000	.000	-,001	-,001	-.535**
	Sig.	.	1.000	.990	.996	.000
	N	93	93	93	93	93
PC2	r	.000	1.000	.000	-.001	-.238*
	Sig.	1.000	.	1.000	.989	.022
	N	93	93	93	93	93
PC3	r	-.001	.000	1.000	.000	.411**
	Sig.	.990	1,000	.	.998	.000
	N	93	93	93	93	93
PC4	r	-.001	-.001	.000	1.000	-.247*
	Sig.	.996	.989	.998	.	.017
	N	93	93	93	93	93
Cent. Size	r	-.535**	-.238*	.411**	-.247*	1.000
	Sig.	.000	.022	.000	.017	.
	N	93	93	93	93	93

Graphically, a similar scatter can be found when plotting PC1 with PC2 compared to that obtained with modern forms analyzed alone. Extinct theropod forms are located at previously empty regions of the avian morphospace, and this is due to extreme values acquainted by them for PC2. This location in morphospace implies an extreme skull morphological configuration in comparison to modern forms; a deeper rostrum (extinct theropods at this region of morphospace), and a more stretched quadrate bone whose position covaries within the trend of variation towards the avian condition (opposite values of the PC). This situation confers extinct forms a deeper appearance of the skull, and within the trend towards opposite regions of morphospace is also accompanied by amplification of the braincase and its "rotation", reflecting an apparent overall flexion of the skull in modern forms.

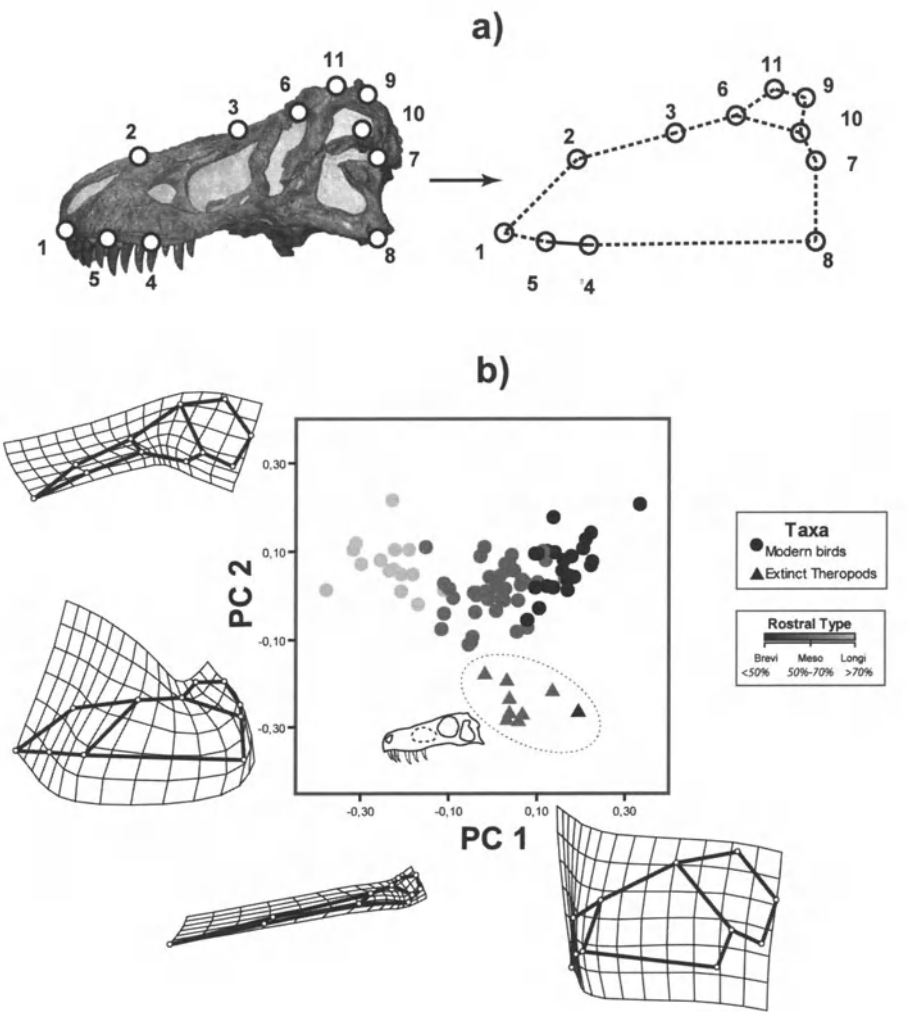

Fig. 4. a) Skull from an extinct theropod (*T. rex*), with landmarks (see also Table 1). Note lack of landmarks at areas within the orbit (e.g. nerves) b) PCA (PC1 and PC2) with extinct forms included. PC1 variation close to that without extinct forms. PC2 shows a trend of craniofacial flexion, but also note variation at quadrate bone (landmarks 7, 8). Scheme of *Herrerasaurus* at region of morphospace only occupied by extinct forms (pointed ellipse). Dark triangle is *Citipati*. Theropods analyzed are: *Herrerasaurus ischigualastensis* (from, Sereno and Novas 1993), *Tyrannosaurus rex* (cast from AMNH 5027), *Coelophysis bauri* (from, Colbert 1989), *Dromaeosaurus albertensis* (from, Currie 1995), *Velociraptor mongoliensis* (from, Currie 1997), *Acrocanthosaurus atokensis* (from Currie and Carpenter 2000), *Allosaurus fragilis* (from, Madsen 1976), *Citipati osmolskae* (IGM 100/978, housed at AMNH), *Albertosaurus libratus* (Cast from ROM 1247)

12. 5. Discussion and conclusions

We have found that most of the morphological diversity of the skull of modern avian forms can be found in a small number of dimensions; the first four dimensions on the avian PCA explain over 80% of total skull variance of a representative sample that comprises all known Orders within Neornithes. From the results, more than 70% of the variation after GPA relies on two main trends: (1) a continuous range of variation in the anterior region of the rostrum (its lengthening or shortening), and (2) angulations or flexions of the craniofacial complex, conferring different architectural appearances to the skull.

A remarkable morphological plasticity is characteristic of the shape of the rostrum and it is a dominant morphological trend in modern birds (Zusi 1993), and this is clearer if we compare their rostral variation with that of other theropod dinosaurs. We have been able to locate it morphometrically, showing that it mostly concerns the premaxilla and part of the maxilla (its anterior area), and that it concentrates in one dimension, strikingly explaining more than half of all the variation between all Orders. This large natural variation can be grouped into the following types: brevirostrals, mesorostrals and longirostrals (Marugán-Lobón and Buscalioni 2003). *Micropsitta* would be a special case of extreme brevirostrality, most likely to be exploring a morphological boundary, whereas *Pelecanus*, an extreme longirostral, falls within an area of morphospace explored by other archosaurian forms (Pterosaurs, e.g. *Pteranodon*; see, Marugán-Lobón and Buscalioni 2003).

Resistant Fit superimposition results (Fig.2) suggest that despite the fact that variation is extremely localized at the anterior region of the rostrum (and therefore the braincase being much more conservative), it cannot be regarded as totally independent. This is because the remainder regions caudal to the rostrum are much more conservative but still vary in some degree. This should not occur if we speak strictly of the Pinocchio Effect. We might thereby suggest that morphological plasticity of the rostrum should be interpreted as affected by different constraints governing its variation, rather than thinking of it as a structure that varies autonomously from the remaining skull (i.e. the braincase), in accordance to adaptive or functional demands.

We have also seen that the skull of modern birds can structurally differ in appearance by an angular relationship that varies between the rostrum and the braincase (Duijm 1951), a craniofacial variation otherwise undistinguishable if measurements were not performed over the whole skull. We have been able to detect and locate this morphological variation with landmark based superimposition techniques. The second dimension of overall variation is associated to shape variation regarding a flexed configuration conferring a rotated appearance to the braincase in regard to the rostrum, in contrast to an opposite condition of unbent morphology. The explained variance of this dimension is 14%, quite significant if we face that the first dimension did account for more than a 50% by itself.

Marinelli (1928) quoted the aforementioned morphological trend as a real morphocline, and differentiated between two extremes that he typified as *straight* skull

types in contrast to those that were *bent*. Duijm (1951) studies followed those of Marinelli, and although he typified extremes as *straight* and *kinked* (bent) ones, his major remark opposed the idea of a morphocline, reasoning that variation should rather be independent between structural units (the rostrum and the braincase). Hofer (1952) found that the straight type could be called *orthocranial* because, among other features, the ventral edge of the rostrum could be found parallel to the cranial floor, but for him, the opposite morphological extreme is a type he named *klinorhynch*, in which only the rostrum would be the structure that bent obliquely downwards in respect to the braincase. Other morphological types (Hofer 1952) were described; *aerorhynch* types, very rare, and only to be found through sagittal slicing of the skull (Order Gaviiformes would be the example for this condition). *Airencephalic* would be a special condition mainly displayed by Strigiformes (i.e. owls) in which the brain is elevated in regard to the rostrum, and *klinocranial*, in which both the rostrum and the braincase are both flexed. Besides Duijm (1951) all authors found and cited variation qualitatively. The former author identified skull types by measuring angles, although he established a baseline for comparisons relying on the idea that a common "natural" posture should be found across taxa, and perhaps misrepresenting observations due to the possible arbitrariness of this premise.

Given that our results (Fig. 3) show a second dimension from which we can differentiate between two very distinct extreme types, straight and kinked (following terminology by Duijm, 1951), we can argue that both types belong to the natural extremes of a real morphocline, as was first noted qualitatively by Marinelli (1928). Namely, penguins (e.g. *Spheniscus*) or the Woodcock (*Scolopax*) are the natural occurrences of such extreme conditions respectively (authors first noted that the extreme straight type should be found on the Cormorant, *Phalacrocorax*, which on our data is certainly a straight type, but not extreme, whereas the Woodcock is always found as the extreme example of its type). This trend of craniofacial covariation, thus, highlights the importance of taking the antorbital cavity (and associated structures and tissues within, see, Witmer 1997) into account, and putting it into play as an important structure bridging morphological covariation between the braincase and the rostrum.

Likewise, other architectural types can be found from the PCA, but interestingly, they all need to be found in association to PC2 (Fig. 3). For instance, in order to construct an airencephalic skull (e.g. Strigiformes), a slight morphological deviation along the axis towards a kinked type must occur, and the same happens with klinorhynch types. In other words, the appearance of other distinctive or special cases of skull variation (any other morphological trend associated to a subsequent dimension, e.g. PC4 for airencephaly, see Fig. 3) is likely to be morphologically integrated with the craniofacial covariation of the braincase and the rostrum.

The straight type (or orthocranial), on the other hand, was thought to be the primitive typology from which all the other types should derive (Duijm 1951; Hofer 1952). Even though developmental and phylogenetic processes were involved in the explanation of this argument, the most favoured idea relied on that this configuration resembles that found in other "reptiles" (Hofer 1952; Starck 1955). On the one hand, this assertion should not be surprising since, as stated

above, flexion of the skull appears to represent an architectural property of the skull (see also, Duijm 1951), underlying therefore almost any skull type. Within a macroevolutionary framework, on the other hand, extinct theropods are found at an extreme of this morphocline, at a previously unexplored region of morphospace (following our analytical steps, although it should probably be ordered conversely; this region of morphospace would have been previously explored in the Upper Triassic by, e.g. *Herrerasaurus*), resembling a severe straightening. Explained variance by this PC2 is higher than that without extinct forms. Additional to their straight condition, variation associates the quadrate bone to change considerably, which covaries with the strong flexion of the braincase, which, at the same time, expands towards an avian configuration. Thus, the observation suggests that major macroevolutionary transformation can be operatively mapped, as results match the expected trend of transformation towards changes probably related through time to a higher degree of cerebralisation (understood as the acquisition of larger braincase volume in modern avian forms), but with the need to be preceded by a more flexible relationship of covariation among structural modules of the skull. Craniofacial morphological diversity depends on rearrangements through covariation of the modules of the structural design of the skull.

As Keller (2002) puts it, however, the usual assumption is that the primary task of scientific explanation is to provide a causal account of a phenomenon. First, we have seen that size is allometrically correlated to all described shape dimensions at different levels of significance (Table 2). Even though herein not explored thoroughly, the assumption that size plays an important role within the novel appearance of modern forms (Padian 2003) becomes evident, especially if we take into account the striking large size some extinct forms could achieve (not shown in our data). Second, former studies have always pointed to the influence the development of large eyes has had over the skull architecture in modern birds (Duijm 1951; Hofer 1952), and even about its role in the evolution of skull kinetics in birds (Bout and Zweers 2001). In addition, other authors have also pointed out that a morphological tradeoff should be associated to the acquisition of larger eyes to a higher degree of cerebralization (Gaup 1906; Marugán-Lobón and Buscalioni 2003) to be affecting the configuration of the skull of modern birds. However, little agreement has been established, almost certainly because the multifactor nature of the events involved muddle its comprehension. In paleobiology, size variation is directly considered to be associated to morphological variation, but the difficulty springs from the fact that size affects form at very different but integrated scales; to each structure or module, and to the whole once structures become integrated through ontogeny. This complex size-shape interaction broadens the riddle once it becomes reflected on patterns of organismic macroevolution.

12. 6 Acknowledgements

The authors would to thank J. Barreiro (MNCN), C. Mehlin (AMNH), M. Norell (AMNH), F. Pastor (MAUV), and P. Sweet (AMNH), for their help with the collections housed in their institutions. M. Bastir, for comments and advice on this manuscript and fruitful discussions on vertebrate morphology and evolution. F. J. Rohlf and W. Al-Garaibeh at SUNY, Stony Brook for their tireless and friendly advice about geometric morphometrics. A. Elewa for inviting us to participate in the making of this book, and J. Mulhall and J.C. Pavón, for English advice on the manuscript. J. Marugán-Lobón is supported by a F.P.U. predoctoral grant from the M.E.C.D. This study is included in the project DGCYT BTE200-0185-C0201.

References

Bang BG (1971) Functional anatomy of the olfactory system in 23 orders of birds. Acta anatomica 79 (Supplement):1-76

Baumel JJ, Witmer LM (1993) Osteologia. In: Baumel JJ, Evans EH, Van der Berge JC (eds) Handbook of Avian anatomy: Nomina Anatomica Avium, 2nd edition. Publications of the Nuttal Ornithological Group Number 23, Cambridge, pp 45-32

Bock WJ (1965) Kinetics of the avian skull. J Morphology 114(1):1-41

Bookstein FL (1991) Morphometric tools for landmark data: Geometry and biology. Cambridge University Press, New York

Bout RG, Zweers GA (2001) The role of cranial kinesis in birds. Comparative Biochemistry and Physiology Part A, 131:197-205

Büller P (1981) Functional morphology of the avian jaw apparatus. In: King AS, McLelland J (eds) Form and Function in Birds, vol 2. Academic Press, London, pp 439-468

Chaterjee S (1999) The rise of birds. 225 Million years of evolution. The John Hopkins University Press, Baltimore, London

Chiappe LM (1995) The phylogenetic position of the Cretaceous birds from Argentina: Anatomy and systematics of the Enantiornithes and *Patagopteryx deferraiisi*. Cour Forsch Senkenb 181:55-63

Colbert EH (1989) The Triassic dinosaur *Coelophysis*. Museum of Northern Arizona Bulletin 57:1–160

Cracraft J (1986) The origin and early diversification of birds. Paleobiology 12(4):383-399

Cracraft J, Clarke J (2001) The basal clades of modern birds. In: Gauthier J, Gall LF (eds) New Perspectives on the Origin and Early Evolution of Birds. Proceedings of the International Symposium in Honor of John H. Ostrom. Special Publication of the Peabody Museum of Natural History, Yale University, New Haven, pp 143-155

Currie PJ (1995) New information on the anatomy and relationships of Dromaeosaurus albertensis (Dinosauria: Theropoda). J Vert Paleo 15 (3):576–591

Currie PJ (1997) Raptors. In: Padian K, Currie PJ (eds) Encyclopedia of dinosaurs. Academic Press, London, p 626

Currie PJ, Carpenter K (2000) *Acrocanthosaurus atokensis* from Antlers Formation, Oklahoma, U.S.A. Geodiversitas 22(2):207–246

Debbaut V, Davis JR (2002) Analysing phenotypic variation: When old-fashioned means up-to-date. J Biosci 27(3):191-193

Duijm M (1951) On the head posture in birds and its relation to some anatomical features. I-II Proc Koninklijke Nederlandse Akademie van Wetenschappen, ser C, Biological and Medical Sciences 54:202-271

Dullemeijer P (1972) Methodology in craniofacial biology. Acta Morphol Neerl-Scand 10:9-23

Feduccia A (1999). The origin and evolution of birds, 2nd edition. Yale University Press, New Haven

Fisher HI (1955) Some aspects of the kinetics in the jaw of birds. Wilson Bulletin 67(3):175-188

Gaup E (1906) Die entwicklung des kopfskelttes in hertwig. In: Hertwig O (ed) Handbuch der Vergleicherden und Experimentellen Entwickelungstehre vol III, pp 573-855

Gauthier J (1986) Saurischian monophyly and the origin of birds. In: Padian K (ed) The Origin of birds and the evolution of flight. Mem Calif Acad Sci 8, San Francisco, pp 1-55

Grant BR, Grant PR (1993) Evolution of Darwin Finches caused by a rare climatic event. Proc R Soc London Ser B, 251:111-117

Hofer H (1952) Der gestalwandel des schädels der säugetiere und vögel, mit besonderer berücksichtigung der Knickungstupen und der shädelbasis. Verhandlungen der Anatomischen Gesellschaft (Jena) 50:102-113

Jerison HJ (1973) Evolution of the brain and intelligence. Academic Press, New York London

Keller EF (2002) Making sense of Life. Explaining biological development with models, metaphors and machines. Harvard University Press, Cambridge

King AS, King DZ (1979) Avian morphology: General principles. In: King AS, McLelland J (eds) Form and Function in Birds, vol 1.Academic Press, London, pp 1-38

Madsen JH Jr (1976) *Allosaurus fragilis*. A revised osteology. Utah Geological and Mineral Survey Bulletin 109:1–163

Marinelli W (1928) Über den schadel der Schnepfe. Paleobiologica 1:135-160

Martin GR (1985) Eye. In: King AS, Mclelland J (eds) Form and function in birds. Academic Press, London, pp 311–374

Marugán-Lobón J, Buscalioni AD (2003) Disparity and geometry of the Skull in Archosauria (Reptilia: Diapsida). Biological Journal of the Linnean Society 80:67-88

McGhee GR (1999) Theoretical morphology. The concept and its applications. Perspectives in Paleobiology and Earth History. Columbia University Press, New York

Morony JJ, Bock WJ, Farrand J (1975) Reference list of the birds of the world. Publications of the Department of Ornithology, American Museum of Natural History, New York

Norell MA, Clark JM, Makovicki PJ (2001) Phylogenetic relationships among Coelurosaurian theropods. In: Gauthier J, Gall LF (eds) New Perspectives on the Origin and Early Evolution of Birds. Proceedings of the International Symposium in Honor of John H. Ostrom. Special Publication of the Peabody Museum of Natural History, Yale University, New Haven, pp 49-67

Ostrom JH (1973) The ancestry of birds. Nature 242:136

Padian K (2001) The false issues of bird origins: An historiographic perspective. In: Gauthier J, Gall LF (eds) New Perspectives on the Origin and Early Evolution of Birds. Proceedings of the International Symposium in Honor of John H. Ostrom. Special

cial Publication of the Peabody Museum of Natural History, Yale University, New Haven, pp 485-499

Padian K (2003) Evolutionary transitions in the origin of birds. J Vert Paleo 23 (Supplement to Number 3):84

Padian K, Chiappe LM (1998) The early evolution of birds. Biol Rev 73:1-42

Proctor NS, Lynch PJ (1993) Manual of ornithology. Avian structure and function. Yale University Press, New Haven

Raff RA (1996) The shape of life; genes, development, and the evolution of animal form. Chicago University Press, Chicago

Richtsmeier JT, Burke Deleon V, Lele SR (2002) The promise of Geometric Morphometrics. Yearbook Phys Anthrop 45:63-91

Rohlf FJ (2003) TPSseries software for morphometric data; TPSrelw v.1.33; TPSdig. v.1.34. Department of Ecology and Evolution, SUNY at Stony Brook, NY.

Rohlf FJ, Marcus LF (1993) A revolution in morphometrics. Trends in Ecology and Evolution 8:129-132

Rohlf FJ, Slice DE (1990) Extensions of the Procrustes method for the optimal superimposition of landmarks. Syst Zool 39:40–59

Sereno PC, Novas FE (1993) The skull and neck of the basal Theropod *Herrerasaurus ischigualastensis*. J Vert Paleo 8(4):451-476

Siegel AF, Benson RH (1982) A robust comparison of biological shapes. Biometrics 38(2):341-350

Slice DE (1994) GRFnd software for morphometric data. Department of Ecology and Evolution, SUNY at Stony Brook, NY

Slice DE (2000) Morpheus et al. software for morphometric data. Department of Ecology and Evolution, SUNY at Stony Brook, NY

Starck D (1955) Die endocraniale morphologie der Ratiten, besonders der Apterygidae and Dinornithidae. Gegenbaurs Morphologisches Jarhbuch 96:14-72

Witmer LM (1997) The evolution of the antorbital cavity of archosaurs: a study in soft tissue reconstruction in the fossil record with an analysis on the function of pneumacity. Mems Soc Vert Paleo, J Vert Paleo 17 (Suplement):1-73

Zusi R (1993) Patterns of diversity in the avian skull. In: Hanken J, Hall B (eds) The Skull. Patterns of structural and systematic diversity, vol 2. The University of Chicago Press, Chicago, pp 391-437

13 Correlation of foot sole morphology with locomotion behaviour and substrate use in four passerine genera

Fränzi Korner-Nievergelt

Zoological Museum, University Zurich, Winterthurerstr. 190, CH – 8057 Zurich, Switzerland, fraenzi.korner@bluewin.ch

13.1 Abstract

In this study, I relate plantar skin morphology (size and shape of pads, papillae and furrows) to locomotor behaviour and use of microhabitat in 37 passerine bird species in 4 distantly related genera (*Carduelis*, *Dendroica*, *Regulus* and *Parus*). If parallel evolution is present plantar skin morphology in the four passerine genera, I expect to find significant predictors among plantar skin traits for habitat use and locomotor behaviour. Plantar skin morphology was obtained by macro-photographs of the feet of wild caught birds. The number of plantar traits was reduced by elliptic Fourier analysis and principal component analysis to 13 morphological traits which were related to ecological factors by logistic regression models.

As expected, I found strong relationships between plantar skin morphology and microhabitat and non-volant locomotor behaviour, whereas the correlation between plantar morphology and aerial behaviour is poor.

I found patterns of parallel evolution in plantar integumentary traits within four distantly related genera. Furthermore, I found significant relationships between substrate use, locomotion behaviour and plantar morphology implying an adaptive function of the plantar integument to locomotion and substrate.

Keywords: Plantar integumentary morphology, elliptic Fourier analysis, ecomorphology, birds.

13.2 Introduction

Efficient foraging is crucial for successful performance of animals. Thus body systems related to foraging are expected to be subject to strong selection. Many studies have shown significant correlation between feeding ecology and

morphological characters (Karr and James 1975; Leisler 1980; Carrascal et al. 1990; Losos 1990; Barbosa and Moreno 1995). In particular, the locomotor system plays an important role in foraging behaviour (Moreno 1991; Moreno and Carrascal 1993; Miles et al. 2000). Most ecomorphological studies of birds have focused on flight and the feeding apparatus (Norberg 1986; Price 1991; Winkler and Leisler 1992; Barbosa and Moreno 1995; Keast 1996). Some studies relate tarsus, toe and claw lengths to locomotion or habitat use (e.g. Blechschmidt 1929; Palmgren 1936; Rüggeberg 1960; Norberg 1979; Raikow 1985; Barbosa and Moreno 1999). Most of these focused on skeletal and muscle morphology, although the toe pads are very pronounced in passerines, and it seems reasonable to assume a function during locomotion (Lennersted 1975a). Whether this assumption is true, or whether the pads have other functions such as insulation (Lennersted 1985), or both, has never been tested. Some authors propose that differences in pad morphology are related to ecological differences between closely related species (Goldcrest *Regulus regulus* vs. Firecrest *R. ignicapillus*, Leisler and Thaler 1982; Golden-crowned kinglet *R. satrapa* vs. Ruby-crowned kinglet *R. calendula*, Keast and Saunders 1991). Up to now, a comprehensive study relating locomotor behaviour and plantar integumentary morphology has never been done.

In this study, I relate external plantar integumentary morphology (size and shape of pads, papillae and furrows) to substrate use and locomotor behaviour in 37 passerine bird species belonging to 4 distantly related genera belonging to three different families: *Parus* (Paridae), *Regulus* (Regulidae), *Carduelis* and *Dendroica* (Fringillidae) (Sibley and Ahlquist 1990). Within the Fringillidae, *Carduelis* belongs to the subfamily Fringillinae, whereas *Dendroica* is phylogenetically related to the Emberizinae (Yuri and Mindell 2002). Within a genus, the selected species cover, where possible, a broad ecological spectrum. This selection of species allows for testing for parallel evolution. Futuyma (1998, p 110) defines parallel evolution as similar developmental modifications that evolve independently. If parallel evolution is present in plantar integumentary morphology in the four passerine genera studied here, I expect to find significant predictors among the traits of the plantar surface for habitat use and locomotor behaviour using regression models. Predicting ecology from morphology is the general approach of an ecomorphological study (Winkler and Leisler 1985; Leisler and Winkler 1991; Bock 1994; Wainwright and Reilly 1994).

13.3. Species and data

13.3.1 Species and sample size

Species were selected so that the sample showed a broad variation in habitat use. Particularly, I first selected species inhabiting an extreme arboreal habitat. The

outermost twigs of conifers provide an extreme microhabitat due to the thin structures (needles) birds have to cling to during locomotion. Therefore, I selected four genera that contain at least one species that forages in the outermost twigs of conifers. Then, I selected congeneric species so that within each genus a broad ecological spectrum was present. However, the species selection was mainly dictated by the range of species caught at the following bird ringing stations during the indicated time: August/September 2000 at Rybachy (RU), October 2000 at Col de Bretolet (CH), August to October 2001 at Powdermill (Pennsylvania, USA) and March 2002 at Bolle di Magadino (CH). For two species, *Parus inornatus* and *P. rufonuchalis*, I used museum specimens preserved in ethanol housed at the British Museum, Natural History Museum Tring, GB.

The sample size ranged from 1 to 13 (median=3) individuals per species.

13.3.2 Morphological data

I took pictures of the plantar foot surface of wild caught live birds using a Nikon camera with a macro lens (Medical-Nikkor 120mm, 1:4) equipped with a ring flash. For standardisation of foot position, I softly pressed the birds' right foot against a sheet of glass (Fig. 1). The pictures, one from the plantar side and one from the lateral, were taken through the glass (Fig. 2). I used the program tpsDig Version 1.30 (Rohlf, 2001) to measure length, width and height of each digital pad and the width of the furrows between the pads. Additionally, I digitised the outline of the proximal pad (the largest pad) on digit I in plantar view, measured its area electronically and counted the number of papillae. The length of the claw on digit I and its curvature were measured and calculated as described by Feduccia (1993).

From each of these measurements, species means were calculated. The species mean shape of the outline of the proximal pad of digit I was obtained by abstracting the outlines by elliptic Fourier decomposition (Ferson et al. 1985). Using this method, the outline is decomposed in a sum of sine- and cosine-functions. The more terms ("harmonics" with four coefficients each) that are added to the function, the closer the outline is described by the function. I used 8 harmonics. The shapes were rotated and stretched to match standard size and direction. From the individual coefficients, species means were calculated and from them, the species mean pad shape was reconstructed (Fig. 3). The elliptic Fourier analyses were carried out on the computer program Morpheus et al. (Slice, 1998).

Fig. 1. Photographic set up for taking pictures of the foot. The bird's right foot was softly pressed against the glass while taking the pictures

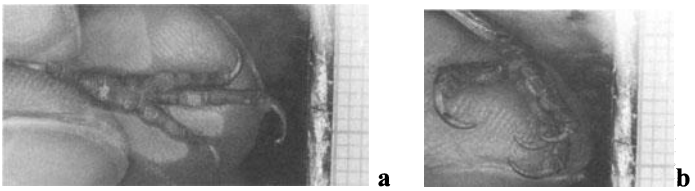

Fig. 2. a) Ventral and **b**) lateral view of the right foot of a *Dendroica magnolia*

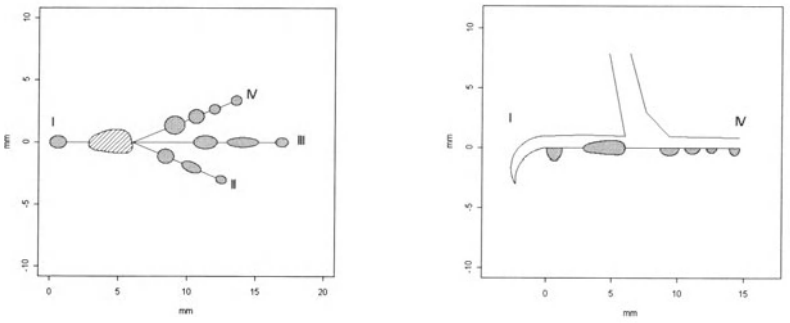

Fig. 3. Reconstruction of the mean right plantar surface of *Dendroica magnolia* in ventral view (left) and lateral view (right). The reconstruction of the pads is based on length, width and height and approximated by ellipses, except for the proximal pad on digit I. This pad was reconstructed via the mean elliptic Fourier coefficients as described in the text. The density of the hatching is proportional to the number of papillae on this pad. The angles between the toes are arbitrarily set to 25° between toe II and III, and 24° between toe III and IV, respectively. In lateral view, the claw of digit I is reconstructed by its length, its height at the base and its inner and outer curvature. The curvatures are approximated by circle segments. The units of the axis are in mm

13.2.3 Behavioural data

Substrates were divided into 7 categories and bird behaviours into 9 categories (Table 1), based on the definitions given in Remsen and Robinson (1990). For

each species, I asked experts (see acknowledgements and Appendix) to specify how often the species uses each substrate and how often the species performs each behaviour. The species experts could choose between three frequencies: never, seldom, often. For 29 species, I received an answer from one to three experts. For 8 species, I extracted the information about substrate use and foraging behaviour from the following literature: Knox and Lowther (2000): *Carduelis cabaret*, Dawson (1997): *C. pinus*, Hunt and Flas-pohler (1998): *Dendroica coronata*, Curson (1994): *D. discolor*, Harrap and Quinn (1996): *Parus carolinensis, P. inornatus. P. rufonuchalis*, and Ingold and Wallace (1994): *Regulus calendula.*

Table 1. Definitions of categories of substrate and behaviour

Category	Description
Substrate	
Needles	coniferous foliage
Leaves	deciduous foliage
Twigs	canopy of trees or bushes, not in foliage
Trunk	trunk of a tree or a bush
Elsewhere	on grass or ground
Vertical	bird contacts with its feet a vertical substrate
Air	bird's feet don't touch any substrate
Behaviour	
Sideways	bird hangs sideways, flank up (Fig. 15.4 a)
Belly up	bird hangs with its belly up (Fig. 15.4 b)
Upside down	Birds head hangs below the body (Fig. 15.4 c)
Flutterhop	hopping supported by fluttering
Hover	flying in place or stalling, combination of the categories "sally-stall" and "sally-hover" defined by Remsen & Robinson (1990)
Flycatch	short bout of flight in order to catch a prey, this category was named by Remsen & Robinson (1990) "sally-strike"
Aerial hawk	longer foraging flight
Beside	the bird's body is situated beside the substrate (e.g in Fig. 15.4 a, c)
Below	bird hangs below the substrate, either flank, belly or tail is pointing upwards (e.g. in Fig. 15.4 b)

The species scores for each microhabitat and behaviour/position category are given in the appendix.

a b c

Fig. 4. Illustration of the behavioural categories **a**) sideways, **b**) belly up, and **c**) upside down

13.2.4 Statistics

All statistical analyses were performed using R 1.5.1 software (R Development Core Team, 2002).

Data transformation and correction for size

The curvature of the claw of digit I was arc-sin and square-root transformed and not corrected for size. All other morphological variables of the plantar morphology were log-transformed and then corrected for size by dividing them by the log-transformed foot span (between digit I and II, Fig. 5). The area of the proximal pad on digit I was divided by the square of the digital span. The number of papillae of the pad was divided by the papillar area of this pad. The digital span itself was divided by the cube root of the birds' weight (Leisler and Winkler 1991). Bird's weights were taken from Dunning (1992).

Reduction of variables

Since the chance of finding significant but biologically irrelevant relationships between dependent and independent variables increases with the number of variables, it is recommended that the number of variables be kept low compared to the number of observations (e.g. Sachs 1978). Furthermore, autocorrelated dependent variables might impair the results of regressions. Therefore, I reduced the original number of morphological variables (57) to 13, which were as little as possible correlated to each other, showed a high variability within the data, and which covered most of the functional aspects of the bird's foot. In order to achieve such a reduction, I performed 6 principal component analyses (PCA) on subsets of functionally related variables. These subsets were: 1) pad lengths, 2) pad widths (12 variables each), 3) pad heights (6 variables), 4) furrow widths (8 variables),

and 5) diverse traits, which did not belong to one of the groups above (number of papillae, pad area, claw length, curvature of claw, foot span, distance from the foot centre to the first pad on each toe (distance 5)) and 6) shape coefficients of the pad outline. Of the PCAs 1) to 4), principal components that explained more than 30% of the variance were selected (Table 2). Of PCA 5), principal components that explained more than 4% of the variance were selected, since the miscellaneous variables cover a number of different morphological functions. These threshold values were arbitrary set. Within each principal component, the variable with the highest loading was retained for further analysis, whereas the others were discarded (Table 2). The 10 selected variables cover a broad range of functional aspects of plantar morphology (Fig.5). The first components of the PCAs 1) to 4) measure size of the corresponding variable set, since all loadings have the same signs. Therefore, the variables selected from these components are interpreted as follows: The length of pad 2 measures general pad lengths, width of pad 11 measures general pad widths, and height of pad 1 represents general pad heights. An alternative method for variable reduction would be factor analysis instead of PCA.

Table 2. The first few components of the five principal component analyses on each group of variables and the selected variables according to their loading values

variable group and number of variables	principal components	proportion of variance	variable with the highest loading	loading
1) pad lengths (12)	1	38.8%	length of pad 2	-0.408
	2	30.8%	length of pad 1	0.446
2) pad widths (12)	1	68.4%	width of pad 11	-0.314
3) furrow widths (8)	1	48.2%	width of furrow 9	-0.438
4) pad heights (6)	1	73.1%	height of pad 1	-0.437
5) miscellaneous (10)	1	56.4%	hind claw	-0.378
	2	15.2%	area of pad 2	0.597
	3	13.2%	curvature of claw of digit I	-0.452
	4	5.4%	distance 5	-0.513
	5	4%	number of papillae	-0.556

The last subset of morphological variables 6) consists of the Fourier shape coefficients of the pad outline. Only the coefficients from the first three harmonics were used. Since the first three coefficients of the first harmonic for all species are 1, 0, and 0 due to standardisation in relation to size, rotation and starting point, they were omitted, and only 12-3=9 coefficients were entered into the principal components analysis. The first two principal components accounted for 77.05% and 13.07% of the variance, respectively.

These components were used as pad shape variables. The meaning of PC1 is seen in the ratio length/width and in the position of the maximal width (Fig. 6). A high value of PC1 means a large ratio and a proximal maximal width. PC2 describes the asymmetry of the pad. The higher the score on PC2, the more convex is the lateral edge of the pad, whereas the medial edge tends to be flatter.

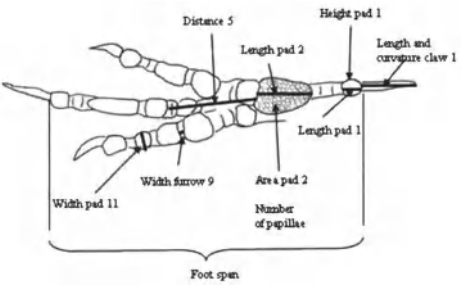

Fig. 5. The variables of plantar morphology that remained after the redundant variables were discarded

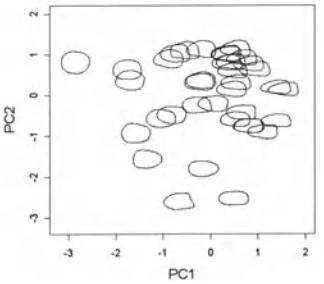

Fig. 6. The first two principal components of the pad shape coefficients; Left=distal, right=proximal, upper=lateral/outer/right, lower=medial/inner/left; along the x-axis (PC1) the pads became narrower and their maximal width changes from distal to proximal; along the y-axis (PC2) they become more asymmetric

Therefore, 13 variables of plantar morphology were selected: lengths of pad 1 and 2, height of pad 1, width of pad 11, width of furrow 9, distance 5, length of the hind claw, the area of pad 2, the curvature of the claw of digit I, the number of papillae on pad 2 (Fig. 5), and two shape coefficients of the outline of pad 2 (Fig. 6). Finally, foot span was used as size variable.

Relationships between ecology and morphology

Significant relationships between microhabitat use or locomotor behaviour and the 13 morphological variables were obtained by applying the following procedure to each of the 16 variables of substrate and behaviour:

(1) A linear regression model was obtained by backward selection from the full linear model with the 13 morphological variables and the factor "genus" (4 levels) as independent variables, and the ecological variable as dependent variable. The influence of single species on the result was obtained by the Cook's distance (Hair

et al. 1995). In one case (twigs) one species had to be omitted due to a Cook's distance higher than 0.5.

(2) The variables remaining in the linear model after the backward selection were used for a proportional odds regression model (Hosmer and Lemeshow 2000; Stahel and Pritscher 2002). Since the ecological variables in this study take ordered discrete values (never, seldom, often), a proportional odds regression, which is a type of ordinal logistic regression, is the appropriate method to determine the significances of single morphological variables in predicting substrate use or behaviour.

Before the odds regression was performed, the means of the ecological scores were rounded to one of the three levels "never", "seldom" and "often". The final model was selected by a stepwise backward method minimising the AIC-criteria.

(3) The final proportional odds regression models were tested by comparing their deviances with the deviances of the null models using a Chi-square test (Stahel and Pritscher 2002).

(4) The goodness of fit of the proportional odds model was tested by a modified Hosmer-Lemeshow test (Hosmer and Lemeshow 2000). This test was originally devised for testing a binary logistic regression: The observations are ordered according to their fitted values.

Then, the observations were summarised in 10 groups. Finally, a Chi-square test on the 10x2 table of observed and fitted values was performed, using 20-10-(2-1)-1=8 degrees of freedom. Applying this test to an ordinal logistic regression with three levels in the dependent variable, the 10x2 table has to be modified to a 10x3 table, and the degrees of freedom for the Chi-square test to 30-10-(3-1)-1=17. A significant Chi-square-test means that the model does not fully explain the variability in the dependent variable.

Two ecological variables, namely "twigs" and "trunk", contain only two levels. Here, instead of the proportional odds regression a binary logistic regression was performed. The models were tested for significance by comparing their residual deviances with the residual deviance of the null model, containing only the intercept (Stahel and Pritscher 2002).

The Hosmer-Lemeshow test was used as a goodness of fit test, as described by Hosmer and Lemeshow (2000).

13.3 Results

The substrate variables, "needles", "trunk" and "vertical" can be accurately predicted by morphological variables of plantar morphology (Table 3). From the variables of locomotor behaviour, only the behaviours related to bipedal locomotion, except "upside down" and "below", can be fully predicted by plantar morphological variables (Table 4). The locomotor variables describing aerial behaviour have a poor fit with plantar morphology (significant goodness of fit test, Table 4). Since I corrected for genus in the regressions, the relationships discovered are parallel within each genus.

Table 3. The proportional odds (or binary logistic) regression models for substrate use. If not otherwise indicated, the results stem from a proportional odds model fit. *: a significant goodness of fit test means that the model does not explain the entire variation of the ecological variable. In bold are significant variables in models with a good fit

substrate	variables in the model	estimated b	se of b	p
needles	**genus**	**.**	**.**	**0.002**
	pad length	**-1.33**	**0.59**	**0.014**
	number of papillae	**-2.15**	**0.83**	**0.004**
	total model			<0.001
	goodness of fit			0.316
leaves	genus	.	.	<0.001
	curvature of claw	2.94	0.99	<0.001
	foot span	-2.15	0.74	<0.001
	total model			<0.001
	goodness of fit			0.002*
twigs[a]	intercept	1.37	0.47	0.004
(binary	number of papillae	-1.07	0.46	0.020
logistic	test of the total model			0.010
regression)	goodness of fit			0.020*
trunk	intercept	-15.28	34.08	0.654
(binary	genus	.	.	0.670
logistic	**length of pad 1**	**-2.65**	**1.19**	**0.026**
regression)	**curvature of claw**	**-3.37**	**1.54**	**0.029**
	test of the total model			0.002
	goodness of fit			0.067
elsewhere	pad length	1.97	0.69	0.001
	length of pad 1	-1.17	0.76	0.106
	length of hind claw	-1.18	0.66	0.061
	area of pad 2	-1.35	0.63	0.022
	curvature of claw	-1.78	0.63	0.004
	total model			0.003
	goodness of fit			<0.001*
vertical	**pad shape component 1**	**-61.67**	**20.23**	**<0.001**
	pad shape component 2	**-53.82**	**21.20**	**0.003**
	pad length	1.39	1.00	0.145
	height of pad 1	**-1.66**	**0.84**	**0.026**
	foot span	1.02	0.75	0.144
	total model			<0.001
	goodness of fit			0.410
air	pad shape component 2	-9.12	5.91	0.113
	pad width	2.11	0.72	<0.001
	length of claw	-1.02	0.67	0.115
	foot span	2.00	0.72	<0.001
	distance 5	1.10	0.62	0.066
	number of papillae	1.97	0.90	0.019
	total model			0.003
	goodness of fit			0.023*

[a]I omitted *Carduelis cannabina* from this analysis due to its too strong influence on the result.

Table 4. The proportional odds regression models for the locomotor behaviour. Legend as in Table 3

locomotion behaviour	variables in the model	estimated b	se of b	p
sideways	**pad length**	**-1.89**	**0.59**	**<0.0001**
	length of pad 1	**2.06**	**0.74**	**0.001**
	foot span	0.76	0.48	0.09
	number of papillae	**1.83**	**0.78**	**0.008**
	total model			0.001
	goodness of fit			0.286
bellyup	**pad length**	**-2.55**	**0.71**	**<0.0001**
	furrow width	-0.75	0.43	0.067
	total model			<0.0001
	goodness of fit			0.090
upside down	pad shape component 2	33.76	15.44	0.010
	pad length	-2.05	0.62	<0.0001
	pad height	0.80	0.42	0.049
	total model			<0.0001
	goodness of fit			<0.0001*
flutter-hop	genus	.	.	0.038
	length of pad 1	1.95	0.87	0.012
	furrow width	0.92	0.58	0.098
	area of pad 2	-1.03	0.54	0.048
	number of papillae	3.07	1.18	0.002
	total model			0.046
	goodness of fit			0.023*
hover	furrow width	-0.96	0.44	0.019
	pad shape component 1	11.21	6.86	0.067
	pad shape component 2	20.22	14.26	0.107
	length of hind claw	-2.29	0.71	<0.001
	number of papillae	-1.87	0.84	0.006
	total model			<0.001
	goodness of fit			<0.001*
flycatch	genus	.	.	0.010
	pad length	1.34	0.91	0.126
	pad width	1.57	0.74	0.020
	area of pad 2	-1.74	0.81	0.019
	distance 5	-2.51	0.91	<0.001
	total model			<0.001
	goodness of fit			<0.001*
aerial hawk	pad shape component 1	-11.46	6.41	0.061
	pad height	1.27	0.70	0.057
	length of hind claw	-1.76	0.69	0.005
	total model			0.008
	goodness of fit			<0.001*
beside	**pad shape component 1**	**-27.61**	**9.09**	**0<0.001**
	pad shape component 2	**-29.64**	**15.10**	**0.037**
	length of pad 1	0.93	0.64	0.139
	number of papillae	**2.49**	**1.06**	**0.008**

Table 4 (cont)

	total model			0.003
	goodness of fit			0.228
below	pad shape component 1	-20.50	6.15	<0.001
	furrow width	-0.81	0.42	0.040
	area of pad 2	-0.59	0.41	0.143
	total model			<0.001
	goodness of fit			0.016*

In particular, I found the following relationships between substrate use and foot morphology within 37 species of 4 genera (Table 3):

1) The higher the proportion of coniferous foliage utilisation in the substrate of a bird, the shorter are their pads and the fewer is the number of papillae on the proximal pad on the first toe (Fig. 7).

2) Birds often foraging on trunks, have a short length of the distal pad of the first toe, and a weakly curved hind claw.

3) Round and symmetric proximal pads with a distal maximal width and a flat distal first toe pad are correlated with a high proportion of vertical structures in the substrate of a bird (Fig. 8).

Most of the non-volant behaviour types can well be predicted by plantar morphology, whereas none of the aerial behaviours can fully be predicted by plantar morphology (Table 4). The significant relationships between plantar morphology and behaviour types are the following:

1) The more a bird hangs sideways, the shorter are its pads except the distal pad on the first toe, which becomes longer (Fig. 9a). Furthermore, the proximal pad of digit I exhibits a high number of papillae.

2) Birds that often hang under the substrate with their belly upwards, have short pads (Fig. 9b).

3) A body position beside the substrate is correlated with symmetric, round proximal pads of digit I exhibiting a large number of papillae.

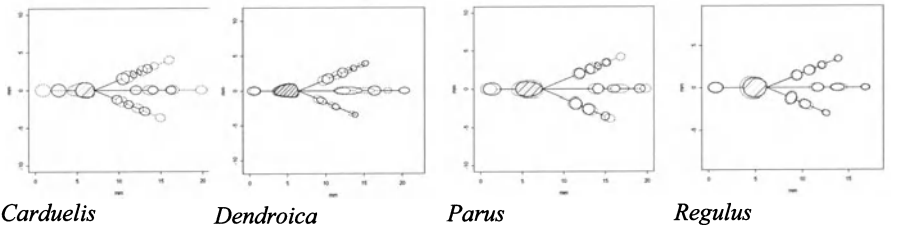

Fig. 7. Mean right plantar morphologies (ventral view) by genus (dotted lines) and the plantar morphology of a typical needle specialist of each genus (solid lines). Within each genus, the needle specialist has a shorter proximal toe pad on the first toe compared to the genus' mean, and fewer papillae (represented by the density of the hatching). For digit numbers see Fig.2

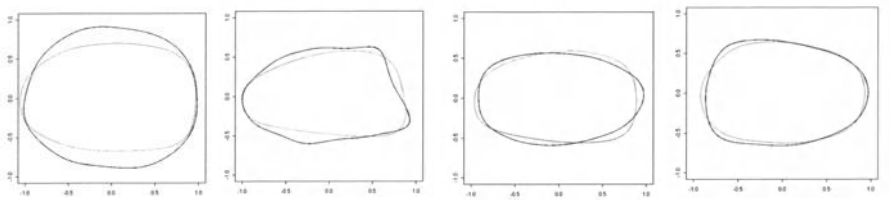

Fig. 8. Mean outline of the proximal pad of digit I by genus (dotted lines) and that of a specialist on vertical structures (solid lines) overlaid. The size of the pads has been standardised. Distal=left, lateral=upper (same orientation as in Fig.2). Within each genus the distal (left) part of the toe pad of the specialist on vertical structures is broader than that of the mean pad of the genus

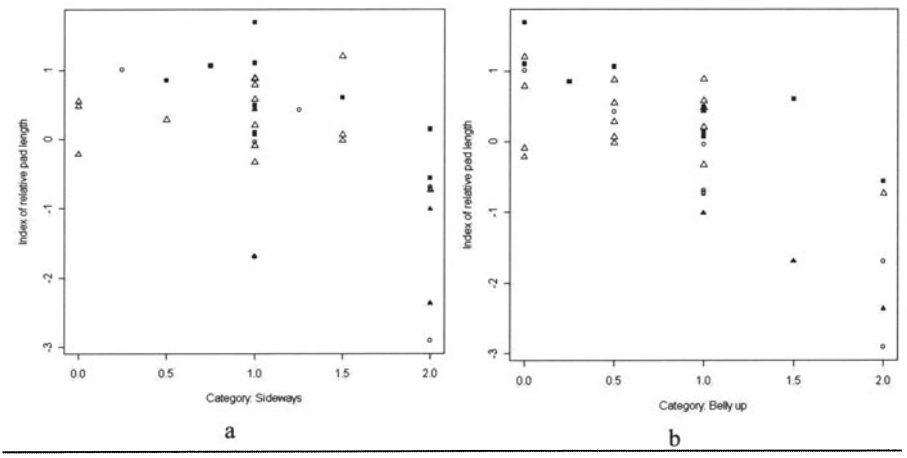

Fig. 9. Relationship of the length of the proximal toe pad of digit I to a) the frequencies of sideways orientation, b) proportion of belly up positions. ○: *Carduelis*, △: *Dendroica*, ▲: *Regulus*, ■: *Parus*

13.4 Discussion

13.4.1 Reconstruction of mean foot sole shapes

It was difficult to fully standardise foot pictures of living birds. The position of the toes varies especially in the distal regions in ventral view (Fig. 2a), due to lateral deflection of the distal phalanges. In such cases, I did not measure the width of the pads. Consequently, the species means of most of the distal pad widths are based

on a lower number of individuals than are the proximal ones. The proximal pads are not affected by toe deflection, and the within species variability (due to methodology or biology) in the shape of the outline of the proximal pad on the hind toe is small, as e.g. in *Dendroica virens* (Fig. 10). However, individual pad shapes might differ considerably from the mean shape. For the following species, only one individual was available for study: *Carduelis barbata*, *Dendroica cerulea, D. discolor*, *D. pinus*, *Parus inornatus*, *P. montanus* and *P. rufonuchalis*.

A higher standardisation of the pictures could have been obtained by using study skins instead of living birds. However, for study skins, the pads are dried and often hollow, and do not show their natural shapes; therefore canceling any possible advantage of using them.

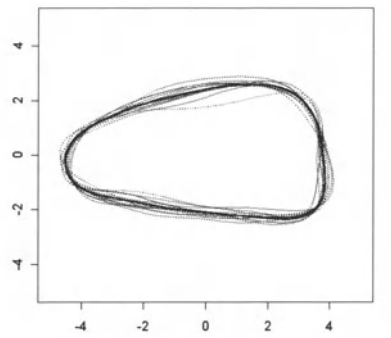

Fig. 10. Within-species variability of the shape of the proximal pad of digit I in *Dendroica virens*. Distal=left, lateral=upper (same orientation as Fig. 2), n=11.

13.4.2 Parallelism

I expected to find correlations of plantar morphology with substrate use and locomotor behaviour only if parallel evolution is present, i.e. each genus shows the same trend of morphological adaptation to substrate or behaviour. For a narrower definition of parallelism see Russell (1979). The fact that I found significant predictors among the foot sole traits for substrate use and behaviour indicates that parallel evolution exists in the majority of the four genera. Few relationships that I found do not show the same trend in each genus. For example, the negative relationship between the length of the proximal pad on digit I and two behavioural categories (sideways and belly up) is not or only weakly pronounced in *Dendroica*, whereas the other three genera show a clear negative relationship (Fig. 10). This observation indicates that for some ecological or behavioural problems, alternative morphological or behavioural solutions might exist, as for example in trunk climbing birds (Richardson 1942).

13.4.3 Functional aspects of plantar morphological traits

Curvature of the hind claw

I found that the curvature of the hind claw is negatively correlated with climbing on trunks. This result contrasts to earlier findings. According to Rüggeberg (1960), clinging and climbing specialists, such as *Certhia*, *Sitta*, *Parus atricapillus*, *Regulus*, *Acrocephalus*, *Carduelis spinus* and *Loxia*, have stronger curved, higher claws compared to the ground living birds *Alauda*, *Locustella* and *Carduelis cannabina*. Also Fedducia (1993) found that tree dwellers and trunk climbers have stronger curved claws than ground living birds. Both authors compared arboreal birds including trunk climbers with ground living ones. Contrastingly, I compared trunk climbers with mostly arboreal birds. Therefore, my results indicate that birds clinging to small twigs might have stronger curved claws than trunk climbers. For trunk climbers, strong (high) claws might be advantageous in order to grip into the rough bark of trunks. Accordingly, Zani (2000) found that the higher the claws of lizards are, the better these animals cling to rough substrate. To fully elucidate the function of well curved claws, experimental studies are needed.

Toe pads: size and shape

Several authors have assumed that toe pads of passerine birds are adapted to their locomotor behaviour and substrate (Rüggeberg 1960; Lennersted 1974; Leisler and Thaler 1982; Winkler and Leisler 1985; Keast and Saunders 1991; Korner-Nievergelt and Leisler in press). However, extensive tests or even descriptions of the relationship between pad morphology and locomotor behaviour and substrate use are lacking. This study describes for the first time statistically significant relationships between pad morphology and locomotor behaviour and substrate use. However, because statistical correlation do not elucidate function, the functional hypothesis I propose here need to be tested experimentally.

Pad length is negatively correlated with needles, and positively associated with foraging on the ground or grass. Furthermore, all body stances deviating from an upright position (sideways, belly up, upside down) are correlated with short pad length. Short pads might enhance the flexibility of the toes. Such flexible toes might be advantageous for clinging with force to a twig or needle. On the other hand, long toe pads might stiffen the toes and provide stability while walking on the ground. Blechschmidt (1929) and Rüggeberg (1960) found that basal (proximal) phalanges are shorter relative to the distal phalanges in arboreal birds than they are in ground foragers. Normally, each pad lies ventral to a phalanx (Lennersted, 1975b). Therefore, the lengths of phalanges and pads might correspond to each other.

The length of the distal pad of digit I is short in trunk climbers. Rüggeberg (1960) already noted that trunk climbers typically have small distal pads, however it is not clear what this "small" refers to: height, length or width. For trunk

climbers it is important to have a large foot span (Rüggeberg 1960; Winkler and Bock 1976; Norberg 1979), whereas tall pads might hinder the claws' ability to hook into the bark.

The height of the distal pad of digit I is small in birds often using vertical structures, but large in birds often found hanging upside down. In order to firmly grip the substrate while hanging upside down, it might be important to have tall distal pads. Such tall pads help closing the grip around a twig, whereas the claws might be less important than in trunk climbers. Similarly, for clinging to vertical structures, it might be important to have a large contact area between the plantar surface and the substrate, which is better provided by flat and long pads. The positive correlation of the length of this pad with hanging sideways supports this hypothesis.

Beside the lengths and heights of pads, their shapes are also important, namely for clinging to vertical structures and holding the body beside the substrate. For clinging to vertical structures (which is highly correlated with holding the body beside the substrate) it is plausible that a symmetric, broad pad with a distal maximal width provides a large contact area between the substrate and the plantar surface and therefore enhances the friction. Such a relationship has, as far as I know, never been described, before.

Papillae

In a descriptive study of pads and papillae of passerines Lennersted (1975b) supposed that the structure of papillae and pads are adapted to the substrate. However, he did not correlate the number of papillae per pad with substrate use. Such studies exist only for geckos (Autumn et al. 2000), lizards (Zani 2000), possums (Rosenberg and Rose 1999) and mice (Krättli 2001). Autumn et al. (2000) described small adhesive structures in the toe pads of geckos which enable them to adhere to smooth surfaces. Similar adhesive lamellae have been found in geckos and lizards (Zani, pers. comm.). However, these hair-like structures are much smaller (diameter ~5 μm) than the papillae of a bird's toe pad (diameter 200-850 μm). Furthermore, the papillae of a bird do not resemble hair-like structures but look more like round cushions. I did not find any hair-like structure on REM-pictures of birds pads (Fig. 11). I looked at four species *Parus ater*, *P. caeruleus*, *Regulus regulus*, and *Phylloscopus trochilus* under four different magnifications (25x, 100x, 500x, and 2000x). It is unlikely that bird's papillae produce an adhesive force due to their microscopic structure. They are simply too large. Bird's pad papillae are with regard to histology and size more similar to the ridges of mammal's toe pads. In mice, the density of these ridges is highly correlated with clinging ability (Krättli 2001). The smaller and more numerous the ridges are, the better is the clinging ability to a thin substrate such as small twigs. We might, therefore, expect, also in birds, a negative correlation between size of papillae and the diameter of the substrate. Respectively, since size of papillae is inversely proportional to the number of papillae per unit area, I would expect a positive correlation between number of papillae and the diameter of the substrate. However, I found a negative correlation between the number of papillae and

foraging in needles, whereas hanging sideways and holding the body beside the substrate were positively correlated with the number of papillae per unit area. Similar observations were made by Lennersted (1975b). He found a reduced number of papillae in birds living on the ground, on tree trunks and on very thin twigs. However, he did not provide a functional interpretation. Furthermore, Lennersted (1975b; 1985) described that Palearctic sedentary passerines have generally few and large papillae, whereas passerines of similar size wintering in tropical Africa have many and small papillae. He supposed an insulating function of the few but large papillae. However, an insulating function of the foot sole might not be important in birds since they can regulate the temperature of their feet by a rete mirabile. I have not found any plausible interpretation for the function of the papillae of a bird's toe pad.

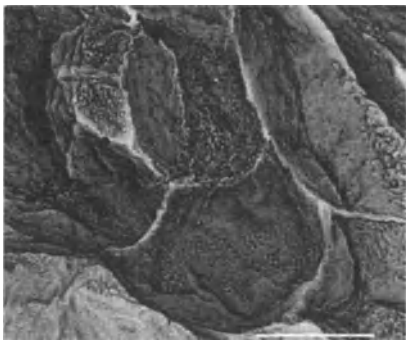

Fig. 11. REM-picture of the pad surface of a typical needle-dweller *Regulus regulus*. No special structures can be seen. White bar: 9 μm

13.5 Acknowledgements

I am deeply indebted to my supervisors Dr. B. Leisler (ecomorphology) and Lisa Pritscher (statistics). Many thanks to the leaders of the ringing stations, who kindly allowed me to take bird foot pictures, Nadya Zelenova (Rybachy) and Bob Mulvihill (Powdermill).

The following experts kindly answered my questions about behaviour: Bruce Byers (BB), Jan Drachmann (JD), Wilhelm Egli (WE), Wolfgang Forstmeier (WF), Tom Fox (TF), Richard T. Holmes (RTH), Jones Jason (JJ), John Kilgo (JK), Pius Korner (PK), Steven Latta (SL), Karin Lindstrom (KL), G. A. Lozano (GAL), Bill McMartin (BM), Chris Rimmer (CR), Juan Carlos Senar (JCS), David Shaw (DS), Robert Smith (RS), Barbara Tschirren (BT), Claudio Venegas (CV), Marc-André Villard (MAV), W. Herbert Wilson (WHW). Dennis E. Slice supported me in morphometrics. H. Jauch produced the REM pictures. M.J. Calvacanti, Pius Korner, James Rohlf and Anathony Russel gave valuable

comments on earlier drafts of the manuscript. This study was financially supported by the SANW, FAN and the Zürcher Hochschulverein.

References

Autumn K, Liang YA, Hsieh ST, Zesch W, Chan WP, Kenny TW, Fearing R, Full RJ (2000) Adhesive force of a single gecko foot-hair. Nature 405: 681-685

Barbosa A, Moreno E (1995) Convergence in aerially feeding insectivorous birds. Netherlands J Zool 45: 291-304

Barbosa A, Moreno E (1999) Hindlimb morphology and locomotor performance in waders: an evolutionary approach. Biol J Linn Soc 67: 313-330

Blechschmidt H (1929) Messende Untersuchungen über die Fussanpassungen der Baum- und Laufvögel. Gegenbaurs Morphol Jahrb 61: 517-547

Bock WJ (1994) Concepts and methods in ecomorphology. J Biosci 19: 403-413

Carrascal LM, Moreno E, Tellería JL (1990) Ecomorphological relationships in a group of insectivorous birds of temperate forest in winter. Holarctic Ecol 13: 105-111

Curson J (1994) New World warblers. Christopher Helm A & C Black, London.

Dawson WR (1997) Pine Siskin. In: Poole A, Gill F (eds) The Birds of North America. The American Ornithologists' Union, The Academy of Natural Science of Philadelphia

Dunning JB (1992) CRC Handbook of Avian Body Masses. CRC Press, London.

Feduccia A (1993) Evidence from claw geometry indicating arboreal habits of *Archeaeoptryx*. Sci 259: 790-793

Ferson S, Rohlf FJ, Koehn RK (1985) Measuring shape variation of two-dimensional outlines. Syst Zool 34: 59-68

Futuyma DJ (1998) Evolutionary Biology. Sinauer Associates Inc, Sunderland Massachusetts

Hair FJ, Anderson RE, Tatham, RL, Black WC (1995) Multivariate Data Analysis. Prentice-Hall Inc. Englewood Cliffs, New Jersey

Harrap S, Quinn D (1996) Tits, Nuthatches & Treecreepers. Christopher Helm A & C Black, London

Hosmer DW, Lemeshow S (2000) Applied logistic regression. John Wiley & Sons Inc, New York

Hunt PD, Flaspohler DJ (1998) Yellow-rumped Warbler. In: Poole A, Gill F (eds) The Birds of North America. The American Ornithologists' Union, Cornell Laboratory of Ornithology and The Academy of Natural Sciences

Ingold JL, Wallace GE (1994) Ruby-crowned Kinglet. In: Poole A, Gill F (eds) The Birds of North America. The American Ornithologists' Union, The Academy of Natural Sciences of Philadelphia

Karr JR, James FC (1975) Eco-morphological configurations and convergent evolution in species and communities. In: Cody ML, Diamond JM (eds) Ecology and Evolution of Communities. The Belknap Press of Harvard University, Cambridge, pp 258-291

Keast A (1996) Wing shape in insectivorous passerines inhabiting New Guinea and Australian rain forests and eucalyptic forest/eucalyptic woodlands. Auk 113: 94-104

Keast A, Saunders S (1991) Ecomorphology of the North American Ruby-crowned *Regulus calendula* and Golden-crowned *R. satrapa* kinglets. Auk 108: 880-888

Knox AG, Lowther PE (2000) Common Redpoll. In: Poole A, Gill F (eds) The Birds of North America. The American Ornithologists' Union, Cornell Laboratory of Ornithology and The Academy of Natural Sciences

Korner-Nievergelt F, Leisler B (in press) Morphological convergence in conifer-dwelling passerines. J Ornithol

Krättli H (2001) Struktur und Funktion des Extremitäteninteguments bei einheimischen Mäuseartigen (Muridae, Rodentia). Ph D thesis, University of Zurich

Leisler B (1980) Morphological aspects of ecological specialisation in bird genera. Ecol Birds 2: 199-220

Leisler B, Thaler E (1982) Differences in morphology and foraging behaviour in the Goldcrest *Regulus regulus* and Firecrest *R. ignicapillus*. Ann Zool Fennici 19: 277-284

Leisler B, Winkler H (1991) Ergebnisse und Konzepte ökomorphologischer Untersuchungen an Vögeln. J Ornithol 132: 373-425

Lennersted I (1974) Pads and papillae on the feet of nine passerine species. Ornis Scand 5: 103-111

Lennersted I (1975a) A functional study of papillae and pads in the foot of passerines, parrots, and owls. Zool Scripta 4: 111-123

Lennersted I (1975b) Pattern of pads and folds in the foot of European Oscines (Aves, Passeriformes). Zool Scripta 4: 101-109

Lennersted I (1985) Foot papillae and pads. In: Campbell B, Lack E (eds) A dictionary of birds. T & A Poyser, Calton, p 670

Losos JB (1990) Ecomorphology, performance capability, and scaling of west Indian Anolis lizards: an evolutionary analysis. Ecol Monogr 60: 369-388

Lovette IJ , Bermingham E (2001) Mitochondrial perspective on the phylogenetic relationships of the *Parula* wood-warblers. Auk 118: 211-215

Miles DB, Sinervo B, Frankino WA (2000) Reproductive burden, locomotor performance, and the cost of reproduction in free ranging lizards. Evol 54: 1386-1395

Moreno E (1991) Musculature of the pelvic appendages of the treecreepers (Passeriformes: Certhiidae): myological adaptation for tail-supported climbing. Canad J Zool 69: 2456-2460

Moreno E, Carrascal LM (1993) Leg morphology and feeding postures in four *Parus* species: An experimental ecomorphological approach. Ecol 74: 2037-2044

Norberg UM (1979) Morphology of the wings, legs and tail of three coniferous forest tits, the Goldcrest, and the Treecreeper in relation to locomotor pattern and feeding station selection. Phil Trans R Soc Lond B. Biol Sci 287: 131-165

Norberg UM (1986) Evolutionary convergence in foraging niche and flight morphology in insectivorous aerial-hawking birds and bats. Ornis Scand 17: 253-260

Palmgren P (1936) Bemerkungen über die ökologische Bedeutung der biologischen Anatomie des Fusses bei einigen Kleinvogelarten. Ornis Fenn 13: 53-58

Price T (1991) Morphology and ecology of breeding warblers along an altitudinal gradient in Kashmir, India. J Anim Ecol 60: 643-664

Raikow RJ (1985) Locomotor systems. In: King AS, McLelland J (eds) Form and Function in Birds. Academic Press, London, pp 57-147

R Development Core Team (2002) R: A language and environment for statistical computing. R Foundation for Statistical Computing, Vienna, Austria. http://www.R-project.org

Remsen JV, Robinson SK (1990) A classification scheme for foraging behaviour of birds in terrestrial habitats. Stud Avian Biol 13: 144-160

Richardson F (1942) Adaptive modifications for tree-trunk foraging in birds. Univ California Publ Zool 46: 317-368

Rohlf FJ (2001) tpsDig Version 1.30 release 29-10-2001. Ecology and Evolution, SUNY at Stony Brook, New York

Rosenberg, HI, Rose R (1999) Volar adhesive pads of the feathertail glider, *Acrobates pymaeus* (Marsupalia, Acrobatidae). Can J Zool 77: 233-248

Rüggeberg T (1960) Zur funktionellen Anatomie der hinteren Extremität einiger mitteleuropäischen Singvogelarten. Z wissensch Zool 164: 1-106

Russell AP (1979) Parallelism and integrated design in the foot structure of gekkonine and diplodactyline geckos. Copeia 1979 (1): 1-21

Sachs L (1978) Angewandte Statistik. Springer, Berlin

Sibley CG, Ahlquist JE (1990) Phylogeny and Classification of Birds, A study in Molecular Evolution. Yale University Press, New Haven and London

Slice DE (1998) Morpheus et al.: Software for morphometric research. Revision 30-01-98. Department of Ecology and Evolution. State University of New York, Stony Brook, New York

Stahel W, Pritscher L (2002) Logistische Regression. (Lecture notes of the post diploma course in applied statistics 2001/2003, ETH Zurich)

Wainwright PC, Reilly SM (1994) Ecological Morphology, Integrative Organismal Biology. The University of Chigago Press, Chigago

Winkler H, Bock WJ (1976) Analyse der Kräfteverhältnisse bei Klettervögeln. J Ornithol 117: 397-418

Winkler H, Leisler B (1985) Morphological aspects of habitat selection in birds. In: Cody M (ed) Habitat Selection in Birds. Academic Press Inc, London. pp 415-434

Winkler H, Leisler B (1992) On the ecomorphology of migrants. Ibis 134: 21-28

Winkler H, Leisler B (1994) Ecomorphological patterns of adaptation and convergence in forest birds. J Ornithol 135: 472-473

Yuri T, Mindell DP (2002) Molecular phylogenetic analysis of Fringillidae, "New World nine-primaried oscines" (Aves: Passeriformes). Mol Phyl Evol 23: 229-243

Zani PA (2000) The comparative evolution of lizard claw and toe morphology and clinging performance. J Evol Biol 13: 316-325

Appendix

Mean ecological scores

The means of the ecological scores are calculated from the answers of the species experts. 0=never, 1=seldom, 2=often. A "li" stands for those species, for which the information stems from the literature (see text). The names of the species experts are given in the acknowledgements. na: missing values.

	needles	leaves	twigs	trunk	elsewhere	vertical	air	side ways	belly up	upside down	flutter hop	hover	flycatch	aerial hawk	beside	Below	expert(s)
Carduelis barbata	0.5	2	1.5	0	1.5	0.5	0	1.3	0.5	0	1	0	0	0	0.5	0	CV, WE
C. cabaret	2	2	2	0	1	2	1	2	2	2	1	0	0	0	2	2	li
C. cannab.	0	0	0	0	2	2	0	1	1	0	1	0	0	0	2	1	JD
C. card.	1	2	2	0	2	2	1	2	1	2	1	0	0	0	2	2	FK
C. chloris	0	0	2	0	1.5	1.5	1	0.3	0	0	2	0	0	0	0.5	0	KL, FK
C. pinus	2	1	1	0	1	2	1	1	2	2	1	1	1	1	2	2	li
C. spinus	2	2	2	0	0	2	1	2	1	2	1	1	0	0	2	2	JCS
C. tristis	0	0	2	0	1	1	1	2	1	1	2	0	0	0	1	0	FK
Dendroica caerulesc.	1	2	1.5	0.5	1	1	1	1	0.5	0	1	1.5	1.5	0.5	1.5	1	MAV RTH
D. castanea	1.5	1.5	1.5	0.5	1	1	1	1	1	0	1	1	1.5	1	1	0	BM, li
D. cerulea	0.5	2	1	0	0	2	1.5	1.5	0.5	0.5	2	0	2	0.5	2	0.5	TF, JJ
D. coronata	2	0	2	1	0	1	1	0	0	0	1	1	1	1	0	0	li
D. discolor	1	1	2	1	2	1	2	1	1	0	1	2	2	1	1	0	li
D. fusca	2	1	2	0	0.5	1.5	0.5	0	1	1	1	1	0	1	1.5	0	TF, FK, li
D. magnol.	2	1	2	0	0	1	1	1	0	1	1	1	1	1	1	0	FK, li
D. palmar.	1.5	1	2	0	2	0	2	1.5	0.5	0.5	1.5	0.5	1	0.5	1	0	WHW, li
D. pensylv.	1	2	1	0	0	1	0	1	0	0	1	0	0	0	1	0	BB
D. petechia	0	2	2	0	0	1	0.5	1.5	0	0	0.5	0	0.5	0	1	0.5	TF, GAL
D. pinus	2	1.5	2	0.5	0.5	1.5	0.5	2	2	2	1	1	2	1	1.5	1	TF
D. striata	1	2	1	0	0	1	0.5	0	0.5	0.5	1	0.5	1	0.5	1.5	0	CR, SL
D. tigrina	2	0	2	0	0	1	2	1	1	0	2	2	2	2	1	1	FK, li
D. virens	2	2	1	0	0	0.5	1	0.5	0.5	0	0.5	1.5	1	1	1	0.5	RS, MAV
Parula [1]ame.	1	2	2	1	na	1	na	1	1	1	2	1	1	0	1	1	JK
Parus ater	2	0	2	0	0	1.8	1.5	2	2	0.5	2	0	0.5	0.5	2	1.8	FK, PK
P. atricap.	1	1	2	0	0	1	1	1	1	1	1	1	0	0	1	1	FK
P. caerul.	0	1	2	1	0	2	1	2	1	1	1	0	0	0	2	1	FK
P. carolin.	0	1	2	1	1	1	1	1	1	1	1	1	1	1	1	1	li
P. cristatus	2	0.3	2	0.5	1.5	0.5	1	0.5	0.3	0	1.5	1.3	0.5	0	0.5	0.3	PK, FK
P. inornat.	1	1	2	1	1	1	1	1	1	1	1	1	1	1	1	1	li
P. major	0	0	2	0	1.5	1	0.5	1	0	0	1	0	0	0	1	0	FK, BT
P. montan.	1.5	0.5	1.5	0	0	2	1	1.5	1.5	1	1	1	0	0	1.5	1.5	WF, FK
P. palustris	0.8	0.8	2	0	1	1.3	0.5	0.8	0.5	0	0.8	0.3	0	0	0.8	0.5	FK, PK
P. rufonu.	1	0	2	1	2	1	1	1	0	0	1	1	1	1	1	0	li
Regulus cale.	2	2	2	0	1	2	2	1	1	1	2	2	2	2	1	1	li
R. ignicap.	1	1	2	0	0	2	2	2	1	1	2	2	1	1	1	1	FK
R. regulus	2	1	2	0	0	2	1	2	2	2	1	0	0	0	2	2	FK
R. satrapa	2	1.5	2	1	1	2	1	1	1.5	0	1	1	1	0	1	1	DS, li

[1] The genus *Parula* is genetically not separable from the genus *Dendroica* and therefore treated as *Dendroica* in this study (Lovette and Bermingham 2001).

14 Maximum-likelihood identification of fossils: taxonomic identification of Quaternary marmots (Rodentia, Mammalia) and identification of vertebral position in the pipesnake *Cylindrophis* (Serpentes, Reptilia)

P. David Polly[1] and Jason J. Head[1, 2]

[1]School of Biological Sciences, Queen Mary, University of London, London E1 4NS, UK, d.polly@qmul.ac.uk; [2]Department of Paleobiology, Smithsonian Institution, Washington D.C. 200013-37012, USA

14.1 Abstract

We applied a Maximum-Likelihood (ML) criterion to the problem of identifying unknown specimens using a database of specimens whose identity was known. Our approach was based on shape, quantified using two-dimensional Cartesian landmarks. We applied the technique to two specific problems: (1) identifying Quaternary marmot skulls (*Marmota*, Sciuridae, Rodentia) to species, and (2) identifying the position of individual elements within the vertebral column of the Red-tailed pipesnake, *Cylindrophis ruffus* (Serpentes, Alethinophidia). The ML criterion finds the best identity by choosing the sample that best fits the unknown. Cross-validation tests indicated that identifications of unknown marmots were correct about 80%-90% of the time. Fossil marmots from two sites (Meyer Cave, Illinois and Little Box Elder Cave, Wyoming) could be assigned to species (*M. monax* and *M. flaviventris* respectively), but marmots from several other localities could not be assigned to a species-level taxon. Snake vertebrae could be allocated to their proper columnar interval more than 80% of the time, with incorrect assignments rarely being more than 10% out of place. Our technique is widely applicable in palaeontology, where the problem of identifying isolated morphological elements can be acute but is often ignored. Our approach allows palaeontologists to base their identifications securely on their morphological data, and to recognize conditions under which a confident identification can or cannot be made.

Keywords: Maximum-likelihood, *Marmota*, *Cylindrophis*, classification, vertebrae, skull.

14.2 Introduction

The identification of palaeontological specimens can often be problematic, especially in the face of morphological variation. Whether the problem is assigning a specimen to a taxon or determining which anatomical element a specimen represents, identifications can be compromised by subjectivity and "small sample" typology. Consequently, assignments are often influenced by external, *a priori* considerations such as geographic and stratigraphic provenance. Many automatic identification methods are available, including neural networks, nearest neighbor classification, and linear discriminant analysis (Ripley 1994; Yang 2002; Behnke 2003). In this paper, we applied a maximum-likelihood (ML) criterion and landmark representations of shape to the problem of identifying unknown specimens using a database of specimens whose identity was known (Hastie and Tibshirani 1996). Our goal was to explore an objective method for identifying fossil materials, and to assess the extent to which the method was able to make accurate identifications.

We applied this approach to two problems. The first was species-level identification of fossil marmots based on their skulls. Marmots (woodchucks, Alpine marmots) have a geographic distribution that covers much of Holarctica (Hoffmann et al. 1997; Barash 1989; Steppan et al. 1999). Most living marmot species are adapted to either montane or steppe habitats and their ranges have been more restricted in interglacial warm periods (including today) than in cooler glacial periods. Consequently, fossil marmots are commonly recovered outside extant distributions, and the group has provided an important example of the effects of climatic change on the geographic ranges of mammals (Stearns 1942; Anteva 1954; de Villalta 1974; Frase and Hoffmann 1980; Graham et al. 1996; Kalthoff 1999). The well-documented geographic reorganization of marmot ranges makes the accurate identification of fossil remains imperative because incorrect assignments obscure patterns of environmentally driven geographic reorganization (Graham and Semken 1987; Polly 2003a). We built a database of skull shapes from the majority of species, including most North American subspecies. We characterized skull shape using landmarks on the ventral cranial surface, and applied an automated ML algorithm that identified unknown individuals against this database.

The second problem was the assignment of isolated snake vertebrae to a particular position in the vertebral column. We explored the possibility of using vertebral shape and ML matching to the problem of assigning isolated vertebrae to subregions of the precloacal vertebral column. The fossil record of snakes consists predominantly of isolated precloacal vertebrae. Because of this, the majority of taxonomic assignments for fossil snakes are based on (often subtle) variations in vertebral shape (e.g. Rage 1984;

Holman 2000). Progressive, quantified intracolumnar variation is well-documented for the vertebral column in snakes (e.g. Hoffstetter and Garyard 1965; Hoffstetter and Gasc 1969; Thireau 1967; LaDuke 1991; Polly et. al. 2001), however this variation is not accounted for in taxonomic assignments, with a few notable exceptions (Szyndlar 1984). In order to reconstruct alpha taxonomy in fossil snakes, taxonomic differences in vertebral shape must be distinguishable from intracolumnar variation. As a first step in separating taxonomy from regional position, we explored the possibility of using vertebral shape and ML matching to assign isolated vertebrae to subregions of the precloacal vertebral column for two snakes within a single species. To do this, we used landmarks to characterize the shape of all the precloacal vertebrae from a single individual. We divided the vertebral column into equal sections, using each section as a statistical sample representing that region, and applied the same ML algorithm to match vertebrae whose position was unknown to one of the regions.

Our approach used the variation in each known sample to estimate a multivariate probability distribution against which each unknown was compared, and is a simplified version of mixture discriminant analysis, or Gaussian ML classification (Hastie and Tibshirani 1996). Identifications were made by finding the sample into whose probability function the unknown best fit, or, put another way, by finding the known sample distribution that maximized the likelihood of the unknown shape. Because we used landmark representations of shape, the unknown was iteratively fit to each sample using Procrustes Generalized Least-Squares (GLS) superimposition, which minimizes the differences among the shapes via translation, scaling, and rotation (Rohlf 1990; Rohlf and Slice 1990). Probability distributions for each sample were estimated from the means and variances of each dimension of each superimposed landmark, and their joint distribution was used to compare the unknown specimen. In the interest of applying this procedure to small samples, we ignored issues of colinearity and covariance, and we discuss the ramifications of that decision. For simplicity, we have confined this study to examples where the unknown individuals are almost certain to have come from a group represented by the samples against which they are being compared. In many palaeontological studies, however, specimens may belong to a new taxon or may be an early member of an evolving lineage whose morphology is not perfectly coincident with living or previously studied fossil species (Polly 2002). We do not deal with this evolutionary problem here, but those attempting to apply our method should consider it carefully. A tree-based ML approach (e.g. Polly 2003a, b) may be preferable in cases where the unknown is not likely to literally be a member of sampled groups.

The application of Procrustes superimposition to problems of identification or classification is not new. Wang et al. (2003) applied Procrustes distance to identify human individuals based on their gait as measured from superimposed frames from films taken while walking. Numerous applications have also been made in the food industry, albeit with a considerably different use of Procrustes alignment (e.g. Muir et al. 1995; Sinesio et al. 2001; Le Fur et al. 2003). Statistical distributions of Procrustes residuals

(the many finer points of which we have sidestepped) have been elegantly described by Dryden and Mardia (1998) and references therein.

Abbreviations: FAMNH, Frick Collection, American Museum of Natural History; ***k***, number of Cartesian dimensions; **IMNH**, Idaho Museum of Natural History; **ISM**, Illinois State Museum; **ML**, maximum-likelihood; ***n***, number of landmarks (except where **N** is explicitly used in the text for numbers of individuals in a sample); **UCM**, University of Colorado-Boulder Natural History Museum; **UCMP**, University of California Museum of Paleontology; **USNM**, United States National Museum of Natural History.

14.3 Materials and methods

14.3.1 Marmots

Nineteen samples of living marmots were assembled to serve as points of comparison and to test the accuracy of identifications (Table 1). The samples represented nine of the fourteen living species, including all but one North American species. For the three major North American species (*M. caligata*, *M. flaviventris*, and *M. monax*) representative subspecies were included.

Living individuals or museum skin specimens can easily be assigned to their proper species. Skeletal or dental remains, such as those found in the fossil record, are much more difficult to classify, however. Diagnostic differences in the skull, including the breadth of the interorbital region, the shape of the postorbital processes, and the relative size of the upper fourth premolar, have been suggested (Howell 1915; Frase and Hoffman 1980), but these qualitative characteristics break down when large, geographically and subspecifically diverse samples are considered.

We applied the ML identification method to six Quaternary palaeontological samples (Table 2). These samples were selected because they included skulls that were sufficiently complete for quantitative comparison with extant material. Palaeontological material included specimens from Moonshiner Cave, Bingham Co., Idaho (White et al. 1984) housed in the Idaho Museum of Natural History; Bear Park Cave, Blaine Co., Idaho (Jefferson et al. 2002) housed in the Idaho Museum of Natural History; Little Box Elder Cave, Converse Co., Wyoming (Anderson 1968) housed in the University of Colorado-Boulder Museum of Natural History; Papago Springs, Santa Cruz Co., Arizona (Skinner 1942; Czaplewski et al. 1999a, b) housed in the American Museum of Natural History; Schlieper's Pit, Pike Co., Illinois housed in the Illinois State Museum; and Meyer Cave, Monroe Co., Illinois (Parmalee 1967) housed in the Illinois State Museum. All of these localities except Papago Springs fall within the cur-

rent geographic range of either *Marmota monax* (the Woodchuck) or *M. flaviventris* (the Yellow-bellied marmot).

Thirty four two-dimensional landmarks were chosen to represent the shape of the ventral side of the cranium (Fig. 1). Only one half of the skull was used so that fossil (or extant) specimens that were broken on one side could still be included. The landmarks were placed as follows: 1. Contact point between incisors; 2. Lateralmost point of the incisor alveolus; 3. Anteriormost point of the anterior palatine foramen; 4. Intersection of the maxillary-premaxillary suture and the palatine foramen; 5. Anteriormost point of the process below the infraorbital fissure; 6. Junction between the anterior zygoma with the lateral wall of the skull; 7. Palatalmost point on the root of the third premolar; 8. Palatalmost point on the root of the fourth premolar; 9. Palatalmost point on the root of the first molar; 10. Palatalmost point on the root of the second molar; 11. Palatalmost point on the root of the third molar; 12. Junction of the maxillary-palatine sutures and the midline; 13. Anteriormost point of the lesser palatine foramen; 14. Anteriormost point of the greater palatine foramen; 15. Posteriormost point of the palatine bones at the midline; 16. Anteriormost point of attachment of posterior superficial masseter on the the zygoma; 17. Posteriormost point of attachment of posterior superficial masseter on the zygoma; 19. Anteriormost point of attachment of the posterior deep masseter on the zygoma; 20. Posteriormost point of attachment of the posterior deep masseter on the zygoma; 21. Junction between posterior of the zygoma and the skull wall; 22. Anterior lacerate foramen; 23. Anterior point of interpterygoid foramen; 24. Boundary of the basisphenoidal-occipital suture and the medial wall of the auditory bulla; 25. Carotid canal; 26. Midpoint of opening to external auditory meatus; 27. Mastoid process; 28. Anteriormost point of the posterior lacerate foramen; 29. Paroccipital process; 30. Hypoglossal foramen; 31. Posteriormost point of the occipital condyle; 32; Anteriormost point of the foramen magnum; 33. Midline of the basisphenoidal-occipital suture; and 34. Midline of the presphenoidal-basisphenoidal suture. It is worth noting that several geometric morphometric studies of marmots have been published (Cardini 2003; Cardini and Tongiorgi 2003; Cardini et al. 2003; Polly 2003).

Table 1. Samples of living marmots whose identity was known. The individual subspecific samples belonging to the three North American species *Marmota caligata*, *M. flaviventris*, and *M. monax* were combined repectively into three larger species samples for final determinations. **ID** is the identifying number of each sample and **N** is the number of individuals

ID	Taxon	Locality	N
1	*M. broweri*	Brooks Range, Alaska, USA	6
2	*M. caligata caligata*	Becharof Lake, Alaska, USA	13
3	*M. caligata cascadensis*	Mt. Ranier, Washington, USA	6
4	*M. caligata nivaria*	Montana and Idaho, USA; Alberta, Canada	10
5	*M. caligata okanagana*	British Columbia, Canada	3
6	*M. caligata oxytona*	Alberta and British Columbia, Canada	8
7	*M. caudata*	N.W.F.P, Pakistan and Kashmir	28
8	*M. flaviventris engelhardti*	Utah, USA	7
9	*M. flaviventris flaviventris*	Donner Pass, California, USA	3
10	*M. flaviventris fortirostris*	White Inyo Mts., California, USA	13
11	*M. flaviventris luteola*	Colorado, USA	12
12	*M. flaviventris nosophora*	Idaho and Montana, USA	22
13	*M. himalayana*	China, Kashmir, and Sikkim	22
14	*M. marmota*	Switzerland	5
15	*M. monax canadensis*	Ontario, Canada	12
16	*M. monax monax*	Illinois, Indiana, and Virginia, USA	28
17	*M. monax rufescens*	Ontario, Canada	8
18	*M. sibirica*	Mongolia and Inner Mongolia, China	21
19	*M. vancouverensis*	Vancouver Island, Canada	7

Table 2. Fossil samples considered for identification. All localities except Papago Springs fall within the geographic range of an extant species of *Marmota*

Locality	Age	N	Extant Species Range
Moonshiner Cave, Idaho	Early Holocene	1	*M. flaviventris*
Bear Park Cave, Idaho	Holocene	2	*M. flaviventris*
Little Box Elder Cave, Wyoming	Late Glacial	1	*M. flaviventris*
Papago Springs, Arizona	Wisonsinan	1	None
Schliepers Pit, Illinois	Holocene	2	*M. monax*
Meyer Cave, Illinois	Lt. Pleist. / Holocene	5	*M. monax*

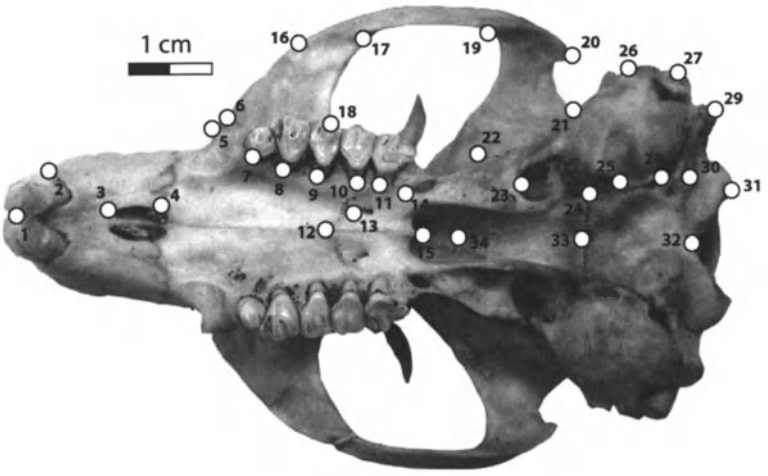

Figure 1. Ventral view of the skull of *Marmota flaviventris engelhardti* from the Colub Mountains, Utah (AMNH 140038) showing the position of the 34 landmarks used to represent skull shape

14.3.2 Snakes

Precloacal vertebrae from two individuals of the Red-tailed pipesnake, *Cylindrophis ruffus* were studied. *Cylindrophis* is an alethinophidian snake traditionally considered basal with respect to Macrostomata (e.g. Kluge 1991; Tchernov et al. 2000) although more recent analyses have reduced clarity of interrelationships (e.g. Slowinski and Lawson 2002). *Cylindrophis ruffus* is a fossorial and littoral taxon about 70 cm long from southeast Asia. We chose *Cylindrophis* because it is an "anilioid" (sensu Cundall

et al. 1993), a group with a long, widely dispersed fossil record (Rage 1984; Gardner and Cifelli 1998; Holman 2000). We considered two individual snakes. The order position of each bone was known in one specimen (USNM 523566), and vertebrae from that snake were used as identification samples. The order position was not known in the second specimen (UCMP 136995). Only precloacal vertebrae were considered because they are the most problematic in terms of positional identification, and constitute the majority of both the snake vertebral column and the fossil record. The first snake had 184 precloacal vertebrae, and the second had 187.

Vertebrae were photographed in anterior view and their shape represented by a series of 14 two-dimensional landmarks (Figure 2). As with the marmot dataset, only one side of each element was digitized because vertebrae are approximately bilaterally symmetrical. Landmarks were placed as follows: 1. midline base of the cotyle; 2. midline dorsal margin of coytle; 3. medialmost contact between vertebral centrum and neural arch; 4. midline dorsalmost point of neural canal; 5. midline dorsal margin of zygosphene; 6. dorsal margin of neural spine; 7. dorsolateralmost point of zygosphenal articular facet; 8. ventromedialmost point of zygosphenal articular facet; 9. medialmost point of prezygapophyseal articular facet; 10 lateralmost point prezygapophyseal articular facet; 11. lateralmost point of prezygapophyseal accessory process; 12. dorsal margin of synapophyseal articular surface; 13. ventral point of synapophyseal articular surface; 14, contact between synapophysis and vertebral centrum.

The vertebrae of the specimen where the order was known were partitioned into equal sized sections. Each section served as an identification sample, allowing unknown specimens to be allocated to a specific region of the precloacal column. No attempt was made to determine a more exact placement of unknowns. Two partitions were tried: one with 18 partitions containing ten vertebrae each, and the second with 10 partitions of eight vertebrae each.

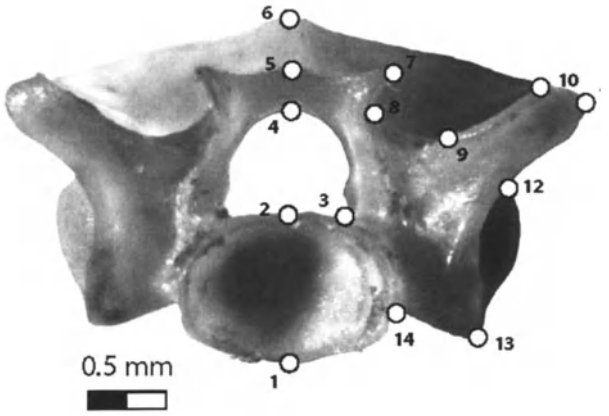

Figure 2. Anterior view of precloacal vertebra 120 from *Cylindrophis ruffus* (USNM 523566) showing the positions of the 14 landmarks used in this study

14.3.3 ML identification procedure

Each unknown specimen was iteratively superimposed with individual known samples and the likelihood calculated. Superimposition was achieved through Procrustes (GLS) analysis, consisting of translation, scaling to unit centroid size, and rotation. The mean (or consensus shape) was subtracted to yield Procrustes residuals. Normal distributions were fit using the mean (zero) and standard deviation of the residuals of the specimens of known identity, where the number of distributions equaled n landmarks * k dimensions.

Identification was treated as a maximum-likelihood (ML) problem. Normally ML is used to estimate distribution parameters from a set of observed data. In this case, the parameters were the mean and variance of the parent distribution (taxon, vertebral position) from which the unknown specimen was drawn, but instead of estimating these using a multi-individual sample and drawing from any possible mean and variance, the algorithm selected the mean and variance of the known sample that best explained the unknown individual. The identity of the best-fit sample was then assigned to the unknown.

The log likelihood of the unknown given a particular sample was calculated as

$$l(u) = \sum_{i=1}^{n*k} \log[f(u \mid s)] \qquad (13.1)$$

where $n*k$ was the number of landmarks times the number of dimensions and $f(u|s)$ was the probability of the unknown residual given the distribution of the known residuals. The latter was calculated from the density function of a normal curve fit to the mean and variance of each of the $n*k$ sets of residuals. Even though sample sizes differed (and were occasionally quite small) the normal distribution rather than the t-distribution is appropriate for ML fitting. The property of the t-distribution of increased spread with decreased sample size makes it inappropriate because the density curves for small samples would be disproportionately large, resulting in a biased referral of unknowns to them.

Our likelihood function disregards two important properties of Procrustes superimposed data, colinearity and covariance, both of which reduce the accuracy of identification. Our decision to disregard was made because these properties were nearly impossible to incorporate when the number of specimens in a sample is smaller than $n*k$, as is often the case for palaeontological studies. Because this study was aimed at practical use, we sacrifice power for wider applicability.

14.3.4 Cross-validation assessment

A "leave-one-out" cross-validation procedure (Hills 1966; Mosteller and Tukey 1968; Stone 1974) was used to assess the effectiveness of the algorithm. Each specimen was iteratively removed from its sample and treated as though its identity were unknown. Its identity was then estimated using the original samples (including its own n-1 parent sample). Cross-validation statistics were then calculated from the known and estimated identities.

For marmots, samples 1, 2, 7, 10, 11, 13, 14, 16, 18, and 19 (Table 1) were used in the cross-validation procedure. A second set of samples (3, 4, 5, 6, 8, 9, 12, 15, and 17), whose identities were known but whose subspecific identity differed from the identification samples, was also tested. Later, some of these were combined into three large samples representing three North American species (see below). For snakes, the 18 sections of ten vertebrae and 10 sections of 18 vertebrae were cross-validated.

Two cross-validation statistics were calculated: (1) the percentage of specimens that were classified correctly, and (2) the percentage of classifications that were correct. The complements of these statistics (the percentages of incorrect classifications) correspond to Type I and Type II error. The second of these is the most important for assessing the probability that an identification made by the algorithm is correct.

14.3.5 Identification of unknowns

The identities of true unknowns were then estimated using the ML procedure. Fossil marmot specimens (Table 2) were matched against the three large samples representing the most geographically widespread North American species. As will be shown below, the accuracy of identification was better with large samples. Individuals from the same parent species were combined to yield three large species samples: *Marmota flaviventris* ($N = 57$), *M. monax* ($N = 48$), and *M. caligata* ($N = 39$). These species currently have wide distributions and are the most likely to be represented in the fossil faunas considered here. For snakes, vertebrae from a disarticulated specimen of *Cylindrophis ruffus* (UCMP 136995) whose positions were not known were matched against the articulated specimen (USNM 523566) whose vertebral order was known. The known specimen was divided both into 18 sections of 10 vertebrae and 10 sections of 18 vertebrae.

14.4 Results

14.4.1 Marmots

The frequency with which marmot specimens were correctly identified was high at 76.0% (Table 3). The best results were obtained for *Marmota monax*, where 100% were correctly identified, while the worst results were for *M. marmota,* with 0%. The taxon to which a misidentified specimen was assigned was not usually the closest phylogenetic relation. Misidentification was related to sample size, however. When the size of the parent sample dropped below ten, the percentage of specimens that were correctly assigned to it dropped dramatically (Figure 3).

The frequency with which identifications were correct was better, with an average of 87.5% of assignments being correct (Table 3). All assignments to *M. broweri*, *M. caligata*, *M. flaviventris luteola*, and *M. vancouverensis* were correct. Conversely, *M. sibirica* assignments were frequently incorrect (42.4%) because specimens belonging to other groups were frequently assigned to *M. sibirica*, even though nearly all *M. sibirica* specimens were themselves correctly identified (90.5%). We presume that the high frequency of assignments to *M. sibirica* and *M. monax* (especially incorrect ones) was due to greater variation in these species, which would make the probability distributions at each landmark broader, thus encompassing variation in other species.

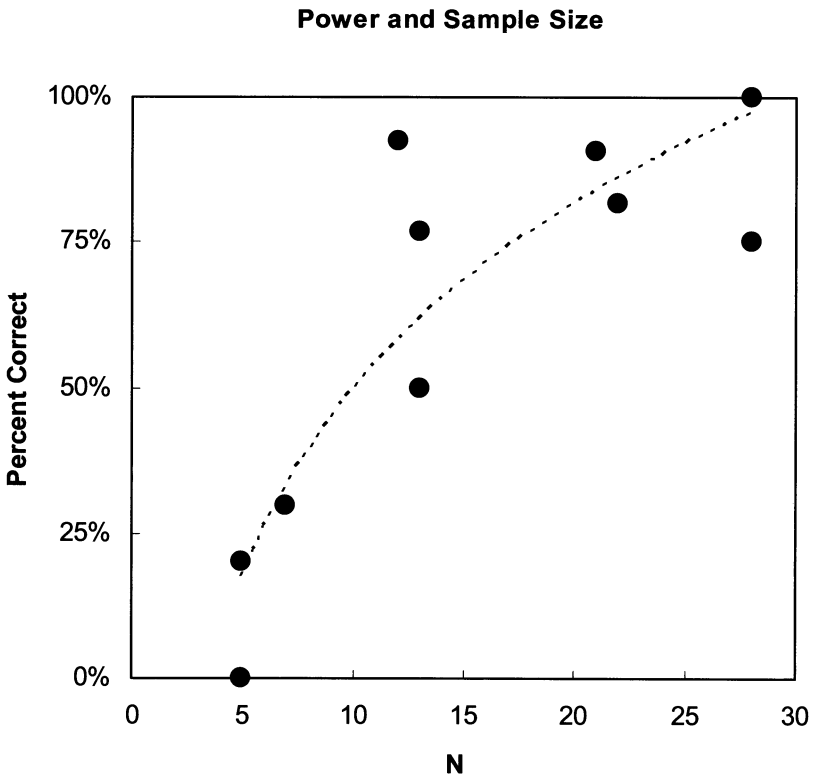

Figure 3. Graph showing relationship between the percentage of specimens correctly identified as a function of the size of the identification sample for that taxon

Results were similar when other subspecies were cross-validated against the original samples. Twenty individuals from subspecies of *M. monax* (*M. m. rufescens* and *M. m. canadensis*) and 32 from subspecies of *M. flaviventris* (*M. f. nosophora, M. f. engelhardti*, and *M. f. flaviventris*) were submitted to the identification procedure using the same identification samples as before. Results were similar in that 100% of the *M. monax* specimens were identified correctly, but only 57.1% of the *M. flaviventris* specimens were correctly assigned (Table 4). Of the 21 *M. flaviventris* that were misidentified, one was assigned to *M. caudata*, 10 to *M. sibirica*, and the remaining 11 to *M. monax*. Of the 10 identifications made as *M. flaviventris*, 100% were correct, while only 64.5% of the identifications as *M. monax* were right. We can thus be much more confident of an identification as *M. flaviventris* than as *M. monax*.

Table 3. Cross-validation statistics for the first set of extant marmots. The true identity columns report how often a specimen belonging to the group at the left was identified correctly. The estimated identy columns report how often a particular identification was correct

	True Identity		Estimated Identity	
	Correct	Incorrect	Correct	Incorrect
M. broweri	20.0%	80.0%	100.0%	0.0%
M. caligata	76.9%	23.1%	100.0%	0.0%
M. caudata	75.0%	25.0%	75.0%	25.0%
M. fl. fortirostris	50.0%	50.0%	85.7%	14.3%
M. fl. luteola	92.3%	7.7%	100%	0.0%
M. himalayana	81.8%	18.2%	66.7%	33.3%
M. marmota	0.0%	100.0%	--	--
M. monax	100.0%	0.0%	84.8%	15.2%
M. sibirica	90.5%	9.5%	57.6%	42.4%
M. vancouverensis	29.6%	70.4%	100%	0.0%

Because large samples make better identifiers, samples representing the three widespread North American samples were pooled for use with the fossil unknowns. These samples were also cross-validated to provide statistics for assessing fossil identifications. The numbers differed slightly, but the pattern of success was the same as the previous tests (Table 5). *M. flaviventris* assignments were correct 100% of the time, while *M. caligata* was correct 79.6%, and *M. monax* 88.2% of the time.

Fossil specimens could be confidently identified in a few, but not all cases. All five Meyer Cave specimens were identified as *M. monax*, the species that currently lives in the area. (Table 6) The cross-validation statistics (Table 5) suggest that the chance that all five specimens could be incorrectly assigned was improbable ($P = 2.3 \times 10^{-5}$). Results from the remaining localities were more problematic. The Schlieper's Pit are also like to be *M. monax*, although one of specimens was identified as *M. caligata* (Table 6). Like Meyer Cave, Schlieper's Pit lies within the current range of *M. marmota*, and the probability that the *M. caligata* identification is wrong is high ($P = 0.204$). The probability that the *M. monax* classification is wrong is lower ($P = 0.118$), making it the best identification. The Little Box Elder Cave was assigned to *M. flaviventris*, which is the species that currently inhabits that area. The frequency with which *M. flaviventris* attributions were correct was 100% (Table 5).

Table 4. Cross-validation statistics for other subspecies samples. The true identity columns report how often a specimen belonging to the species at the left was identified correctly. The estimated identy columns report how often a particular identification was correct

	True Identity		Estimated Identity	
	Correct	Incorrect	Correct	Incorrect
M. monax	100.0%	0.0%	64.5%	35.5%
M. flaviventris	32.2%	67.8%	100.0%	0.0%
M. caudata	--	--	0%	100.0%
M. sibirica	--	--	0%	100.0%

Table 5. Cross-validation statistics for combined North American species samples. The percentage correct for the estimated identities (column 3) was used a measure of confidence for the fossil identifications

	True Identity		Estimated Identity	
	Correct	Incorrect	Correct	Incorrect
M. caligata	100.0%	0.0%	79.6%	20.4%
M. flaviventris	77.2%	22.8%	100.0%	0.0%
M. monax	93.8%	6.2%	88.2%	11.8%

Marmots from the remaining localities could not be confidently identified. The two Bear Park Cave marmots were assigned to *M. caligata* and *M. monax*, neither of which currently lives in the area, which is currently inhabited by *M. flaviventris*. *M. caligata* lives about 100 to 150 km north and *M. monax* has a range that extends into northern Idaho, with the nearest populations about 500 km away. The locality is Holocene in age, but geographic range shifts on the order of 100s of kilometers could easily have occurred within that time. In fact, the presence of two different species at the site is plausible. Cross-validation was not high enough to be conclusive, with 20.4% of *M. caligata* assignments and 11.8% of *M. monax* assignments likely to be incorrect.

Table 6. Identifications of individual fossil specimens. The log likelihood statistic for each match is also reported

Specimen No.	Locality	Estimated Identity	Ln Likelihood
IMNH 21589	Moonshiner Cave, Idaho	*M. caligata*	71.71
IMNH 38025	Bear Park Cave, Idaho	*M. caligata*	74.84
IMNH 38027	Bear Park Cave, Idaho	*M. monax*	73.65
UCM 23606	Little Box Elder Cave, Wyoming	*M. flaviventris*	68.75
FAMNH 42828	Papago Springs, Arizona	*M. caligata*	63.22
ISM 491788	Schliepers Pit, Illinois (surface)	*M. monax*	57.77
ISM 491778	Schliepers Pit, Illinois (surface)	*M. caligata*	68.75
ISM Unnumb.	Meyer Cave, Missouri	*M. monax*	63.13
ISM Unnumb.	Meyer Cave, Missouri	*M. monax*	63.54
ISM Unnumb.	Meyer Cave, Missouri	*M. monax*	70.81
ISM Unnumb.	Meyer Cave, Missouri	*M. monax*	68.45
ISM Unnumb.	Meyer Cave, Missouri	*M. monax*	63.56

The Moonshiner Cave and Papago Springs marmots were also ambiguous. The one available specimen from Moonshiner was referred to *M. caligata* , although the site now lies within the range of *M. flaviventris*. As with Bear Park, Moonshiner Cave lies within a few hundred kilometers from populations of *M. monax* and *M. caligata* so the presence of any of the three species during the Early Holocene is plausible. The Papago Springs specimen was also referred to *M. caligata*, with the same caveat that there is more than 1 in 5 chance that the identification is wrong. If the true identity were nearby *M. flaviventris*, as has been suggested in previous literature, there would be a 22.8% chance that the identification was incorrect, and then a 46% chance that the misidentification was *M. caligata.*

14.4.2 Snakes

Cross-validation statistics for assigning individual vertebrae to one of 18 sections were good, with 66.1% of vertebrae were assigned to their correct region (Table 7). Of those that were incorrectly assigned, 88.5% were assigned to the section immediately adjacent the true one, and an additional 11.5% were only two sections away. The probability of correct identification was not randomly distributed however. Both the first and last sections had 100% of their vertebrae correctly identified. In both sections, misidentifications are limited to middle sections, whereas in mid-regions misidentification can be made both anteriorly and posteriorly, increasing the chance of a wrong assignment. Consequently, the percentage correct was lower for middle sections. The

greatest percentage of incorrect assignments was also in the middle region (73% for section 7 and 69% for section 9). The ends of the region had low percentages of incorrect assignments, although the lowest was section 5 (10%).

Results were better when the number of sections was decreased to 10 and the bin size increased to 18 (Table 8). With this arrangement 81.7% of vertebrae were correctly assigned. Of those incorrectly assigned, 94% were assigned to a section immediately adjacent and the remaining 6% were only two sections away.

Table 7. Cross-validation statistics for the placment of individual precloacal vertabrae of *Cylindrophis ruffus* (USNM 523566) to one of 18 sections of the precloacal column with bin size of 10. Overall success rate was 61% of vertebrae correctly assigned to position

	True Identity		Estimated Identity	
Section	Correct	Incorrect	Correct	Incorrect
1	100%	0%	83%	17%
2	70%	30%	78%	22%
3	60%	40%	75%	25%
4	80%	20%	80%	20%
5	90%	10%	90%	10%
6	60%	40%	67%	33%
7	30%	70%	27%	73%
8	40%	60%	57%	43%
9	40%	60%	31%	69%
10	50%	50%	63%	38%
11	80%	20%	57%	43%
12	30%	70%	60%	40%
13	70%	30%	54%	46%
14	80%	20%	57%	43%
15	60%	40%	86%	14%
16	80%	20%	80%	20%
17	70%	30%	88%	13%
18	100%	0%	83%	17%

Vertebrae from a second individual were identified using the sections from the first, first dividing the trunk into eighteen sections with bin size of 10 and then into ten sections with bin size of 18. When the more numerous but smaller bins were used, the results were disappointing (Figure 4a). The majority of assignments were made to the 5th section (69.5%), with the second most to the fourth (15.0%). The remaining 15% of

assignments were scattered fairly evenly across sections 6 to 18. The expectation was that 5.5% of vertebrae should have been assigned to each section. The preponderance of assignments to sections 4 and 5 was most likely the result of greater shape variance in this region, which attracted the ML function. Results using ten sections with bin size of eighteen were much better (Figure 4b). Some assignments were made to each section, with the most to section 7 (21.9%) and the least to section 1 (3.7%). The expectation was 10% of the vertebrae assigned to each section, and these results agree well with that. These results and those presented in Table 8 suggest that the position of precloacal vertebrae can be assigned to the nearest 10% of the vertebral column with a high degree of confidence. Thus, intracolumnar variation in snake vertebral morphology can be recognized and accounted for prior to taxonomic assignments.

Table 8. Cross-validation statistics for placement of individual vertebrae to one of 10 sections with bin size of 18. Overall succes rate was 82% of vertebrae correctly assigned

	True Identity		Estimated Identity	
Section	Correct	Incorrect	Correct	Incorrect
1	100.0%	0.0%	35.7%	64.3%
2	50.0%	50.0%	90.0%	10.0%
3	83.3%	16.7%	78.9%	21.1%
4	72.2%	27.8%	86.7%	13.3%
5	66.7%	33.3%	80.0%	20.0%
6	88.9%	11.1%	76.2%	23.8%
7	88.9%	11.1%	88.9%	11.1%
8	88.9%	11.1%	84.2%	15.8%
9	83.3%	16.7%	88.2%	11.8%
10	94.4%	5.6%	94.4%	5.6%

14.5 Discussion

The identification procedure used in this study took two important mathematical shortcuts in the interests of applicability to palaeontological samples. The pros and cons of adopting our procedure are worth discussing. In both cases, our decision to cut corners was to accommodate small sample sizes of the sort that palaeontologists normally have.

Our first shortcut was to ignore colinearity in the Procrustes residuals. Procrustes, or generalized least-squares (GLS) superimposition, removes variation due to scale,

translation, and rotation, and, consequently, introduces colinearity, or redundancy, into the resulting shape variables (Gower 1975; Dryden and Mardia 1998; Rohlf 1999). In practical terms, that means that there were fewer informative variables than there were Procrustes residuals; however, our likelihood function was summed over all $n*k$ residuals. Despite its inelegance, this decision did not affect the results because the redundancy was the same for each of the identification samples and no bias was introduced.

The second shortcut was to ignore covariance among the Procrustes residuals, a decision with potentially detrimental effects. The covariance of two variables affects their joint probability distribution, but our ML did not take this into account. Figure 5 illustrates the effect of covariance on a joint probability distribution using a simple bivariate example. The ellipses represent 95% confidence intervals (CI) associated with the data. The solid ellipse is the true bivariate CI based on the variances and covariances of the data. In theory it encompasses 95% of the population and represents the probability boundary that would be used to statistically assess sample membership (*i.e.,* Z-test with α=0.05). The dashed ellipse represents the 95% CI of a probability distribution that has x and y variances equal to those of the data, but with no covariance. While the areas encompassed by the two are equal, their shape and orientation in the variable space are different. Two "unknowns" are represented by stars. The first would fall outside the statistical definition of the sample, but the second falls within it. When covariances are not used in estimating the CI, then the first unknown falls within the boundary, but the second is excluded. Consequently, both Type I and Type II errors increase when covariances are ignored.

Our ML algorithm did not take into account covariances, so suffers from the consequent loss of power. The probability density curves we used were estimated from the mean and variance of each set of Procrustes residuals as though each varied independently. Despite that, the cross-validation statistics were surprisingly high, even though they were not always high enough to make confident identifications of individual fossil samples in the case of the marmot skulls.

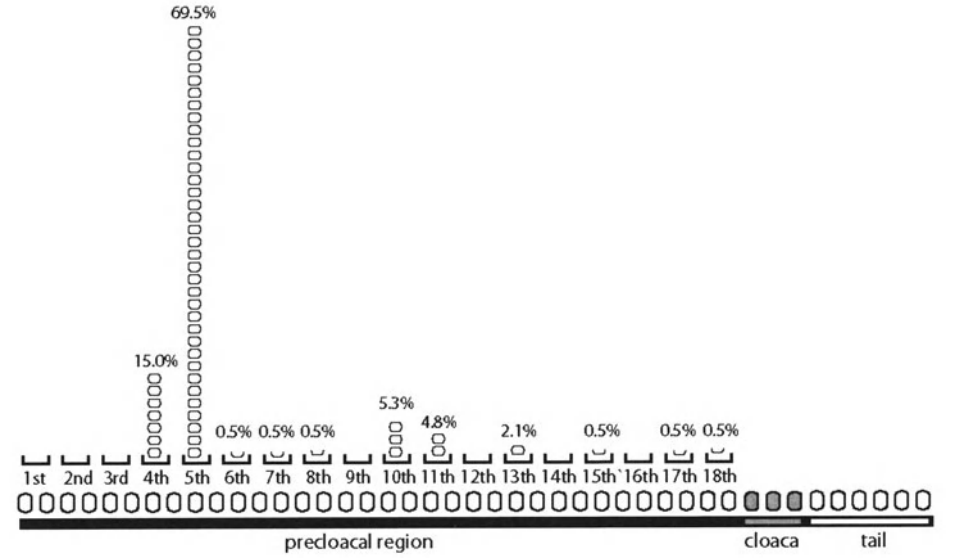

Figure 4. Results of identification of unknown vertebrae of a single individual of *Cylindrophis ruffus* (UCMP 136995) using sections from another single individual of the same species (USNM 523566). The assignments are graphically represented as bins in the precloacal region of a snake. **A.** Eighteen sections with bin size of 10. Most of the unknown vertebrae were placed in the fifth section (69.5%). None were placed in the first three sections, and only a few in the last sections. **B.** Ten sections with bin size of 18. Identifications were much more plausibly distributed across the length of the precloacal region

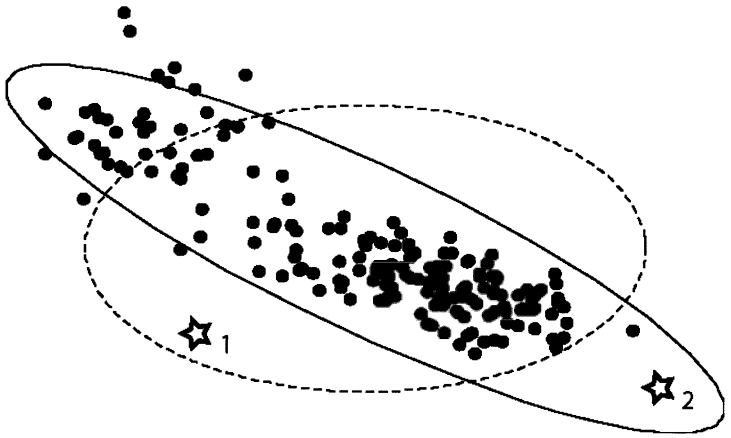

Figure 5. The effect of ignoring covariances on ML identifications. These bivariate data (black points) have a strong covariance and their 95% confidence ellipse (solid line) is aligned along their major axis. If a probability distribution were estimated individually from the x and y traits without consideration of their covariance, the 95% ellipse would have a different shape and orientation (dashed line). Conclusions about the identity of two unknowns (stars) would depend on whether covariances were incorporated. When they are, 1 falls outside the 95% confidence interval, but 2 within it. The reverse is true when covariances are ignored. The effect of ignoring covariances is reduced identifying power

Both colinearity and covariance could have been removed from our data by rotating them to their principal component axes using Singular Value Decomposition (SVD). SVD identifies a reduced number of orthogonal, or uncorrelated, axes for colinear data. However, the number of axes is limited by the number of individuals in a sample when the latter is smaller than the number of non-redundant variables. That was the case in this study. When complicated morphology, such as vertebrae or skulls, is studied from palaeontological or recent museum samples the number of landmarks times the number of dimensions will often exceed the number of individuals in a sample. In this study 28 landmarks (56 variables) were used to represent marmot skull shape, and 14 landmarks (28 variables) for snake vertebrae. Only one marmot sample (the combined *M. flaviventris* sample) and no snake samples were large enough to overcome this issue. Had the data been projected onto their principal components, then the number of variables would have been different for each sample, equal to the number of individuals in it. The ML statistic, which is summed over all variables in the sample, would not have been comparable among samples.

14.6 Conclusions

Quantitative methods for assessing fossil samples should be a high priority for palaeontologists. We often accept weak evidence for assigning newly collected specimens to species-level taxa or for identifying the type of element represented by a specimen in cases where many similar elements make up the fossilizable parts of an organism (e.g. vertebrae, leaves, teeth, echinoid plates, etc.). The non-morphological logic that we adopt in reaching decisions about identity can often compromise the interpretations that we draw from the faunal data. For example, the marmots from Papago Springs have been presumed to be *Marmota flaviventris* (Skinner 1942; Frase and Hoffmann 1980; Czaplewski et al. 1999a, b) because of the close proximity of the site to the current geographic range of that species. However, important conclusions about shifting geographic ranges of mammal species in relation to climate have been drawn from the occurrence of marmots at Papago Springs (Stearns 1942; Anteva 1954; de Villalta 1974; Frase and Hoffmann 1980). Given that range shifts are known to have occurred, some of them quite dramatic, why might the marmots from Papago Springs not belong to a more geographically distant species, such as *M. caligata*, as weakly suggested by our results? Similarly, the majority of identifications of fossil snakes have incorporated geographic provenance in generic- and species-level assignments of vertebral remains. The subsequent uses of geographically-derived assignments as evidence in paleoclimatic and biogeographic reconstructions (e.g. Holman 1995) is fundamentally circular and ultimately untestable (Bell et al. in press). Our understanding of the extent to which geographic reoganization, migration, and environmental response hinges on the ability to make morphology-based taxonomic assignments. A quantitative, statistical, morphological approach will give the most scientifically reliable results.

When only single specimens are available, the possibility of reliable identifications may remain remote, even when quantitative procedures are adopted. We found that individual skull specimens could be accurately classified 80%-100% of the time when a large identification sample was available. But even that level of accuracy was not always enough to confidently identify an individual fossil specimen. Even a 10% error rate is enough to undermine confidence when several different species could have plausibly been present at a locality. For example, if ten or more skull specimens been available from Papago Springs, we would have been able to confidently assess their collective species identity, but with only a single individual, the only viable conclusion was that the species identity was uncertain. Similarly, analysis of a larger sample of *Cylindrophis*, accounting for ontogenetic variation and sexual dimorphism will provide greater explanatory power for the abilities and limitiations for these methods in recognizing regional variation in the vertebral column of snakes.

14.7 Acknowledgements

Our thanks go to Dr. Ashraf Elewa for inviting this contribution and for his help in editing. Christopher Bell (University of Texas at Austin), Chris Conroy (Museum of Vertebrate Zoology), Denny Diveley (American Museum of Natural History), Judith Eger (Royal Ontario Museum), Robert D. Fisher (National Museum of Natural History), Linda Gordon (National Museum of Natural History), Frederick Grady (National Museum of Natural History), Russ Graham (Denver Museum of Natural History), Robert Hoffmann (National Museum of Natural History), Sharon Jansa (Bell Museum, University of Minnesota), Paula Jenkins (The Natural History Museum, London), Larry Martin (University of Kansas), Colin McCarthy (The Natural History Museum, London), Meng Jin (American Museum of Natural History), Gary S. Morgan (New Mexico Museum of Natural History), Chris Norris (American Museum of Natural History), James L. Patton (Museum of Vertebrate Zoology), Kevin Seymour (Royal Ontario Museum), Norm Slade (University of Kansas), George Stanley (University of Montana), Jessica M. Theodor (Illinois State Museum), Mary E. Thompson (Idaho Museum of Natural History), Peter Robinson (University of Colorado), Richard W. Thorington, Jr. (National Museum of Natural History), and George Zug (National Museum of Natural History) provided access to, and information about, specimens in their care. Anna Kay Behrensmeyer (National Museum of Natural History) and Chris Bell (University of Texas at Austin) provided facilities for image processesing. This work was supported by a grant from the UK Natural Environment Research Council (NERC GR3/12996) to PDP and a Nation Science Foundation Bioinformatics Postdoctoral Fellowship (NSF 98-162, award number 0204082) to JJH.

References

Anderson E (1968) Fauna of the Little Box Elder Cave, Converse County, Wyoming: the Carnivora. University of Colorado Studies, Series in Earth Sciences 6:1-59

Anteva E (1954) Climate of New Mexico during the last glaciopluvial. Journal of Geology 62:182-191

Barash DP (1989) Marmots: social behavior and ecology. Stanford University Press, Stanford

Behnke S (2003) Heirarchical neural networks for image interpretation. Springer, New York

Bell CJ, Head JJ, Mead JI (in press) Synopsis of the herpetofauna from Porcupine Cave, Colorado. Chapter in Biodiversity Response to Environmental Change in the Middle Pleistocene. In: Barnosky AD (ed) The Porcupine Cave Fauna from Colorado. University of California Press, Berkeley

Cardini A (2003) The geometry of the marmot (Rodentia : Sciuridae) mandible: Phylogeny and patterns of morphological evolution. Syst Biol 52:186-205

Cardini A, Tongiorgi P (2003) Yellow-bellied marmots 'in the shape space': sexual dimorphism, growth, and allometry of the mandible. Zoomorphology 122: 11-23

Cardini A, Tongiorgi P, Sala L, O'Higgins P (2003) Skull form and evolution in Marmota (Rodentia, Sciuridae). In: Ramousse R, Allaine D, Le Berre M (eds) Proceedings of the IV Marmot World Conference. International Network on Marmots, Lyon, pp. 67-72

Cundall D, Wallach V, Rossman DA (1993) The systematic relationships of the snake genus Anomochilus. Zoological Journal of the Linnean Society, 109:275-299

Czaplewski NJ, Peachey WD, Mead JI, Ku TL, Bell CJ (1999a) Papago Springs Cave revisited, Part I; Geologic setting, cave deposits, and radiometric dates. Occasional Papers of the Oklahoma Museum of Natural History 3:1-25

Czaplewski NJ, Mead JI, Bell CJ, Peachey WD, Ku TL (1999b) Papago Springs Cave revisited, Part II: Vertebrate paleofauna. Occasional Papers of the Oklahoma Museum of Natural History 5:1-41

de Villalta JF (1974) Presencia de la marmota y otros elementos de la fauna estépica en la pleistoceno catalán. Speleon [Barcelona] 21:119-124

Dryden IL, Mardia KV (1998) Statistical Shape Analysis. John Wiley & Sons, Chichester, England.

Frase BA, Hoffmann RS (1980) Marmota flaviventris. Mammalian Species 135:1-8

Gardner JD, Cifelli RL (1998) A primitive snake from the Cretaceous of Utah. In Unwin DM (ed). Cretaceous Fossil Vertebrates. Special Papers in Palaeontology 60: 87-100

Gower JC (1975) Generalized Procrustes analysis. Psychometrika 40:33-51

Graham RW, et al. (1996) Spatial response of mammals to late Quaternary environmental fluctuations. Science 272:1601-1606

Graham RW, Semken HA (1987) Philosophy and procedures for paleoenvironmnetal studies of Quaternary mammalian faunas. In: Graham RW, Semken HA, Graham MA (eds.) Late Quaternary Mammalian Biogeography and Environments of the Great Plains and Prairies. Illinois State Museum: Springfield, Ill., pp. 1-17

Greene HW (1997) Snakes: the Evolution of Mystery in Nature. University of California Press, Berkeley

Hastie T, Tibshirani R (1996) Discriminant analysis by Gaussian mixtures. Journal of the Royal Statistical Society B, 58: 155-176

Hills M (1966) Allocation rules and their error rates. Journal of the Royal Statistical Society B, 28: 1-31

Hoffmann RS, Koeppl JW, Nadler CF (1979) The relationships of the amphiberingian marmots (Mammalia: Sciuridae). Occasional Papers of the Museum of Natural History, University of Kansas 83:1-56

Hoffstetter R, Garyard Y (1965) Observations sur l'osteologie et la classification des Acrochordidae (Serpentes). Bulletin du Muséum National d'Historie Naturelle, 36:677-696

Hoffstetter R, Gasc J-P (1969) Vertebrae and ribs of modern reptiles., In: Gans C (ed) Biology of the Reptilia, Volume 1 (Morphology): 201-310. Academic Press, London

Holman JA (1995) Pleistocene Amphibians and Reptiles in North America. Oxford Monographs on Geology and Geophysics 32. Oxford University Press, New York

Holman, JA (2000) Fossil snakes of North America. Origin, evolution, distribution, paleoecology. Indiana University Press, Indianapolis

Howell AH (1915) Revision of the American marmots. North American Fauna, 37: 1-80

Jefferson GT, McDonald HG, Akersten WA, Miller SJ (2002) Catalogue of Late Pleistocene and Holocene fossil vertebrates from Idaho. Idaho Museum of Natural History Occasional Paper 37:157-192

Kalthoff DC (1999) Ist Marmota primigenia (Kaup) eine eigenständige Art ? Osteologische Variabilität pleistozäner Marmota-Populationen (Rodentia: Sciuridae) im Neuwieder Becken (Rheinland-Pfalz, Deutschland) und benachbarter Gebiete. Kaupia 9:127-186

Kluge AG (1991) Boine snake phylogeny and research cycles. Miscellaneous Publications of the Museum of Zoology, University of Michigan 178:1-58

Kretzoi M (1954) Marmot remains from Debrecen. Földtani Közlöny 84:75-77

LaDuke TC (1991). Morphometric variability of the precaudal vertebrae of Thamnophis sirtalis sirtalis (Serpentes: Colubridae), and implications for interpretation of the fossil record. Ph.D. dissertation, City University of New York

Le Fur Y, Mercurio V, Moio, L, Blanquet J, Meunier JM (2003) A new approach to examine the relationships between sensory and gas chromatography-olfactometry data using generalized procrustes analysis applied to six French chardonnay wines. Journal of Agricultural and Food Chemistry 51:443-452

Mosteller F, Tukey JW (1968) Data analysis, including statistics. In: Lindzey G, Aronson E (eds) Handbook of Social Psychology Vol. 2. Addison Wesley

Muir DD, Hunter EA, Banks JM, Horne DS (1995) Sensory properties of hard cheese – identification of key attributes. International Dairy Journal 5:157-177

Parmalee PW (1967) A recent cave bone deposit in southwestern Illinois. Bulletin of the National Speleological Society 29:119-147

Polly PD (2002) Phylogenetic tests for differences in shape and the importance of divergence times: Eldredge's enigma explored. In: MacLeod N, P. Forey (eds) Morphology, Shape, and Phylogenetics, Taylor and Francis, Inc., pp. 220-246

Polly PD (2003a) Paleophylogeography: the tempo of geographic differentiation in marmots (Marmota). Journal of Mammalogy 84:278-294

Polly PD (2003b) Paleophylogeography of Sorex araneus: molar shape as a morphological marker for fossil shrews. Mammalia 68:233-243

Polly PD, Head JJ, Cohn MJ (2001) Testing modularity and dissociation: the evolution of regional proportions in snakes (Serpentes, Vertebrata). In: Zelditch M (ed) Beyond Heterochrony: The Evolution of Development. pp. 305-335, John Wiley & Sons, New York, NY

Rage J-C (1984) Encyclopedia of Paleoherpetology, part 11, Serpentes. Gustav Fischer Verlag, Stuttgart

Ripley BD (1994) Neural networks and related methods for classification. Journal of the Royal Statistical Society B, 56: 409-456

Rohlf FJ (1999) Shape statistics: Procrustes superimpositions and tangent spaces. Journal of Classification 16:197-223

Sinesio F, Guerrero L, Romero A, Moneta E, Lombard JC (2001) Sensory evaluation of walnut: an interlaboratory study. Food Science and Technology International 7:37-47

Skinner MF (1942) The fauna of Papago Springs Cave, Arizona. Bulletin of the American Museum of Natural History 80:143-220

Slowinski JB, Lawson R (2002) Snake phylogeny: evidence from nuclear and mitochondrial genes. Molecular Phylogeny and Evolution, 24:194-202

Stearns CE (1942) A fossil marmot from New Mexico and its climatic significance. American Journal of Science 240:867-878

Steppan SJ, Akhverdyan MR, Lyapunova EA, Fraser DG, Vorontsov NV, Hoffmann RS, Braun MJ (1999) Molecular phylogeny of the marmots (Rodentia: Sciuridae): tests of evolutionary and biogeographic hypotheses. Syst. Biol. 48:715-734

Stone M (1974) Cross-validatory choice and assessment of statistical predictions. Journal of the Royal Statistical Society B, 36: 111-147

Szyndlar, Z. 1984. Fossil snakes from Poland. Acta Zoologica Cracoviensia, 28:1-156

Tchernov E, Rieppel O, Zaher H, Polcyn MJ, Jacobs LL (2000) A fossil snake with limbs. Science 287:2010-2012

Thireau M (1967) Contribution a l'etude de la morphologie caudale et de l'anatomie vertebrale et costale des genres Atheris, Atractaspis, et Causus (Viperides de l'Ouest african). Bulletin du Museum Nationale Historie Naturalle, Paris, (2):454-470

Wang L, Tan TN, Hu WM, Ning HZ (2003) Automatic gait recognition based on statistical shape analysis. IEEE Transactions on Image Processing 12:1120-1131

White JA, McDonald HG, Anderson E, Soiset JM (1984) Lava blisters as carnivore traps. Carnegie Museum of Natural History Special Publication 8:241-256

Yang T (2002) Cellular networks and image processing. Nova Science Publishers, Huntington, NY

15 Geometric morphometrics of the upper antemolar row configuration in the brown-toothed shrews of the genus *Sorex* (Mammalia)

Igor Y. Pavlinov

Zoological Museum, Moscow M.V.Lomonosov State University, 125009 Moscow, Bol'shaya Nikitskaya Str. 6, igor_pavlinov@zmmu.msu.ru

15.1 Abstract

Under brief consideration is geometric morphometric analysis of the shape of anterior part of the upper toothrow including incisive, antemolars and 1st molariform in several species of the shrew genus *Sorex* (Mammalia: Soricidae). 12 landmarks were used to describe configuration of the toothrow, and thin-plate spline and Procrustes analyses were applied to reveal species differences. It is shown a possibility for variation of the antemolar row configuration among (and possibly within) shrew species to be studied strictly numerically by means of the geometric morphometrics. It is recommended that tooth base be included in the descriptions of the shape of anterior part of the upper toothrow if differences by overall configuration are to be revealed.

Key words: *Sorex*, brown-toothed shrews, antemolar variation, geometric morphometrics.

15.2 Introduction

Relative height of antemolars, or unicuspids, is of taxonomic importance in the brown-toothed shrews of the genus *Sorex* (Mammalia). This feature allows to discriminate species inhabitating the same geographic area, and it is important in recognizing subspecies in some instances (e.g. Dolgov 1968).

The upper antemolars are 5 small unicuspid teeth situated in the maxillar toothrow between enlarged incisive anteriorly and 1st molariform posteriorly (Fig. 1, *a*). Individual antemolars are usually identified by enumeration from the most anterior to the most posterior one. They differ in their height, the first two or three of them being the largest and the 5th one being the smallest. These differences are

traditionally described in various ways, a common pattern of these description being the estimation of the antemolar heights relative to each other, provided that a baseline is being fixed parallel to horizontal axis of the skull.

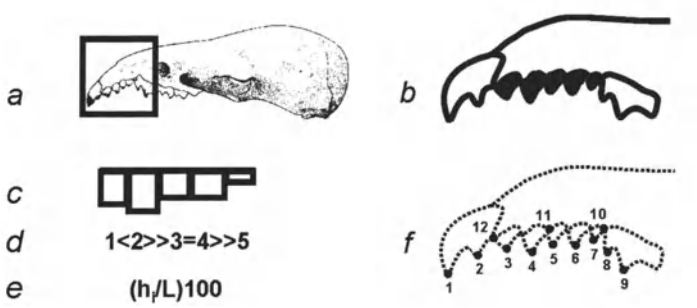

Fig. 1. Antemolars of the brown-toothed shrews and their descriptions: ***a***– position of the antemolar row on the shrew skull (shown by quadrate), ***b***– the anterior portion of the toothrow from incisive to molariform, antemolars shown by dark; descriptions of the antemolars by: ***c***– a "palisade", ***d***– an "antemolar formula", ***e***– indices, and ***f***– landmarks

The most simple way is direct observation of antemolar row drawing (Fig. 1, *b*; Dolgov 1968). Its specific, more formalized representation is a kind of "palisade" in which each tooth is indicated by a "picket" with its relative height equivalent to the one of corresponding tooth (Dolgov in lit.; Fig. 1, *c*). Such a drawing or a pictogram with specific combination of tooth heights is interpreted as a morphotype, and samples can be compared numerically by calculated morphotype frequencies in population studies.

In taxonomic diagnoses and identification keys, so called "antemolar formula" is applied in which algebraic symbols are used to show relative height of adjoining teeth denoted by respective numbers (Pavlinov et al. 2002). For instance, the formula "1<2>>3=4>>5" (Fig. 1, *d*) indicates that the 1st tooth is lower than the 2d, the 2d is significantly higher than the 3d, the 2d is as high as the 4th, and the 4th is much higher than the 5th.

A more laborious and hence less popular approach is based on measuring height of each tooth in the antemolar row and calculating of respective indices using antemolar row length as a common denominator (Viktorov and Kuzyakin 1974; Fig. 1, *e*). Such indices can be used as quantitative traits in statistical comparisons of populations and species.

It is evident that the first two methods of expression of antemolar proportions are based on semi-qualitative evaluation of the tooth heights and so they are not especially precise. Only the last method is strictly numerical; however, it provides estimation of relative height of each tooth separately and of configuration of the entire toothrow. Thus, none of the above approaches to analysis of antemolar proportions in the shrews is both strictly numerical and exhaustive.

There is a strictly numerical approach to analysis of shape transformations of morphological objects known as geometric morphometrics (GM) (Bookstein 1991; Rohlf 1993). It is based on the description of morphological objects by a set of landmarks placed at certain points. In our particular case, these landmarks could be placed rather precisely at tips of antemolars, and their configuration free of reference to any baseline makes the total antemolar row the shape in the GM sense. It makes GM a promising approach to study variation of the antemolar proportions among brown-toothed shrews.

Very preliminary results of a pilot project of exploration of variation of upper antemolar proportions in the genus *Sorex* by means of GM methods are presented here. The main task of the present publication is to show basical possibilities of GM in such kind of investigations.

Dental nomenclature for the shrews is adopted mainly after Dannelid (1998), his "1st molariform" being named here just "molariform" for sake of convenience.

15.3 Materials and methods

The following 8 species of the brown-toothed shrews of the genus *Sorex* are included in the study sample (with number of specimens indicated parenthetically): *S. araneus* (9), *S. buchariensis* (5), *S. caecutiens* (10), *S. camtschaticus* (5), *S. isodon* (8), *S. minutus* (7), *S. roboratus* (9), *S. vagrans* (6). The sample includes species some of which are known to be much similar to each other while others being most dissimilar (Dolgov 1985). Only right toothrows of non-adult specimens with minimally worn dentitions were studied. The specimens belong to the collection of Moscow Zoological Museum.

The specimen images were outlined using Stemi S6 Binocular and then scanned. Each skull was aligned under the binocular in such way that the sagittal plane of the former became parallel to the focal plane of the latter. This is achieved when tips of both right and left antemolars taking the same position in the toothrow (i.e., denoted by the same number) coincide with each other.

Landmarks are placed at the following focal points (Fig. 1, *f*). Landmarks 3 to 7 correspond to tips of the antemolars: they allow to describe and to study the shape of the antemolar tips row alone. Landmarks 1, 2 designate tips of the incisive, while landmarks 8, 9 designate tips of parastyle and paracone of the molariform, respectively. At last, landmarks 10 to 12 designate the base of antemolar toothrow: they are placed at the points at which respective tooth crown bases crossed on the horizontal skull projection. Two sets of landmarks were studied independently, one including all 1–12 landmarks and another with landmarks 3–7 only. The entire set allowed to study overall configuration of the anteriors part of the toothrow, while the reduced set was used to study antemolar tips only.

The landmarks were fixed and their x,y coordinates were digitized by TPSDig (Rohlf 2001a). Consensus configurations for each shrew species were calculated based on each of 1–12 and 3–7 landmark sets using TPSSplin (Rohlf 1997), and all subsequent comparisons were based on the consensuses only. The same program was used for pairwise comparison of species consensus configurations with overall consensus calculated for the entire sample.

The shape differences in the entire sample were studied using TPSRelw (Rohlf 2001b). The following options were adopted for both datasets. The parameter alpha was set to 0, and the uniform components were included in the analysis. Procrustes distances between consensuses were calculated for each of 3–7 and 1–12 landmark sets using TPSSplin, and their respective matrices were compared using Mantel test in the NTSYSpc (Rohlf 1998).

15.4 Results

Analysis of the complete set of landmarks by the TPS method indicates that percentage of total variance explained by a particular RW decreases rather monotonously from the 1st to the 7th one. 45.6 per cent of total variance is explained by RW1 and about 31 per cent of total variance is explained by RW2. Highest contribution to the total variance belongs to landmarks 5–7 corresponding to the tips of 3d to 5th antemolars, respectively. The sum of squares attributed to each of these landmarks is equal to about 0.23 while variation at other landmarks is characterized by sums of squares not exceeding 0.08. These three landmarks provide the greatest input into both 1st and 2d RWs total variances.

Visualization of transformation along RW axes using vector mode (Fig. 2, *a*) indicates the following pattern. As far as RW1 is concerned, there is a predominating change of height of 3rd and 5th antemolars which go in opposite direction. A more slight change of height of the molariform is positively correlated with that of 3rd antemolar, while transformation of 4th antemolar is positively correlated with that of 5th one. The gGradient of the toothrow shape changes along RW2 is more complex and involves nearly all teeth. Changes in height of 3rd and 5th antemolars are negatively correlated with those of 2nd and 4th antemolars and the molariform. Besides, change of distance between tips of the incisive is positively correlated with displacements of tips of 1st and 2nd antemolars and the molariform; it is negatively correlated with displacements of tips of 3rd and 5th antemolars.

When the reduced set of landmarks is analyzed, most of the overall dispersion is attributed to the RW1 (69.1 per cent) and much less to RW2 (27.7 per cent). Unlike the analysis of the entire data set, landmarks 4–5 corresponding to the tips of 2d and 3d antemolars contribute most to the total variance. The sums of squares attributed to each of these landmarks is equal to 0.47 and 0.32, respectively, while those of other landmarks does not exceed 0.07. This means that transformation of shape of antemolars row becomes more localized if their bases and other teeth of

anterior portion of upper dentition are excluded from the analysis. Landmark 4 provides greatest input into RW1 while landmark 5 occurs with high input both in RW1 and RW2.

Graphic representation of transformations of the antemolar tips row indicates

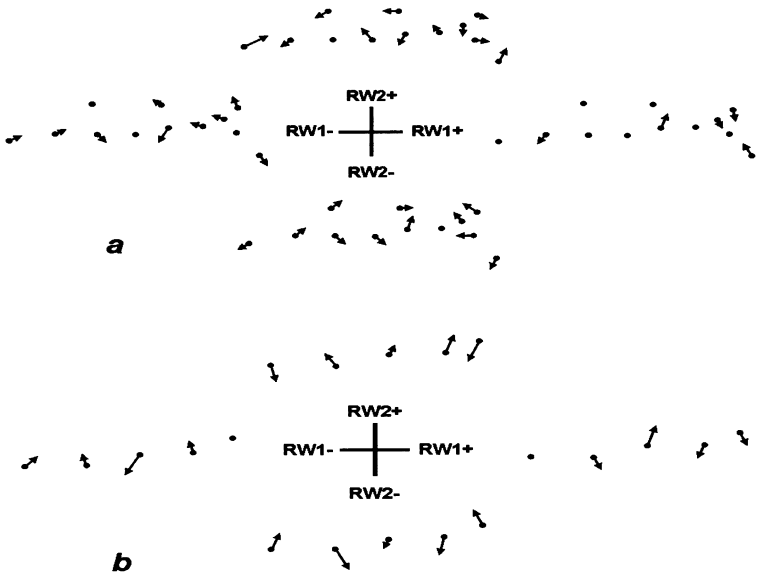

Fig. 2. Transformations of the toothrow shape along 1st and 2d relative warps (RW1 and RW2, respectively) described by: ***a***– all landmarks, ***b***– landmarks 3-7

the following (Fig. 2, *b*). Position of landmark 4 changes most prominently along RW1 being negatively correlated with displacements of other landmarks. Along RW2, landmarks 4–6 slide in opposite direction to that of landmarks 2 and 7.

To sum up, the above results allows to fix the following basical transformations of shape of anterior portion of upper dentition in the brown-toothed shrews. Height of the 3d antemolar is most variable among the teeth studied here. Taking its variation as a "focal point", two different trends in shape transformations can be identified.

One of them defined by RW1 involves negative correlation of height of 3d antemolar with heights of both other antemolars and the molariform. Specific to this trend is minimal changes of general proportions of antemolars, that is it involves mainly transformation of shape of the antemolar tips row. Contrary to this, a prominent change of overall height of molariform is included in this trend, while variation of incisive cusps is minimal.

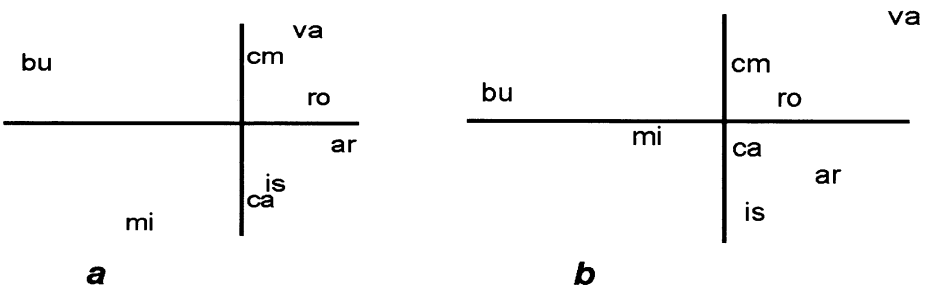

Fig. 3. Distribution of the toothrow consensus configurations of the shrew species in the shape spaces of 1st and 2d relative warps (horizontal and vertical axes, respectively) calculated for: ***a***– all landmarks, ***b***– landmarks 3-7. The species are: ar- *araneus*, bu- *buchariensis*, ca- *caecutiens*, cm- *camtschaticus*, is- *isodon*, mi- *minutus*, ro- *roboratus*, va- *vagrans*

Another trend defined mainly by RW2 is characterized by the following features. When only the shape of the antemolar tips row is considered (landmarks 3–7), 2d and 4th antemolars become positively correlated with the 3d one. When general proportions of antemolars are included (the entire set of landmarks), correlation of most of antemolars with the 3d one remains nearly the same as in the previous trend. Peculiar to the trend under consideration is that nearly the entire dentition studied here is involved in the transformations. Change of overall height of the molariform is still evident but now it is negatively correlated with that of 3d antemolar. Besides, incisive length is now involved in the toothrow transformations: it increases while height of the 3d antemolar decreases, and vice versa.

Similarity among *Sorex* species studied here is roughly the same for both complete and reduced landmark data sets (Fig. 3). This is approved by numerical comparison of Procrustes distance matrices: Mantel statistics $Z_M = 2.71$, $p<0.99$. *S. buchariensis* appeared to be most specific; *S. minutus* also takes a quite remote position. Other species, when compared by all landmarks, cluster in the following way: *S. camtschaticus* + *S. vagrans*, *S. roboratus* + *S. araneus*, *S. caecutiens* + *S. isodon*. When compared by landmarks 3–7, *S. roboratus* becomes closer to *S. caecutiens*, and *S. araneus* is closer to *S. isodon*.

Peculiarities of particular species by shape of anterior part of the upper toothrow can be best illustrated by the transformation grid. Here, overall consensus configuration is used as a common reference, on which four species are superimposed that take opposite positions on the RW1 and RW2 axes calculated for the entire dataset (Fig. 4).

It is easy to see that *S. araneus* differs from the other species by rather enlarged anteriormost part of dentition relative to its posteriormost part. Antemolars of this species decrease rather evenly from 1st to 5th. In *S. buchariensis*, ratio of these two parts of dentition is opposite: the molariform is very high relative to incisive and 1st antemolar. Besides, enlarged 3d antemolar which is as high as 2d one is

peculiar for this species. Dentition of *S. minutus* is least transformed, it just slightly differs from the reference by antemolar ratio only: the 3d one is just little smaller then the 2d one, similar to *S. buchariensis*. *S. vagrans* differs both from the reference and other species by very high 4th antemolar and by elongated tip of the incisive.

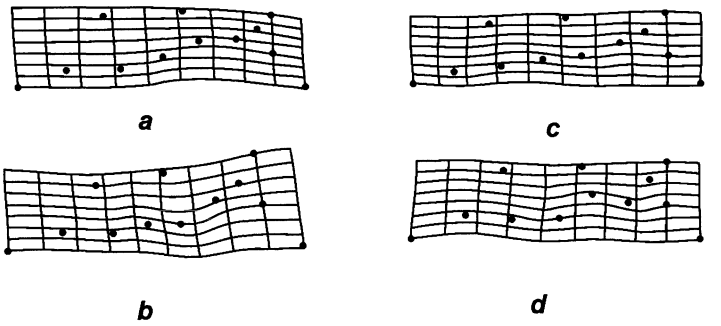

Fig. 4. Grids showing transformation of shapes of consensus configurations of anterior part of the upper toothrow in the shrew species: ***a***– *araneus*, ***b***– *buchariensis*, ***c***– *minutus*, ***d***– *vagrans*

15.5 Conclusions

Similarity pattern among *Sorex* species by shape of anterior part of the upper toothrow agrees largely with subgeneric classification of that genus established previously by traditional methods on the basis of dental morphology (see Pavlinov and Rossolimo 1987, for references and discussion). Thus, *S. buchariensis* is allocated to subgenus *Eurosorex*; *S. camtschaticus* and *S. vagrans* are members of subgenus *Otisorex*; *S. minutus* belongs to subgenus *Dolgovia* in some of the most "splitting" classifications. *S. roboratus*, *S. caecutiens*, and *S. isodon* are usually placed together as members of a separate (yet unnamed) species group; *S. araneus* is similar to them by its dentition though it has a quite different karyotype.

From this, one may conclude that GM reveals some "evident" features of the shapes analyzed here. On the one hand, this is not surprising, as it was the primary background of selection of the species for this pilot project that their mutual differences be quite clear-cut. On the other hand, the fact that the results of the present analysis well agree with anticipations seems to certify GM applicability to in-

vestigations of variation of shape of the anterior part of upper toothrow both among and eventually within shrew species of the genus *Sorex*.

When studying the shape under consideration, it is advisable to landmark not only antemolar tips row but the tips of adjacent teeth as well as the base of antemolar toothrow. This allows to explore both the variation in the configuration of antemolar tips row and in the relative height of elements of the anterior portion of the upper toothrow.

15.6 Acknowledgements

I am highly indebted to Dr. M.V. Zaitsev and to Prof. F.J. Rohlf for discussion of the above results, to an anonymous reviewer for useful criticisms, and to Prof. A.M.T. Elewa for inviting me to contribute to this volume.

References

Bookstein FL (1991) Morphometric tools for landmark data: geometry and biology. Cambridge, Cambridge Univ. Press

Dannelid E (1998) Dental adaptations in shrews. In: Wojcik JM, Wolsan M (eds) Evolution of Shrews. Mamm. Res. Inst., Bialowieza (Poland), pp 157-174

Dolgov VA (1968) Specifics and variation of odontological traits of Palaearctic brown-toothed shrews (Mammlia, *Sorex*) (in Russian). Arch. Zool. Mus. Moscow Univ. 10: 179-199. (in Russian)

Dolgov VA (1985) Brown-toothed shrews of the Old World. Moscow Univ. Publ., Moscow. (in Russian)

Pavlinov IYa, Kruskop SV, Varshavski AA, Borissenko AV (2002) Terrestrial mammals of Russia. KMK Sci Press, Moscow. (in Russain)

Pavlinov IYa, Rossolimo OL (1987) Systematics of mammals of the USSR. Moscow Univ. Publ., Moscow. (in Russian)

Rohlf FJ (1993) Relative warps analysis and example of its application to mosquito wings. In: Marcus LF, Bello E, Garcia-Valdecasas A (eds) Contributions to morphometrics. C.S.C.I., Madrid, pp 131-160

Rohlf FJ (1997) TPSsplin: thin-plate spline, version 1.16. N.Y., State Univ. at Stony Brook (program)

Rohlf FJ (1998) NTSYSpc, version 2.02k. N.Y., State Univ. at Stony Brook (program)

Rohlf FJ (2001a) TPSdig, version 1.31. N.Y., State Univ. at Stony Brook (program)

Rohlf FJ (2001b) TPSrelw: relative warps, version 1.23. N.Y., State Univ. at Stony Brook, (program)

Viktorov LV, Kuzyakin AP (1974) Scaling the size ratio of upper antemolars in brown-toothed shrews. In: Ecological and faunistic investigations in vertebrates of the Central Region. Ryazan, Pedagogical Inst., pp 23-26. (in Russian)

16 Geometric morphometrics in paleoanthropology: Mandibular shape variation, allometry, and the evolution of modern human skull morphology

Markus Bastir and Antonio Rosas

Department of Paleobiology, Museo Nacional de Ciencias Naturales, CSIC, 28006 Madrid, Spain, mbastir@mncn.csic.es

16.1 Abstract

Twenty 3D landmarks were digitized on adult mandibles from Atapuerca, Sima de los Huesos (AT-SH) (N=8), Neanderthals (N=17) and modern humans (N=82). The 3D data was converted into 2D data for Thin-Plate splines analyses. Multivariate regression of partial warps and uniform component scores on size and bootstrap analyses were used to test three hypotheses of allometry. The mandible was divided into a supra- and infra-alveolar part, which are developmentally distinct components. Separate analyses for each component revealed that all species displayed greater allometric variation at the supra-alveolar unit than at the infra-alveolar unit. The infra-alveolar unit showed allometric variation patterns associated to spatial position of the mandible within the craniofacial system. In the supra-alveolar unit the formation of a retromolar space was identified as positive allometric effect in all three species. However, this effect was morphologically different and stronger in Neanderthals and AT-SH hominids than in humans. These findings are discussed in the framework of possible evolutionary modifications of the overall skull design.

Keywords: Atapuerca, Neanderthals, infra-alveolar canal, complex morphological systems, Procrustes techniques.

16.2 Introduction

In paleoanthropology, the morphological variation of the skull has been of classical importance. Currently two major models exist regarding the evolution of modern humans (Henke and Rothe 1994). One model, that of a Lower Pleistocene

"Multiregional Origin" of modern humans proposes a continuity of morphological patterns (Wolpoff et al. 2001) whereas the "Out of Africa"-Model suggests a more recent (later Middle Pleistocene) origin in Africa and predicts a discontinuous pattern of morphological variation (Stringer 2003). These models are particularly interesting regarding the evolution of Neanderthals. While in model of multiregional origin, Neanderthals and modern humans comprise one phylogenetic line, in the Out of Africa model they belong to different species (Rosas and Bermúdez de Castro 1998). However, recent discoveries favor the Out of Africa model (Bermúdez de Castro et al. 1997; White et al. 2003).

From a morphological point of view, these phylogenetic models are built on different ways to interpret and comprehend morphological variation (Aiello and Dean 1990; Henke and Rothe 1994). The possibility of such disjunctive interpretation of both models demonstrates the need of knowledge about the organization of possible biological factors underlying morphological variation (Bastir in prep).

In the light of craniofacial biology, morphological variation is the result of interrelated and complex structural, historical and functional factors, which become modified during ontogeny and phylogeny (Moss and Young 1960; Atchley and Hall 1991; Enlow and Hans 1996; Moss 1997; Rosas 2001; Lieberman et al. 2002; Bastir et al. 2003). All these factors play together in order to produce one composite morphological result. In this developmentally, and thus dynamically oriented line of reasoning, one important factor of morphological variation is allometry, i.e. the covariation of size and shape. Although allometry represents one of the oldest known biological principles, it is in many respects still an unresolved issue (Klingenberg 1998). One current problem relates to the question, whether or how allometry is a useful tool for phylogenetic analysis (Ackermann and Krovitz 2002; O'Higgins et al. 2001; Bastir and Rosas in revision). Some recent studies found parallel allometric trajectories which are either interpreted as evidence for ontogenetically early pattern determination in humans and Neanderthals (Ponce de León and Zollikofer 2001) and even phylogenetic proximity among chimpanzees and hominins (Ackermann and Krovitz 2002). Other studies did not find clear systematic relations between allometric trajectories and phylogenetic relations (O'Higgins et al. 2001, Bastir and Rosas in revision). Surprisingly, even within humans parallel and divergent allometric trajectories were identified questioning their taxonomic usefulness (Vidasdottir et al. 2002). This evidence suggests that further study in that direction is needed.

One methodological problem in most of these studies is that usually one principal component of shape variation -that one, which is most correlated with size- is taken as the representative variable of growth allometry. However, it is known that often more than one principal component can show allometric variation (O'Higgins et al. 2001; Vidasdottir et al. 2002; Bastir et al. 2003). As this fact may influence the analysis and recognition of shape changes produced by pure allometry, one straightforward way to avoid these problems is the use of regression models of shape on size (Bookstein, 1996; Loy et al., 1996; Zelditch et al. 2001). Procrustes based geometric morphometry of landmark data (Rohlf and Slice 1990) is an ideal tool for this kind of allometric analysis because it is based on the operational separation of size and shape, which provides a high analytical resolution

(Bookstein 1991, 1996; Rosas and Bastir 2002). This analytical resolution is affected, however, by the numeric relations of sample size, groups and landmarks like in any other multivariate statistic procedure and resampling techniques can sometimes provide solutions. In this sense, the question of allometric parallelism or divergence is also a question of methods. But there is also a morphological interest, that addresses the morphological nature of allometric shape changes.

The present study analyzes static allometric variation of mandibles from modern humans, Neanderthals and from their putative ancestors, *Homo heidelbergensis* by regression approaches. It tests the null hypothesis that no difference exists in the allometric variation among the mandibles of these hominins (H1) and analyzes the allometric variation in morphology by pairwise comparisons and superposition of allometric trajectories (Zelditch et al. 2001). The morphological analysis of the mandible provides various advantages. It is a paradigmatic key-object for the study of complex morphology, a notion, which characterizes any morphological structure that is "comprised by a number of developmental parts and processes" (Atchley and Hall 1991:105). The mandible is further one of the best-represented bones in the human paleontological record (Rosas 1992). In addition, the study of mandibular allometry is specifically interesting regarding the evolution of classic Neanderthals. In a series of previous investigations with conventional morphometric techniques, it was convincingly demonstrated that the mandibular morphology of the hominids from Atapuerca, Sima de los Huesos (AT-SH) (*H. heidelbergensis*) display a principally allometric pattern of shape variation (Rosas 1997, 2000). The evolutionary relevance of this AT-SH mandibular allometry consists of the fact that smaller individuals display a series of primitive characters, while larger AT-SH individuals present clearly derived (Neanderthal-like) morphologies as a retromolar space, a mental foramen close to M1 and a symphyseal curvature. This allometric pattern formation in the AT-SH mandibles is the second hypothesis (H2) to be tested.

In the present study, we divided the mandible into two parts (functional matrix components) (Moss and Young 1960; Enlow and Hans 1996). We performed separate analyses of the part superior to the alveolar nerve canal and the part inferior to it. These parts differ developmentally, because bone remodeling (i.e. bone resorption and bone deposition) is regionally different (Enlow and Hans 1996). The infra-alveolar part contains structural information about the spatial position of the mandible within the complete craniofacial systems and properties of the growth process and the associated modifications (e.g. total mandibular, matrix and intramatrix rotations, sensu (Björk 1969; Skieller et al. 1984; Björk 1991). The part superior to the alveolar nerve canal in humans is characterized ontogenetically by external resorption and internal deposition (Enlow and Hans 1996). The supra-alveolar component has a strong functional component that relates to occlusion and the masticatory system. In the mandible this system consists of the muscle insertion sites, the dentition and the alveolar process.

Mastication is a main function of the viscerocranium, which is known to scale positively with body size (Biegert 1957; Emerson and Bramble 1993). Thus, the third hypothesis (H3) tests if the supra-alveolar, functional part of the mandible shows stronger allometric variation than the infra-alveolar, structural part.

16.2 Material and methods

We collected 20 3D-landmarks with a MicroScribe 3DX® digitize. These landmarks are [(1) M3; (2) M1; (3) Canine, (4) Mental foramen, (5) Inferior basal border, (6) Preangular notch, (7) Gonion; (8) Ramus Flexure, (9) Condylion, (10) Mandibular notch, (11) Coronoid, (12) Anterior ramus, (13) Retromolar space, (14) Mandibular foramen, (15) Infradentale, (16) B-point, (17) Menton, (18) Gnathion, (19) Foramen genioglossum, (20) Internal Infradentale] (Fig. 1).

Details of measurements, error evaluation and data processing are described elsewhere (Rosas, Bastir 2002). The human mandibles (N=82) were digitized at the Institute of Anthropology (European sample; N=45) of the University of Coimbra in Portugal and at the Natural History Museum (African sample N=37) in London, with female and male individuals in roughly similar contributions.

The Atapuerca SH sample is a unique collection of mandibles, which belong most probably to one biological population (Bermúdez de Castro et al. 2001). Although the total sample consists of at least twenty-nine different specimens (Rosas 1995), eight of these mandibles are almost complete, and were used in the present study [five females: AT-607, AT-950, AT-952, AT-2193, AT-3888; and three males AT-300, AT-605, AT-888; (Rosas et al., 2002a)]. The original mandibles are housed the MNCN, Madrid. The Neanderthals (Krapina J, La Chapelle, Aubesier 11, MonteCircceo 2 and 3, La Ferassie 1, La Quina 5 and 9, St. Cesaire, Regourdou 1, Amud 1, Tabun 1 and 2, Bañolas, Zafarrayah, Spy 1, and Kebara) were digitized at the Natural History Museum, London, and mostly on casts (except Tabun 2) and at the MNCN, Madrid.

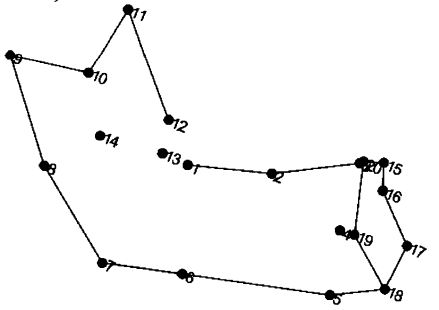

Fig. 1. Landmark scheme on the mean shape of a human mandible

16.3 Geometric morphometry

Geometric morphometry of landmark coordinates provides an ideal tool kit for testing hypotheses of allometry. This is, because at the core of these methods is the separation between two components of biological form, i.e., size and shape (Bookstein 1991). Procrustes superimposition techniques (translation, rotation and

scaling) aim to minimize the offset between homologue landmarks, and size is obtained as a scaling factor termed "centroid size" (Kendall 1977; Rohlf and Slice 1990; Bookstein 1991), which is defined as the square root of the sum of the squared distances between the centroid and each of the landmarks (Bookstein 1991). Shape is the residual geometric information remaining, once superimposition techniques ruled out location, scale and rotational effects (Kendall 1977).

16.3.1 Thin-plate splines

A specific category of shape variables derives from thin-plate splines, i.e., the partial warps and uniform component scores (Bookstein 1991). Thin-plate splines (TPS) quantify the shape differences between two objects by deforming the first specimen into the second one. First, both configurations are Procrustes superimposed. Second, a hypothetical infinitely thin metal plate (grid) is fitted over the reference configuration, which is then deformed vertically until it matches exactly the target shape (Bookstein 1991). The warping of the grid reflects the mismatch of homologue landmarks. This deformation is characterized by certain amounts of bending energy, which can be used for the derivation of shape descriptors, the partial warps and uniform component scores (α=0) (Rohlf et al. 1996). In the present study, the Procrustes mean shape of all specimens of a given species is transformed by TPS into each of the individuals. The TPS transformation yields a data matrix in which each specimen is defined exactly in the shape space by the obtained partial warps scores and its centroid size. This was performed separately for humans, AT-SH hominids and Neanderthals. Detailed technical description of these methods can be found in Bookstein (1991).

16.3.2 Missing data

The present geometric morphometric study is based on landmark coordinates. Whereas in Procrustes analysis missing landmarks are not so much a problem, since the superimposition can be performed on a set of the largest number of common preserved points (Slice 1998), the TPS method does not permit missing data. TPS analysis is currently also most effectively performed on two-dimensional data, thus the 3D coordinates of partially fragmentary fossils needed a specific preparation. First, a Generalized Procrustes Superimposition (Rohlf and Slice 1990) was performed in 3D altogether on all specimens. The group specific mean shapes were calculated and centroid size was extracted as the common scaling factor. All the specimens were rotated into lateral view. Then the missing values of the corresponding group mean shapes were replaced in the aligned data. For the AT-SH sample the sex-specific mean values were used (Rosas and Bastir 2002; Rosas et al. 2002a), whereas for the Neanderthal sample the unsexed group specific mean was used. The medio-lateral coordinate dimension was removed and the specimens were rescaled by the previously extracted centroid size. Finally,

the bilateral landmarks were averaged, so that the data could be exported into the TPS-software data format by Morpheus (Slice 1998).

16.3.3 Geometric morphometric software and data analyses

The allometric patterns of shape variation were calculated by multivariate regressions of shape on log-transformed centroid size (Bookstein 1996) by VecCompare, VecLand (IMP-software) (Sheets 2001), and tpsRegr (TPS-software) (Rohlf 1998). The fit of the regression models was evaluated by the explained variance of the model and by Goodall's F-test (1991) (Rohlf 1998). The differences in significantly allometric models were evaluated by bootstrapping procedures (N=300), described in detail in (Zelditch et al. 2001, 2003). This conservative test compares the angles of allometric vectors between two samples (VecCompare). By bootstrapping procedures a within-group angle range is evaluated for each sample and compared with the between-group angle. If the between-group angle is larger than the 95% range of the bootstrapped within-group angles, the between-group angle is judged significantly different and the allometries are different (Zelditch et al. 2001, 2003). The allometries are compared by VecLand and depicted as displacement vector for each species on each landmark.

16.4 Results

The allometric shape changes as expressed by regressions on log centroid size are shown in Figure 2. The overall allometric patterns show little shape variation in humans and higher variation among the fossils. (Table 1). This table gives the descriptives of the fit of the regression models of the supra-and infra-alveolar units evaluated by tpsREGR (Rohlf 1998). The supra-alveolar components were all highly significantly allometric. Infra-alveolar components showed less clear relations. In all cases, AT-SH hominids revealed the best fit of the data. The bootstrap comparisons for the significant models of the total mandible and the supra-alveolar unit are given in Table 2. The angle ranges were generally high and did not contribute to distinguish between the species and lend support to Hypothesis 1 of similar slopes. Hypothesis 2 is corroborated because Figures 2a, c indicate the presence of a retromolar space and a posterior position of the mental foramen in AT-SH hominids (by an anterior migration of M1).

Table 1. Fit of Regressions (tpsREGR)

System	Humans		Neanderthals		Atapuerca	
	% expl. var.	sig.	% expl. var.	sig.	% expl. var.	sig.
supra-alveolar	8,1	0,000	21,1	0,000	57,74	0,000
infra-alveolar	3	0,005	9	ns	27	ns

ns (not significant)

Table 2. Supra-alveolar models. Bootstrapping angles in decimal degrees (VecCompare6). Between: indicates between group angle, G1, G2 give the 95% C.I. of ranges within the group listed in G1 / G2

G1 / G2	between	G1	G2	Difference
Humans / Atapuerca-SH	108	103,5	34	ns
Humans / Neanderthals	112,6	91	49,8	ns
Atapuerca-SH / Neanderthals	92,5	35,9	93,3	ns

ns (not significant)

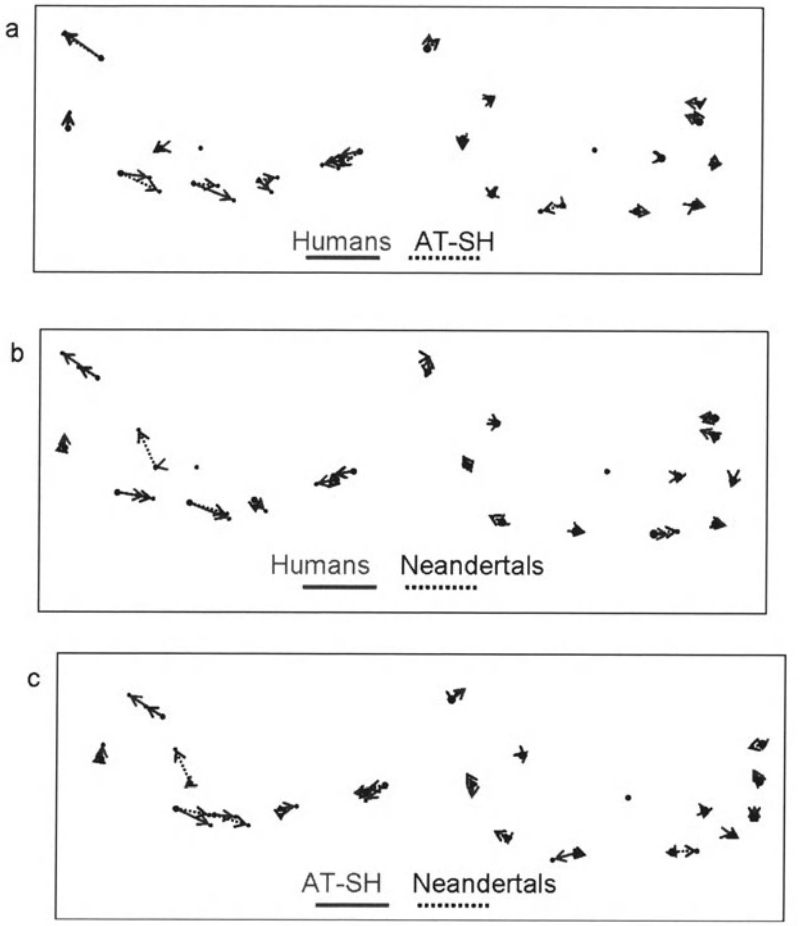

Fig. 2. Pairwise comparison of superposed allometric variation patterns. a) humans, AT-SH; b) humans, Neanderthals, c)AT-SH, Neanderthals. Left column: functional unit. Right colum: structural unit

The superposed allometric tendencies of the developmental components contribute further to understand the allometric patterns (Fig. 2). As listed in Table 1, the supra-alveolar unit displays much more allometric variation than the infra-alveolar unit., which supports Hypothesis 3. The supra-alveolar components show also a very similar overall morphological pattern (Fig. 2, left column). All species produce an anterior shift at the molar dentition as a positive allometric effect, but with different vertical and horizontal components. These changes are accompanied by other more individualized modifications of the ramus shape. The infra-nerve units show only minor allometric changes.

19.5. Discussion

In the present study we analyzed the allometric variation in mandibles of modern humans and Middle Pleistocene hominins. Geometric morphometrics were used to test hypotheses about allometric shape variation. Hypothesis 1 predicted parallel allometric trajectories among all species. Hypothesis 2 predicted that larger individuals from Atapuerca-SH should display derived morphological traits, typical for Neanderthals and Hypothesis 3 predicted higher allometric variation at the functional mandibular part. All hypotheses received support from the analytical design of the present study

Hypothesis 1. The findings indicate that no significant difference exists in static allometric variation patterns between the analyzed hominin species. Although this is similar to the study of Ponce de León and Zolikofer (2001) who reported parallel trajectories in postnatal ontogenetic allometries, our results are not directly comparable. This is, because in the present study static allometric variation patterns were analyzed and three different kinds of allometry can be distinguished, ontogenetic, static and evolutionary allometry (Cheverud 1982; Klingenberg 1998).

While ontogenetic allometry contains information about the dynamics of growth and development of a given species, static allometry describes size-shape relations that are obtained in later ontogeny (Godfrey and Sutherland 1996; Rosas and Bastir 2002) or because of specific functional or developmental relationships. Adult allometry is thus not a direct substitute for ontogeny. The relationship between all three kinds of allometry is that growth allometries have their effect on adult variation, which is subjected to natural selection and other evolutionary phenomena (Klingenberg 1998). A possible interpretation of the interspecific comparison may be that the analyzed species share static allometric slopes with different morphological consequences that are obtained earlier in ontogeny. Insofar the present results fit to the findings of Ponce de León. and Zolikofer (2001).

The present results support Hypothesis 2 in that large individuals in AT-SH showed derived morphological traits such as the presence of a retromolar space (Rosas 1992, 1997). It is particularly interesting that the formation of the retromo-

lar space, the mental foramen position and the symphyseal curvature are present in all three species as a positive allometric, but therefore also continuous effect, which is therefore in line with other findings (Franciscus and Trinkaus 1995; Rosas 1997).

A particular problem of static allometry in this respect is that it does not contain information about the developmental dynamics that lead to the evolution of a particular morphology. Thus, to investigate the question, which kind of allometric changes may have contributed to these particular morphological modifications in the AT-SH-Neanderthal lineage requires a comparative analysis of the traits among all three kinds of allometry. Changes in rate or time can only be distinguished in the comparative analysis of ontogenetic data that contain a reference for time (Klingenberg 1998). In the present study, nevertheless, the morphological nature of allometric variation patterns was of interest and not their heterochronic nature. This question deserves further analysis.

Another reason for cautiousness in comparisons of the present results with other studies of allometric variation is of methodological nature. This study applied a thin-plate spline regression approach to the study of allometry (Bookstein 1996; Loy et al. 1996; Zelditch et al. 2001) instead of using relative warps (Ponce de León and Zolikofer 2001). The present approach captures thus, by definition, all variation associated to modifications of size, while in relative warps analysis, the fractions of pure allometry can be morphologically distributed across various relative warps (O'Higgins et al. 2001; Vidasdottir et al. 2002; Bastir et al. 2003).

Of particular interest seems the test of Hypothesis 3. The results indicate that the separation of the mandible in specific developmental units contributes to locate the allometric effect of shape variation. Table 1 and Figure 2 show that specifically the unit associated with strong functional aspects displays high allometric variation, with different vertical and horizontal modifications at the ramus and the posterior limit of the corpus. This is not only coherent with the fact that precisely functional associations can be detected in static allometries (Klingenberg, 1998) but also supports the view that the viscerocranium, i.e. the masticatory apparatus (Biegert, 1957, Emerson and Bramble 1993), and the facial part of the respiratory system (Enlow and Hans 1996) show strong positively allometric associations with body size or body mass.

The difference of allometric and non-allometric variation patterns and their relative independence within the mandible lends support to a major aspect of the functional matrix hypothesis (Moss and Young 1960), which predicts that different and partially independent functional (micro-skeletal) units can be integrated within the same individual bone. In this respect the findings support the division of these units in functional and structural terms, although it should be noted that other mandibular divisions at other phenomenological scales are possible (Klingenberg et al. 2003).

The structural component has shown considerably decreased allometric variation (Table 1). However, its structural nature may not only be indicated by the lack of allometric variation, but also by the fact that this part contains information about the spatial position of the mandible within the whole craniofacial system (Skieller et al. 1984; Björk 1991). Figure 2a indicates that large modern human

individuals show a more vertical morphological pattern, in which larger individuals tend to increased vertical ramus proportions and decreased horizontal corpus proportions, with a backwards reorientation, retraction of the symphysis. This retraction is produced by spatially induced bone resorption (Enlow and Hans 1996).

These modifications may be interpreted in terms of allometric changes in later ontogeny (Godfrey and Sutherland 1996; Rosas and Bastir 2002) which produce different spatial positions in the mandible in larger individuals with respect to the cranium. In a recent analysis of static allometric variation of the whole skull, it was shown that in larger individuals, independent from sexual dimorphism, the whole viscerocranium was inferiorly expanded (Rosas and Bastir 2002). Such a displacement is likely a consequence of general postnatal facial growth effects within a principally vertical skull design in humans and has been associated to specific mandibular rotations and remodeling patterns (Enlow and Hans 1996).

This situation should be theoretically different in the hominin fossils because their increased facial projection and prognathism (Aiello and Dean 1991; Bastir 1998) would require less spatial adaptation in mandibles of larger individuals. It is interesting nevertheless, that also in the more prognathic fossils morphologies - associated to spatial adjustments- can be observed at the orientation and morphology of the symphysis, which are morphologically similar to those of modern humans and causally related to a vertical skull design (Enlow and Hans 1996). It is difficult to understand this, but this problem offers one indication for future investigation that should address the analysis of remodeling patterns at the symphysis of those hominins (Martinez-Maza and Rosas 2002). A comparative paleohistological analysis could indicate whether the observed similarity in morphology relates to similar biological processes between modern humans and fossil hominins.

19.7 Conclusions

The present study has shown that geometric morphometric analysis of allometric variation and the superposition of allometric trajectories on individual landmarks offers a series of interesting question that are important for the understanding of the evolution of the modern human skull. While the interpretation of static allometry in terms of phylogenetic relations is difficult, the study has shown that allometric shape variation of the hominin mandible is localized at the functional part, related to mastication. In this area in all species a tendency to form a retromolar space was observed. Another mandibular unit that has been associated to structural factors reveals less allometric variation. It permits however inferences to the spatial position of the mandible within the entire skull. Similar morphological modifications at the symphysis among all three species are discussed with respect to spatial directions of growth displacement but conclusions about comparability of symphyseal similarity must await further study of the paleo-histology of the involved structures.

16.9. Acknowledgements

We thank Dr. Elewa for inviting us to participate in this volume as well as Dr. Sheets and Dr. Zelditch for suggestions and discussions on earlier drafts of this manuscript. We are grateful to Dr. Eugenia Cunha (University of Coimbra), Dr. Louise Humphrey, Mr. Robert Kruszynski and Prof. Chris Stringer (NHM-London) for permissions to study the material in their charge and for the support during the time of data recording. This study was partly supported by the SYS-Ressources of the NHM-London (MB), the Luso-Español Project MEC: HP: 1995-0031 and the Atapuerca project BXX2000-1258-C03-01. MB is supported by a FPI pre-doctoral grant of the Spanish Ministry of Science MCyT.

References

Ackermann, R R & Krovitz G E (2002) Common Patterns of Facial Ontogeny in the Hominid Lineage. Anatomical Record 269:142-147

Aiello L, Dean C (1990) An introduction to human evolutionary anatomy. London: Academic Press Harcourt Brace & Company

Atchley WR, Hall BK (1991) A model for development and evolution of complex morphological structures. Biological Reviews 66:101-157

Bastir M. (1998) 3D- Analysis of Prognathism.The Morphological Variation of Homo sapiens Populations and Fossil Casts, Some Aspects of Biomechanics and Functional Morphology. Master thesis, University, Vienna.

Bastir, M, Rosas A, Kuroe K (2003). Petrosal orientation and mandibular ramus breadth: Evidence of a developmental integrated petroso-mandibular unit. American Journal of Physical Anthropology DOI: 10.1002/ajpa.10313

Bastir M, Rosas A (2004.) Facial heights: Implications of postnatal ontogeny and facial orientation for skull morphology in humans and chimpanzees. American Journal of Physical Anthropology 123S, 60-61

Bastir M, Rosas A, Sheets DH (2004) The morphological integration of the hominoid skull: A Partial Least Squares and PC analysis with morphogenetic implications for European Mid-Pleistocene mandibles. In: Slice D (ed) Developments in Primatology: Progress and Prospects: Kluwer Academic/Plenum (in press)

Bastir M (in prep) Structural and systemic factors of morphology in the hominid cranio-facial system. A geometric morphometric analysis of integrative aspects in the morphological variation of humans with implications for the Atapuerca SH hominids and European hominid evolution. Doctoral Dissertation, Autonoma University of Madrid, Madrid

Bastir M, Rosas A (in revision) The hierarchical nature of morphological integration in the posterior face of modern humans and great apes. American Journal of Physical Anthropology

Bermúdez de Castro JM, Arsuaga JL, Carbonell E, Rosas A, Martínez I, Mosquera M. 1997. A Hominid from the Lower Pleistocene of Atapuerca, Spain, Possible Ancestor to Neanderthals and Modern Humans. Science 276: 1392-1395

Bermúdez de Castro JM, Sarmiento S, Cunha E, Rosas A, Bastir M (2001) Dental size variation in the Atapuerca-SH Middle Pleistocene hominids. Journal of Human Evolution 41: 195-209

Biegert J (1957) Der Formwandel des Primatenschädels und seine Beziehungen zur ontogenetischen Entwicklung und den phylogenetischen Spezialisationen der Kopforgane. Gegenbaurs Morphologisches Jahrbuch 98: 77-199.

Björk A (1969) Prediction of mandibular growth. America Journal of Orthodontics 55: 585-599

Björk A (1991) Facial growth rotation - reflections on definitions and cause. Proceedings Finnish Dental Society 87: 51-58

Bookstein FL (1991) Morphometric tools for landmark data. Cambridge: Cambridge University Press

Bookstein FL (1996) Combining the Tools of Geometric Morphometrics. In: Marcus LF (ed) Advances in Morphometrics. New York: Plenum Press. pp 131-151

Cheverud JM (1982) Relationships among ontogenetic, static an evolutionary allometry. American Journal of Physical Anthropology 59:139-149

Emerson SB, and Bramble DM (1993) Scaling, allometry and skull design. In: J Hanken and BK Hall (eds) The skull. Chicago: University of Chicago Press, pp 384-421.

Enlow DH, Hans MG (1996) Essentials of Facial Growth. Philadelphia London New York: W.B. Saunders Company

Franciscus RG, Trinkaus E (1995) Determinants of retromolar space presence in Pleistocene *Homo* mandibles. Journal of Human Evolution 28: 577-595

Godfrey LR, Sutherland MR (1995) Flawed inference: why size-based tests of heterochronic processes do not work. Journal of Theoretical Biology 172: 43-61

Goodall, C 1991) Procrustes methods in the statistical analysis of shape. J R Statistical Soc, B. 53: 285-339

Henke W, Rothe H (1994) Paleoanthropologie. Berlin, Heidelberg, New York: Springer Verlag

Kendall DG (1977) The diffusion of shape. Advances in Applied Probability 9: 428-430

Klingenberg CP (1998) Heterochrony and allometry: the analysis of evolutionary change in ontogeny. Biological Reviews 73: 79-123

Klingenberg CP, Mebus K, Auffray J-C. (2003). Developmental integration in a complex morphological structure: how distinct are the modules in the mouse mandible? Evol Dev 5: 522-531.

Loy A, Cataudella S, Corti M. (1996) Shape changes during the growth of the sea bass; *Cecentrarchus labrax,* (TELEOSTEA: Perciformes) in relation to differenct rearing conditions. In: Marcus LF (ed) Advances in Morphometrics. New York: Plenum Press. pp 399-405

Martinez-Maza C, Rosas A. (2002) Bone remodeling in the Atapuerca-SH mandibles. Implications for growth patterns in middle pleistocene hominids. American Journal of Physical Anthropology 115: 107-108

Moss M, Young RW (1960) A Functional Approach to Craniology. American Journal of Physical Anthropology 45: 281-292

O'Higgins P, Chadfield P, Jones N (2001) Facial growth and the ontogeny of morphological variation within and between the primates Cebus apella and Cercocebus torquatus. Journal of Zoology, London 254: 337-357

Ponce de León M, and Zollikofer C (2001) Neanderthal cranial ontogeny and its implications for late hominid diversity. Nature 412:534-538

Rohlf FJ. (1998) tpsREGR. Version 1.27 New York: Ecology & Evolution, SUNY at Stony Brook (http://life.bio.sunysb.edu/morph)

Rohlf FJ, Slice D (1990) Extensions of the procrustes method for the optimal superimposition of landmarks. Syst. Zool. 39: 40-59

Rosas A. (1992) Ontogenia y Filogenia de la mandíbula en la evolución de los homínidos. Aplicación de un modelo de morfogénesis a las mandíbulas fósiles de Atapuerca. Doctoral Dissertation, Universidad Complutense, Madrid

Rosas A (1995) Seventeen new mandibular specimens from the Atapuerca/Ibeas Middle Pleistocene Hominids sample (1985-1992). Journal of Human Evolution 28: 533-559

Rosas A (1997) A gradient of Size and Shape for the Atapuerca sample and Middle Pleistocene hominid variability. Journal of Human Evolution 33: 319-331

Rosas A (1998) Modelos de crecimiento en mandíbulas fósiles de homínidos. Atapuerca, un nuevo paradigma. In: Atapuerca y la Evolución Humana. Madrid: Fundación Ramón Areces. pp 239-275

Rosas A (2000) Ontogenic approach to variation in Middle Pleistocene hominids. Evidence from the Atapuerca -SH mandibles. Human Evolution 15: 83-98

Rosas A (2001) Occurrence of Neanderthal Features in Mandibles From the Atapuerca-SH Site. American Journal of Physcial Anthropology 114: 74-91

Rosas A, Bastir M (2002) Thin-Plate Spline Analysis of Allometry and Sexual Dimorphism in the Human Craniofacial Complex. American Journal of Physical Anthropology 117: 236-245

Rosas A, Bastir M, Martínez Maza C, Bermúdez de Castro JM (2002a) Sexual Dimorphism in the Atapuerca-SH hominids. The evidence from the mandibles. Journal of Human Evolution, pp 135-141

Rosas A, Bastir M, Martinez-Maza C (2002b) Morphological integration and predictive value of the mandible in the craniofacial system of Hominids: A test with the Atapuerca SH mandibular sample. Collegium Anthropologicum 26: 171-172

Rosas A, Bermudez de Castro JM (1998) The Mauer mandible and the evolutionary significance of Homo heidelbergensis. Geobios 31: 687-697

Sheets DH. (2001) IMP, Integrated Morphometric Package. (http://www.canisius.edu/~sheets/morphsoft.html) Sheets, David H

Skieller V, Björk A, Linde-Hansen T (1984) Prediction of mandibular growth rotation evaluated from a longitudinal implant sample. American Journal of Orthodontics 86: 359-370

Slice DE. (1998) Morpheus et al.: software for morphometric research. Version 01-01-00, New York, Department of Ecology and Evolution, State University, Stony Brook

Stringer C (2003) New perspectives on the Neanderthals. Evolutionary Anthropology 11: 58-59

Viðarsdóttir US, O'Higgins P, and Stringer C (2002) A geometric morphometric study of regional differences in the ontogeny of the modern human facial skeleton. Journal of Anatomy 201: 211-229

White T, Asfaw B, DeGusta D, Gilbert H, Richards G, Suwa G, Howell CF.(2003) Pleistocene Homo sapiens from Middle Awash, Ethiopia. Nature 423: 742-747.

Wolpoff MH, Hawks J, Frayer DW, Hunley K (2001) Modern Human Ancestry at the Peripheries: A Test of the Replacement Theory. Science 291: 293-297

Zelditch ML, Sheets DH, Fink WL. (2001) The spatial complexity and evolutionary dynamics of growth. In: Zelditch ML (ed) Beyond Heterochrony. New York: Wiley Liss. pp 145-194.

Zelditch ML, Lundrigan BL, David Sheets H, and Garland T (2003) Do precocial mammals develop at a faster rate? A comparison of rates of skull development in Sigmodon fulviventer and Mus musculus domesticus. Journal of Evolutionary Biology 16: 708-720

17 3-D geometric morphometric analysis of temporal bone landmarks in Neanderthals and modern humans

Katerina Harvati

Department of Anthropology, New York University, 25 Waverly Place, New York NY 10003, USA, katerina.harvati@nyu.edu

17.1 Abstract

The temporal bone is often described as one of the most diagnostic areas for Neanderthals. It is the location of several traits thought to differentiate Neanderthals from modern humans, including some proposed Neanderthal derived traits. Most of these are difficult to capture with traditional measurements and are usually described qualitatively. This study built on previous work in applying the techniques of geometric morphometrics to the complex morphology of the temporal bone, with the purpose of quantifying the differences observed between Neanderthal and modern human temporal bone morphology. The sample included 270 modern humans from 9 populations spanning the extremes of the modern human geographical range, 14 Neanderthals and 6 Late Paleolithic Europeans. The data were collected as 3-D landmark coordinates and the specimen configurations were superimposed using Generalized Procrustes Analysis. The fitted coordinates were analyzed using multivariate statistics. The temporal bone landmark analysis successfully separated Neanderthals from modern humans. Most of the previously described temporal bone traits contributed to this separation, although a few differences from previous analyses were found.

Keywords: Neanderthals, Kabwe, modern human origins, temporal bone.

17.2 Introduction

The temporal bone is one of the most diagnostic anatomical areas for Neanderthals. Neanderthal features include the small mastoid process relative to the juxtamastoid eminence (Boule and Vallois 1957; Vallois 1969; Santa Luca 1978; El-yaqtine 1996; Dean et al. 1998); the origin of the petro-tympanic crest at the most inferiorly projecting part of the tympanic and the coronal orientation of the tym-

panic plate (Vallois 1969; Vandermeersch 1985; Elyaqtine 1996; Schwartz and Tattersall 1996); a wide, shallow and medially closed-off glenoid fossa (Vallois 1969); and the strong supramastoid crest (Boule and Vallois 1957; Vallois 1969). Most of these traits are difficult to measure directly with caliper measurements. Previous studies by the author (Harvati 2001a, b, 2002, 2003) pursued their quantitative evaluation using 3-D geometric morphometrics of temporal bone landmarks in Neanderthals and modern human groups. Perhaps the greatest advantage of this technique is that it provides a means of quantifying shape differences of variable traits which cannot be directly linearly measured (Dean 1993; Harvati 2001a).

The present paper builds on the author's earlier work by including a greater number of fossil specimens. This is of particular importance for the Upper Paleolithic European specimens, of which only four were included in Harvati (2001a, b, 2003). Some of the fossil specimens for which only casts were available earlier are here represented by the original specimens. This enhances the quality of the data, as some temporal bone landmarks are more difficult to locate on casts. Finally, shape differences along principal components were visualized here using Morphologika (O'Higgins and Jones 1999) rather than GRF-ND (Slice 1992). As in Harvati (2001a, b, 2003) Neanderthals are shown to be very clearly differentiated from modern humans in their temporal bone traits.

17.3 Materials and methods

A sample of nine modern human populations (Andamanese, Australian, Austrian Berg, W. African Dogon, Greenland Inusguk, Melanesian Tolai, Western Eurasian, Khoisan, Afalou/Taforalt Epipaleolithic), totaling 270 specimens, and several Middle and Late Pleistocene fossil specimens were analyzed (Table 1). For further details on the modern human samples see Harvati (2001a, 2003). Thirteen osteological landmarks were digitized (Table 2, Figure 1), following Howells (1973). Data were collected as three-dimensional coordinates using a portable digitizer Microscribe 3DX. All data were collected by the author. Measurement error was calculated for each landmark based on ten replicates of the same specimen. Error was assessed for each landmark by calculating the deviation around the mean distance of that landmark from the centroid (mean of all coordinates). Measurement error ranged from 0.06 to 0.34 mm and was similar across all landmarks. Minimal reconstruction was allowed during data collection for specimens where very little damage was observed. The landmark coordinates were superimposed using Generalized Procrustes Analysis (Rohlf 1990; Rohlf and Marcus 1993; Slice 1996; O'Higgins and Jones 1998) in Morpheus (Slice 1994-1999) and Morphologika (O'Higgins and Jones 1999). Using reflection of right and left, specimens preserving different sides were combined in one dataset. Data were reconstructed by reflecting right-left homologous landmarks, so that landmarks preserved on different sides could be combined to form a more complete composite configuration.

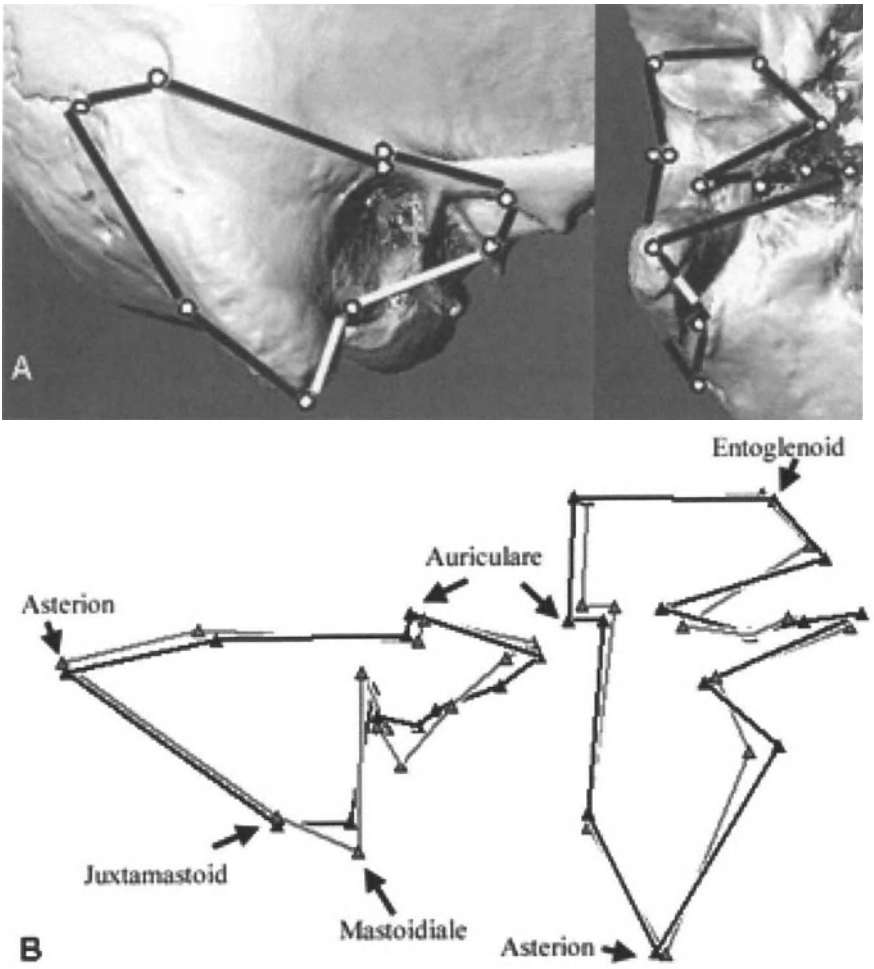

Fig. 1. A. Landmarks used in the analysis in lateral and ventral view; B. Modern human (grey) and Neanderthal (black) mean configurations

The fitted coordinates (Slice 2001) were analyzed using a principal components analysis (PCA); a canonical variates analysis (CVA) on the first 15 PCs (83.4 % of the total variance); Mahalanobis D^2 correcting for unequal sample sizes (Marcus 1990); and a discriminant analysis, which treated the Upper Paleolithic specimens as unknown, to be classified into one of the predefined species level by posterior probability. The robustness of this analysis was further tested by conducting a cross-validation test on the entire dataset. An ANOVA was performed on the PCA scores to determine the significance of species effects along each component, and a Bonferroni test (*alpha* set to 0.05) was performed on all pairwise compari-

sons of the population and species means of PC scores, in order to detect significant differences between groups. Shape differences along the principal components separating Neanderthals, or other fossils, from modern humans were explored in Morphologika.

17.4 Results

PC 1 (12.7 % of the total variance) separated Kabwe from the rest of the sample. The shape differences between Kabwe and modern humans along PC 1 include a more inferiorly positioned mastoid portion of the temporal bone, a shorter mastoid process and more posteriorly placed tip of the juxtamastoid eminence and a wider glenoid fossa.

Table 1. Sample of fossil specimens used. Asterisks indicate specimens for whic casts were used

Neanderthal:	Saccopastore 2
	La Chapelle
	La Ferrassie 1
	La Ferrassie 2
	Spy 1
	Spy 2
	La Quina 5
	La Quina 27
	Circeo 1
	Gibraltar 1
	Krapina C
	Krapina 39-1
	Amud 1
	Shanidar 1*
Upper Paleolithic Europeans:	Cro Magnon 1
	Abri Pataud
	Predmosti 3*
	Predmosti 4*
	Mladec 2
	Mladec 5*
Mid. Pleistocene specimens:	Kabwe

Neanderthals were separated from modern humans along PCs 2, 3 and 5 (0.9, 8.9 and 6.3 % respectively; Figure 2). The clearest separation is shown along PC 5

Table 2. List of temporal bone landmarks used

1. Asterion
2. Stylomastoid Foramen
3. Most medial point of the jugular fossa
4. Most lateral point of the jugular fossa
5. Lateral origin of the petro-tympanic crest
6. Most medial point of the petro-tympanic crest at the level of the carotid canal
7. Porion
8. Auriculare
9. Parietal Notch
10. Mastoidiale
11. Most inferior point on the juxtamastoid crest (following Hublin 1978)
12. Deepest point of the lateral margin of the articular eminence
13. Most inferior point on the entoglenoid process

although there is some overlap along all these components. All three PCs showed a statistically significant species effect in the ANOVA ($p < 0.0001$ for PC 2, $p = 0.0019$ for PC 3 and $p < 0.0001$ for PC 5), and Neanderthal mean scores were significantly different from those of modern humans. When examined at the level of the population, Neanderthal mean scores were not significantly different from those of the San and Inugsuk along PC 2 and those of the Andamanese along PC 3. Neanderthal scores were significantly different from all modern human groups along PC 5. The Upper Paleolithic specimens and Kabwe fell within the modern human 95 % confidence ellipse and outside the Neanderthal cluster along these axes, although some specimens fell within the area of overlap of the confidence ellipses of the two groups. Along PCs 2 and 3 five Neanderthal specimens (Amud 1, Quina 5, Spy 1, Guattari 1 and La Ferrassie 2) overlapped with modern humans. Only two Neanderthals (Amud 1 and Spy 2) fell within the modern human 95 % confidence ellipse along PC 5.

The shape differences that separated Neanderthals from modern humans along these PCs can be summarized as follows: Neanderthals showed a more superiorly positioned tip of the mastoid process; the tip of the juxtamastoid eminence was more inferiorly, anteriorly and medially placed; the petro-tympanic crest was more coronally oriented; porion and auriculare more posteriorly, and the medial end of the petro-tympanic crest more posteriorly and medially placed (Figure 3).

The possibility that these shape differences were related to allometric scaling was explored. As previously found, temporal bone centroid size for Neanderthals was found to fall well within the range of modern human temporal bone centroid size and mean Neanderthal centroid size was not significantly different from the mean modern human centroid size (Figure 4). Among modern human populations there were significant differences in mean centroid size. The Epipaleolithic Afalou/Taforalt population showed the greatest centroid size and was significantly different from all other modern human populations except the Upper Paleolithic European sample. Both of these populations have been described as highly robust (see discussion in Harvati 2001a). Kabwe showed a very high centroid size.

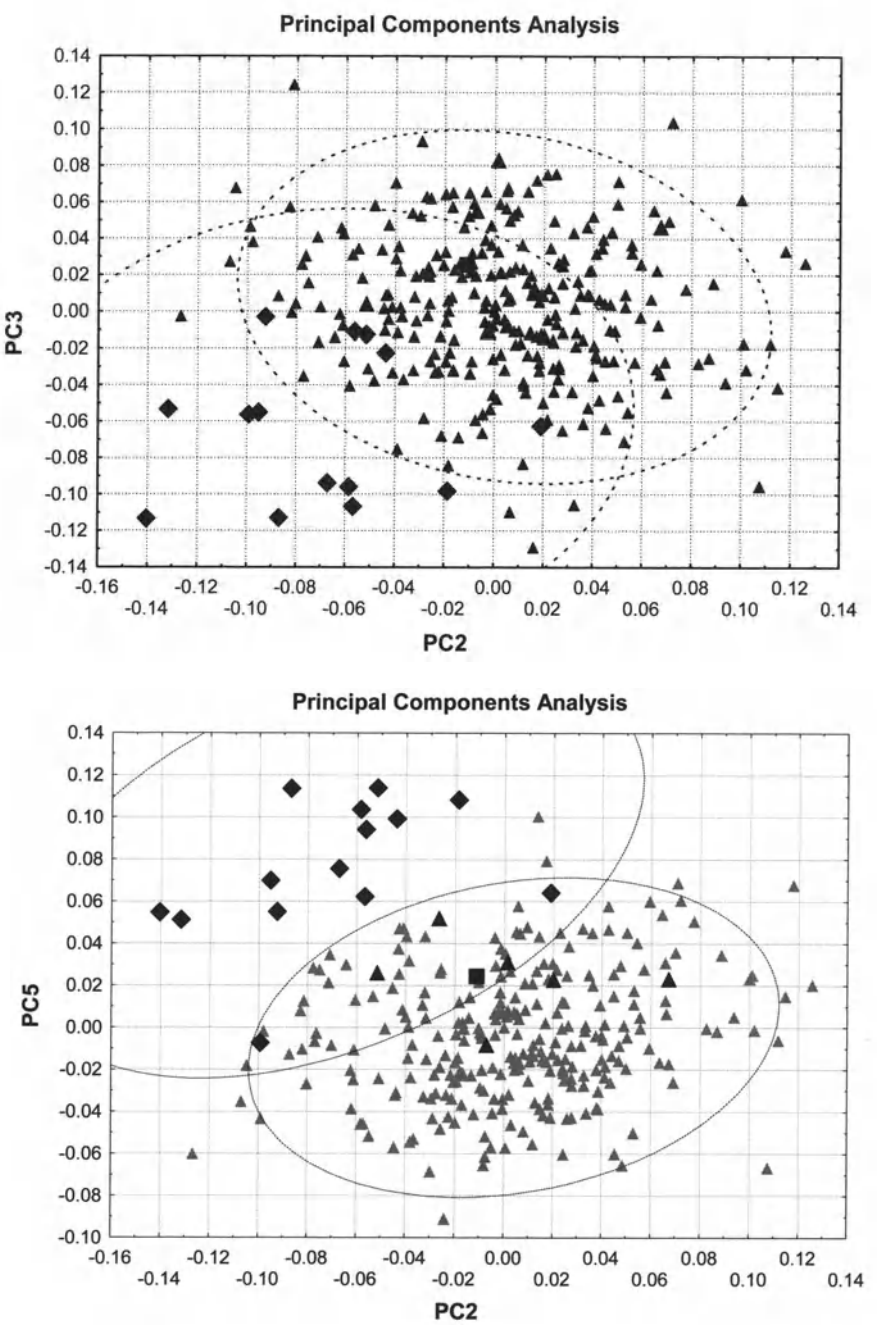

Fig. 2. PCA components 2 and 3 (top) and 2 and 5 (bottom). Neanderthals: black diamonds; Recent modern humans: grey triangles; Upper Paleolithic: black triangles; Kabwe: black square. Dotted lines represent 95 % confidence ellipses

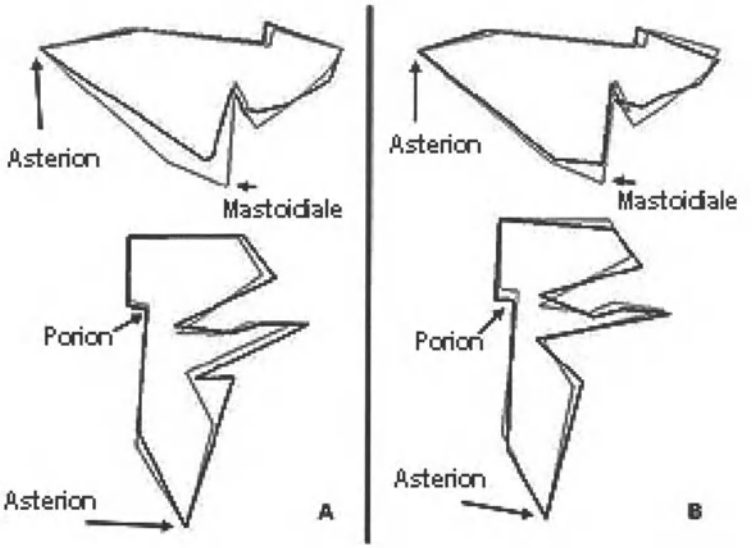

Fig. 3. Shape differences between the Neanderthals and modern humans along A. PCs 2 and 3; B. PCs 2 and 5. Neanderthal configuration shown in black, modern human in grey

A correlation analysis was performed on the PCs 2, 3 and 5 and centroid size. These were all found to be significantly correlated with centroid size, although the correlation coefficients were quite low, indicating weak correlations (PC2: r^2=0.022 p=0.0117; PC3: r^2=0.061 p<0.0001; PC 5: r^2: 0.222 p<0.0001). When the PCs were plotted against centroid size, all three showed a similar pattern of relatively strong correlation between PC score and centroid size within modern humans, but not across modern humans and Neanderthals. The plot of PC5, which scored the highest correlation, against centroid size is shown in Figure 4. Therefore, although it appears that the shape differences described along these components are to some extent size-related among modern humans, they are do not seem to be related to temporal bone centroid size in Neanderthals.

The CVA was performed at the population level, so as not to bias the results by predetermined species. Canonical axis 1 (Figure 5) separated Neanderthals from all other specimens. No Neanderthal fell within the modern human 95 % confidence ellipse along the first two canonical axes, although Amud 1 is the closest specimen to modern humans. Kabwe and the Upper Paleolithic Europeans fell within the modern human 95 % confidence ellipse along canonical axes 1 and 2. Canonical axis 1 was not correlated with centroid size.

The Mahalanobis squared distances (Table 3) among populations were calculated. Neanderthals were very distant from modern human groups. The smallest D^2 between Neanderthals and any modern human population was to the Inugsuk. This distance was larger than the largest distance found between modern human groups. The Upper Paleolithic European specimens were much closer to modern humans than to Neanderthals. Kabwe was found to be approximately equally

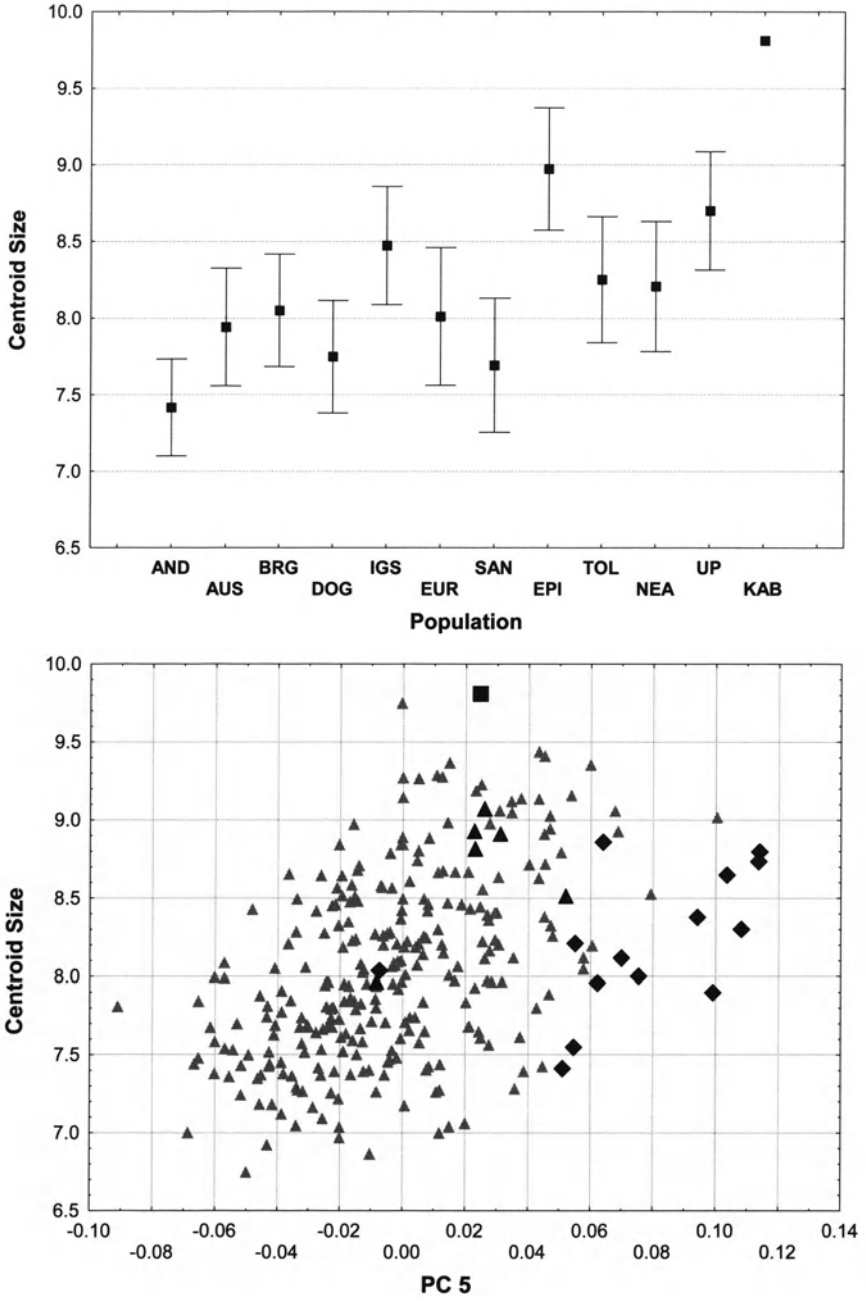

Fig. 4. Means and standard deviations of temporal bone centroid size by population (top); Centroid size plotted by Principal Component 5 (bottom)

distant from Neanderthals and modern humans, but closer to some modern human populations. In the discriminant analysis all Upper Paleolithic specimens were classified as modern human with a posterior probability of 1.00. In the cross-validation test all modern humans, and all but one Neanderthal specimen (Amud 1), were classified correctly.

17.5 Discussion

17.5.1 Modern humans

As reported previously (Harvati 2001a, b, 2003), the modern human mean configuration is characterized by a medio-laterally narrow tympanic area and glenoid fossa, a relatively sagittal orientation of the petro-tympanic crest and a large mastoid process (Figure 1).

17.5.2 Neanderthals

The Neanderthal mean configuration differed from the modern human one in having a more laterally placed auriculare and porion and a somewhat inferiorly placed entoglenoid pyramid and root of the articular eminence, showing a wider glenoid fossa and tympanic area; a more coronal orientation of the petro-tympanic crest; a smaller mastoid process; and a more medially placed juxtamastoid eminence, indicating a wider digastric fossa; (Figure 1). The juxtamastoid eminence appeared only slightly larger than that of modern humans, although it was at the same height, or even lower, than the Neanderthal mastoid process. A shorter mastoid portion of the temporal bone and a stronger supramastoid crest, as indicated by a more lateral placement of auriculare relative to porion, were traits that were previously found to characterize Neanderthals relative to modern humans (Harvati 2003). These features were not found to differ between these two groups in the present analysis. The above differences were found to separate Neanderthals from modern humans in the PCA. The large Mahalanobis D^2 between Neanderthals and modern humans confirms that temporal bone traits are very successful in separating Neanderthals from modern humans.

As in previous analyses, Amud 1 consistently overlapped with the modern human range along the axes that separated Neanderthals from modern humans in the PCA. It was also found to be closest to modern humans along the first canonical axis in the CVA and was the only Neanderthal to be misclassified as modern human in the cross-validation test of the discriminant analysis. As reported previously (Suzuki 1970; Stringer and Trinkaus 1981; Harvati 2003), Amud 1 has a large mastoid process and is intermediate between Neanderthals and modern hu-

mans in the orientation of its petro-tympanic crest and the position of its articular eminence.

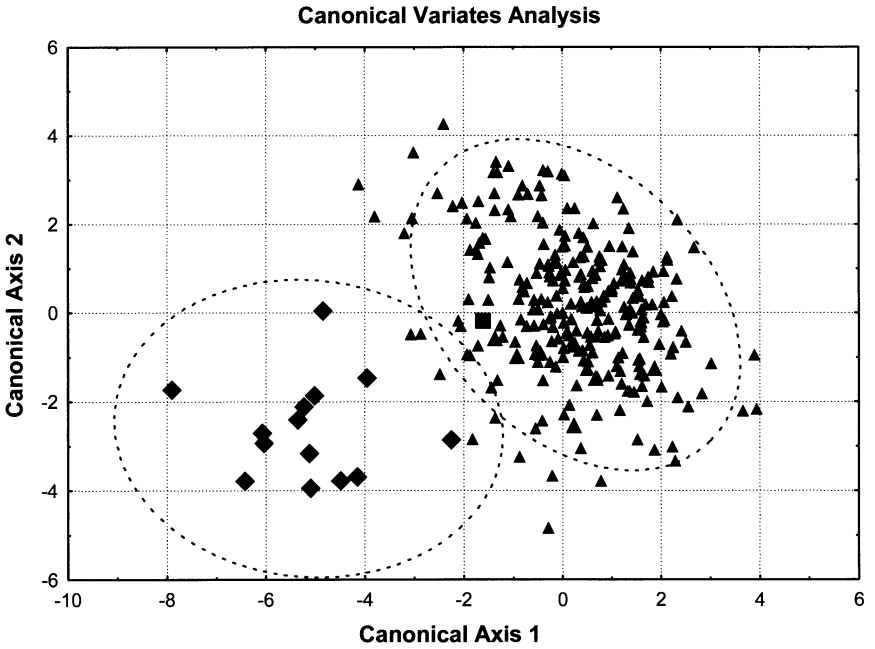

Fig. 5. CVA axes 1 and 2. Symbols as in Fig. 2

17.5.3 Upper Paleolithic Europeans

As previously found, the mean configuration for these specimens was very similar to that of modern humans. The Mladec specimens are often cited as showing Neanderthal affinities (e.g. Kidder et al. 1992). Mladec 2 showed some similarities to the mean Neanderthal configuration in having a large juxtamastoid eminence and small mastoid process. Despite these limited similarities Mladec 2 never clustered with Neanderthals in either the PCA or the CVA and was identified as modern human in the discriminant analysis. Mladec 5, which was not included in the previous analysis, was very similar to the modern human mean configuration, never clustered with Neanderthals and was classified as modern human. The Upper Paleolithic group was very distant from Neanderthals in Mahalanobis D^2. Their distances to other modern human groups were equivalent to those found among recent human populations.

17.5.4 Kabwe

As was reported in Harvati (2001b, 2003), this specimen differed from both the modern human and the Neanderthal mean configuration. showing relatively small

Table 3. Mahalanobis squared distances among populations. All distances are significant to the 0.0001 level, exept where indicated: NS non-significant, * significant to the 0.05 level, ** significant to the 0.01 level. Nea: Neanderthals, And: Andamanese, Aus: Australian, Brg: Austrian Berg, Dog: W. African Dogon, Epi: Afalou/Taforalt Epipaleolithic, Igs: Greenland Inusguk, Eur: W. Eurasian, San: Khoisan, Tol: Melanesian Tolai, UP: Upper Paleolithic Europeans

	Kabwe	**Nea**	**And**	**Aus**	**Brg**	**Dog**
Kabwe	0.00					
Nea	**23.18	0.00				
And	*18.26	47.50	0.00			
Aus	NS14.48	42.25	15.70	0.00		
Brg	*17.97	47.63	15.28	8.42	0.00	
Dog	*20.48	37.62	14.30	10.55	11.96	0.00
Epi	*19.40	43.14	15.68	17.27	8.12	9.50
Igs	**28.31	32.48	20.25	8.41	12.61	12.05
Eur	*20.18	44.75	11.20	5.54	2.64	5.49
San	NS11.94	40.42	27.05	15.65	17.39	7.50
Tol	*18.01	42.88	15.04	**1.83	5.98	9.13
UP	NS12.75	35.42	15.05	15.43	9.80	17.43

	Epi	**Igs**	**Eur**	**San**	**Tol**	**UP**
Kabwe						
Nea						
And						
Aus						
Brg						
Dog						
Epi	0.00					
Igs	21.56	0.00				
Eur	6.58	9.14	0.00			
San	20.39	22.59	15.67	0.00		
Tol	13.02	8.63	3.65	14.66	0.00	
UP	12.36	14.53	12.60	20.60	14.96	0.00

and posteriorly placed mastoid and juxtamastoid processes, a sagittal orientation of the petro-tympanic crest, a medio-laterally wide glenoid fossa, and a supero-

inferiorly shorter mastoid portion of the temporal bone. These shape differences contributed to the separation of Kabwe along the first PC axis. As found previously Kabwe did not show a strong supramastoid crest, despite such descriptions in the literature (Dean et al. 1998; see Elyaqtine 1995 for a different assessment). Kabwe shared with modern humans the more sagittal orientation of the petro-tympanic crest and the absence of a tympanomastoid fissure, as noted previously (Elyaqtine 1995; Schwartz and Tattersall 1996; Martínez et al. 1997; Dean et al. 1998) possible derived traits of modern humans. Kabwe was very distant in Mahalanobis D^2 from both modern humans and Neanderthals, although it was closer to the former.

17.6 Conclusions

As reported in Harvati (2003) most previously described Neanderthal temporal bone features were supported by this analysis, including the small size of the mastoid process, the orientation of the petro-tympanic plate and the great width of the glenoid fossa. Unlike previous findings, a strong supramastoid crest was not found in Neanderthals relative to modern humans. The large size of the juxtamastoid eminence in Neanderthals was found to be less important in differentiating this group from modern humans than the small size of the mastoid process. Kabwe differed in its temporal bone landmark configuration from both modern humans and Neanderthals but was found to share possible modern human autapomorphic traits. The Upper Paleolithic specimens, including the two Mladec specimens, showed essentially modern human patterns of temporal bone morphology.

17.7 Acknowledgements

I thank the curators and collections managers of several museums in Europe, Israel and the US who kindly allowed me to study the fossil and recent collections in their care. I am also grateful to Bill Howells, Eric Delson, Les Marcus, Michelle Singleton and David Reddy and two anonymous reviewers for their comments. This research was supported by NSF (Dissertation Improvement and NYCEP RTG), the American Museum of Natural History, and the Onassis and CARE Foundations.

References

Boule M, Vallois HV (1957) Fossil Men. Dryden Press, New York

Dean D (1993) The middle Pleistocene *Homo erectus* / *Homo sapiens* transition: New evidence from space curve statistics. Ph D thesis, City University of New York

Dean D, Hublin JJ, Holloway R, Ziegler R (1998) On the phylogenetic position of the pre-Neanderthal specimen from Reilingen, Germany. J Hum Evol 34:485-508

Elyaqtine M (1995) Variabilité et évolution de l'os temporal chez *Homo sapiens*. Comparaisons avec *Homo erectus*. Thèse, Université Bordeaux I, n° d'ordre 1321, 215

Elyaqtine M (1996) L'os temporal chez *Homo erectus* et *Homo sapiens*: Variabilité et évolution. *Revue d'Archaeometrie* 20: 5-22

Harvati K (2001a) The Neanderthal problem: 3-D geometric morphometric models of cranial shape variation within and among species. Ph D thesis, City University of New York

Harvati K (2001b) Models of shape variation within and among species and the Neanderthal taxonomic position: a 3-D geometric morphometric approach on temporal bone morphology. J Hum Evol (Abstracts of the Paleoanthropology Society Meeting) 40: A9-A10

Harvati K (2002) Models of shape variation between and within species and the Neanderthal taxonomic position: A 3D geometric morphometrics approach. BAR International Series 1049:25-30

Harvati K (2003) Quantitative analysis of Neanderthal temporal bone morphology using 3-D geometric morphometrics. Am J Phys Anthropol 120: 323-338

Howells WW (1973) Cranial Variation in Man: A Study by Multivariate Analysis of Patterns of Difference Among Recent Human Populations. Papers of the Peabody Museum of Archaeology and Ethnology, Harvard University, vol 67

Hublin JJ (1978) Le torus occipital transverse et les structures associées: Évolution dans le genre *Homo*. Thèse, Université Pierre et Marie Curie, Paris VI

Kidder JH, Jantz RL, Smith FH (1992) Defining modern humans: A multivariate approach. In: Bräuer G Smith FH (eds) Continuity or Replacement: Controversies in *Homo sapiens* Evolution. A. A. Balkema, Rotterdam, pp 157-177

Marcus LF (1990) Traditional morphometrics. In: Rohlf FJ Bookstein FB (eds) Proceedings of the Michigan Morphometrics Workshop. Special Publication, The University of Michigan Museum of Zoology, Ann Arbor, pp 77-122

Martínez I, Arsuaga JL (1997) The temporal bones from Sima de los Huesos middle Pleistocene site (Sierra de Atapuerca, Spain). A phylogenetic approach. J Hum Evol 33: 283-318

O'Higgins P, Jones N (1998) Facial growth in *Cercocebus torquatus*: an application of three-dimensional geometric morphometric techniques to the study of morphological variation. J Anat 193: 251-272

O'Higgins P, Jones N (1999). *Morphologika*. University College London, London

Rohlf JF (1990) Rotational fit (Procrustes) methods. In: Rohlf FJ, Bookstein FL (eds) Proceedings of the Michigan Morphometrics Workshop. The University of Michigan Museum of Zoology, Ann Arbor, pp 227-236

Rohlf JF, Marcus LF (1993) A revolution in morphometrics. Trends in Ecology and Evolution 8: 129-132

Santa Luca AP (1978) A re-examination of presumed Neanderthal-like fossils. J Hum Evol 7:619-636

Schwartz JH, Tattersall I (1996) Toward distinguishing *Homo neanderthalensis* from *Homo sapiens*, and vice versa. L'Anthropologie 34: 79-88

Slice DE. (1992, 1994 Copyright). GRF-ND: Generalized rotational fitting of n-dimensional landmark data. Department of Ecology and Evolution, State University of New York, Stonybrook, New York

Slice DE (1994-1999 Copyright). Morheus et al.: Software for Morphometric Research. Department of Ecology and Evolution, State University of New York, Stonybrook, New York

Slice DE (1996) Three-dimensional generalized resistance fitting and the comparison of least-squares and resistant fit residuals. In: Marcus LF, Corti M, Loy A, Naylor GJP, Slice DE (eds) Advances in Morphometrics. NATO ASI Series. Plenum Press, New York, pp 179-199

Slice DE (2001) Landmark coordinates aligned by Procrustes analysis do not lie in Kendall's shape space. Systematic Biology 50: 141-149

Stringer CB, Trinkaus E (1981) The Shanidar Neanderthal crania. In: Stringer CB (ed) Aspects of Human Evolution. Taylor and Francis, London, pp 129-165

Suzuki H, Takai F (1970) The Amud Man and His Cave Site. Academic Press of Japan, Tokyo

Vallois HV (1969) Le temporal Néanderthalien H 27 de La Quina. Étude anthropologique. L'Anthropologie 73: 524-400.

Vandermeersch B (1985) The origin of the Neanderthals. In: Delson E (ed) Ancestors: The Hard Evidence. Liss, New York, pp 306-309

Index